Hypothermic encapsulation of bone marrow stem cells in alginate hydrogel beads.

Conor James Robinson

MSc

University of Glasgow

Submitted in fulfilment of the requirements of the Degree of Doctor of Philosophy (PhD)

Centre for the Cellular Microenvironment

School of Molecular Bioscience

College of Medical, Veterinary and Life Sciences,

University of Glasgow,

Glasgow

G12 8QQ

September 2025

Abstract

The bone marrow niche microenvironment (BM) is highly complex. It is home to haematopoietic stem cells (HSCs) and, most importantly, long-term HSCs (LT-HSCs) reside here in close proximity to osteoblasts and are responsible for producing all blood and immune cells (Nombela-Arrieta et al., 2013). Mesenchymal stem/stromal cells (MSCs) that form all bone, cartilage, muscle and fat cells, also reside in BM (Fink & Zachar, 2011; Gang et al., 2004; B. Johnstone et al., 1998; Nishimura et al., 2015; Mathew et al., 2011). Cytokines expressed by MSCs are known to regulate HSC quiescence – a low metabolic state adopted for long-term survival –, cell cycle entry and differentiation (Fereydani et al., 2024).

HSCs are at the forefront of medical science. They have been used for decades in stem cell transplants and remain the most effective method of treating damaged bone marrow (Khaddour et al., 2023). Due to the increasing average lifespan of the population, the natural occurrence of malignant mutations in HSCs and the resultant blood disorders are ever more present in our global society (Jaiswal & Ebert, 2019). HSC genetic damage also occurs as a side effect of many widely used drugs, such as chemotherapeutic agents, and while we know this damage leads to leukaemia, we currently have no curative treatments, and prognosis is poor; further emphasising the need for research into the area (Ezoe, 2012).

Unfortunately, HSCs are notoriously sensitive to cryopreservation and culture under traditional 2D culture methods (Branco et al., 2024; Rimac et al., 2023). Combined with being a very rare cell type – 0.01% of the total blood population – this makes them incredibly expensive and therefore relatively inaccessible to many institutions for research purposes (Lee-Six et al., 2018). Further, much of the research into culturing HSCs aims to expand the population and encourages an activated cell-state (Cheng & Scadden, 2009). This is not comparable to how the most clinically relevant LT-HSC population reside *in vivo,* and therefore, a way to maintain quiescent HSCs and present them for drug testing should be of utmost importance to give insight into this critical yet under-researched cell type and the diseases that impact them.

There is also now a societal push towards improved ethical standards and reduced environmental impact of research, which threatens to move beyond a point where current and developing techniques can keep up. For example, while not legally required, the medicines and healthcare products regulatory agency requires animal testing for medicines before human clinical trials (The Use of Animals in Pharmaceutical Research,

ABPI, 2025). This is largely due to a lack of adequate and well-tested alternatives, and therefore, foundational research on how human models could be created, such as this project, is necessary to meet phase-out targets by the current government (Labour-Party-Manifesto-2024, 2024.).

Work produced by the LifeTime centre for doctoral training intends to discover and develop non-animal technologies in collaboration with industry, charities and the NHS with real-world medical applications (About Us – LifETIME CDT, 2025). The goal of this thesis was to develop a methodology which could improve access and reduce the cost of rare and expensive bone marrow stem cells to enable their use more widely in clinical and research applications and in turn, aid advances in this area of work. More specifically, hypothermic temperatures and alginate hydrogels were used to encapsulate human primary stem cells and induce the low-metabolic state of quiescence. The experimental methodology and optimum temperature for single MSCs were first confirmed to be 15 °C using viability staining as proposed by Atelerix, which is currently used as an environmentally friendly and animal-free preservation alternative (Swioklo et al., 2016). Following this, the surface marker expression of monolayer and encapsulated MSCs was compared. CD34+ haematopoietic cells were then encapsulated, stored, and their surface marker expression analysed to determine the optimum temperature, media and media supplementation for encapsulation. Donor variability prevented meaningful conclusions; however, haematopoietic stem and progenitor cells (HSPCs) were maintained more effectively than others. Raising questions about the applicability of using CD34+ cells as ‘HSCs’, for only a very small number of these cells have functional properties of stem cells.

Next, MSC spheroids were encapsulated and their viability and surface marker expression compared to non-encapsulated and monolayer controls. The optimum media and temperature were analysed, with similar trends observed between conditions. Surface marker expression indicated that aggregation may induce phenotypical changes, but this was not enhanced by encapsulation. Further, the surface stiffness of gels without cells, with cells, with spheroids, and with cells and spheroids was analysed, and a stiffness in line with that used to induce osteogenic differentiation in literature was observed (Chaudhuri et al., 2016). Finally, a more extensive panel was used to analyse CD34s to determine which subsection of HSPCs was maintained under encapsulation, and colony-forming assays were performed to assess functional capacity.

The core findings of the study showed that MSC spheroids are viable for longer than

single MSCs when encapsulated in alginate at hypothermic temperatures, and that aggregation induces surface marker changes that indicate low motility and immunosuppressive abilities. Further, this process does induce quiescence within the quiescence-capable subpopulations of HSPCs and does so less favourably for more mature subpopulations. Therefore, this method could potentially be used for the storage and transport of this cell type, in addition to alternate uses such as a scaffold with which to present HSPCs or MSC spheroids in a simple model for research, drug testing or as a ready-to-use cell therapy.

The project exclusively uses directly applicable human primary cells, uses no animal products and is fully biocompatible. Cell-laden alginate has wide-reaching applications; however, this work could be used specifically to improve access to stem cells for future research and, therefore, assist in the development and reduce costs of non-animal testing methods and models, whilst itself being more environmentally friendly than current alternative transport and storage methods.

Table of Contents

List of tables

List of Figures

Acknowledgments

Firstly, I want to thank the EPSRC for funding this work. I'd also like to thank the LifeTime Centre for Doctoral Training and Professors Matthew Dalby and Manuel Salmeron-Sanchez for letting me be part of the LifeTime CDT programme and the Centre for the Cellular Microenvironment, along with their advice and mentorship. Special thanks to Dr Monica Tsimbouri for being everyone's "lab mum"; for the insurmountable technical and emotional support, guidance and understanding, I will be forever grateful. To Dr Alisdair McDonald, I want to extend similar thanks for technical support, advice and friendship.

To my friends in Glasgow and the CDT with whom I shared this journey, I'll miss you all and wish you the utmost success with whatever you do next! In particular, thank you, Emma, for being my 'lab bestie' (although I could have gotten by without all those emotions of yours). Hannah and I love you dearly.

On that, I thank my fiancé, Hannah, for moving to Scotland with me (even though I reassured you I wouldn't move here in the first place), for loving me when I worked stupid hours, when I was over-socialised and sat in silence for a weekend, for feeding me, watering me and facing me towards the sun.

Lastly, and most importantly, my parents. For supporting me through my rather turbulent journey of school, academia and life. Encouraging me to be curious, allowing me to stumble along my own path, make my own mistakes, yet motivating me to keep going in whatever capacity I could. This work, this last decade of higher education, is as much your achievement as it is mine.

Thankyou.

Authors Declaration

I declare that, except where explicit reference is made to the contribution of others, this dissertation is the result of my own work and has not been submitted for any other degree at the University of Glasgow or any other institution.

Printed Name: CONOR ROBINSON

Signature:

Abbreviations

ADC	Adult stem cell
ADSC	Adipose stem cells
AECs	Arteriolar endothelial cells
ALL	Acute lymphoblastic leukaemia
ALP	Alkaline phosphatase
AML	Acute myeloid leukaemia
AMP	Adenosine 5'-monophosphate
A-MSC	Adipose derived mesenchymal stem/stromal cell
Ang-1	Angiopoietin-1
ATP	Adenosine triphosphate
BIT	Bovine Insulin Transferrin
BM	Bone marrow
BM-HSC	Bone marrow haematopoietic stem cell
BM-MSC	Bone marrow mesenchymal stem/stromal cell
BMP-2	Bone morphogenetic protein 2
BSA	Bovine serum albumin
BSP	Bone sialoprotein
CAR	CXCL12 abundant reticular
CB	Cord blood
CB-HSPC	Cord blood-derived HSPC
CB-MSC	Cord blood mesenchymal stem/stromal cell
CD	Cluster of differentiation
CDK	Cyclin-dependant kinase
CF	Colony forming
CFU	Colony forming unit
CHIP	Clonal haematopoiesis of indeterminate potential
CH	Clonal haematopoiesis
CLP	Common lymphoid progenitor
CMP	Common Myeloid Progenitor
CPA	Cryopreservation agent
CXCL-12	C-X-C Motif chemokine ligand 12
CXCL4	C-X-C motif chemokine ligand 4
CXCR4	C-X-C Motif chemokine receptor type 4
DKK1	Dickkopf-related protein 1
DMEM	Dulbecco's modified eagle's medium
DMSO	Dimethyl sulfoxide
ECM	Extracellular matrix
ECs	Endothelial cells
E-MSC	Embryonic stem cell derived mesenchymal stem/stromal cell
ESC	Embryonic stem cells
FACS	Fluorescent activated cell sorting
FGF2	Fibroblast growth factor 2
Flt-3	Feline McDonough sarcoma like tyrosine kinase 3
FSC-a	Forward scatter area

FSC-W	Forward scatter area width
g-CSF	Granulocyte-colony stimulating factor
GF	Growth factor
Gfi-1	Growth factor independent 1 transcriptional repressor
HGF	Hepatocyte growth factor
HIF	Hypoxia induced factor
HLA	Human leukocyte antigen
HLA-DR	Human leukocyte antigen -DR isotype
HLTM	Human long term culture medium
hPSC	Human pluripotent stem cell
HRP	Horseradish peroxidase
HS	Human serum
HSC	Haematopoietic stem cell
HSPC	Haematopoietic stem and progenitor cell
IGF-1	Insulin-like growth factor 1
I-HSC	Intermediate haematopoietic stem cell
IL	Interleukin
IMDM	Iscove's modified Dulbecco's medium
iPSC	Induced pluripotent stem cell
Lef1	Lymphoid enhancer-binding factor 1
LIF	Leukaemia inhibitory factor
LRP5/6	Low density lipoprotein receptor-related proteins 5 and 6
LTC	Long term culture
LT-HSC	Long term haematopoietic stem cell
MKs	Megakaryocytes
MPL	Myeloproliferative leukaemia protein
MPP	Multipotent progenitors
MSC	Mesenchymal stem/stromal Cell
MSX2	Msh homeobox 2
OB	Osteoblast
Oct-4	Octamer-binding transcription factor 4
Opn	Osteopontin
OSX	Osterix
PB	Peripheral blood
PB-HSPCs	Peripheral blood- derived HSPCs
PBS	Phosphate buffered saline
PGE2	Prostaglandin E2
RGB	Red, Green, Blue
RGD	Arginylglycylaspartic acid
ROS	Reactive oxygen species
RT	Room temperature
RUNX	Runt-related transcription factor
SCF	Stem cell factor
SCT	Stem cell transplant
SDF-1	Stromal cell-derived factor-1

SECs	Sinusoidal endothelial cells
SFRP1	Secreted frizzled-related protein 1
SIRT1	Sirtuin 1
SOX2	Sex determining region Y-box2
SSC-A	Cide scatter area
STC-1	Stanniocalcin 1
ST-HSC	Short term haematopoietic stem cell
TCF7	Transcriptional factor 7
TGF-β	Transforming growth factor beta 1
THPO	Thrombopoietin
TLE2	Transducin-like enhancer protein 2
TNF-α	Tumour necrosis factor alpha
TSG-6	Tumour necrosis factor - inducible 6 protein
UC-MSC	Umbilical cord mesenchymal stem/stromal cell
VCAM-1	Vascular adhesion molecule 1
VEGF	Vascular endothelial growth factor
VW-MSC	Vascular wall mesenchymal stem/stromal cell
YAP	Yes-associated protein 1

Chapter 1. Introduction

The advancement of medicine and enhanced public health are dependent on research. Research taking place, predominantly, within universities and therefore specific research groups, which are loss-making enterprises reliant on external funding from governments and research councils (Annual TRAC 2022-23 Sector Summary and Analysis by TRAC Peer Group, 2024). As a result, relatively expensive techniques and materials become limitations and hindrances in research involving them. Haematopoietic stem cells (HSCs) are widely used in the treatment of leukaemia in stem cell transplants (SCT), and it's currently of research interest to target haematopoietic illnesses at their source – diseased HSCs (Khaddour et al., 2023; Jaiswal, 2020). Treating malignant stem cells would then prevent the disease from ever bearing fruit. However, even with this hypothesis being a gateway to vast avenues of research - such as the highly fashionable emergence of gene editing – high costs are unavoidable (Park & Bao, 2021). This issue is to be addressed in this project.

The first hurdle is comparability to *in vivo* cells. As HSCs cannot be reliably cultured, and the best efforts using complex and expensive model systems, it means research involving them is difficult (Branco et al., 2024). Since there is no universally standard culture method, it also means the comparability of data is limited. Furthermore, most currently existing models aim to expand the HSC population or render most cells in an activated state (Cheng and Scadden, 2009). Considering the most primitive and clinically relevant HSC population resides in a quiescent state for most of their time, it is these that we should be targeting as a starting point for illnesses. Also, *in vitro* models should start aiming to maintain HSCs in this state – something as yet not achieved reliably without gene editing (Ikonomi et al., 2020; Nakamura-Ishizu et al., 2014; Shiroshita et al., 2022; Yamada et al., 2013).

The second obstacle is cost. Compared to other cell types, the cost per cell for HSCs is exceptionally high. They are expensive to buy, require expensive media supplements to maintain, and their population cannot be expanded (Branco et al., 2024). They are also an incredibly rare cell type occupying a tiny percentage of the cells in the body, and harvesting is highly invasive (Lee-Six et al., 2018).

Thirdly is accessibility. HSCs are a highly sensitive cell type with variable recovery rates upon traditional freeze/thaw cryogenic cycles, resulting in low

yields from samples frozen for storage, transport, or both (Rimac et al., 2023). Contrastingly, in developing countries where modern infrastructure is not in place, cold-chain transport is not available to provide frozen or refrigerated samples at all (Ashok et al., 2017; Gligor et al., 2018; Yahia, 2010). This means that not only are institutions in these areas unable to participate in research using HSCs, but HSCs are unavailable to provide lifesaving stem cell treatments. Subsequently, we need a method with which to provide these cells into the harshest of environments without the need for freezing, or a method that allows them to be isolated and kept short-term to prep for surgery.

Mesenchymal stem/stromal cells (MSCs) are also of great interest in a clinical setting due to their ability to home to injury sites and exhibit anti-inflammatory, immunomodulatory effects and bone regenerative effects, among many others (Piuzzi et al., 2017) (Chandanala et al., 2024; Yuan et al., 2022). In fact, aggregated MSCs known as MSC spheroids are also now of clinical interest, with differing abilities compared to single-cell MSCs, such as enhanced anti-inflammatory abilities (Bartosh et al., 2010).

This project is undertaken as part of the LifeTime centre for doctoral training, which, in collaboration with charities, industry and the NHS, intends to discover and develop non-animal technologies with real-world medical applications (About Us – LifETIME CDT, 2025). The aim is to facilitate scientific advancements by improving access to rare, yet clinically important, bone marrow (BM) HSCs (BM-HSCs) and BM-MSCs by making a simplified, cost-effective method of maintaining them *in vitro* to then be used as a storage and/or delivery method. This will be based on existing work on single-cell MSCs performed by the stakeholder company Atelerix Ltd, who use alginate hydrogels to induce a quiescent state in the cells, enabling short-term storage and cell maintenance at hypothermic temperatures (Swioklo et al., 2016). This work will have a wide range of additional potential applications, as *in vitro* maintenance of quiescent HSCs will enable research and testing to take place on the cells in a comparative state to those most difficult to target *in vivo,* while potential use as a delivery method for MSC spheroids would have useful clinical applications (Genovese et al., 2014).

1.1 Stem Cells

There are three distinct stem cell types: pluripotent, multipotent and unipotent. Human pluripotent stem cells (hPSCs) can expand indefinitely and form any cell in the body (Odorico et al., 2001). The only naturally occurring form of hPSCs are embryonic stem cells, isolated from the inner cell mass of a blastocyst between 4 and 7 days old (National Research Council (US) and Institute of Medicine (US) Committee on the Biological and Biomedical Applications of Stem Cell Research., 2002). In vivo, they will form all three germ layers of embryonic tissue. However, in 2006, through pluripotency gene transduction, induced pluripotent stem cells (iPSCs) were created which possess many similarities to embryonic stem cells like flexible lineage commitment, without the ethical concerns (Takahashi & Yamanaka, 2006).

Contrastingly, adult multipotent stem cells are found in a specific area or tissue of fully developed mammals, with this location known colloquially as a stem cell 'niche' (He et al., 2009). They are the most primitive cell in their respective lineage and, through differentiation, are able to become any other cell within it. The exception is transdifferentiation - a mechanism through which a cell undergoes genetic reprogramming and switches to a cell of a different lineage - which can occur with both mature progenitor and primitive stem cells (Song & Tuan, 2004).

If the most primitive cell in a system has only one progenitor, it is known as a unipotent stem cell. Examples include germline stem cells, which produce sperm in the testis, and a population of cells in the mammary gland exclusively responsible for the formation of a single mammary epithelial cell type (Shahrabi et al., 2016; Visvader & Lindeman, 2011).

Adult stem cells do not generally have indeterminate proliferative or multilineage potential without *in vitro* modification chemically or at the gene level (Krampera et al., 2007). However, they can temporarily exit the cell cycle and enter a state of reduced metabolism known as quiescence, while being able to re-enter later (de Morree & Rando, 2023). Further, unlike their progeny, stem cells are not generated anew when needed. Instead, through a process called self-renewal, the population of stem cells present at birth will repopulate themselves (He et al., 2009). Self-renewal requires entrance back into the cell cycle, something that can also be triggered as a response to injury. Over time, this cloning can lead to replicative senescence, where the recapitulative

capacity of the stem cell pool reduces; something demonstrated by reduced regenerative capacity displayed by older people compared to the young (Huang et al., 2022; Krasnova et al., 2023; Shao et al., 2013).

1.1.1 Mesenchymal Stem/Stromal Cells

MSCs are pluripotent and can commit to several lineages via adipogenesis, osteogenesis, chondrogenesis and myogenesis, which will lead to the formation of fat, bone, cartilage and reticular tissue, respectively (Fink & Zachar, 2011; Gang et al., 2004; B. Johnstone et al., 1998; Nishimura et al., 2015; Mathew et al., 2011). Subsequently, MSCs can be isolated from a range of locations, with the most common being from adipose tissue (A-MSCs), umbilical cord (UC-MSCs), cord blood (CB-MSCs) or the bone marrow (BM-MSCs) (Pittenger et al., 2019; Tsuji et al., 2014; Zeddou et al., 2010). In fact, MSCs have now been isolated from nearly every tissue in the body (Crisan et al., 2008; da Silva Meirelles et al., 2006). As MSCs exist in numerous forms and stages of commitment, efforts have been made to define the primitive, and most clinically relevant, MSC population. The minimum criteria proposed by the Mesenchymal and Tissue Stem Cell Committee of the International Society for Cellular Therapy covers cell properties and cluster of differentiation (CD) surface markers. Surface markers are protein molecules in the form of receptors that coat the surface of cells, typically identified by a ‘CD’ number notation (Markides et al., 2019). Firstly, the cells must exhibit plastic adherence in standard cell culture conditions. Secondly, they must be CD105, CD73 and CD90 positive and CD45, CD34, CD14 or CD11b, CD79α or CD19 and HLA-DR negative. Lastly, they must be able to differentiate into osteoblasts, adipocytes and chondrocytes *in vitro* (Dominici et al., 2006). However, additional insight suggests that more stringent criteria are required. It is now known that MSCs are better described as ‘stromal’ rather than ‘stem’ cells, due to the heterogeneous nature of the population. Within the plastic adherent population stated in the criteria, many cells are already lineage committed and therefore lack multilineage and colony-forming capabilities, while only a small subset retains these ‘stemness’ properties (Kuroda et al., 2010; Lv et al., 2014). Therefore, it is proposed that a more extensive criterion would be for MSCs to possess multilineage potential, have colony-forming (CF) potential and be positive or negative for a more extensive group of surface markers. It is also important to note that MSCs from different sources will have

different marker expression. For example, while CD271 is a good indicator of CF ability in BM-MSCs, it is not a marker expressed on CB-MSCs or UC-MSCs (Jones et al., 2002; Zeddou et al., 2010). In fact, the 2023 review by Fonseca *et al.* indicates a variety of markers currently used through literature for characterising MSCs, which are CD44, CD271, CD29, CD90, CD105, CD166, CD73, CD146 and Stro-1 (Fonseca et al., 2023).

1.1.1.1 MSC Surface Markers

CD44 is an adhesion molecule that interacts primarily with hyaluronic acid (HA) as well as extracellular matrix ligands such as collagen and fibronectin (FN).(Sneath & Mangham, 1998) It is involved in cell-cell adhesion during the aggregation of macrophages, lymphocytes and fibroblasts (Sneath & Mangham, 1998). As well as lymphocyte activation and homing (Arch et al., 1992; Haynes et al., 1989; Jalkanen et al., 1986). It is critical for MSC homing to injury sites, as damaged tissue shows increased HA concentration (Bian et al., 2013; Dovedytis et al., 2020; Ouhtit et al., 2020). However, fresh BM-MSCs lack CD44 expression but gain it in culture (Qian et al., 2012). CD44 is also of interest in most cancers, with expression changes resulting in tumour growth, invasion and metastasis (Sneath & Mangham, 1998). CD44 regulates A-MSC differentiation into chondrocytes by modulating Smad2/3 and ERK1/2 pathways (Xu et al., 2020).

CD271 low-affinity nerve growth factor receptor [LNGFR]) is most known for its role in the development of melanoma, with its expression correlating to metastatic cell conversion from healthy melanocytes (Filipp et al., 2019). Its expression correlates to an MSC population with enhanced tissue repair and both osteogenic and chondrogenic potential (Álvarez-Viejo et al., 2015; Hermida-Gómez et al., 2011; Müller et al., 2019). Further, it is expressed exclusively on the only subset of MSCs with CF and engraftment potential (Kuçi et al., 2010). However, the exact abundance of this subset is unclear. For example, for A-MSCs, it could be anything from 20 to 98%, while for BM-MSCs from 2 to 30% (Camilleri et al., 2016; Cao et al., 2024; Quirici et al., 2002; Sober et al., 2023).

The CD29 (Integrin $ß_1$) family are heterodimers comprised of the CD29/$ß_1$ chain associated with one of six different α-chains (Hemler, 1990). Through the $α_1$ and $α_2$ (collagen), $α_3$ (laminin) and $α_5$ (Arginylglycylaspartic acid (RGD) binding) heterodimers, CD29 is critical for cellular interaction with the ECM and cell migration (Caixia et al., 1991; Ode et al., 2011; Sun et al., 2023). Further,

interaction with the α_5 and β_1 chain of the integrin leads to the induction of intercellular adhesion (Caixia et al., 1991).
CD29 is also involved in numerous cancers. For example, $\alpha_1\beta_1$ is a marker of two-thirds of colon cancers and promotes the invasion of cancer cells (Boudjadi et al., 2015); blocking $\alpha_2\beta_1$ enhances osteosarcoma treatment outcomes (C. Yu et al., 2020); $\alpha_3\beta_1$ promotes metastasis of breast cancer cells, is a biomarker for bladder cancer, and $\alpha_3\beta_1$ targeting is a non-small cell cancer treatment (Jin et al., 2020; Ndoye et al., 2021; Zou et al., 2020).

CD90 (THY-1) is a cell adhesion glycoprotein observed in multipotent MSC populations, with its expression diminished in differentiated progenitors (Moraes et al., 2016a). It contains an RGD-like peptide and a heparin-binding domain, which enables interaction with cells and surfaces, therefore playing a role in cell adhesion and migration (Valdivia et al., 2023).

CD105 (Endoglin) CD105 is an accessory co-receptor of transforming growth factor beta 1 (TGF-ß) (Cheifetz et al., 1992; Meurer & Weiskirchen, 2020; Wong et al., 2000). While TGF-ß can be used to induce chondrogenic, regulate osteogenic and inhibit adipogenic differentiation in MSCs, CD105 expression is not affected based on TGF-ß abundance (Zhao & Hantash, 2011). In fact, while it was postulated that CD105 was representative of multilineage potential, the truth of that is questionable. For example, Cleary *et al*. demonstrated that CD105 expression is not indicative of chondrogenic potential in BM-MSC (Cleary et al., 2016). While Anderson *et al*. showed that it was CD105- MSCs that were more prone to adipocyte and osteocyte differentiation (Cleary et al., 2016). However, CD105-negative MSCs show enhanced immunomodulation capacity compared to CD105-positive MSCs, which correlates with MSC spheroids having enhanced immunomodulation capacity (Pham et al., 2019) (Thai et al., 2024).

CD166 (activated leukocyte cell adhesion molecule [ALCAM]) is a type 1 membrane protein found on a variety of cell types, including OBs, MSCs and HSCs (Chitteti et al., 2013; Cho et al., 2023; Ferragut et al., 2021; Smith et al., 2017). It can interact with other CD166 proteins as well as CD6, enabling cell-cell adhesion during monocyte migration and leukocyte metastasis (Smith et al., 2017). CD166 expression on OBs also correlates with their ability to maintain HSCs due to its expression being directly correlated to Runt-related transcription factor 2 (RUNX2) (Chitteti et al., 2013, 2014). While loss of CD166 expression on

niche HSCs correlates with reduced long-term potential (Hooker et al., 2015; Jeannet et al., 2013).

CD73 is a 5'-nucleotidase that metabolises adenosine 5'-monophosphate (AMP) to adenosine and is critical in MSC immunosuppressive capability (Chandanala et al., 2024; Colgan et al., 2006).
It is also expressed on MSCs, which have enhanced haematopoietic cytokine expression and subsequently enhanced haematopoietic maintenance.(Galgaro et al., 2021) Other MSC characteristics that correlate to increased CD73 expression include enhanced proliferation rate, homing and migration, immunomodulation and osteogenic potential, and decreased chondrogenic potential (Burand et al., 2020; Galgaro et al., 2021; Ode et al., 2011; Suto et al., 2017).

CD146 (melanoma cell adhesion molecule [MCAM])
While it is expressed on endothelial cells (ECs), muscle cells and pericytes, CD146 was first identified due to its high expression in many tumours (Joshkon et al., 2020). In particular, overexpression is a hallmark of cancers, particularly those that are progressive and metastatic, by enhancing interactions between the cell and the ECM (Wang et al., 2020). Traditionally, its role is in cell adhesion, migration and is highly linked to angiogenesis (Joshkon et al., 2020). However, expression in MSCs correlates with differentiation and immunoregulatory capacity (Ma et al., 2021; Wang et al., 2020). It can also indicate MSC commitment to vascular smooth muscle cells and is upregulated in normoxia but downregulated in hypoxia (Espagnolle et al., 2014; Tormin et al., 2011).

1.1.1.2 Relevance and applications of MSCs

Regenerative medicine can be described simply as 'the replacement or regeneration of human cells, tissue or organ to restore or establish normal function' (Mason & Dunnill, 2008). It is in this field that MSCs are of great interest as stem cell therapies, defined as systemic or local. Local therapies involve the injection of cells close to the wound site, resulting in a large dose with low amounts of non-specific dosing. Systemic therapies involve a non-local administration, relying on MSCs travelling to the damaged site. This enables treatment to invasive or inaccessible locations but often results in non-specific dosing with many cells accumulating in organs like the kidneys (Sukmana et al., 2023; Ullah et al., 2019).

Systemic therapies are based on *in vivo* observations that MSCs have displayed homing capabilities in response to signals produced after tissue damage and migrate accordingly (Ponte et al., 2007; Ullah et al., 2019). They do so by leaving their classic niche tissues and entering circulating blood, travelling and accumulating at the site of injury, guided by a concentration gradient of stress and inflammation-based chemokines and growth factors (Rochefort et al., 2006; Xiao Ling et al., 2016; Yuan et al., 2022). They are of interest for regenerative medicine because once homed to the site of damage, MSCs display immunomodulatory and anti-inflammatory effects by inhibiting the M1 macrophage (which secretes pro-inflammatory cytokines) phenotype and inducing M2 (which secretes anti-inflammatory cytokines) (Chandanala et al., 2024; Yuan et al., 2022).

MSCs also have a highly complex secretome which acts as an intercellular signalling system to communicate with other MSCs, as well as to cells involved in immunosuppressive, regenerative and antimicrobial systems, among others (Fernández-Francos et al., 2021). This involves the secretion of pro-inflammatory cytokines such as interleukin 6 (IL-6), cell regulatory cytokines such as stem cell factor (SCF), and antimicrobial peptides like LL-37 (O'Hagan-Wong et al., 2016; Saleh et al., 2015; Yagi et al., 2020).

Thanks to their secretory profile and broad differentiation capacity, MSCs are being utilised in medical research for numerous illnesses. According to clinicaltrial.gov, as of March 2025, there are currently over 1500 clinical trials using MSCs. The broad areas of which are the immune, musculoskeletal, cardiovascular and central nervous systems. (Yang et al., 2018) (Mousaei Ghasroldasht et al., 2019; Piuzzi et al., 2017; Villa et al., 2016) (Xu et al., 2020) (M. Ge et al., 2018)

1.1.2 Haematopoietic Stem Cells

Hematopoietic stem cells (HSCs) are a name given to the most primitive cells within the haematopoietic system. First characterised in 1988 by Spangrude *et al.*, who demonstrated that HSCs could reconstitute the blood cells and therefore save lethally irradiated mice (Spangrude et al., 1988). It wasn't until 1994 that Morrison *et al.* separated and defined three separate populations within this 'HSC' subset, defining long-term HSC (LT-HSC) and short-term (ST-

HSC) populations, which have multilineage potential, and multipotent progenitors (MPPs), which do not (Morrison & Weissman, 1994). We continue to use their surface marker panel as guidelines to this day, with human HSCs being described as lineage negative (Lin-) CD34+CD38-CD45RA-, while haematopoietic stem/progenitor cells (HSPCs) are purely Lin-CD34+CD38- **(Figure 1)**.
Over time, a long and highly complex hierarchy has been shown to exist, more like a differentiation gradient, with increasingly more differentiated cells originating from a highly quiescent, long-term population (**Figure 1)**. Regardless, there are still a few markers used to sort haematopoietic cells into sub-populations. Lin- means a cocktail of antibodies was used to deplete the population of cells committed to myeloid and lymphoid pathways (Thermofisher, 2025). CD34 is a surface marker expressed on just 1.5% of the BM mononuclear population (Krause et al., 1996). Its exact purpose is still unconfirmed, but there's evidence to show it plays a role in cell adhesion and homing to the BM (Healy et al., 1995; Nielsen & McNagny, 2009). Lin- mononuclear CD34+ cells exhibit oligopotency but not necessarily multipotency. Multipotency is exhibited within Lin-CD34+CD38- cells, with CD38 playing a role in cell activation and proliferation (Morandi et al., 2019). Lastly is to separate this population based on CD45RA and CD90. The function of CD45RA in HSCs is unknown; however, CD90 is involved in inflammation and wound healing (Kisselbach et al., 2009). CD45-CD90+/CD90lo cells are considered LT-HSCs, with active cells having engraftment capacity ≥3-4 months as well as CD90+ cells being able to produce CD90- cells but not vice-versa, confirming the hierarchy (Cheng et al., 2020; Majeti et al., 2007). However, there is an inconsistency in the literature, as in some cases ST-HSCs, I-HSCs and MPP are considered the same cell type classified as CD90-CD45RA- and have no long-term recapitulation or self-renewal ability, with those that do considered LT-HSCs (Stemcell Technologies, 2025; Laurenti et al., 2015). In others, ST-HSCs are considered CD90+ but still grouped with MPPS in terms of properties (Ribeiro-filho et al., 2019). While in other cases ST-HSCs are considered separate from MPPS via CD49 expression, yet both are considered CD90-CD45RA- (Mann et al., 2022). With alternate surface markers Flk2, CD150 and CD48, the expression of MPPs have been categorised and split into groups 1 to 4 (Pietras et al., 2015; Wilson et al., 2008). All are CD90-CD45RA-, though MPP1 have recapitulative capabilities up to 4 months, have self-renewal capabilities and are very similar to descriptions elsewhere of LT-HSCs. Whereas

MPP 2-4 have limited reconstitution capabilities under a month, and no self-renewal ability - more like historical descriptions of ST-HSCs. This functional description is in line with observations that CD90-CD45RA- cells are still capable of full haematopoietic recapitulation but require at least 7 times the cell numbers compared to CD90+CD45RA- cells, which correlates to only 1 in 4 MPPs having this ability (Majeti et al., 2007). However, this begs the question as to how we define these various populations and whether we should base subpopulations on functional capabilities rather than by surface marker expression. It appears that over time, what was once considered a short-term HSC with 1 month reconstitution ability is now widely considered to be an MPP, while the ST-HSC population now resides closer functionally to LT-HSCs, but are just lacking CD90 expression and the ability to produce other CD90+ cells. Stemcell Technologies considers long-term Lin-CD34+CD38-CD45RA-CD90+CD49f+ cells as 'true' HSCs and Lin-CD34+CD38-CD45RA-CD90-CD49f- cells as MPPs (Stemcell Technologies, 2025). As displayed in **Figure1** this is the definition that shall be adhered to heron unless additional refinement is specified, with the abbreviation MPP encompassing MPP 2-4 – those without long-term reconstitution and inability to enter quiescence - while multipotent stem cells/MMP1 encompasses both I-HSCs and ST-HSCs as they all have the same reconstitution properties, ability to enter quiescence, and are indistinguishable using the markers described. To avoid confusion with MSCs (mesenchymal stem/stromal cells), multipotent stem cells/MPP1 shall instead be referred to as ST-HSCs from here on. The entire CD34+CD38- population will be referred to as HSPCs to reflect the mixed population, and Lin-CD34+CD38-CD45RA- cells as HSCs as it encompasses LT-HSCs, I-HSCs, ST-HSCs, and MPP1-4. Lin-CD34+CD38-CD45RA+ are lymphoid progenitor cells (LPC). Lastly, CD34+ will be used to describe the CD34+ mononuclear BM haematopoietic cells population.

In terms of population breakdown, the cell source is critical. For example, Majeti *et al.'s* 2007 study showed that within the Lin-CD34+CD38- HSPC population, for bone marrow, 30.3±18.9% were LT-HSCs, 37.7±14.1% ST-HSCs/MPPs and 24.7±11.8% LPC, whereas in cord blood, this is 25.2±10.3% LT-HSCs, 49.8±11.4% ST-HSCs/MPPs and 18.4±8.4% LPC (Majeti et al., 2007). While we can't know for certain, animal and computer models have enabled us to gather approximations of the number of HSCs present in the body and the rate

with which they expand and/or self-renew. However, these Figures have been highly variable over the years. Caitlin *et al*. suggested in 2002 that the number of HSCs per animal is conserved in mammals at around 10000, and then in 2011 suggested a replication rate of once every 40 (25-50) weeks and an adult population around 11000, with around 1000 actively involved in haematopoiesis (Abkowitz et al., 2002; Catlin et al., 2011).

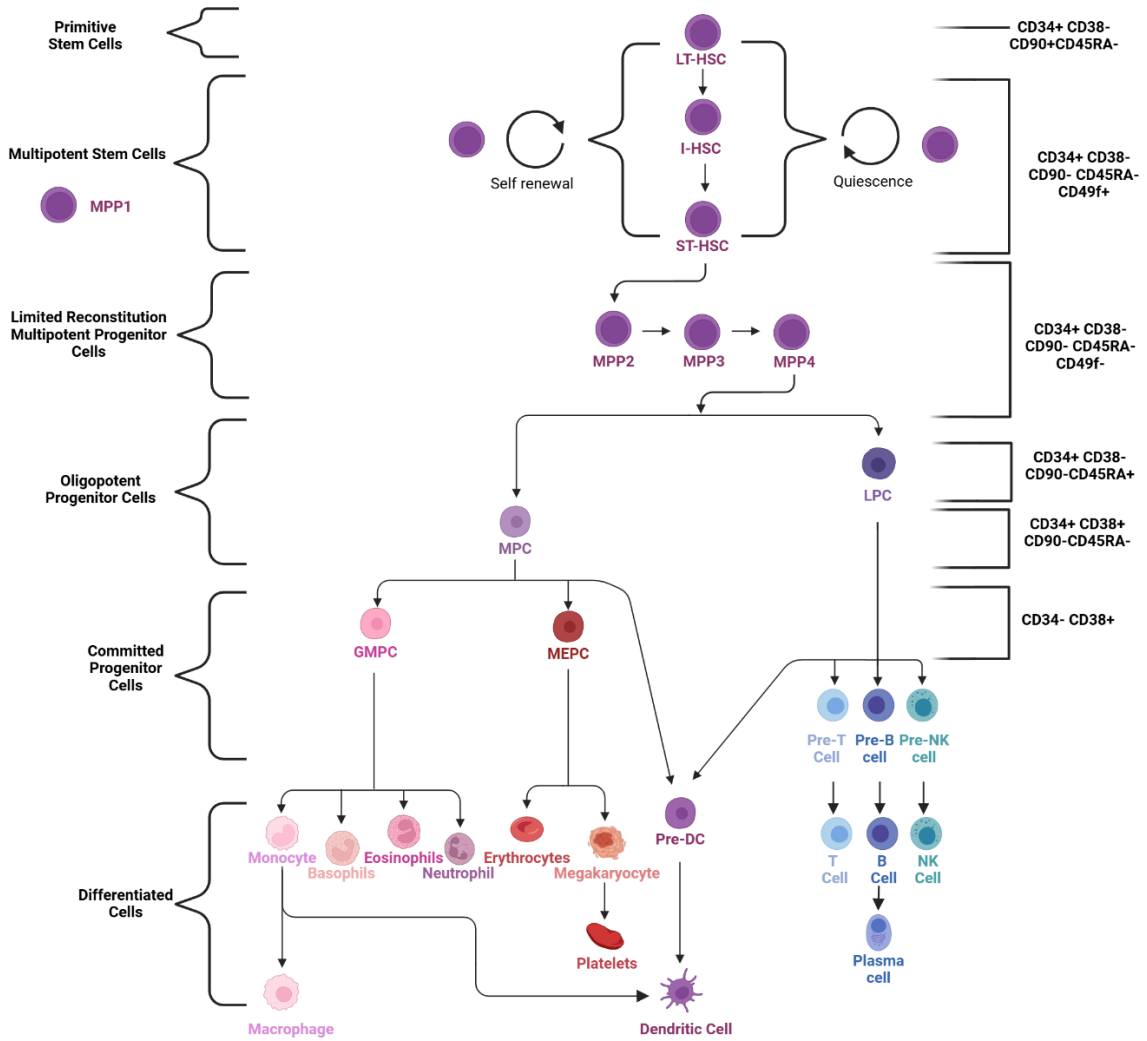

Figure 1. Differentiation pathway of HSCs. LT-HSC Long-term HSC, I-HSC intermediate HSC, ST-HSC short-term HSC, MPC Myeloid progenitor cell, LPC Lymphoid progenitor cell, GMPC Granulocyte/Macrophage progenitor cell, MEPC Megakaryocyte/Erythroid progenitor cell, Pre-DC Pre-dendritic cell, Pre-NK Pre-natural killer cell.
Created on Biorender.com.

With the study of a 59-year-old man in 2018, Lee-Nix *et al.* estimate a number of HSCs actively involved in cell production to be between 50,000 and 200,000 (Lee-Six et al., 2018).And finally, in 2023, Boyle *et al.* estimate the number of cell divisions of primitive HSCs to be around 56 times over an 85-year lifespan, with half of those divisions occurring within the first 24 years(Boyle et al., 2023).

Considering CD34+ cell numbers in bone marrow of ~$1.4x10^6$ cells kg^{-1} and one human having around 3 kg of marrow in their entire body, then one person has roughly $4x10^6$ cells kg^{-1} CD34+ BM cells (Kasow et al., 2007; Nombela-Arrieta & Manz, 2017). It is no surprise, then, that when trying to purchase BM-HSCs or BM-CD34+ cells, they are at least £1000-£2000 for $1x10^6$ cells (Lonza Bioscience, 2025). This makes them a very expensive cell type to use in either a clinical setting or a research one. Prices of £1000 for 1 million cells for research purposes are unsustainable to all but incredibly well-funded laboratories or those that can access donations from hospitals.
In addition, HSCs are renowned for being poorly suited to culture under traditional 2D cell-culture methods due to LT-HSCs' previously mentioned limited proliferative capabilities. This results in senescence, differentiation, loss of differentiation capacity and dilution of this population when cultured *in vitro* (Bowman & Zon, 2009; Kumar & Geiger, 2017).
With clinically relevant numbers of HSPCs in limited supply, various *in vitro* HSPC expansion methods have been developed, but so far with limited success. Initial efforts used a cocktail of some HSC regulatory cytokines and transitioned into specific HSPC expansion media (Costa et al., 2018; Qiu et al., 2004; Sei et al., 2019). This then transitioned to more complex modelling systems to be covered in **section 1.4**, but these methods of increasing complexity bring their own inherent costs, making us no closer to a cost-effective way of accessing HSCs.

1.1.2.1 Relevance of HSCs

As the most primitive form of all cells, the body has no way of repopulating a depleted stem cell population, whether this be due to disease, side effects of medications or naturally through ageing. Further, the limited full-scale recapitulative ability of the native LT-HSC pool means blood cell depletion due to disease would take a long time to recover, if at all. This is why depleting the

population is avoided, or if unavoidable, treated with an SCT. While the most implemented use of HSCs in a clinical environment is widely as a marrow transplant, in recent years, it is actually a transplant of HSPCs – a haematopoietic stem cell transplant (HSCT) (Khaddour et al., 2023). In fact, mobilising HSPCs into the peripheral blood (PB-HSPCs) and using granulocyte-colony stimulating factor (g-CSF) to collect has made HSPC harvesting far less invasive than BM-HSC harvesting, and is now more prevalent (Bolan et al., 2001). The purpose of HSCT is for implanted cells to repopulate the bone marrow after disease or treatments like chemotherapy deplete the original host population (Lee & Hong, 2020). As a result, the implanted population must have full BM recapitulation capabilities, and so samples are enriched purely for the CD34+ cells (Morgan et al., 2017). This is because while LT-HSCs are required for long-term recovery, immediate recapitulation is thanks to more mature, proliferative CD34+ progenitors (Cheng et al., 2020). Therefore, a mixture of all HSPCs must be present in the sample. The number of cells required for HSCT is determined by body mass, typically in the range of 2 to $10x10^6$ cells kg^{-1} (Erdal et al., 2023). However, as previously stated, clinically relevant numbers of HSCs are not easily accessible, and further, to be used for HSCT, they must be a human leukocyte antigen (HLA) match to the patient (Gragert et al., 2014).

HSCT can be autologous (use the patient's own cells) or allogenic (using cells donated by another) (Aljagthmi & Abdel-Aziz, 2025; Khaddour et al., 2023). The advantage of autologous transplants is that they lack the risk of donor compatibility; however, while a useful option before a treatment that will deplete the marrow population, like chemotherapy, it is not a viable option for those with already diseased marrow cells, other illnesses or the elderly who have already depleted marrow (Al Hamed et al., 2019).
Allogenic cells come from healthy donors; however, to minimise the risk of rejection, donor compatibility is determined in the following order: HLA-matched and related donor, HLA-matched but unrelated donor, cord blood and finally haploidentical (half HLA-matched) (Bartenstein & Deeg, 2010). It is access to cells of an appropriate HLA match that limits the availability of HSCT treatment options, as only 25% of people have an HLA-matched relative, while HLA-matched non-relative donors for ethnic minorities can fall as low as 10% (Bartenstein & Deeg, 2010). There is also a significant risk involved with non-

complete donor matches. These are most commonly graft-versus-host-disease (GVHD), resulting in rejection of the transplanted cells/tissue, organ failure and infections (Tanaka et al., 2016).

HSCs are also of great interest in research in the form of gene editing – the process of correcting, disrupting or inserting a specific segment of DNA to alter the properties and characteristics of an organism or cell (National human genome research institute, 2019). Another advancement in the area is gene editing. For HSCs, autologous transplants using cells which have had the malignant mutation corrected can be carried out. For example, a 32-base pair deletion in the CCR5 gene has been shown to result in resistance to 5-tropic human immunodeficiency virus (HIV-1) infection (DiGiusto et al., 2016). While gene correction of the sickle cell disease mutation in CD34+ cells could yield an effective treatment and restore 'normal' functionality (Hoban et al., 2015). However, in 2014, confirmed by various studies including the above, it appears that gene correction is more efficient within less primitive sub-populations, suggesting different approaches are required if aiming for full recapitulation with the edited lineage (Genovese et al., 2014).

1.2 The bone marrow niche microenvironment and its regulation of stem cell behaviour

Stem cells populate certain locales. The one most relevant to this work is known as the bone marrow niche microenvironment (**Figure 2)**. The niche is in red bone marrow - a semi-solid tissue located in trabecular or 'spongy' bone -and is home to a variety of cell types (Morrison & Scadden, 2014). Specifically, MSCs and HSCs reside here in close proximity, along with their progeny. There are also two distinct regions within the marrow – with a gradient between them – that exhibit differences in stiffness and oxygen concentration and cell, ECM protein and cytokine composition. These are known as the endosteal niche – the outer region of the marrow closest to the bone - and the perivascular niche – areas surrounding blood vessels (Braham et al., 2018; Nombela-Arrieta et al., 2013; Tormin et al., 2011). In fact, it's close to the vasculature within the endosteal region where quiescent HSCs are believed to reside, with a combination of features controlling their behaviour and maintaining each subpopulation. Specifically, Itkin *et al.* reported that the arterial vessels support quiescent

HSCs while sinusoidal vessels activate HSPCs and are responsible for trafficking to and from the marrow (Itkin et al., 2016).

1.2.1 Cellular composition of BM and their extracellular profiles

The cellular component of the BM mostly comprises the progenitor cells of HSCs and MSCs, like OBs, pericytes and lymphocytes. They primarily interact through short-distance cytokine signalling, with long-distance signalling typically coming from farther afield in response to things like injury (Bentley, 1981; Rebar, 1993). The most widely reported cytokines associated with HSC regulation are displayed in **Table 1.**

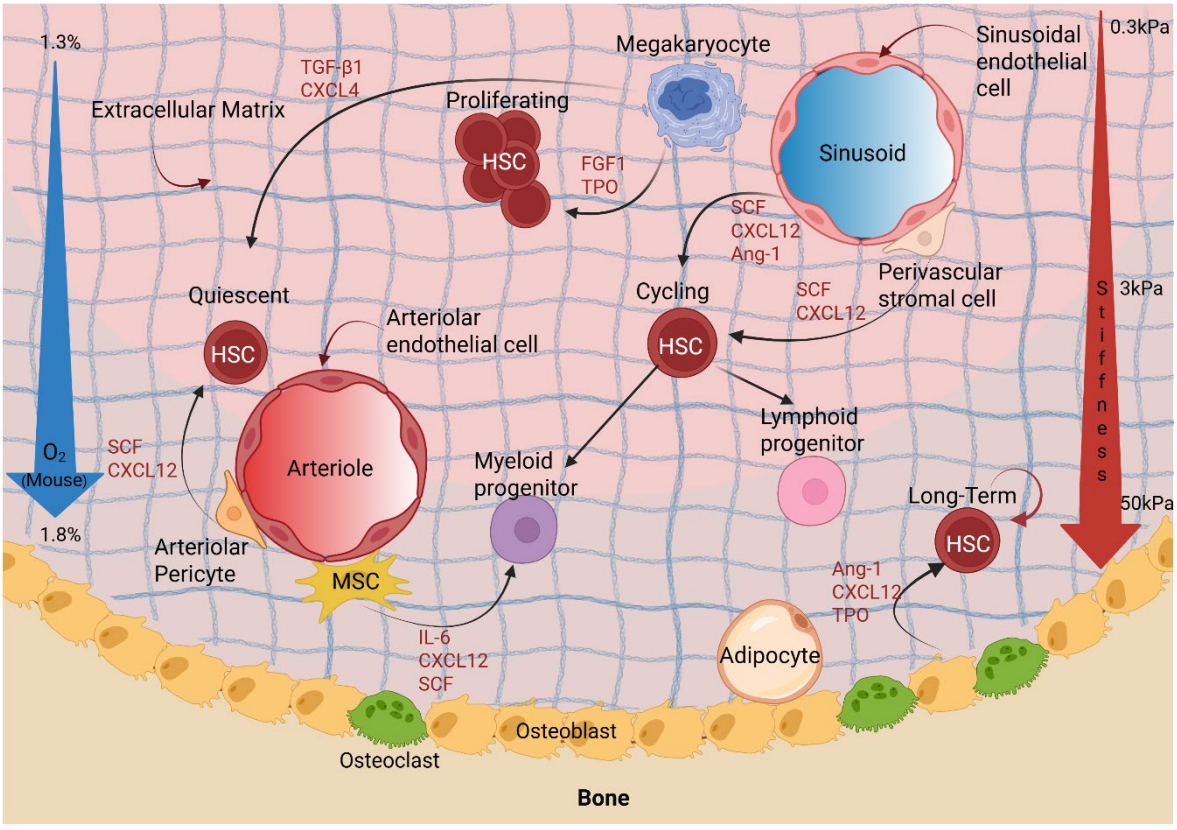

Figure 2. Schematic of the bone marrow niche microenvironment demonstrating the locations of HSC populations and their regulatory components within the niche. Created on Biorender.com.

Table 1. Summary of the commonly documented extracellular molecules within the BM niche, their source, and their purpose regarding HSC maintenance.

Molecule	Source(s)	Purpose for HSCs
THPO	OBs, MSCs(Yoshihara et al., 2007).	Regulation of HSC quiescence (Yoshihara et al., 2007).
Ang-1	OBs, MSCs(Arai et al., 2004; Chen et al., 2021).	Induces HSC adhesion to bone, increases quiescence (Arai et al., 2004).
SCF	ECs (Ding et al., 2012), Perivascular cells (Ding et al., 2012), Osteoprogenitors (Shah et al., 2017) MSCS (Waskow, 2019).	Regulation, migration, differentiation, prevents apoptosis and in and induces cell cycle entry of HSCs (Broudy, 1997; Domen & Weissman, 2000; Shah et al., 2017)
SDF-1/CXCL12	Pericytes, OBs,(Jung et al., 2006), BM MSCs(Schajnovitz et al., 2011).	Homing of MSCs and HSCs to the bone marrow, HSC maintenance by regulating cell cycling (Ding et al., 2012).
IL-6	Macrophages, fibroblasts, T cells, and MSCs (O'Shea et al., 2019).	Directs HSC production of progenitors and the myeloid lineage commitment of them (Mirantes et al., 2014).
IL-3	T Cells, Macrophages (O'Shea et al., 2019).	Promotes haematopoietic progenitor cell growth (O'Shea et al., 2019).
Flt-3	ECs, fibroblasts, Myeloid cells (Stirewalt & Radich, 2003).	Promotes HSPC proliferation and CFU development (Stirewalt & Radich, 2003).

1.2.1.1 Cell types in the bone marrow

Osteoblasts.

Osteoblasts (OBs) line the endosteal region of the marrow where LT-HSCs reside, although they are not frequently in direct contact (Malara et al., 2014; Nombela-Arrieta et al., 2013). Animal research has shown that the reduction of OB numbers in transgenic mice results in a substantial decrease in haematopoietic progenitor cells (HPCs) (Visnjic et al., 2004). This is due to OBs secreting numerous HSC regulatory cytokines thrombopoietin (THPO), angiopoietin (Ang-1), SCF, Osteopontin (Opn) and C-X-C motif chemokine ligand12 (CXCL12) (Arai et al., 2004; Jung et al., 2006; Yoshihara et al., 2007). Further, immature OBs with high RUNX2 expression have been shown to promote HSC expansion (Chitteti et al., 2013). As a result, OBs are considered integral for maintaining the LT-HSC population.

Megakaryocytes.

Megakaryocytes (MKs) are responsible for platelet production and express extracellular matrix components FN, laminin (LM) and collagen (Malara et al., 2014). They are also integral to directing HSPC behaviour. By expressing C-X-C motif chemokine ligand (CXCL4), MKs can regulate HSC cell cycle activity and induce a quiescent state (Bruns et al., 2014). They also secrete Ang-1, stimulate osteoblast proliferation and secrete IGF-1, which induces HSC proliferation (Heazlewood et al., 2013; Zhou et al., 2015).

Endothelial cells.

ECs line the blood vessels and come in two forms in the BM. HSCs reside in direct contact with vasculature within the endosteal region of the marrow (Nombela-Arrieta et al., 2013). Sinusoidal endothelial cells (SECs) experience higher levels of ROS and secrete CXCL12 (Maan et al., 2020). Arteriolar endothelial cells (AECs) have been demonstrated as the core supplier of SCF in the marrow (Xu et al., 2018). AEC SCF is expressed to maintain HSCs, as well as for expansion as part of development. While deletion of SCF expression in AECs results in depleted HSC numbers (Ding et al., 2012). AECs also express netrin-1, which maintains quiescence and self-renewal in HSCs (Renders et al., 2021).

MSCs.

MSCs are found in various forms and sub-populations throughout the body. In BM,

collectively these sub-populations secrete nearly all the critical HSC-maintaining cytokines (CXCL12, SCF, Ang-1, THPO, Opn, IL-6), albeit not necessarily the primary source (Fereydani et al., 2024). Therefore, the specific subpopulations have differing roles in the haematopoietic pathway.

CD146+ MSCs have displayed trilineage capacity, reside closely to HSCs in the niche, and their expression of key HSC-maintaining cytokines means their addition in long-term culture (LTC) assays resulted in increased colony formation over 8 weeks compared to conventional assays (Sacchetti et al., 2007; Sorrentino et al., 2008). Nestin+ MSCs have been shown to promote HSC quiescence and express SCF and CXCL12 (Kunisaki et al., 2013). CD271+ and CD271+/CD146low MSCs line bone and are located in direct contact with and maintain quiescent HSCs, while CD271+/CD146+ MSCs are perivascular and maintain the proliferative HSC population (Fonseca et al., 2023; Tormin et al., 2011).

Perivascular Stromal Cells/Pericytes.

Cells that reside in the perivascular region of the marrow share largely the same properties and surface markers as BM-MSCs, and in the past have been considered the same cells (Mizuno et al., 2018; Sá da Bandeira et al., 2017). However, pericytes are a cell type distinct from MSCs, typically further split into CXCL12-abundant reticular (CAR), leptin receptor+ (LepR+) and nestin+ (Nes+) cells (De Souza et al., 2016).

Defined by uncharacteristically high expression of CXCL12, CAR cells also express high levels of SCF and possess adipogenic and osteogenic differentiation capability (Aoki et al., 2021; Sugiyama et al., 2006). In accordance with this, short-term ablation of CAR cells in mice impairs adipogenic and osteogenic differentiation potential of marrow cells, secretion of SCF and CXCL12 and resultant HSC health (Omatsu et al., 2010). Interestingly, leptin receptor-expressing CAR cells are the sub-population with the greatest CXCL12 and SCF expression and differentiation capacity (Aoki et al., 2021).

There is obviously an overlap between CAR and LepR+ cells, and therefore, the properties are also similar. LepR+ cells express Ang-1, SCF and CXCL12, and knockout variants of LepR+ cells impair HSC maintenance (Ding et al., 2012; Ding & Morrison, 2013). They can differentiate osteogenically and adipogenically and induce differentiation of both lineages in other stromal cells (Gao et al., 2023).

Nes+ cells are rare – occupying~0.002% of BM cells – but associate closely with HSCs along arterioles and modulate HSC behaviour (Kunisaki et al., 2013). They exist in a largely quiescent state, much like the HSCs alongside them; however, they possess far greater CFU potential compared to Nes-. They share features with other pericytes with multilineage differentiation capacity and high expression of CXCL12 and SCF.

Adipocytes.

Development of 'fatty marrow' is a reversible process which occurs with age and results in adipocytes establishing themselves within the red bone marrow. It was initially shown that adipocytes inhibit haematopoiesis, and their presence within the marrow correlates with decreased levels of HPCs (Naveiras et al., 2009). However, over time, a greater understanding of the heterogeneity of adipogenic populations has resulted in findings which indicate positive affiliations to a healthy haematopoietic system (Tratwal et al., 2021). It is now believed that while adipogenic progenitors and adipocytes cannot maintain haematopoiesis, indicated by adipocyte-rich BM having reduced numbers of ST-HSCs and HPCs, it does instead contain fully functional, CFU-capable LT-HSCs, indicating adipocytes can maintain this long-term population (Wilson et al., 2018; Zhu et al., 2013; Zinngrebe et al., 2020). This is only logical, as adipocytes are known to secrete many HSC-regulating cytokines, such as CXCL12, IL-6, SCF (Coppack, 2001; Kim et al., 2014; Zhou et al., 2017).

1.2.1.2 Cytokines

Ang-1 and its receptor Tie2.

Ang-1 induces HSCs' quiescence, protecting the cells from stress and apoptosis and preserving their long-term recapitulative potential (Arai et al., 2004). In fact, Tie2 – the receptor for Ang-1 –is uniquely expressed in the subpopulation of HSCs, which are quiescent and adhere to osteoblasts in the niche. However, this process is highly sensitive. Over-saturation with Ang-1 will impair the bone marrow and lead to HSC senescence (Sim et al., 2021).

CXCL12 and its receptor CXCR4.

The fact that BM-HSCs were discovered in contact with cells highly expressing CXCL12, also known as stromal-derived factor 1 (SDF-1), resulted in the CXCL12-abundant reticular cell type being coined (Sugiyama et al., 2006). Deletion of the CXCL12 receptor (CXCR4) resulted in release and subsequent loss of HSCs

into the cell cycle (Sugiyama et al., 2006). In contrast, the addition of CXCL12 into HSC culture inhibits entry into the cell cycle and therefore maintains the quiescent state in LT-HSC (Nie et al., 2008). It also enhances the engraftment of cells with recapitulative capability, and it is critical for the homing of stem cells to the bone marrow (Broxmeyer et al., 2003; Jung et al., 2006; Xiao Ling et al., 2016).

IL-3 and 6.

Aged BM is a more inflammatory environment, and therefore, the concentrations of inflammatory cytokines are higher (Jahandideh et al., 2020). The result of this is increased proliferation and differentiation of HSPCs (King & Goodell, 2011). Secreted by cells such as macrophages, T cells and mast cells, IL-3 directs the proliferation and differentiation of HSPCs and mobilises quiescent HSCs (Nitsche et al., 2003). While IL-3-supplemented cytokine media displays enhanced proliferation (Bryder & Jacobsen, 2000). Similarly, IL-6 is secreted by a variety of cells, such as macrophages, ECs and fibroblasts, and is upregulated 105-fold during inflammation (Akira et al., 1993; Damas et al., 1992). However, the same data suggest IL-6 will inhibit erythroid progenitor activity and yet, through CCAAT/enhancer binding protein alpha (CEBPα) suppression, can increase HSC self-renewal and proliferative ability (Schürch et al., 2014; Valletta et al., 2020; Zhang et al., 2004).

Opn.

Opn is produced in the niche by osteoblasts and can direct the migration of HSCs towards the endosteal region, and can suppress HSC proliferation (Nilsson et al., 2005; Stier et al., 2005). Opn is therefore critical for stem cell pool size maintenance; however, aged BM sees a reduction in Opn expression, and therefore less control (Guidi et al., 2017). This is observable with Opn knock-out HSPCs unable to reconstitute BM, and Opn-deficient marrow results in peripheral blood containing increased lymphocytes and decreased erythrocytes (Li et al., 2018).

SCF and its receptor c-KIT

SCFs' primary functions are to mobilise HSPCs from BM into the blood, encourage cell cycle entry and increase both short and long-term recapitulative ability of the circulating population (Broudy, 1997; Mcniece et al., 1994; Yan et al., 1994, 1995). It has long been deemed critical for HSC culture, as it is responsible for

the activation of otherwise inactive progenitors (Bernstein et al., 1991). Although some conflicting information does exist, for example, a dose of SCF prior to lethal irradiation dose results in >80% survival, supposedly due to HSCs entering a state of radioprotective quiescence (Zsebo et al., 1992). The SCF receptor c-KIT is also expressed at different levels to enable subpopulations of LT-HSCs to be distinguished. Quiescent HSCs that are highly proliferative when transplanted possess intermediate levels of c-KIT, whereas high c-KIT expression describes a population with limited expansion capability and no long-term recapitulative ability upon transplantation (Grinenko et al., 2014).

THPO and its receptor, MPL.

Zhang *et al*. analysed the expression of 20,475 different genes in LT-HSCs, HSPCs, MPPs and their progenies (Y. H. Zhang et al., 2018). They showed that LT-HSCs express much greater levels of myeloproliferative leukaemia protein (MPL) (the receptor for THPO) compared to HSPCs, MPPCs, monocytes, neutrophils, erythrocytes and NK, T, and B cells. Therefore, MPL could be used as a marker of LT-HSCs. THPO is critical for HSC maintenance by regulating the cell cycle, and while MPL is found on quiescent HSCs, there is conflicting evidence as to whether its role is to maintain quiescence or to induce self-renewal and expansion (De Graaf and Metcalf, 2011) (Fox et al., 2002; Yoshihara et al., 2007; de Graaf et al., 2010). Therefore, it is likely that time, concentration, synergy with other cytokines or a mixture of all three that allows THPO to have such wide control over HSC fate. Further, THPO induces angiogenesis, indicating it enhances Tie2 expression and resultant adherence to osteoblasts (Arai et al., 2004; Lamanuzzi et al., 2021). THPO also influences HSCs indirectly by stimulating megakaryocytic proliferation and maturation, and lineage commitment of HSCs (Kaushansky, 2009).

In contrast to the commonly held belief, there is evidence to suggest the primary source of THPO in BM is extrinsic. The primary source of circulating THPO is produced by liver hepatocytes, and the expression is more than double that of osteoblasts and LepR+ cells (Decker et al., 2018). It was found that this circulating form has greater regulatory behaviour over HSCs than any other. Links between the liver and haematopoietic system are established, as a common complication of liver damage is thrombocytopenia (Lim & Cuker, 2022). Defined by reduced platelet numbers, thrombocytopenia in this case is caused by the

reduction of THPO expression, subsequent reduced megakaryocyte proliferation and maturation, and therefore a reduction in platelet production. This extends to BM, as research shows that the lack of resilience to injury and infection in those with thrombocytopenia is due to severely compromised BM-HSCs (De Graaf & Metcalf, 2011; Nautiyal et al., 2024).

FLT-3 and its receptor, FLT-3R.

In healthy bone marrow, FMS-like tyrosine kinase 3 ligand (FLT-3) is expressed on HSPCs but is lost upon commitment to B cells, T cells, megakaryocytes or erythrocytes (Karsunky et al., 2003; Rosnet et al., 1996). However, mutation of the Flt-3 gene is found in ~30% of acute myeloid leukaemia (AML) cases, making it one of the most common and has one of the worst prognoses (Stirewalt & Radich, 2003). In fact, the receptor is found on most leukemic cell lines.(Anne Turner et al., n.d.) Expression of FLT-3L is widespread in mature haematopoietic lineage cells such as myeloid, B and T cells, as well as in endothelial cells and fibroblasts (Quentmeier et al., 2003; Solanilla et al., 2000; Wodnar-Filipowicz, 2003). While it's agreed that FLT-3L is critical for HSPC growth, this is only when used synergistically with other cytokines; studies have shown that FLT-3L does little on its own (Banu et al., 1999; Brashem-Stein et al., 1996; Broxmeyer et al., 1995). It’s believed that FLT-3L induces the mobilisation of HSPCs and their subsequent expansion and differentiation. For example, one study found that FLT-3L-deficient mice have a 10-fold decrease in CLPs and subsequently B and T cell levels, while common myeloid progenitor (CMP) and HSC levels are unaffected (Sitnicka et al., 2002). Though a different study saw reductions in both CMPs and CLPs (McKenna et al., 2000).

1.2.1.3 EVs

First thought as waste carriers, it is now well documented that extracellular vesicles (EVs) are secreted by nearly all types of cells (Johnstone et al., 1987; Van Niel et al., 2018). Separated into two populations based roughly on size - exosomes (30-150nm) or microvesicles (50-1000nm) - EVS contain many of the components of their parent cell, such as nucleic acids and proteins (Batsali et al., 2020; Zhou et al., 2020). As a result, EVs are an integral part of the intercellular signalling system: acting as stable carriers of biological messages throughout most, if not all, physiological processes (Simeone et al., 2020). Subsequently, research into the use of EVs in targeted drug delivery and

diagnostics has accelerated in recent years (Butler et al., 2018; Kumar et al., 2024).

1.2.2 The ECM

The extracellular matrix (ECM) is a three-dimensional network that is secreted, remodelled, and adhered to by the cells that reside there, dictating the physical properties of a tissue and acting as a reservoir for proteins and cytokines (Frantz et al., 2010). This relationship is symbiotic, and the ECM exerts influence over the residing cells. The ECM can be broken down into two areas: the interstitial matrix is the overarching structural component of the network, while the pericellular matrix, specifically the basement membrane, is directly adjacent to cells (Bandzerewicz & Gadomska-Gajadhur, 2022). Inspired by these two regions, the wider physical cell environment, such as substrate stiffness, or local environment like surface topography, can be used to direct cell behaviour *in vitro*. Increasing surface stiffness can direct differentiation of MSCs into neurons, adipocytes, chondrocytes, myocytes, and osteoblasts, while grooved surfaces can improve nerve regeneration of Schwann cells (Lv et al., 2017; Scaccini et al., 2021). Similarly, localised biological interactions have been mimicked *in vitro*. Growth factors bound to the ECM are released in a controlled fashion during remodelling, something replicated using hydrogels for use in cell models (Bandzerewicz & Gadomska-Gajadhur, 2022; Wang et al., 2019).

1.2.2.1 Stiffness

Unlike most other tissues and organs, the bone marrow varies in stiffness over a comparatively large range. The endosteal region close to the bone has a stiffness of 40-50 kPa, the perivascular niche is around 3 kPa, and the central region is 0.3 kPa (Zhang et al., 2019). This is unlike other soft organs, which range from 5-10 kPa (Kidney), 20-40 kPa (Intestine) or 0.5-1 kPa (Fat) (Handorf et al., 2015). An *in vitro* study showed HSCs undergo increased migration on stiffer gels (40-100 kPa) than softer ones (<40 kPa), indicating a preference for the endosteal niche (Lee-Thedieck et al., 2012). In agreement, stiffer 2D and 3D gels (35 kPa) have also been shown to preserve LT-HSCs better than softer ones (2 and 8 kPa) (Shi et al., 2024).

1.2.2.2 Fibrous Proteins

The interstitial ECM comprises two structural components: proteoglycans and fibrous proteins (Frantz et al., 2010). Proteoglycans are the bulk component,

forming a hydrated gel-like material in which fibrous proteins are embedded (Alberts et al., 2002). However, it is the fibrous proteins which have material characteristics, the main ones of which are: collagen, elastin and FN (Frantz et al., 2010). The collagens are a family of proteins, the most prevalent being type I, II, III, V and XI. They are the most abundant protein in mammals, and their fibrils are woven in a variety of ways depending on the tissue in which they reside to resist tensile forces. For example, in tendons, they align parallel, whereas in skin, they form a mesh to withstand forces on any axis (Alberts et al., 2002; Fratzl, 2008). Most ECM proteins also exist in a non-fibrillar form, which inhabit the pericellular matrix. Collagen type IV, for example, is prevalent in the pericellular matrix surrounding chondrocytes in cartilage (Bandzerewicz & Gadomska-Gajadhur, 2022).

Elastin is the dominant protein in tissues with high elasticity, such as skin. It is approximately one thousand times more flexible than collagen, and to stop tissues from tearing, the fibres of the two are interwoven (Alberts et al., 2002; Kristensen & Karsdal, 2016).

As a new ECM is made, FN is one of the first proteins assembled. This is because FN fibrils initiate the assembly of and integrate with other ECM proteins, such as collagen. FN also has RGD binding domains, which make it crucial for cell interaction with the pericellular ECM through integrins (Alberts et al., 2002; Dallas et al., 2006).

1.2.2.3 Oxygen gradient

The bone marrow is a hypoxic environment; however, there is a gradient of oxygen (**Figure 2)**. The lowest oxygen concentration is found in the deep sinusoidal region >40μm from bone; however, as a soft environment, this is not suitable for HSC residence (Xiao et al., 2022). Spencer *et.al.* demonstrated that in mice, the local oxygen tension in the endosteal perivascular region is roughly 1.8% and 1.3% in deeper sinusoidal regions (Spencer et al., 2014). Therefore, the oxygen gradient within the bone marrow corresponds to areas of stiffness, and the literature for humans agrees; the endosteal region possesses a low oxygen concentration, high stiffness, and is home to the quiescent HSC population, while the proliferative population is found in the highly vascularized and soft perivascular niche (Mohyeldin et al., 2010; Nombela-Arrieta et al., 2013; Tormin et al., 2011).

It is well reported that stem cells (and others) respond to hypoxia with enhanced self-renewal and long-term survival capabilities. The ability of cells to respond to hypoxia is mediated via hypoxia-inducible factors (HIFs). HIF1-α inhibition results in HSC activation, while HIF-1 stabilisation stimulates anaerobic glycolysis (Wielockx et al., 2019). MSCs also respond to hypoxic environments, and distinct subpopulations exist. For example, Tormin *et al*. demonstrated a CD271+ CD146-/low population of MSCs residing in the endosteal region and supported quiescent HSCs, whereas the CD271+ CD146+ population were found in the perivascular region near a proliferative HSC population (Mohyeldin et al., 2010; Tormin et al., 2011).

1.3 Bone marrow diseases

Diseases of the bone marrow are haematopoietic disorders. While the initial malignancy often arises in an immature population, the symptoms become apparent when such a malignancy is maintained in the progeny cell population, or the progeny themselves are the disease and symptom-defining cells (Testa, 2010). Emergence over the last 25 years of age-related haematological disorders is of great interest. Where an increase in lifespan has seen limitations to haematopoiesis become evident, with reduced haematopoietic function and regenerative capabilities in the elderly because of replicative senescence, and therefore insufficient numbers of progeny cell types leading to diseases like anaemia, or malignant genetic mutations leading to cancers (Dong et al., 2020; Lee & Hong, 2020; Zhang et al., 2023). Further, the medications used to treat diseases, such as chemotherapies, are often responsible for off-target effects, resulting in widespread *in vivo* damage. This is particularly prevalent within the bone marrow, potentially causing secondary cancer growths (Jaiswal et al., 2014). It is in the grounds of marrow diseases that drives the need for readily available stem cells for HSCT to treat bone marrow disorders, as well as for use in testing to devise treatments which do not have detrimental effects on the bone marrow cell population.

1.3.1 Leukaemia

Leukaemia is a disease that encompasses cancers of blood cells, and while treatments for leukaemia's are seemingly increasingly effective, there remains a high chance of relapse in both adults and children (Fielding et al., 2007; Lee & Hong, 2020; Oriol et al., 2010; Rheingold et al., 2024). The prognosis and chance

of relapse are influenced by numerous factors such as age and type of cancer; however, the prognosis of relapsed leukaemia in both adults and children is still dismal (Fielding et al., 2007; Oriol et al., 2010; Rheingold et al., 2024). After treatment, assessing the measurable residual disease (MRD) determines if malignant cells are left. While relapse can occur in patients without MRD, there is a correlation between MRD and relapse (Khaldoyanidi et al., 2022; Kruse et al., 2020).

It is of recent discovery that often MRD, relapse, and the cancer as a whole are often due to what is known as a leukemic stem cell (LSC). First discovered in 1999, LSCs are not necessarily stem cells that have mutated but cells which have mutated to gain characteristically stem cell-like functionalities such as quiescence, self-renewal, multipotent differentiation, and expansion capabilities (Holyoake et al., 2001; Khaldoyanidi et al., 2022; Testa, 2010). Due to these characteristics, drugs targeting highly proliferative cells – the hallmark sign of cancers and focus of treatments - do not target LSCs, and as a result, drug and clinical trials are focusing on targeting LSCs specifically, even if their quiescence makes them poor at taking up drugs (Khaldoyanidi et al., 2022).

1.3.2 CHIP

Gene mutations within the haematopoietic system result in diseases such as anaemia and leukaemia (Stieglitz & Loh, 2013; National Centre for Biotechnology Information (US), 1998). Clonal haematopoiesis of indeterminate potential (CHIP) occurs when a cell develops a gene mutation that results in unregulated proliferation and dilution of the healthy cell population (Steensma et al., 2015). Age-related gene mutation accumulation is a normal process; 10-20% of people over 70 have CHIP clones within their haematopoietic system (Jaiswal & Ebert, 2019; King et al., 2019; Winter et al., 2024). That being said, having CHIP clones does not guarantee CH, and CHIP mutations can also be caused by additional factors like obesity or exposure to toxic chemicals through smoking or chemotherapy (King et al., 2019; Weeks & Ebert, 2023). While CHIP mutations do not guarantee illness, they are strongly associated with increased risk of hematologic cancer, all-cause mortality (dying of any disease), coronary heart disease and ischemic stroke (Jaiswal et al., 2014).

1.3.3 Off-target effects

As LSCs and CHIP were identified, it became apparent that the gene mutations were sometimes a result of off-target effects of widely used medications and treatments. Chemotherapies are the go-to treatment for most solid-tumour cancers by targeting proliferating cells rapidly (Nygren, 2001). They are highly toxic and have a range of side effects (van den Boogaard et al., 2022). Over time, we have learned that the side effects are a result of not just short-term DNA damage, but long-term damage as well (Sjöberg et al., 2023; van den Boogaard et al., 2022). For example, approved in 1978 and 1983 respectively, Cisplatin and Etoposide have been used widely ever since as treatments for numerous cancers such as brain, lung and testicular (Dasari & Bernard Tchounwou, 2014; Reyhanoglu & Tadi, 2023). However, both have also been directly linked to secondary leukaemia, and cisplatin causes anaemia, likely due to genetic damage to HSCs (Brenez et al., 1990; American Society of Health-System Pharmacists, 2024; Ezoe, 2012; Wood & Hrushesky, 1995).

1.4 Engineered models

When it comes to scientific research and product testing, there is an ever-growing emphasis on the 3Rs:

Replace: substitute sentient beings with non-sentient alternatives wherever possible.

Reduce: If animal use is unavoidable, the number used to obtain the required information must be kept to a minimum.

Refine: Those animals being used must be treated in the most human way possible (Hubrecht & Carter, 2019).

First put forward in 1959 by Russell and Burch of the Universities Federation for Animal Welfare (UFAW), the original emphasis was catered more towards issues long since rectified (Russell, 1959). Issues such as achieving ‘reduction’ by reducing environmental variables or disease, now catered more towards efficient experimental design, or ‘replacement’ of sentient beings with lesser forms such as mammals for fish, rather than using non-sentient materials. While the 3Rs were formed from an animal welfare perspective, the arguments for moving away from the ‘gold standard’ of animal models are supported scientifically. Results from animals are not fully translatable to humans, hence the need for human trials post animal testing. Large numbers of products see no ill effect in animals but are still unsuccessful in humans; of the 90% of drugs that fail during

clinical trials, 50% of these are due to safety or efficacy (Dowden & Munro, 2019; Takebe et al., 2018; Van Norman, 2019). As a result, *in vitro* human models are deemed the next advancement in product testing as a complementary study to animal testing, or maybe one day as a full replacement. This concept became United States law in December 2022 as part of the FDA modernisation act 2.0, which recognised alternative testing options that can be used to justify the safety of a therapeutic for human trials (Stresser et al., 2023).
With recreating a whole human body an unrealistic goal, models instead aim to mimic specific locations on a smaller scale, and in more recent times look to combine elements from established models to form more complex and physiologically comparable systems. It is in this area where medical research is being directed, specifically the treatment of cancers, where the microenvironment is so important.

1.4.1 Cell models

1.4.1.1 Pitfalls of traditional cell culture

The creation of a model must consider various *in vivo* characteristics of the desired environment, such as those covered in **1.2**, stiffness, cytokines and other cells. From a traditional approach using 2D culture ware, there are immediate pitfalls regarding comparability to *in vivo* environments. Firstly, adherent cells in culture flasks grow in a monolayer with only sideways interactions with neighbouring cells, while non-adherent cells will settle in a layer on the bottom with equally minimal cell-cell contact (Kapałczyńska et al., 2016). Secondly, polystyrene and glass are the two most common cell culture vessel materials. In comparison to human tissue, the stiffness of polystyrene (~1 GPa) and Glass (~70 GPa) is similar only to Bone (~5 GPa) and is orders of magnitude greater than that of most tissues (1-50 kPa) (Fekete et al., 2018; Handorf et al., 2015; Turner et al., 1999). This is problematic when research has shown surface stiffness can direct differentiation, cellular senescence, and various other cell behaviours (Handorf et al., 2015; Lv et al., 2017; Navarrete et al., 2017). Thirdly is that the body is a dynamic environment (with specific exceptions) with constant nutrient and oxygen exchange (Lipreri et al., 2022; Ozturk et al., 2006). Cells are highly dependent on local paracrine signalling molecules to communicate, and with a fluid environment, these signals can reach further, faster. Leading to more dynamic behaviours. They also receive signals from more distant areas of the body, from injury sites or hormones

(Rochefort et al., 2006; Xiao Ling et al., 2016; Yuan et al., 2022). Finally, the cell environment is also inhabited by numerous other cell types, all expressing their own signals, and the synergistic relationships cannot be mimicked with simple supplementation to the growth medium (Bowlin et al., 2024; Mehrasa et al., 2014).

1.4.1.2 Cell aggregates

Cellular aggregates are referred to somewhat interchangeably in wider literature as 3D cell cultures, organoids or spheroids (Simian & Bissell, 2017). However, there are distinct differences. 3D cell cultures are the umbrella term for alternative methods to traditional 2D monolayer culture, which include aggregates, but also describe scaffolds, bioreactors, microfluidics and many others (Cacciamali et al., 2022). Organoids are formed when stem or progenitor cells grown on a 3D support form complex structures partially resembling, genetically and histologically, an organ from which the cells originate. They typically contain cells of various maturities, differentiated from the original stem/progenitor parents, and can be cultured and expanded long term (Gunti et al., 2021; Simian & Bissell, 2017; Corning, n.d.).

Spheroids, on the other hand, are a simpler construct, self-assembling without structural support, and typically consisting of just one or two cell types that remain heterogeneous. They cannot be expanded or regenerated, and do not highly resemble their native tissue (Gunti et al., 2021; Simian & Bissell, 2017; Corning, n.d.). They are, however, used extensively for the study of tumour sites which are similar in their gradient of metabolic activity through the aggregate (Halfter et al., 2016; Quereda et al., 2018; Tomás-Bort et al., 2020). They are also used to temporarily maintain the properties of certain cell types, for example, MSC spheroids have been shown to enhance HSC differentiation potential and induce recovery from senescence (Frith et al., 2010; Krasnova et al., 2023).

1.4.1.3 Co-culture, feeder layers and synergistic engraftment

When combining more than one cell type into a culture, it is typically as one of two forms: feeder layers or as co-cultures.

Feeder layer cells are adherent cells that are grown underneath a non-adherent culture or in/under a 3D structural support, which have a secretory profile (either naturally occurring or through gene editing) that will support or direct

the growth of the additional cells in the culture (Llames et al., 2015). They are treated with radiation or mitomycin to prevent proliferation and therefore supply a continuous supply of the desired secretome with less frequent media changes (Ponchio et al., 2000). This is advantageous as proteins added to media will degrade and/or be taken up over time, resulting in an inconsistent concentration. It also means that for cell types like MSCs, intercellular signals are not removed from culture regularly (Fernández-Francos et al., 2021).
Feeder layers are of use because serum-free media supplementation is often expensive, and cytokines are unstable for prolonged periods of time at 37 °C. This leads to diminishing concentrations over time due to cellular uptake and cytokine degradation, and therefore, concentrations are not controlled. In comparison, a feeder layer will produce a continuous supply of cytokines into solution, which are used and replenished at a rate dependent on the number of feeder cells used. This provides much greater control compared to supplementation in media changes.
Cocultures are used to investigate the interactions between two or more cell types, either as a simple monolayer system or as part of a more complex 3D system (Goers et al., 2014; Jing et al., 2010; Levorson et al., 2014). They are also used to help improve the culturing ability of cell types like HSCs, which, when grown under traditional 2D monoculture methods, do not exhibit *in vivo* behaviours or characteristics. Co-culture also expands on the benefits of a feeder layer by considering the changeable nature of cellular uptake of supplements. If in co-culture, crosstalk between the cell types will direct how much of a specific cytokine is produced, for how long, and this provides much greater comparability to *in vivo* conditions. It also means you have two or more cell types which are of use for analysis and further experiments, widening the scope of the experiment.
MSCs have also been used alongside HSCs in synergistic SCT to enhance engraftment and reduce GVHD. In 2021, Li *et al*. reviewed 19 studies and concluded that MSC co-infusion improved engraftment and reduced GVHD (Li et al., 2021).

1.4.1.4 Nutrient exchange and dynamic culture

The progression from multicell systems was to mimic other biological functions, such as flow rate and nutrient exchange, more accurately. Bioreactors utilise dynamic conditions to mimic the flow of liquid environments like blood, or the constant nutrient and oxygen exchange present in tissues due to interstitial fluid (Lipreri et al., 2022; Ozturk et al., 2006). If demand for stem cells increases, large-scale cell production for SCT will likely occur in a bioreactor format due to the ease of scaling. This would typically be in the form of a spinner flask or rotating bioreactor (K. et al., 2011). A different approach is using a perfusion bioreactor with a fixed substrate through which the media flows (Rödling et al., 2017). Also using dynamic conditions, 'organ on-a-chip' microfluidic devices are widely utilised in research due to their highly customisable, micro-scale cultures that are ideally suited for drug testing platforms and for labs with limited space. It is possible to have multiple inlet tubes and compartments to alter media composition, flow rates and connect separate cell populations (Aleman et al., 2019; Glaser et al., 2022).

1.4.2 Hydrogels

The interest in hydrogels has risen exponentially over the last 50 years (Yahia et al., 2015). They are formed using water-soluble polymers that are crosslinked to form a viscoelastic 3D network. This new hydrophobic material has a high capacity for water retention, without disrupting the structure (Abu Shmeis, 2022; Revete et al., 2022). Already fully integrated into society, hydrogels have widespread uses in agriculture(Palanivelu et al., 2022) the food industry(Nazir et al., 2017; Zhang et al., 2020) and extensively for biomedical applications such as drug delivery (Qiu & Park, 2001), wound healing (Aswathy et al., 2020; Hancock et al., 2011), tissue engineering and regenerative medicine (Lee & Mooney, 2001). As a result, many hydrogels are already known for their biocompatibility and customisability, creating a solid foundation for future research. From a cell research standpoint, hydrogels are typically used in either 2D as a substrate, 2.5D where cells are seeded on top or underneath a gel, or as a 3D scaffold within which cells are seeded (Caliari & Burdick, 2016; Leisten et al., 2012; Wang & Pelham, 1998). Whether they're derived from natural sources or man-made, the material properties of the gel, such as stiffness and porosity, are integral to how the gel influences cell behaviour. However, the properties are highly specific not just to the type of polymer used to form the gel but the

concentration, temperature, pH and length of time during the cross-linking stage of gel manufacture (Lee et al., 2014).

1.4.2.1 Synthetic gels

Polyacrylamide (PA) hydrogels have been widely used in biological sciences since the 1960s for DNA separation via electrophoresis. However, since the 90s, it was also utilised as a substrate for the growth of cells (Wang & Pelham, 1998). PA gels can be synthesised to have stiffness across a full physiologically relevant range from 0.3 to 300 kPa, tuneable viscoelasticity and porosity, while proteins and cell binding motifs can easily be attached covalently to enable cell binding and customisable growth conditions (Protick et al., 2022; Syed et al., 2015; Wang & Pelham, 1998). While these properties were first utilised as 2D coatings for cell culture, this has developed into 3D constructs and combination gels for cell encapsulation (Rana et al., 2016; Shi et al., 2024). The stiffness flexibility means PA gels are utilised from very soft bone marrow models to very stiff vascularized bone models (Derkus et al., 2020; Shi et al., 2024).

A similar gel widely used in cell culture is polyethene glycol (PEG). It has the same tunable properties as PA, and can also be customised to add binding domains, proteins and growth factors. It is also highly biocompatible, enabling cell encapsulation (Lin & Anseth, 2008). To modify the crosslinking density and therefore stiffness, typically the concentration or molecular weight of PEG is adjusted, and this results in easy formation of gels with stiffness from 200 Pa to 1000 kPa (Lee et al., 2014; Seitz et al., 2024). This also gives a wide range of uses from modelling the blood-brain barrier to bone tissue engineering (Ahmad et al., 2024; Si et al., 2024).

1.4.2.2 Gels formed from naturally occurring molecules

The most abundant protein in the ECM is collagen, and subsequently, collagen hydrogels – typically type I collagen – have been investigated and reviewed extensively for their use in cell culture (Antoine et al., 2014; Caliari & Burdick, 2016; Lee & Mooney, 2001; Shenoy et al., 2022). Other than being biocompatible, an advantage of collagen is its tunability. For example, the density of the collagen fibre network and therefore porosity can be increased using higher pH or increased collagen concentration during cross-linking, with lower pH also forming thicker fibres (Sarrigiannidis et al., 2021). Collagen also contains naturally occurring cell-binding sites, which means no additives or

modifications are usually needed to make a hospitable environment. Optimising the fabrication process can therefore result in a wide variety of stiffness and porosities. Antoine *et al.* used pH, concentration and temperature to form gels with stiffness from 540 Pa to 10.7 kPa, with pore sizes from 1.2 to 3.2 μm, to mimic normal and cancerous breast tissue, respectively (Antoine et al., 2015). While Cummings *et al.* produced gels with stiffness of 191 to 242 kPa for use in blood vessel substitutes (Cummings et al., 2004).

Similar in properties to collagen is fibrin. It is biocompatible, has cell binding sites, and can make customisable hydrogels (Cummings et al., 2004; Mosesson, 2005). However, it is only useful for gels with relatively low bulk stiffness. Increasing fibrin concentration results in increased strength but reduced cell viability, and while stiffnesses up to 184 kPa were achieved by Linnes *et al.,* this involved a long acetone treatment, which would be toxic to cells if encapsulated (Linnes et al., 2007). They are, however useful alternative for gels with a softer desired stiffness of 0.9 to 30 kPa, or in a complementary mixture with other gels (Cummings et al., 2004; Sanz-Horta et al., 2023). With uses as models with compressive moduli akin to skin, or to induce chondrogenic differentiation in MSCs and cartilage repair (Ho et al., 2010; Murphy, Whitehead, et al., 2017).

1.4.2.3 Alginate

Another naturally occurring molecule, and that of choice for this study, is sodium alginate, a polysaccharide isolated from brown seaweed, which can be cross-linked to form a highly biocompatible hydrogel with widespread uses from drug and cell therapy delivery systems to soil conditioner (Aderibigbe & Buyana, 2018; Lee & Mooney, 2012; Severino et al., 2019; Shin et al., 2023; Smith & Miri, 2010). It is the material of choice for this project due to it being the core material for the product range of Atelerix – the stakeholder company for this work (see **1.4.4.4**) – who have been investigating it for a decade as a method to encapsulate cells and induce quiescence (Swioklo & Connon, 2016). Other benefits include it and all components for gelation and degradation being animal-free, as well as being well established in the medical sector, which should make it easier to translate work further down the line into medical/modelling/testing applications. The hydrogel material itself lacks binding domains, so it is usually modified to contain RGD domains or mixed with

a secondary material such as collagen or Matrigel (Neves et al., 2020; Stowers et al., 2019). Gelation time, temperature, type of crosslinker and crosslinker and gel concentration are all able to influence the material properties of alginate, while temperature and pH (as long as it's over 4) have limited impact, making it of interest for use at physiological conditions (Akbarzadeh Solbu et al., 2022). Through tuning, alginate gels with a broad range of stiffnesses are possible, with reports from 0.5 Pa in a mammary epithelium model to 900 kPa available (Chan et al., 2011; Stowers et al., 2019).

The sodium alginate molecular structure consists of 1,4-linked residues of ß-D-mannuronic acid (M) and α-L-guluronic acid (G), which exist in blocks as consecutive (-GGG-/-MMM-) or alternating (-GMGM-) monomers to form a polymer chain (see **Figure 3)** (Andersen et al., 2015; Draget & Taylor, 2011). In solution, these chains exist in a random coil secondary conformation due to the electrostatic repulsion between the negative functional groups on adjacent monomers, resulting in a viscous liquid (Andersen et al., 2015). When crosslinked, the alginate contracts into a solid, with greater contractions correlated to increased crosslinking (Ramdhan et al., 2019).

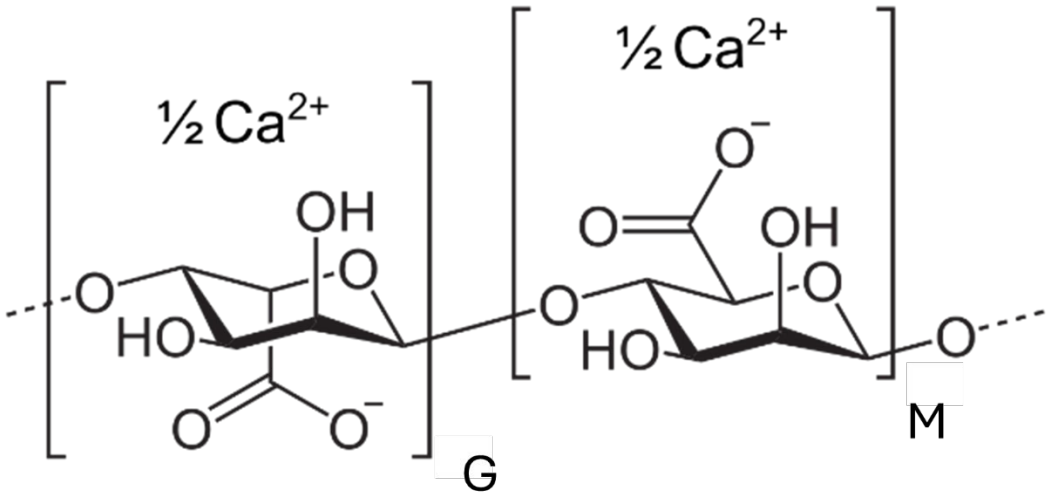

Figure 3. Skeletal formula of calcium alginate 'GM' repeat unit, where M is ß-D-mannuronic acid, and G is α-L-guluronic acid.

When crosslinked ionically, solidification occurs instantaneously upon introduction of the polymer and the cation. This typically occurs via the formation of ion-bridges between G residues. Therefore, alginate with naturally or artificially increased numbers of G units will crosslink more, a phenomenon described by Drageta *et.al.,* where greater numbers of GG residue blocks in calcium-alginate chains increase stiffness, whilst greater numbers of MM blocks increase elasticity (Drageta et al., 2001). In addition, this means that for 3D alginate constructs, the ions need to reach throughout the gel to solidify fully. This is achieved in one of two ways. Firstly, via diffusion over time from a larger reservoir/bath within which the alginate solution is dropped and submerged, allowing a short period of time for diffusion to occur relative to the size of the construct (Ramdhan et al., 2019). This often results in high crosslinking density on the surface, which decreases towards the centre (Paiboon et al., 2023). Or secondly, via internal gelation, where gelation occurs via the release of cations from a molecule suspended or dissolved within the sodium alginate, triggered by an additive such as an acid (Paiboon et al., 2023). This offers a more uniform crosslinking, but additives such as acetic acid, used to release calcium from dissolved Ca-EDTA, would be toxic to cells (Paiboon et al., 2023). It is also of note that the reactivity of ionic crosslinking ions typically falls with reducing temperature, and this will result in slower crosslinking (Lee & Mooney, 2012).

Covalent crosslinking is also possible if the polymer backbone is modified to contain the necessary functional groups. For example, methacrylate can be attached and then crosslinked using a photo initiator and UV light (Andersen et al., 2015). Carrying out covalent crosslinking alongside ionic crosslinking enables further customisation of the gel properties. Covalently crosslinking the outer layer of alginate microbeads makes them more stable *in vivo* due to the inability of chelating agents to break the bonds, slowing the degradation rate of alginate-based grafts with encapsulated islets aimed to treat type I diabetes (Somo et al., 2020). However, the difficulty in breaking covalent bonds would generally contradict a core reason why alginate is utilised in models and tissue engineering – ease of gel degradation to enable biodegradation *in vivo,* retrieve cells or allow cell remodelling.

Ramdhan *et.al.* showed that with internal gelation (using $CaCO_3$ incorporated alginate), increased crosslinking time results in a more homogenous gel, while increased cation concentration results in quicker initial crosslinking, all plateau around 2 hours (Ramdhan et al., 2019). By increasing the concentration of polymer, you increase the number of potential crosslinking sites and therefore can decrease the pore size of the gel. For example, Solbu *et.al.* showed that for internally gelated alginate, pore size was <360nm for 2.0% w/v alginate, <1230nm for 1.0% w/v and <1230nm for 0.5% w/v, with averages of 136±62nm, 172±110nm and 265±213nm, respectively (Akbarzadeh Solbu et al., 2022). Similarly, increasing crosslinker concentration resulted in greater crosslinking and decreased pore size. They also compared 20mM and 25mM $CaCO_3$ with 1.5% w/v alginate and found pore sizes of 92±80nm and 83±74nm, respectively. While these trends are the same using diffusion, the pore size itself is comparatively smaller. Simpliciano *et.al.* demonstrated an average pore size of 5.2±0.9nm for 1.5% w/v Na-alginate cross-linked with 1.5% w/v (0.1M) $CaCl_2$, while Chen *et.al.* showed 1% w/v Na-alginate in 0.1gml^{-1} (0.9M) $CaCl_2$ resulted in beads with pore size ranging from 5 to 100nm, but dominant sizes being 30 to 50nm (W. Chen et al., 2013).
Regardless of crosslinking method, retaining pore sizes in the nm range is important in biological applications to enable adequate nutrient diffusion in and out of the gel to maintain cells. 3%w/v sodium alginate linked in 0.1M $CaCl_2$ linked for 30 minutes, were created by Wells and Sheardown to determine the release rates of BSA (66.4kDa), Lysozyme (14kDa) and Chymotrypsin (25kDa) (Wells & Sheardown, 2007). After 10 hours, 90% of the BSA was released into the surrounding solution, compared to 65% of lysozyme and 75% of chymotrypsin. The BSA is electronegative and the others electropositive, so this indicates that diffusion rates are dependent on charge and not just size. It also means that molecules smaller than BSA should have no trouble diffusing in and out of alginate.

The properties of alginate can also be altered by using different cations. However, while smaller ions form stronger bonds and would typically displace heavier ions from a complex, alginate has an affinity for heavier alkali earth metals such that they bind with the following hierarchy: $Ba^{2+}>Sr^{2+}>Ca^{2+}>>Mg^{2+}$ (Key & Ball, 2014; Ručigaj et al., 2024). In addition, Ba^{2+} can also bind to M

residues, explaining the increased strength of the binding in Ba^{2+} crosslinked alginate (Zimmermann et al., 2007). This results in Ba^{2+} forming more stable gels than the more commonly used Ca^{2+}, exhibiting reduced swelling when submerged in saline, indicating crosslinks were held more effectively and reduced ion diffusion out of the gel into solution (Darrabie et al., 2006). Further, by using trivalent cations such as Fe^{3+}, triple crosslinks can be used to greatly enhance the strength of the gel beyond that of divalent cations (Ručigaj et al., 2024).

1.4.2.4 Uses of alginate hydrogels in medical bioscience

Historic wound dressings were designed to provide a physical barrier and keep the wound dry, while modern wound dressings are now designed to also aid in wound healing (Boateng et al., 2008). Many alginate dressings, such as Kaltostat™ and Algisite™ are widely available commercially and are dry, fibrous dressings that gel when absorbing wound fluid, and then reapply this moisture as water to the affected area and even promote tissue formation (Algisite M Calcium Alginate Dressing - MedicalDressings, 2025; Kaltostat Sterile Alginate Haemostatic Dressing - MedicalDressings, 2025; Boateng et al., 2008). Some more complex dressings are functionalised to be bioactive and are therefore more specialised, with examples reducing scar formation by binding SDF-1 or having increased antimicrobial properties by incorporating silver (Rabbany et al., 2010; Wiegand et al., 2009).

Alginate encapsulation can be used as a carrier for drugs, proteins and cells with tunable release profiles and can also be used to present cells for microarray, high-throughput screening systems (Lee & Mooney, 2012). For example, the release of cells can be controlled by varying degradation rates, drug release can be customised by the method of attachment to the polymer and can also reversibly attach growth factors like VEGF (Lee & Mooney, 2012; Sun & Tan, 2013). An early method of cell therapy via cell encapsulation is of pancreatic islets, which are released upon gel degradation, whilst anti-inflammatory drug flurbiprofen can be released via diffusion and chemotherapy doxorubicin can be released by hydrolysis (Lee & Mooney, 2012). As a drug testing format, encapsulated MCF-7 cells can be treated with chemotherapeutic drugs, doxorubicin and paclitaxel (Sabhachandani et al., 2016). Alginate for bone regeneration typically utilises a combination of MSCs/osteo-induced MSCs and bone-inducing proteins such as BMP-2 to direct bone re-growth at the injury site

(Kanczler et al., 2010; Weng et al., 2006). Similarly, regeneration of cartilage can be carried out by encapsulating chondrogenesis-induced MSCs and TGF-β (Ma et al., 2003; Park et al., 2009).

1.4.3 HSC expansion and/or maintenance models/systems

General limitations of both 2D and 2.5D cultures can be directly translated to the difficulty with culturing HSCs. Limitations which have resulted in extensive investigation into 3D methods of improving the expansion and/or maintenance of HSPCs. Attempts to culture HSCs take primary inspiration from BM. As covered in 1.2.1, the influence of MSCs within the HSC niche is well established, and therefore co co-culture methodology and reasoning is well refined.
It is agreed that serum-free medium with the supplementation of cytokines and an MSC feeder layer or coculture is necessary to increase CD34+ proliferation and reduce apoptosis (Bowlin et al., 2024; Mehrasa et al., 2014).

While additional cytokines are sometimes used, it is generally agreed that cytokine supplementation for HSC maintenance should include SCF, THPO and Flt-3 (Costa et al., 2018; Flores-Guzman et al., 2013; Mehrasa et al., 2014). The use of feeder layers was verified by the finding of 3 distinct groups of HSCs developing when cultured on an MSC monolayer, with more mature cells in suspension, cycling HSCs above the MSCs and primitive cells below the MSCs (Jing et al., 2010). However, the specific source of the MSCs was somewhat overlooked until a comparative study in 2021 by Bucar *et al*. showed that A-MSCs are preferable to BM-MSCs and UC-MSCs (Bucar et al., 2021). In addition, clinical trials have demonstrated that MSC feeder layer expanded HSPCs show enhanced engraftment ability during HSCT (de Lima et al., 2012).

1.4.3.1 Small molecules and EVs

In addition to culturing with the standard conditions, numerous small molecules have been investigated to expand LT-HSC populations for HSCT, with some even entering clinical trials (Branco et al., 2024; Cohen et al., 2023; de Lima et al., 2008; Parikh et al., 2018; Wagner et al., 2016). They typically look to inhibit LT-HSC differentiation or ST-HSC and progenitor proliferation pathways and/or promote expansion of LT-HSCs. UM171 inhibits lysine-specific histone demethylase 1A (LSD1), which in turn blocks differentiation while maintaining consistent proliferation rates, resulting in propagation of LT-HSCs (Subramaniam et al., 2020). This led to successful clinical trials in 2023 that demonstrate

enhanced patient survival with UM171-expanded HSCT compared to non-treated (Cohen et al., 2023). While nicotinamide (NAM) inhibits sirtuin 1 (SIRT1) and therefore differentiation, but also enhances proliferation of progenitors with enhanced bone marrow homing and engraftment (Peled et al., 2012). NAM expanded HSPCs were used successfully in a 2018 phase I/II clinical trial for treatment of sickle cell disease, while the phase 3 trial study, completed in 2025, demonstrated enhanced engraftment across patients with a variety of haematological disorders (Parikh et al., 2018; Wagner et al., 2016; Horwitz, 2021).

MSC-derived EVs have been demonstrated as regulators of both healthy and malignant haematopoietic systems.(Butler et al., 2018) In fact, EVs isolated from MSCs in malignant environments will induce malignant haematopoiesis in healthy cells, while healthy MSC EVs can restore normal haematopoiesis (Batsali et al., 2020). Further, exosomes will induce proliferation in ST-HSCs, while microvesicles expand LT-HSCs (Budgude et al., 2025).

1.4.3.2 Hydrogels in HSC models

The core component for many models is a biomaterial to form the structural component of the niche, with customisable stiffness and porosity lending itself to use as a scaffold. Thought must be given to ensure the pore size will enable cells to migrate into the material if desired, or if encapsulated, small enough to keep cells within. CB-derived CD34+ (CB-HSPCs) cells cultured in highly porous scaffolds of PCL, PLGA, fibrin and collagen were easily removed by pipetting (Ventura Ferreira et al., 2012). The MSC supported models showed enhanced expansion compared to those without, while the fibrin scaffolds showed the greatest CD34+ expansion, phenotype maintenance, morphological, migratory and adhesive properties and highest engraftment and multilineage differentiation in transplanted mice. While by encapsulating MSCs within collagen hydrogels and seeding HSPCs on top, their migration into the construct can be observed (Leisten et al., 2012). The population that does not migrate are mature, committed and proliferative progenitors, while those that do are a primitive, clonal population. A smaller pore size for these collagen gels meant the two populations were easily separated as cells were retained within the gel once migrated. These gels also showed that UC-MSCs were inferior to BM-MSCS at maintaining primitive HSPC phenotype.

1.4.3.3 Multifaceted model approaches

The progression from gel + cell systems was to mimic other biological functions, such as flow rate and nutrient exchange, more accurately (Chatterjee et al., 2021). Song *et al.* encapsulated BM-MSCs within alginate micro-gels and cultured them in a rotating wall bioreactor with HSPCs and saw increased CFU, CD34+ and total cell numbers compared to static and lone HSPC with cytokine cultures (K. et al., 2011). Rödling *et al.* colonised a PEG hydrogel with MSCs and HSCS, which was then placed inside a perfusion bioreactor (Rödling et al., 2017). Static conditions were observed to favour CD34 maintenance, while dynamic conditions encouraged erythroid lineage commitment and loss of CD34+; logical observations based on the residency of these cell types within the haematological system.

Aleman *et al.* connected four chambers, each with cell populations from different regions of the bone marrow, to assess homing preferences of normal and malignant HSPC populations (Aleman et al., 2019). While Glaser *et al.* encapsulated ECs, BM-MSCs and HSPCs in a fibrin hydrogel and inserted them inside a device that mimicked both the endosteal and perivascular environments (Glaser et al., 2022).

1.4.3.4 Maintaining a quiescent phenotype

Most literature searches regarding the *in vitro* culture of quiescent HSCs involve gene editing or forced gene expression, for example, by forced expression of F-box and WD-40 domain protein 7 (Fbxw7) (Iriuchishima et al., 2011). However, low serum, low cytokine, high fatty acid and hypoxic conditions do render quiescent HSC culture possible (Kobayashi et al., 2019; Shiroshita et al., 2022). In particular, higher TPO and SCF concentrations can trigger cell cycle entry and differentiation. The HSCs can be isolated and selected using flow or artificially inducing quiescence using CRISPR-Cas9 genome editing, which grants a higher yield but lacks full physiological comparison.

1.4.4 Cell storage

1.4.4.1 Traditional cryopreservation

When storing and transporting cells, the typical storage technique is that of cryopreservation. This technique uses dimethyl sulfoxide (DMSO) as a cryopreservation agent (CPA) with a cooling rate of 1ºC per minute to a temperature below -135 ˚C. Cells are then thawed rapidly at over 100 ˚C a

minute to 37 °C (Rowley, 2009). However, this technique has pitfalls, the most prevalent of which is ice crystal formation. Mazur *et al*. first hypothesised that it was intracellular ice formation causing decreased viability (Mazur et al., 1972). A theory now widely accepted and reviewed, it is commonplace to use CPAs to inhibit ice crystal formation along with other issues such as solute effects, osmotic shock and supercooling among others (Chang & Zhao, 2021; Elliott, 2013; Gurruchaga et al., 2018; Lin et al., 2023; Murray & Gibson, 2022; Poisson et al., 2019). However, CPAs are often toxic and can cause severe side effects if cells frozen with them are used for transplants (Berz et al., 2007; Hornberger et al., 2019; Morris et al., 2014). There also remains debate over whether cryopreservation impacts cell properties and functions, with MSCs reviewed thoroughly by Bahsoun *et al*. and their opinion being that methods vary too greatly in research to make a solid conclusion (Bahsoun et al., 2019). Further, HSCs are renowned for variable recovery after cryopreservation. Recovery of mobilised PB CD34+ cells post cryopreservation was reported as 73.7% and 68.1% for autologous and allogenic samples, respectively (Rimac et al., 2023). While in general, these figures lie between 40 and 80%, they are mostly around 70% (Gokarn et al., 2023; Johannsen et al., 2016; Purtill et al., 2020; Rimac et al., 2023; Turney et al., 2019). Cell recovery is critical, as recovery of HSPCs can be considered a strong indicator of the functionality of the population, as well as disrupting the dosage a patient would receive (Cottle et al., 2022; Lee et al., 2008).

1.4.4.2 Hypothermic storage

Attempts to utilise hypothermia in a clinical setting started in the early 50's, based on the assumption that reduced temperature would reduce metabolism and therefore prolong cell life out of the body (SWAN et al., 1955). By the 90s, a preservation solution to maintain refrigerated whole organs was used for various organs, and by the 2000s, isolated cells were now stored short-term at 4 °C (Olinga et al., 1997; Southard & Belzer, 1995). For BM-MSCs, Veronesi showed that 18 hours at 4 ºC in saline maintained viability above 80% (Veronesi et al., 2013). While CB-HSPCS, PB-HSPC and BM-HSPCs are maintained better at 4 °C compared to 20 °C (Fry et al., 2013). However, viability does not guarantee functional capacity. A second study showed these conditions resulted in decreased CFU-forming and tri-lineage differentiation potential compared to

fresh (Sohn et al., 2013).

Subsequently, less rudimentary buffers were implemented and gave improved results. Using combinations of human serum albumin (HSA), glucose, and platelet lysate allowed storage for two days (Gálvez et al., 2014; Gálvez-Martín et al., 2014). While using 40 mM trehalose enabled UC-MSCs to remain 90% viable for 7 days and 70% viable after 3 weeks (Di et al., 2012).

There is also reason to believe that 4 °C may not be the optimum hypothermic storage temperature, as studies with a variety of cell types have indicated that ambient temperatures may be more suitable. For example, the optimum storage temperature for epithelial cells and hamster ovary cells in suspension was 16 °C and 17 ºC, respectively (Hunt et al., 2005; Pasovic et al., 2013).

1.4.4.3 Hydrogels as a storage method

Hydrogels have been used as anti-freeze agents for a range of applications. Primarily as a coating, Zhiyuan *et al.* formed an anti-freeze hydrogel by grafting PDMS chains onto a polyelectrolyte network (He et al., 2020) while Guo *et al.* created a PMAA multilayer hydrogel to control ice nucleation and propagation (Guo et al., 2018). However, hydrogels have also been used to protect cells during freezing for storage (Chang & Zhao, 2021; Gurruchaga et al., 2018; C. Zhang et al., 2018).

Encapsulation of cells within hydrogels as a cryoprotectant has also been investigated using synthetic polymers, such as Jain *et al.*, using a dextran-based polyampholyte gel (Jain et al., 2014). However, the most widespread use is that of Alginate (Zhang et al., 2018).

The first example of alginate being used as a cryoprotectant was presented in 1996 by Inaba *et al.*, who encapsulated rat islets and then stored them in liquid nitrogen (Inaba, 1996). While Malpique *et al.* used alginate encapsulation to store brain cell neurospheres in liquid nitrogen, resulting in reduced recovery time post-thawing and less fragmentation (Malpique et al., 2010). Gryshkov *et al.* also used alginate to encapsulate MSCs and demonstrated that on thawing, they have greater metabolic activity compared to those not encapsulated (Gryshkov et al., 2014). However, hydrogels are not frequently reported to be used as room temperature storage for cells. Chen et al. stored mouse embryonic stem cells (ESCs) and human MSCs for 5 days at 18-22 °C in calcium alginate (B. Chen et al., 2013). And gorodestsky et al. used fibrin hydrogels to encapsulate

and store cells in a sealed cryovial for 6 days at 24 °C (Gorodetsky et al., 2011). While my stakeholder company, Atelerix, is the dominant reporter of this use, with primary examples for A-MSCs and keratocytes (corneal stromal cells) (Isaacson et al., 2018; Swioklo et al., 2016).

1.4.4.4 Atelerix

Atelerix "provide patented alginate hydrogel technology to stabilise cells, tissues, blood products, viruses and vectors at room temperature" (About Us | Atelerix, 2025). Their products are of interest to those seeking short-term storage of biological material without access to cold-chain transport infrastructure. The methodology utilises hypothermic temperatures and a non-adherent environment due to alginate encapsulation to induce quiescence in cells. Atelerix gels are also animal-free and contain no toxic components, making them safe to handle and dispose of. They each come with protocols, and the biological material can be recovered quickly and is ready to use. 6 products are currently available: CYTOSTOR™, for the storage of cells, viruses, vectors and mRNA-LNPs, LEUKOSTOR™ for storing fresh leukapheresis, TISSUEREADY™ for organoids, spheroids and microtissues, TISSUEREADY PLUS™ for tissue, WELLREADY™ for storing cells in a well-plate format, and BLOODREADY™ for blood samples (Atelerix: Innovative Cell Preservation, n.d.).

They have produced research papers to demonstrate their findings for mouse embryonic stem cells, A-MSCs and corneal epithelial cells (Branco et al., 2022; B. Chen et al., 2013; Wright et al., 2012). In addition, on the compatibility section of their website, they define the recommended product, storage temperature, seeding density and storage length for a large variety of sample types (Samples Preserved | Atelerix, n.d.).

1.5 Conclusions

Investigation into the bone marrow niche microenvironment over the last 25 years has seen revelations in the way we perceive stem cells and how they may be utilised in broader applications than commonly used transplants. A highly complex environment, modelling the bone marrow has become the go-to method for research into the cell populations residing there *in vivo*. These models have become increasingly refined; however, there is a lack of a reliable and widely accepted method for creating one.

While an ageing population has accelerated research into age-related diseases

and regenerative medicine, a more ethically aware society has driven the conversion to increasingly sustainable methods, materials and practices. However, these practices are more complex than traditional animal models, and with complexity comes cost. To make them a viable alternative, *in vitro* human models must give both improved results as well as competitive pricing. Further, while feasible in research, a highly complex system may be less favourable in pharmaceutical or medical settings where high-throughput testing is required. Therefore, a compromise must be made between ethicality, complexity, accuracy and cost. One way to do so is to utilise materials already approved for use in the medical setting, rather than creating novel materials that could fail at one of the countless stages of the approval processes. Another is to make cells more available to enable research, form a greater understanding of the bone marrow and therefore the components which can be cut to form cheaper, simpler, yet equally effective methods for current and future treatments.
This advancement is imperative because the importance of HSPCs within the medical sector is well established, along with the benefits of MSC spheroids over single cell MSCs, and yet their uses are far from maximised. Being able to transport these cells without cold-chain infrastructure would enable treatments and research in developing countries, whilst also being more environmentally friendly. In turn, increased cell accessibility should lead to decreased costs, again encouraging their use and future development.
Atelerix have displayed the methodology for short-term storage of cells within a biocompatible, FDA-approved material. However, the variability in viable encapsulation time for different cell types means there’s no guarantee this system works universally. Therefore, there remains a need to determine if this will work on HSCs and MSC spheroids.

1.6 Aims and objectives

The following thesis intends to investigate the effects of alginate encapsulation on primary human BM-MSC spheroids and primary human CD34+ BM-HSPCs, with emphasis on aligning with the precedent set out by the training programme within which this project is facilitated in minimising the use of animals in research and providing research with direct, real-world applications. Use of alginate rather than other biomaterials is advantageous because all components used for both gelation and gel degradation are biocompatible and animal-free;

the natural lack of binding sites prevents cell interaction with the matrix and helps induce quiescence, and gelation and gel degradation is quick, simple, and is not harmful to cells. Primary stem cells will be used exclusively so that any findings are directly applicable to increasing the availability of primary stem cells for use in research and medicine.

To do this, the impacts of encapsulation of single-cell MSCs will first be explored using viability and flow cytometry. Secondly, viability and flow cytometry will be performed on HSPCs. Next, the same will be performed on MSC spheroids. The result would be to demonstrate whether HSPC and MSC spheroid encapsulation would be a viable method of alternate storage, and in extension, whether they would be adequate as a ready-to-use drug testing platform. With consideration of transport and experiment length, a time criterion of 2 weeks was decided for functional cell survival, with this not being a viable method if this timeframe was not met.

Chapter 2. Materials and methods

2.1 Isolation of cells from donor samples and donor identification

All cells used for this work were from donated primary bone marrow samples from either Queen Elizabeth University Hospital, Glasgow or the University Hospital, Ayr and were anonymised by the School of Infection & Immunity, Glasgow, before use.

Samples were run through a 70 μm mesh strainer, washed with Dulbecco's Modified Eagle Medium high glucose with sodium pyruvate, without glutamine (DMEM) (Gibco, Cat# 21969035) and added to a Ficoll Paque (Merck, Cat#GE17-1440-02) gradient solution. The mononuclear layer was then extracted, washed with flow buffer (2mM EDTA (Invitrogen, Cat# 15575-020), 0.5% Bovine Serum Albumin (BSA) (Sigma Aldrich, Cat# A7906-100G) in 9.88gL^{-1} Phosphate Buffered Saline (PBS)), and the CD34+ population selected using a MACS positive selection kit. CD34+s were frozen in Alburex20 Human Albumin (CSL Behring) with 0.11 gml^{-1} Dimethyl sulfoxide (DMSO) (Sigma Aldrich, Cat#34869-100ML) or used immediately, while the CD34- population was seeded into tissue culture flasks. MSCs and other adherent cells were cultured until distinct colonies of MSCs formed. As other adherent cells in the population are more adherent, a short trypsinisation using Trypsin-EDTA (ThermoFisher Scientific/ Invitrogen, Cat#15400054) could then be used to remove the MSCs, which were then reseeded.

HSC Donors 1, 2 and 3 are patients 2345, 2346 and 2437, donor 5 was a pooled population of donors 2506 and 2507, donor 6 was a pooled population of donors 2502 and 2501. Donor 4 was a vial purchased from StemCell Technologies Cat# 70002.4. Records were not kept for all MSC donors.

A large number of MSC donors were used throughout this study, and there was no donor continuity between experiments, so each shall be referred to as a 'biological replicate' to avoid confusion. In contrast, the six HSC donors were assigned their own number, colour and symbol to demonstrate continuity between experiments.

2.2 Cell Culture

Any adherent cell cultures were passaged at 70% confluence using Trypsin-EDTA (ThermoFisher Scientific/ Invitrogen, Cat# 15400054), unless before flow

cytometry, in which case TrypLE was used instead.

Primary MSCs were expanded using DMEM (Gibco, Cat# 21969035), supplemented with 0.27 $\mu g ml^{-1}$ of Amphotericin B (Gibco, Cat# 5290-026), 89 units/89 $\mu g ml^{-1}$ of penicillin-streptomycin (Sigma Aldrich, Cat# P0781-100ml), 2.4 mM L-Glutamine (Sigma Aldrich, Cat# G7513-100ml) 1X dilution of 10X Non-Essential Amino Acids (Gibco, Cat# 11140-035) and 20% Fetal Bovine Serum (FBS) FBS (Gibco, Cat# A5256701). The cells were transitioned to 10% FBS (Gibco, Cat# A5256701) at Passage 5, and this was used thereafter.

S1/S1 fibroblasts were cultured using 172 units/172 $\mu g ml^{-1}$ of penicillin-streptomycin (Sigma Aldrich, Cat# P0781-100ml), 4.8 mM L-Glutamine (Sigma Aldrich, Cat# G7513-100ml) and 12.5% FBS (Gibco, Cat# A5256701).

M2-10B4 fibroblasts were cultured using 172 units/172 $\mu g ml^{-1}$ of penicillin-streptomycin (Sigma Aldrich, Cat# P0781-100ml), 4.8 mM L-Glutamine (Sigma Aldrich, Cat# G7513-100ml) and 9% FBS (Gibco, Cat# A5256701).

On the day before their experiment, frozen primary CD34+s were thawed and cultured overnight using Iscove's Modified Dulbecco's Medium (IMDM) (Gibco, Cat# 12440053) supplemented with 10% BIT (Stemcell technologies, Cat# 09500), 10 $ng ml^{-1}$ Recombinant Human SCF (Peprotech, Cat # 300-07), 10 $ng ml^{-1}$ Recombinant Human Flt-3 (Peprotech, Cat# 300-19 and 5 $ng ml^{-1}$ Recombinant Human THPO (Peprotech, Cat# 300-18). Fresh CD34+ cells were encapsulated without culture.

2.3 Spheroid formation, culture and collection

MSCs were thawed and grown for at least 2 weeks before use, and the media was changed every 3-4 days. AggreWell™ 400 24-well plates, with each well containing 1200 micro-wells, were used to form spheroids of approximately 200 cells per spheroid. The protocol followed is provided by Stemcell technologies (Stemcell technologies, 2017). Anti-adherence solution (Stemcell technologies, Cat#07010) was added to each well of the AggreWell™ 400 plate and centrifuged at 1300g for 5 minutes. Each well was rinsed twice with 0.5ml of pre-warmed 9.88 $g L^{-1}$ PBS and then with 200 µl of DMEM (Gibco, Cat# 21969035). Finally, 1ml of a 2.4×10^5 MSCs per ml solution of cells was added to each well, and the cells were allowed to settle by gravity into the microwells. The plate was then centrifuged at 100g for 3 minutes and then placed into an incubator.

After allowing 2 days to aggregate, the spheroids were removed from the plate

and encapsulated within alginate at 10,000 spheroids per ml of gel **(See 2.2.4)**. When handling spheroids, plasticware was either rinsed with 2% FBS (Gibco, Cat# A5256701) to prevent spheroids from adhering. The beads were stored at 15+/- 0.5 ºC, or at 20+/- 0.5 ºC, while the control spheroids were kept in the plate at 37 ºC, with media changes every 3-4 days.

2.4 Hydrogels

Alginate hydrogel beads from the Atelerix BeadReady™ kit (Atelerix, Cat# BR-MNS) were prepared using the Atelerix BeadReady™ protocol. Component A was mixed 1:1 with the cell suspension, and 100 µl of gel mix was then added dropwise from above through a 21G needle to an 800µl bath of crosslinker and stored in 1.1ml of media (or scaled appropriately) (Atelerix, n.d.). The seeding density of each cell type/aggregate was determined using the guide provided by the company and scaled appropriately so that the diameter and subsequent volume the cells would occupy, so as not to destabilise the network and properties of the gel.

This protocol produced alginate beads of approximately 2.5 mm in diameter. To recover cells/aggregates from gel beads, the storage media was removed and replaced with an equal volume of the dissociation buffer. The vessel was re-sealed and agitated gently for ~ 10 minutes until the beads had dissolved, then centrifuged at 350 rcf for 10 minutes to pellet cells for use.

The temperature or the experiment storage conditions were strictly controlled, with the use of a fridge at 4 +/- 1 ºC, another at 15+/- 1 °C, room temperature controlled using an insulated storage box inside a cupboard in an environmentally controlled laboratory set at 20 °C and measured to remain within +/- 1ºC and a cell incubator for 37 +/- 1 °C.

2.5 Cell encapsulation density

Cell density for encapsulation was based on previous experiments by Atelerix and the median recommended density from the Bead Ready Protocol – for MSCs, this is around $2x10^6$ cells ml^{-1}. However, this was halved for this project to $1x10^6$ cells ml^{-1}. (Damala et al., 2019; Swioklo & Connon, 2016).

Using this density, the recommended total cell volume was calculated. For MSCs, the average diameter of suspension MSCs is anywhere from 15 to 30µm (Drobek et al., 2023; Ge et al., n.d.; Zanetti et al., 2015). Therefore, a rough mean estimate was decided as 22µm, and the total volume of $1x10^6$ cells was 5.6 µl.

For HSCs, a diameter of around 8 µm would suggest a seeding density of $2x10^7$cells ml^{-1}; however, due to cell availability, this number was not practical (Y. Gao et al., 1998). Therefore, HSCs were seeded at $1x10^7$ cells ml^{-1} and occupied a volume of 2.6 µl.

The diameter of 200 cell spheroids was measured to be around 100µm **(Figure 5),** which resulted in a seeding density of $1x10^4$ spheroids ml^{-1} occupying a volume of 5.2 µl.

2.6 Viability

2.6.1 Single cell viability

As per the protocol provided by Thermofisher, 0.5 µl Calcein AM solution and 2 µl ethidium homodimer-1 solution (LIVE/DEAD™ viability/cytotoxicity kit, for mammalian cells, ThermoFisher Scientific/Invitrogen, Cat#L3224) were combined in 1ml of cell storage media (to maintain structural integrity of the gel) to make a staining solution. 4 alginate beads were washed with 1X Dulbecco's phosphate-buffered saline (DPBS) with Calcium and Magnesium (DPBS++) (Gibco, Cat# 14040133), submerged in 400 µl of staining solution and incubated for 30 minutes at 37 °C. The gels were then washed with PBS++ and imaged using an EVOS M7000 microscope.

The imaging was carried out using the z-stack function to take three 50-slice stacks of each gel, totalling 9 stacks per batch. The number of live (green) and dead (red) cells for each stack was counted, and the live cells were divided by the total cell number to give a percentage viability **(see Figure 4)**. As the rate of Calcein hydrolysis will increase in more metabolically active cells, the intensity of the signal can also be compared to determine cell activity.

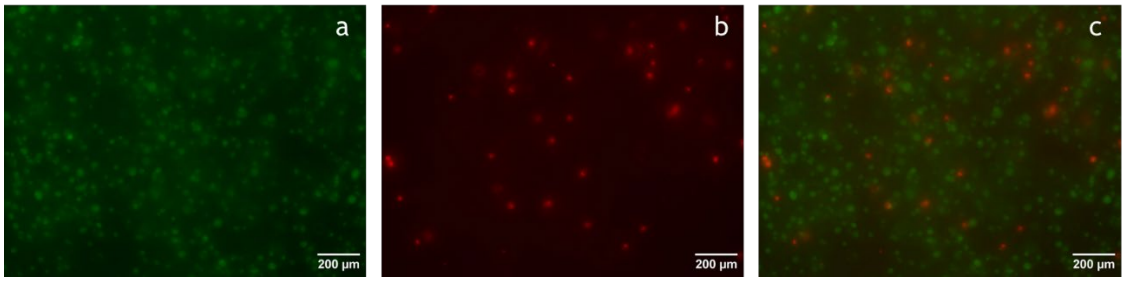

Figure 4. Single-cell MSC viability example of z-stack image of IMDM gels on day 1 for a) green (alive), b) red (dead), c) merged channel stain.

2.6.2 Spheroid viability

The staining solution for spheroid viability was 1µl Calcein AM and 4µl ethidium homodimer-1 (LIVE/DEAD™ viability/cytotoxicity kit, for mammalian cells, ThermoFisher Scientific/Invitrogen, Cat# L3224) in 1ml cell storage media. To stain, 4 beads were submerged in staining solution for an increased time of 1 hour at 37 °C **(see Figure 5)**. 1 hour staining gave a brighter signal due to increased time for dye to be hydrolysed; therefore, less exposure was required for imaging, and less background is present. They were then washed with DPBS++ (Gibco, Cat# 14040133), and the gels were separated into individual wells of a 96-well plate. 200µl of dissolution buffer was then added to each bead, and the plate was agitated for 10 minutes to dissolve the gel. Spheroids were allowed to settle on the base of each well and then imaged on an EVOS M7000 microscope. Each spheroid was imaged using a z-stack, with the bounds set to the top and bottom of the spheroid. This provided an image of the most intense regions through the spheroid, the brightness of which could then be quantified to provide a ratio between the green and red fluorescence intensity.

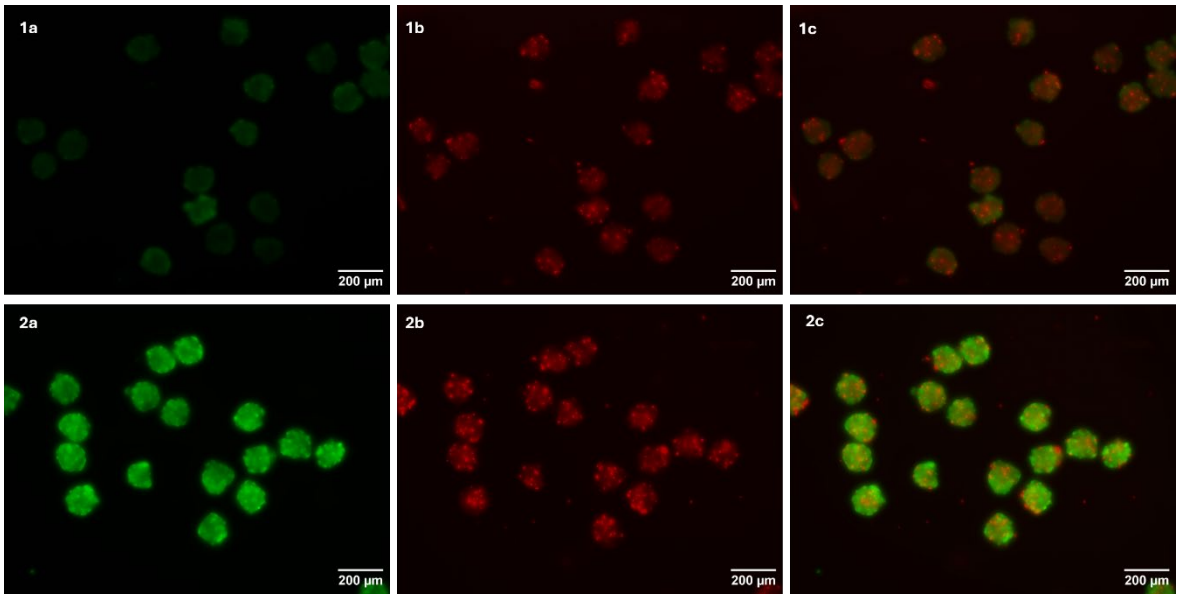

Figure 5. Example MSC spheroid viability staining z-stack images. Figures 5.1) 30 min stain and 5.2) 1 hr stain, with a) merged, b) dead, c) live.

2.7 Flow cytometry

2.7.1 Staining procedures

Antibody and dye volumes assume 1 ‘test’ representing 50,000 cells. Anhydrous Zombie Violet dye was resuspended in 100 µL of DMSO (Sigma Aldrich, Cat# 34869-100ML) to create a working solution, which was then used at a concentration of 0.05 µl per test. Sytox blue viability dye was also used at 1µl per test but does not require pre-hydration. Thermofisher antibodies were used at 1 µl per test, and Miltenyi Biotec antibodies were used at 0.4 µl per test. Gating strategy and panels displayed in **2.7.2.1**. Measurements taken on an Attune Nxt flow cytometer (ThermoFisher Scientific/Invitrogen, SN: 2AFC234440621).

2.7.1.1 Antibody compensation

UltraComp eBeads (Compensation Beads) (ThermoFisher Scientific/Invitrogen, Cat# 01-2222-42) were first vortexed thoroughly, and Eppendorf’s labelled - one for each antibody used in the panel. One drop of the beads was added to each tube, and then 1 µl of the respective antibody was added. This was then vortexed and centrifuged briefly to settle it to the bottom of the tube. They were then incubated for 30 minutes in the dark at 4 °C. Finally, 1 ml of flow buffer was added and mixed thoroughly before use.

2.7.1.2 Viability dye compensation

When using amine-reactive beads

Using the ArC™ Amine Reactive Compensation Bead Kit (ThermoFisher/Invitrogen, Cat# A10346), positive amine-reactive beads were vortexed thoroughly, and one drop was added to an Eppendorf with 0.1 µl of viability dye. The tube was vortexed and centrifuged briefly. It was then incubated at room temperature for 30 minutes in the dark. After, the negative control beads were vortexed, and one drop was added to the Eppendorf with the positive beads, along with 1 ml of PBS. This was mixed briefly and then vortexed thoroughly before use.

When using cells

2 ‘tests’ of cells were washed with PBS. One was then stored at 4 ºC and the other centrifuged and resuspended in 100 µl of 0.04gml^{-1} formalin (37% paraformaldehyde (PFA) stabilised with 10% methanol) (Sigma Aldrich, Cat#F8775). These cells were then incubated at 37 ºC for 30 minutes.

Afterwards, 500µl of PBS was added, mixed briefly and then centrifuged at 450g. This was then resuspended in 50µl flow buffer. Then, the test cells stored at 4 ºC were centrifuged and resuspended in 50 µl of flow buffer. Once both samples were ready, a viability dye working solution was made using flow buffer at 0.5µl of dye in 500µl of buffer. 50µl of the viability dye working solution was then added to both samples and incubated at room temperature in the dark for 30 minutes. They were then washed with 500µl flow buffer and resuspended in 500µl flow buffer. They were then vortexed thoroughly before use.

2.7.1.3 Staining cells

3 test of cells were split between 3 Eppendorf tubes and washed with PBS.
A zombie dye viability dye master mix of 0.2µl of dye in 200µl of PBS was pre-made, of which 50µl was added to each tube of cells. They were stained in the dark at room temperature for 30 minutes, during which an antibody master mix was prepared. The master mix contained three tests' worth of each antibody in the panel, with the mix made up to 150 µl with flow buffer. After viability staining, the cells were then washed with flow buffer. Then, 50µl of the antibody master mix was added, the cells were resuspended, and then stained in the dark at 4 °C for 45 minutes. The cells are then washed with flow buffer once more, resuspended in 500µl of flow buffer and analysed.
If using Sytox Blue, the antibody mastermix was prepared the same as above, but also included three tests of Sytox Blue dye, and the viability staining occurred as part of the antibody staining panel. The rest of the process was the same. If any Super Bright stains were used, 1 µl per test of Super Bright buffer was added to the master mix to avoid non-specific binding of the fluorophore.

If using spheroids.
Before staining, spheroids were dissociated using pre-warmed TryplE at 100 µl per 1000 spheroids, by aggregating them gently at 37 ºC until they dissociated. Once dissociated,10% FBS in DMEM with a volume double or greater than that of the TryplE volume was added to neutralise it and then centrifuged at 250 rcf for 5 minutes.

2.7.2 MSC gating strategies

2.7.2.1 MSC gating strategy 1

The gating strategy and panel utilised across **Figures 12-15** for monolayer MSC experiments is presented in **Figure 6.** Unstained cells were gated based on side

scatter – area (SSC-A) and forward scatter – area (FSC-A), and then FSC-A and forward scatter- height (FSC-H) to remove debris. Next, cells were gated for a negative response to the cell viability dye (Sytox Blye dead cell stain, ThermoFisher Scientific, Cat# S34857) (which permeates into dead cells, not live cells) for laser VL1. Then, cells were gated for a negative response to the HSC lineage cocktail (HSC Lineage Cocktail, ThermoFisher Scientific, Cat# 22-7778-72) for laser BL1 and CD34 (CD34-APC, Miltenyi Biotec, Cat# 130-113-176) for laser RL1 to remove any non-mesenchymal-lineage cells. The remaining cells were then assessed for positive expression for CD166 (CD166 PE, ThermoFisher Scientific, Cat# 12-1668-42) for laser BL2, CD73 (CD73 PerCP-eFluor 710, ThermoFisher Scientific, Cat# 46-0739-42) for laser BL3, CD146 (CD146 PE-Cy7, ThermoFisher Scientific, Cat# 25-1469-42) for laser BL4, CD90 (CD90 AlexaFlour 700, ThermoFisher Scientific, Cat# 56-0909-42) for laser RL2, CD105 (CD105 APC-eFluor 780, ThermoFisher Scientific, Cat# 47-1057-42) for laser RL3, CD44 (CD44 eFluor506, ThermoFisher Scientific, Cat# 69-0441-82) for laser VL2, CD271 (CD271 Super Bright 600, ThermoFisher Scientific/Invitrogen, Cat# 63-9400-42) for laser VL3 and CD29 (CD29 Super Bright 702, ThermoFisher Scientific, Cat# 67-0299-42) for laser VL4.

The following were omitted from the gating panel due to compensation issues –
For biological replicate 1: CD45 (BL1), CD166 (BL2), CD90 (RL2), CD44 (VL2), CD271 (VL3)
For biological replicate 2: CD90 (RL2), CD44 (VL2), CD271 (VL3)
For biological replicate 3: CD90 (RL2), CD44 (VL2), CD271 (VL3)

These values were omitted due to the viability dye being used -Sytox Blue- exhibiting substantial spectral overlap with these channels, and this resulted in false-positive results.

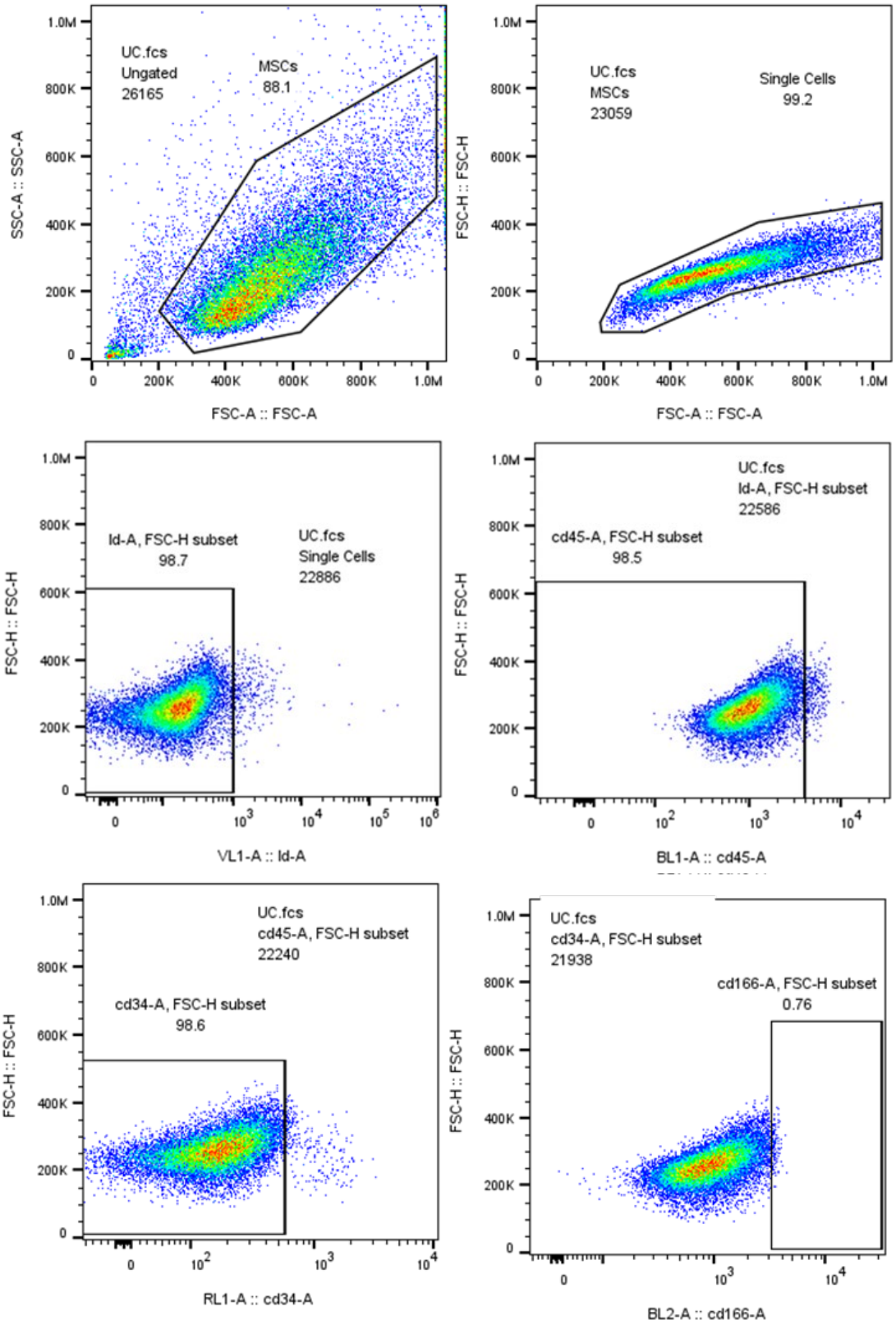
UC.fcs
Ungated
26165
MSCs
88.1
SSC-A :: SSC-A
FSC-A :: FSC-A
UC.fcs
MSCs
23059
Single Cells
99.2
FSC-H :: FSC-H
FSC-A :: FSC-A
Id-A, FSC-H subset
98.7
UC.fcs
Single Cells
22886
FSC-H :: FSC-H
VL1-A :: Id-A
UC.fcs
Id-A, FSC-H subset
22586
cd45-A, FSC-H subset
98.5
FSC-H :: FSC-H
BL1-A :: cd45-A
UC.fcs
cd45-A, FSC-H subset
22240
cd34-A, FSC-H subset
98.6
FSC-H :: FSC-H
RL1-A :: cd34-A
UC.fcs
cd34-A, FSC-H subset
21938
cd166-A, FSC-H subset
0.76
FSC-H :: FSC-H
BL2-A :: cd166-A

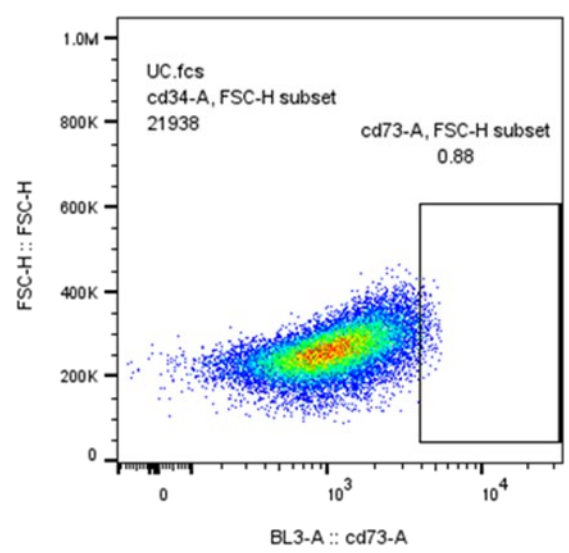
UC.fcs
cd34-A, FSC-H subset
21938
cd73-A, FSC-H subset
0.88
FSC-H :: FSC-H
BL3-A :: cd73-A

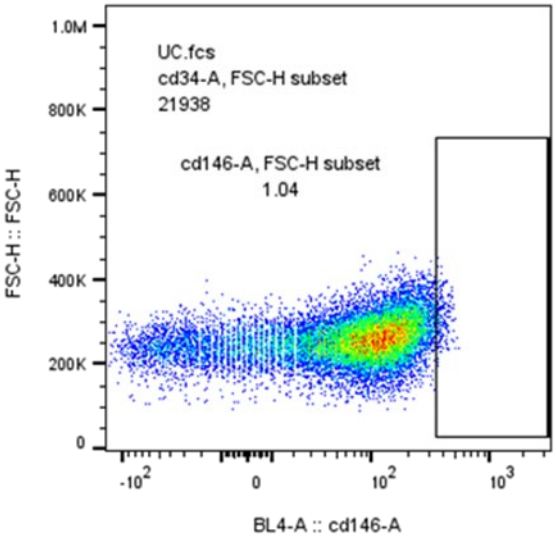
UC.fcs
cd34-A, FSC-H subset
21938
cd146-A, FSC-H subset
1.04
FSC-H :: FSC-H
BL4-A :: cd146-A

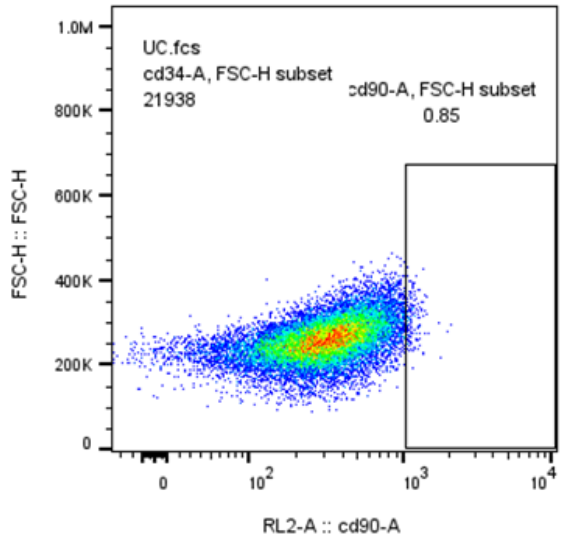
UC.fcs
cd34-A, FSC-H subset
21938
cd90-A, FSC-H subset
0.85
FSC-H :: FSC-H
RL2-A :: cd90-A

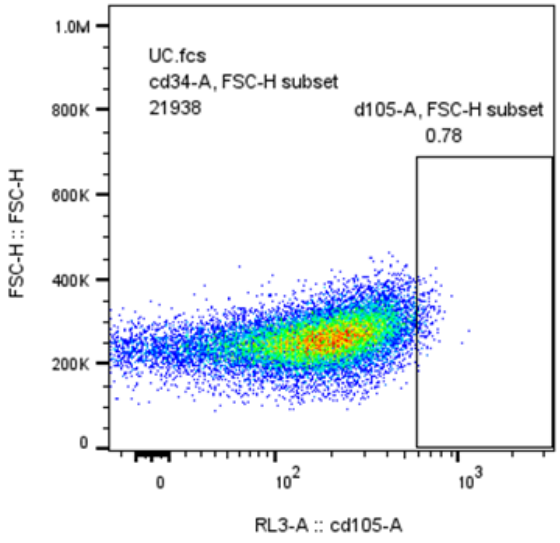
UC.fcs
cd34-A, FSC-H subset
21938
d105-A, FSC-H subset
0.78
FSC-H :: FSC-H
RL3-A :: cd105-A

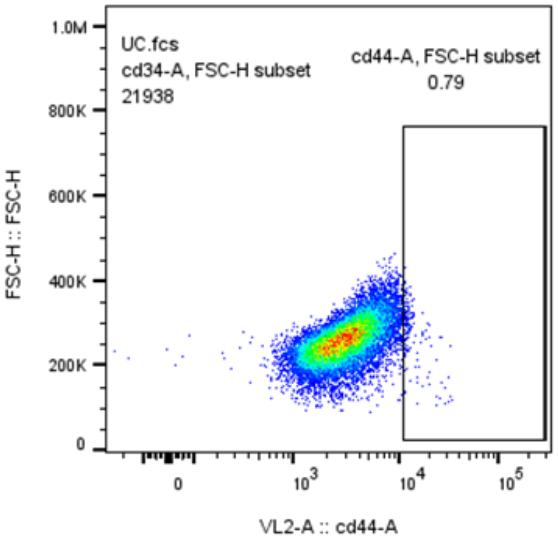
UC.fcs
cd34-A, FSC-H subset
21938
cd44-A, FSC-H subset
0.79
FSC-H :: FSC-H
VL2-A :: cd44-A

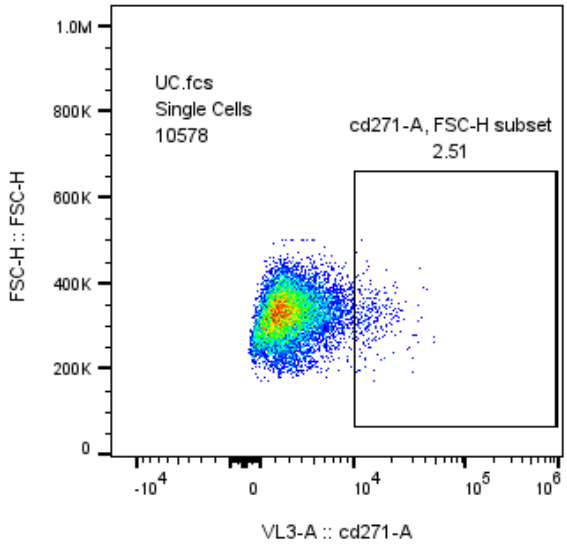
UC.fcs
Single Cells
10578
cd271-A, FSC-H subset
2.51
FSC-H :: FSC-H
VL3-A :: cd271-A

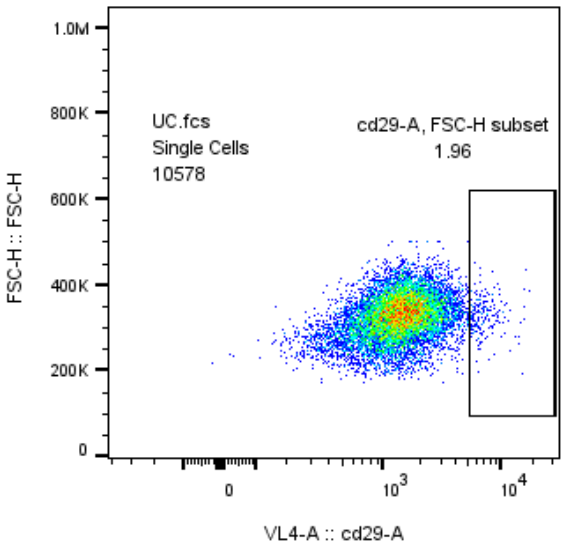

Figure 6. MSC flow panel Gating strategy used in Figures 12, 13, 14 and 15 for monolayer MSC flow cytometry panel, FSC – Forward scatter, SSC – Side scatter A – area, H – height. Cells gated to remove debris, multiplets, negative gating for negative marker mix, negative gate for CD34. Positive expression for other markers was recorded from this gated population. Sytox Blue is used as the viability dye.

2.7.2.2 MSC gating strategy 2

The gating strategy and panel utilised across **Figures 17-20, and 26-29** for encapsulated MSC and MSC spheroid experiments is presented in **Figure 7.** Unstained cells were gated based on side scatter – area (SSC-A) and forward scatter – area (FSC-A), and then FSC-A and forward scatter- height (FSC-H) to remove debris. Next, cells were gated for a negative response to the cell viability dye (Sytox Blye dead cell stain, ThermoFisher Scientific, Cat# S34857) (which permeates into dead cells, not live cells) for laser VL1. Then, cells were gated for a negative response to the HSC lineage cocktail (HSC Lineage Cocktail, ThermoFisher Scientific, Cat# 22-7778-72) for laser BL1 and CD34 (CD34-APC, Miltenyi Biotec, Cat# 130-113-176) for laser RL1 to remove any non-mesenchymal-lineage cells. The remaining cells were then assessed for positive expression for CD166 (CD166 PE, ThermoFisher Scientific, Cat# 12-1668-42) for laser BL2, CD73 (CD73 PerCP-eFluor 710, ThermoFisher Scientific, Cat# 46-0739-42) for laser BL3, CD146 (CD146 PE-Cy7, ThermoFisher Scientific, Cat# 25-1469-42) for laser BL4, CD90 (CD90 AlexaFlour 700, ThermoFisher Scientific, Cat# 56-0909-42) for laser RL2, CD105 (CD105 APC-eFluor 780, ThermoFisher Scientific, Cat# 47-1057-42) for laser RL3, CD44 (CD44 eFluor506, ThermoFisher Scientific,

Cat# 69-0441-82) for laser VL2, CD271 (CD271 Super Bright 600, ThermoFisher Scientific/Invitrogen, Cat# 63-9400-42) for laser VL3 and CD29 (CD29 Super Bright 702, ThermoFisher Scientific, Cat# 67-0299-42) for laser VL4.

The following were omitted due to compensation issues – Biological replicate 1: Negatives (BL1), CD166 (BL2), CD90 (RL2), CD44 (VL2), CD271 (VL3)

Biological replicate 2: CD90 (RL2), CD44 (VL2), CD271 (VL3)

Biological replicate 3: CD90 (RL2), CD44 (VL2), CD271 (VL3)

These values were omitted due to the viability dye being used -Sytox Blue- exhibiting substantial spectral overlap with these channels, and this resulted in false-positive results.

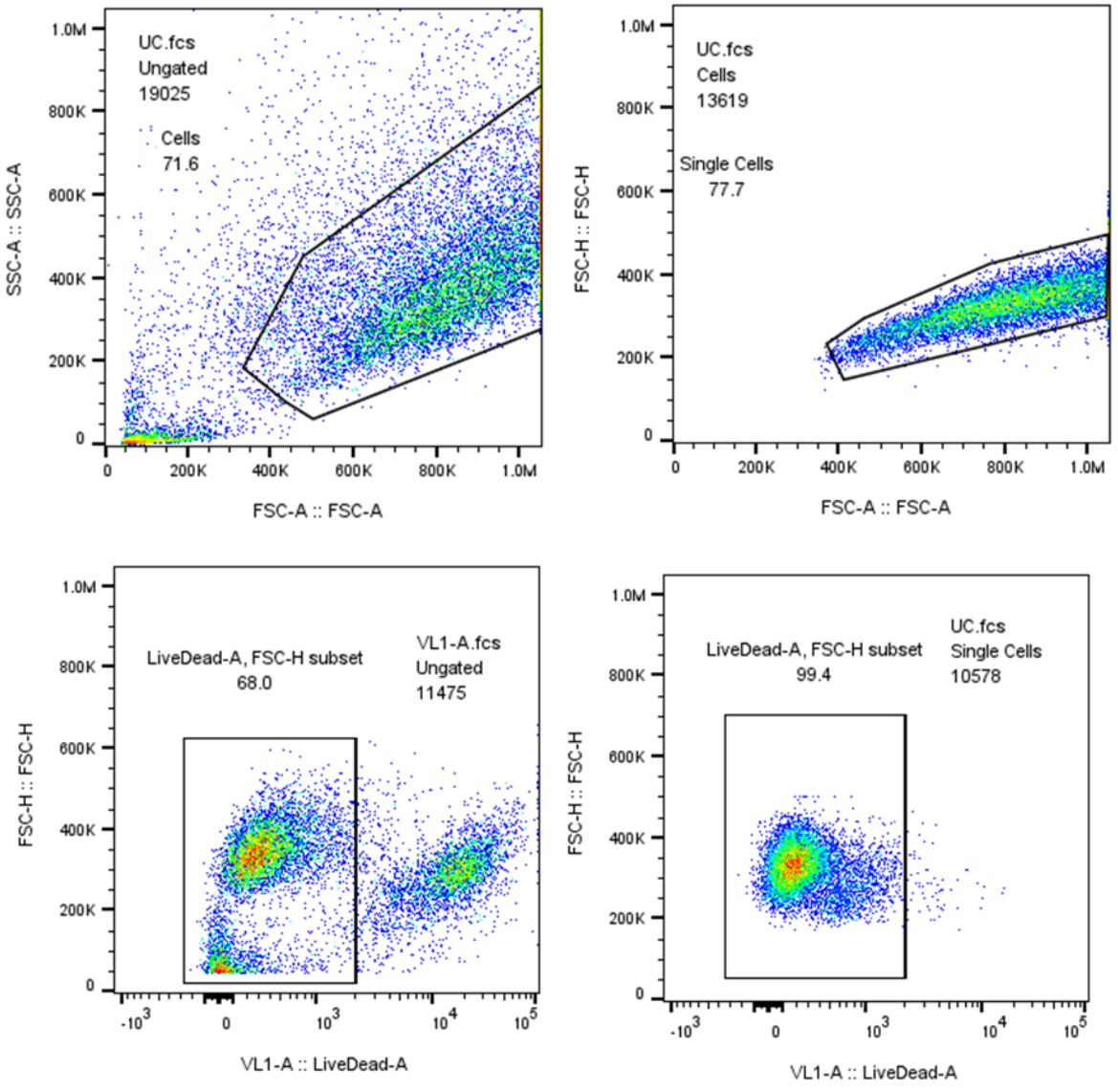

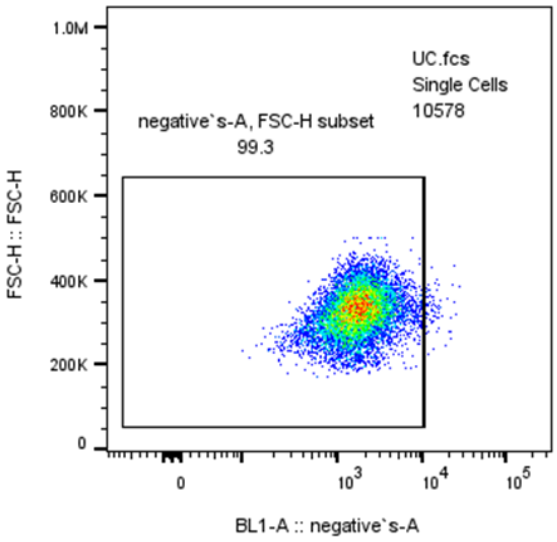
UC.fcs
Single Cells
10578
negative`s-A, FSC-H subset
99.3
FSC-H :: FSC-H
BL1-A :: negative`s-A

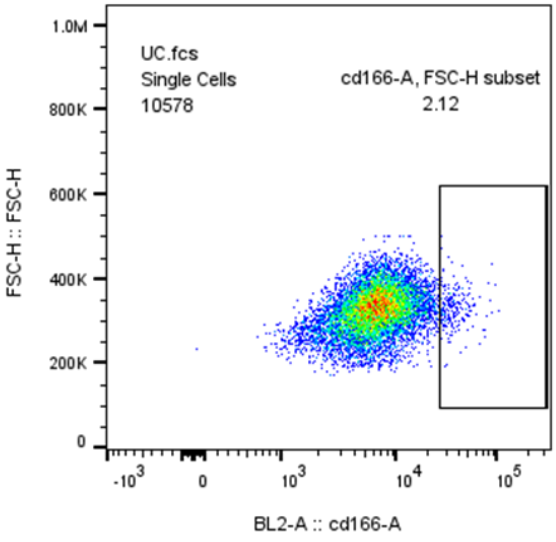
UC.fcs
Single Cells
10578
cd166-A, FSC-H subset
2.12
FSC-H :: FSC-H
BL2-A :: cd166-A

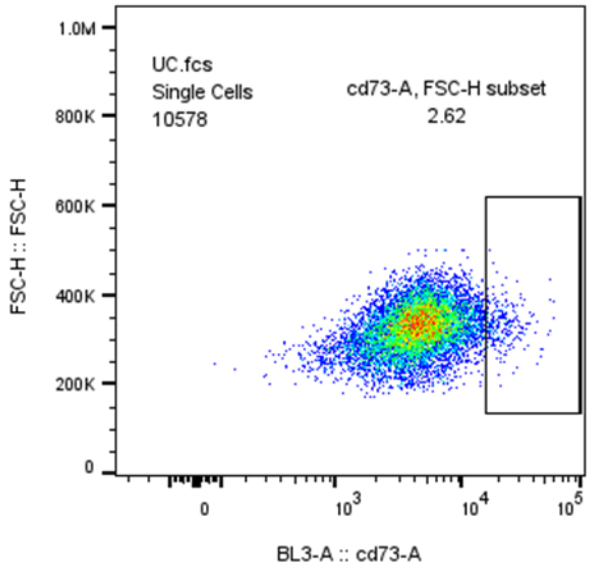
UC.fcs
Single Cells
10578
cd73-A, FSC-H subset
2.62
FSC-H :: FSC-H
BL3-A :: cd73-A

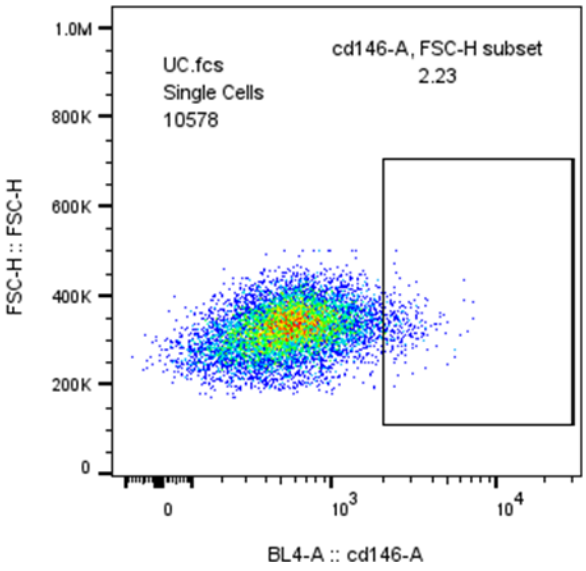
UC.fcs
Single Cells
10578
cd146-A, FSC-H subset
2.23
FSC-H :: FSC-H
BL4-A :: cd146-A

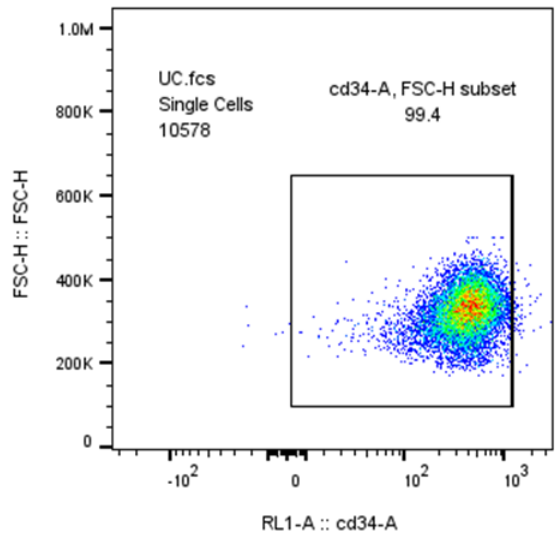
UC.fcs
Single Cells
10578
cd34-A, FSC-H subset
99.4
FSC-H :: FSC-H
RL1-A :: cd34-A

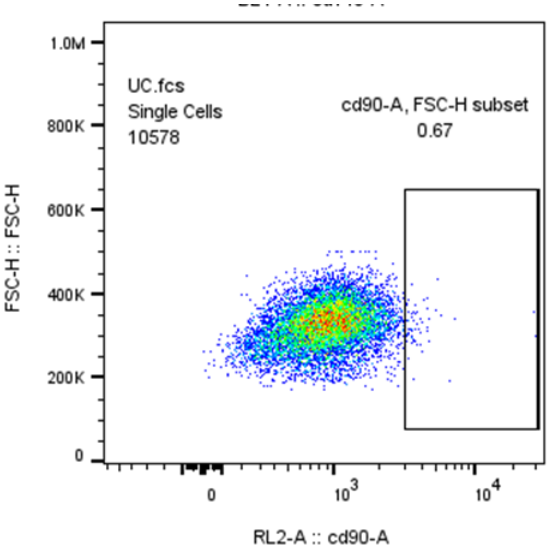
UC.fcs
Single Cells
10578
cd90-A, FSC-H subset
0.67
FSC-H :: FSC-H
RL2-A :: cd90-A

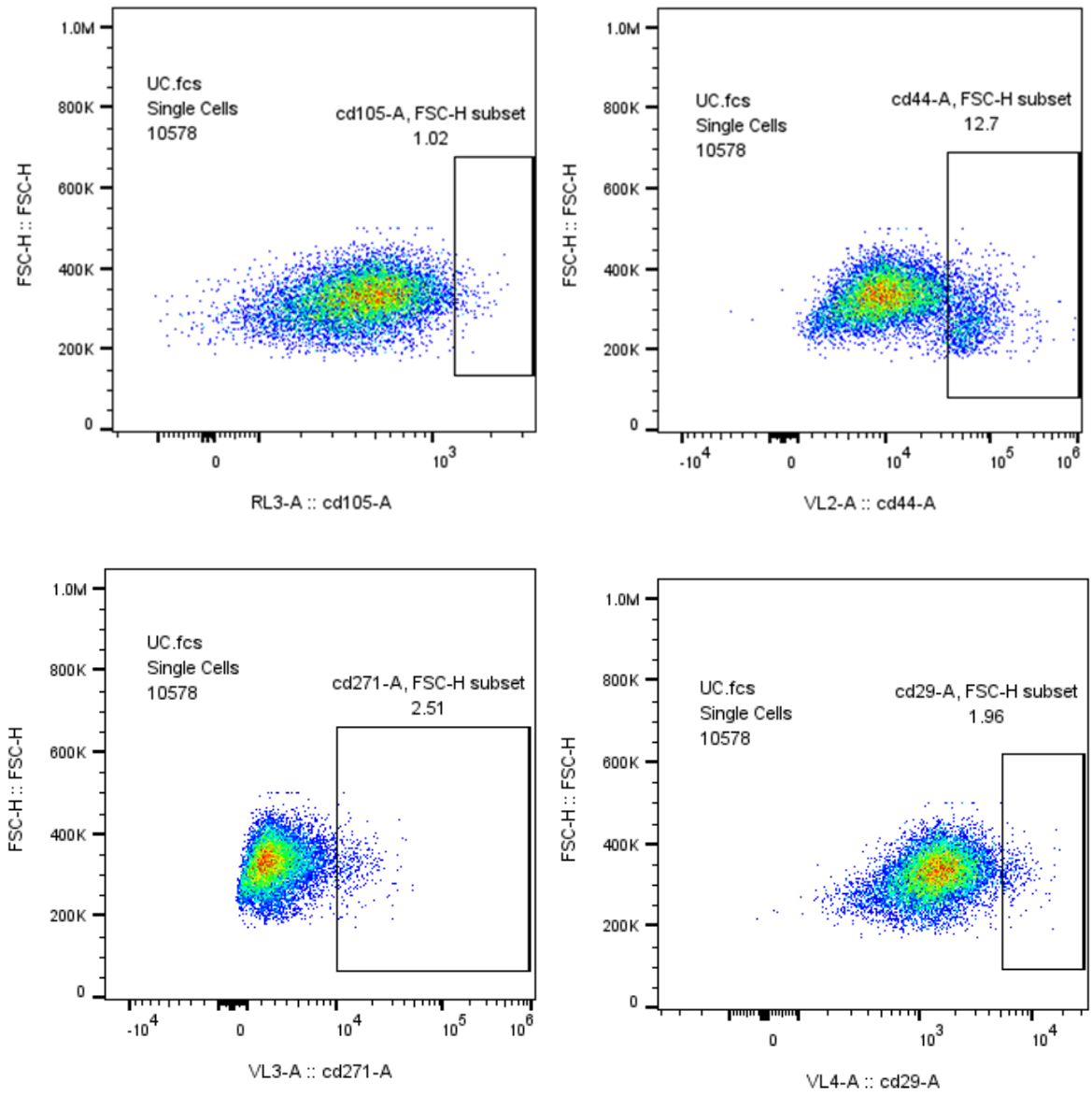

Figure 7. Gating strategy for the MSC flow cytometry panel for single and spheroid MSCs used in Chapter 4, Figures 17, 18, 19, 20, 26, 27, 28 and 29. FSC – Forward scatter, SSC – Side scatter A – area, H – height. Based on unstained control (UC), cells were gated to remove debris, multiplets, negative gating for CD34, and negative gating for negative marker mix. Positive expression for other markers was recorded from this gated population. Sytox Blue is used as a viability dye.

2.7.2.3 MSC gating strategy 3

Issues with the viability dye used in initial experiments, analysed using gating strategies 1 and 2 (**Figures 6 and 7),** resulted in a change to zombie violet and a change in instrument and analysis setup displayed in **Figure 8,** for data displayed in **Figures 30 and 31.** Unstained cells were gated based on side scatter – area (SSC-A) and forward scatter – area (FSC-A), and then FSC-A and forward scatter-

height (FSC-H) to remove debris. Next, cells were gated for a negative response to the cell viability dye (Zombie Violet Fixable Viability Kit, BioLegend, Cat# 423113) (which permeates into dead cells, not live cells) for laser VL1. Then, cells were gated for a negative response to the HSC lineage cocktail (HSC Lineage Cocktail, ThermoFisher Scientific, Cat# 22-7778-72) for laser BL1 and CD34 (CD34-APC, Miltenyi Biotec, Cat# 130-113-176) for laser RL1 to remove any non-mesenchymal-lineage cells. The remaining cells were then assessed for positive expression for CD166 (CD166 PE, ThermoFisher Scientific, Cat# 12-1668-42) for laser BL2, CD73 (CD73 PerCP-eFluor 710, ThermoFisher Scientific, Cat# 46-0739-42) for laser BL3, CD146 (CD146 PE-Cy7, ThermoFisher Scientific, Cat# 25-1469-42) for laser BL4, CD90 (CD90 AlexaFlour 700, ThermoFisher Scientific, Cat# 56-0909-42) for laser RL2, CD105 (CD105 APC-eFluor 780, ThermoFisher Scientific, Cat# 47-1057-42) for laser RL3, CD44 (CD44 eFluor506, ThermoFisher Scientific, Cat# 69-0441-82) for laser VL2, CD271 (CD271 Super Bright 600, ThermoFisher Scientific/Invitrogen, Cat# 63-9400-42) for laser VL3 and CD29 (CD29 Super Bright 702, ThermoFisher Scientific, Cat# 67-0299-42) for laser VL4.

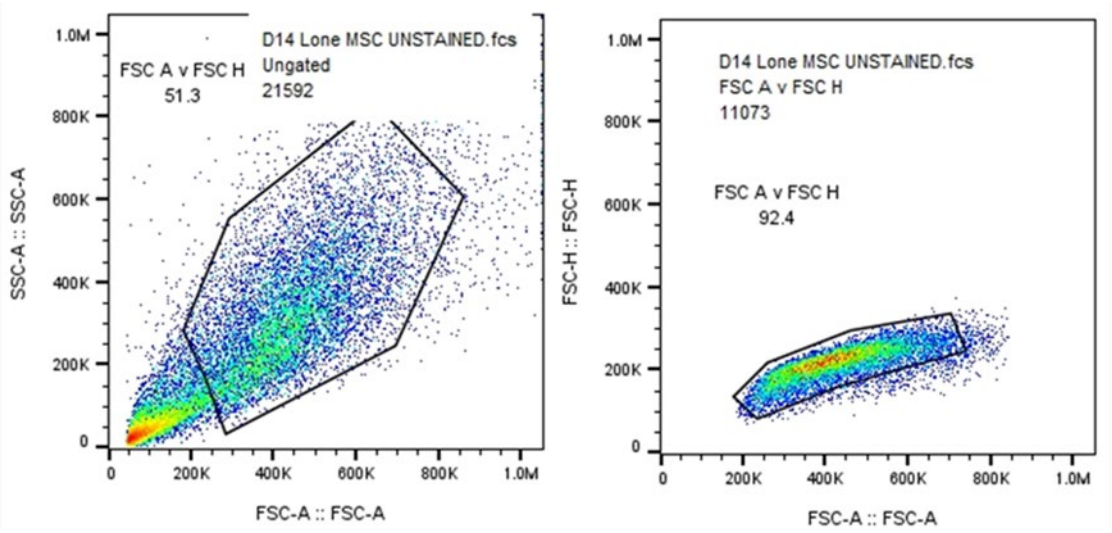

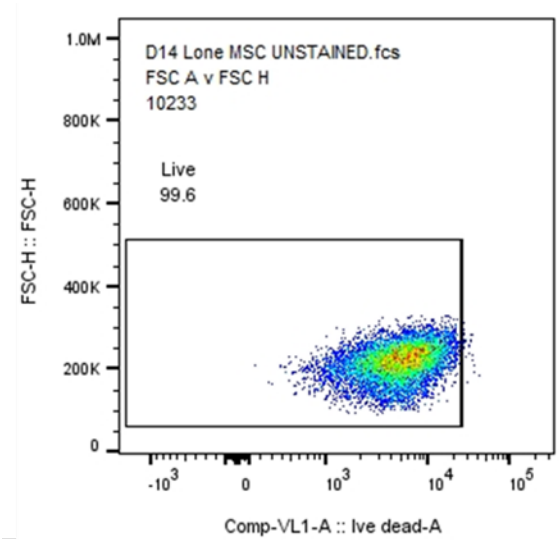
D14 Lone MSC UNSTAINED.fcs
FSC A v FSC H
10233
Live
99.6
FSC-H :: FSC-H
Comp-VL1-A :: Ive dead-A

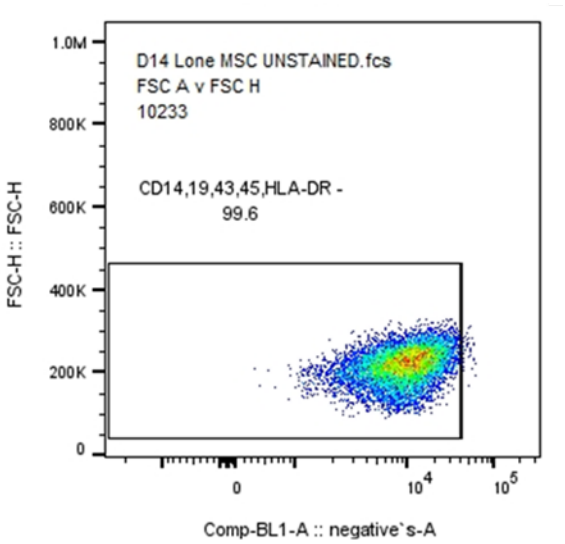
D14 Lone MSC UNSTAINED.fcs
FSC A v FSC H
10233
CD14,19,43,45,HLA-DR -
99.6
FSC-H :: FSC-H
Comp-BL1-A :: negative`s-A

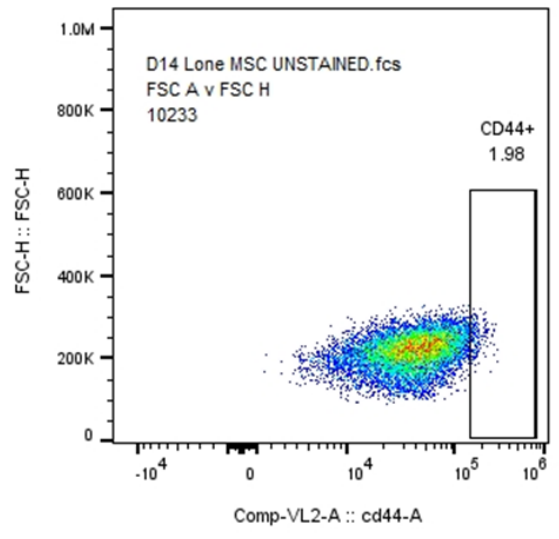
D14 Lone MSC UNSTAINED.fcs
FSC A v FSC H
10233
CD44+
1.98
FSC-H :: FSC-H
Comp-VL2-A :: cd44-A

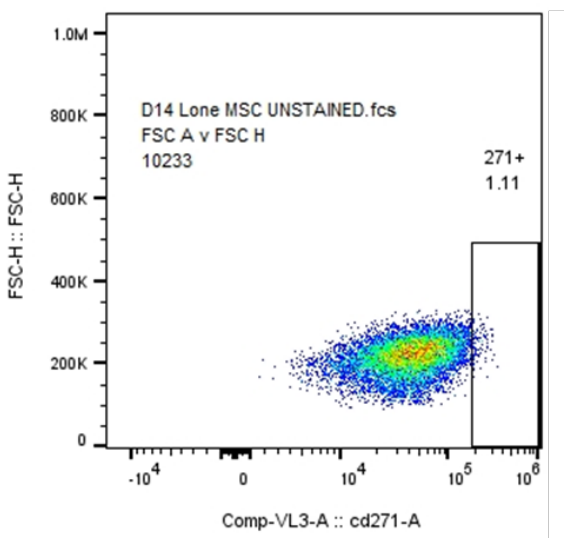
D14 Lone MSC UNSTAINED.fcs
FSC A v FSC H
10233
271+
1.11
FSC-H :: FSC-H
Comp-VL3-A :: cd271-A

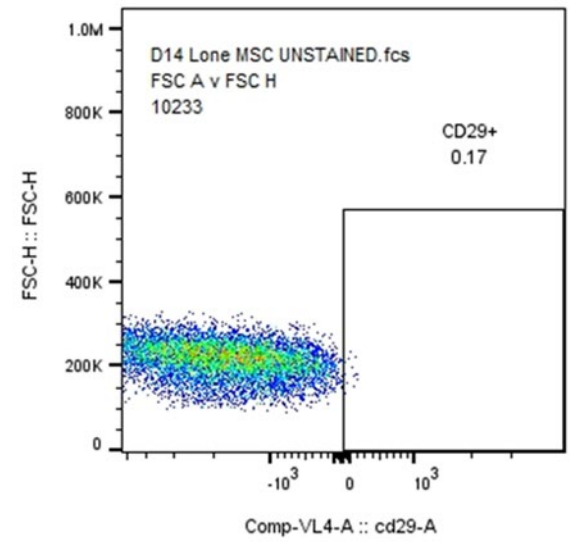
D14 Lone MSC UNSTAINED.fcs
FSC A v FSC H
10233
CD29+
0.17
FSC-H :: FSC-H
Comp-VL4-A :: cd29-A

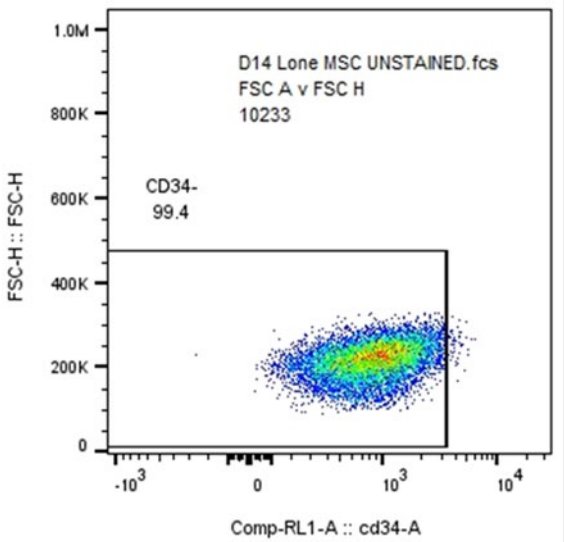
D14 Lone MSC UNSTAINED.fcs
FSC A v FSC H
10233
CD34-
99.4
FSC-H :: FSC-H
Comp-RL1-A :: cd34-A

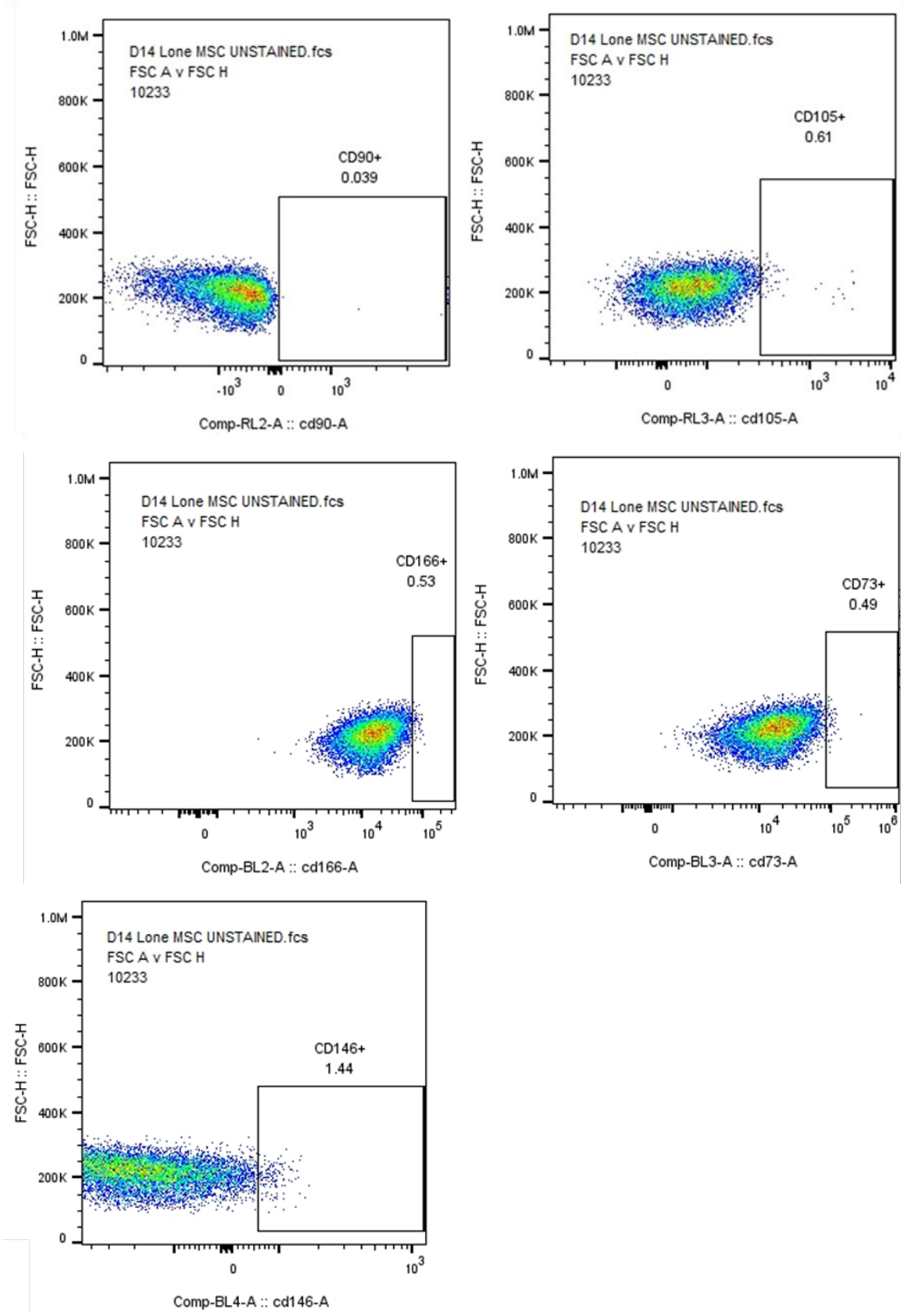

Figure 8. MSC Flow Gating strategy for Figures 30 and 31. MSC flow cytometry panel using an unstained control. FSC – Forward scatter, SSC – Side scatter A – area, H – height. Cells were gated to remove debris, multiplets, negative gating for viability dye, negative marker mix, and analysed using positive gates for other markers.
Zombie violet is used as the viability dye.

2.7.3 HSC gating strategies

2.7.3.1 HSC gating strategy 1

The gating strategy and panel utilised in **Figure 22** for encapsulated HSC experiments is presented in **Figure 9.** Unstained cells were gated based on side scatter – area (SSC-A) and forward scatter – area (FSC-A), and then FSC-A and forward scatter- height (FSC-H) to remove debris. Next, cells were gated for a negative response to the cell viability dye (Sytox Blye dead cell stain, ThermoFisher Scientific, Cat# S34857) (which permeates into dead cells, not live cells) for laser VL1. Then, cells were gated for a positive response to the HSC lineage cocktail (HSC Lineage Cocktail, ThermoFisher Scientific, Cat# 22-7778-72) for laser BL1 and CD45 (CD45 APC eFluor770, Miltenyi Biotec, Cat# 130-110-635) for laser RL3. The remaining cells were then assessed for expression of CD34 (CD34-APC, Miltenyi Biotec, Cat# 130-113-176) for laser RL1, and CD38 (Anti-human CD38 PE-Cy7, ThermoFisher Scientific/Invitrogen, Cat# 25-0388-42) for laser BL4.

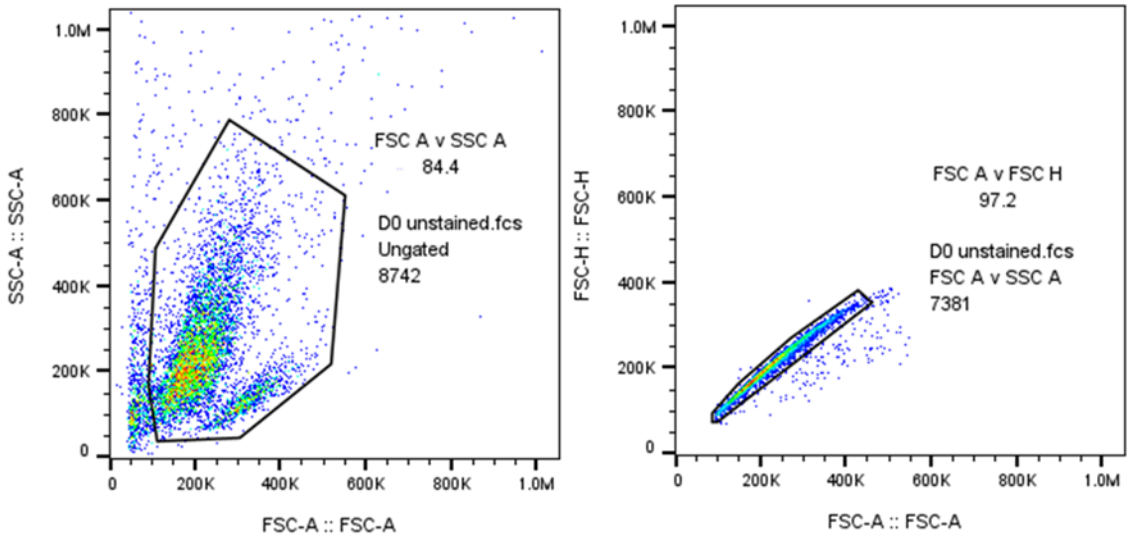

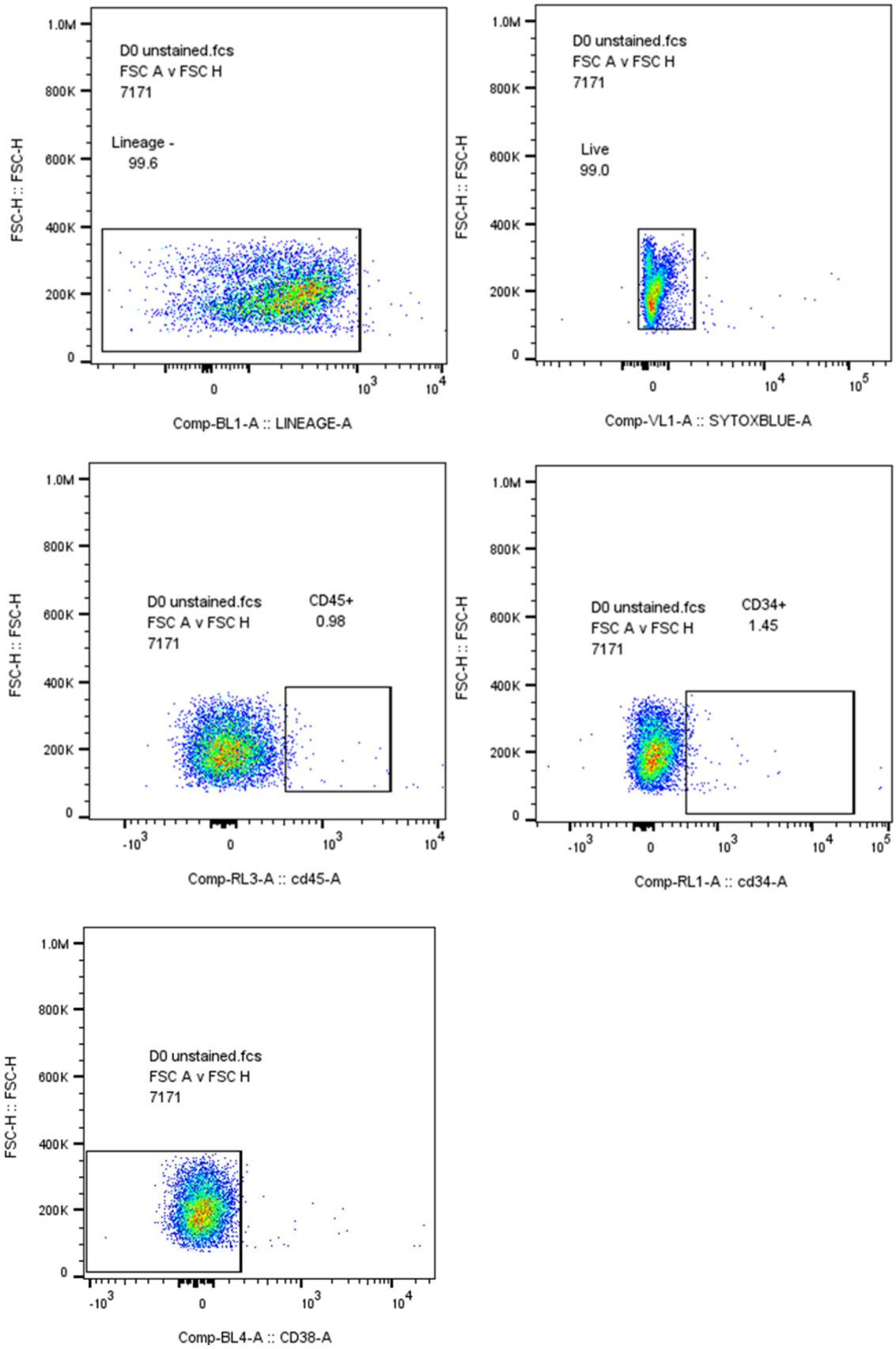

Figure 9. HSC Flow panel used in Figure 22. Gating strategy for HSC flow cytometry panel, FSC – Forward scatter, SSC – Side scatter A – area, H – height. Cells gated to remove debris, multiplets, negative gating for viability dye, negative marker mix and CD38, positive gate for CD45 and CD34. Sytox Blue is used as the viability dye.

2.7.3.2 HSC gating strategy 2

Issues with the viability dye used in initial experiments resulted in a change to zombie violet and a change in instrument and analysis setup for data obtained in **Figure 9**, along with a change in gating strategy and panel to accommodate a more complex analysis with additional surface markers. The gating strategy and panel utilised in **Figure 33** for encapsulated HSC experiments is presented in **Figure 10.** Unstained cells were gated based on side scatter – area (SSC-A) and forward scatter – area (FSC-A), and then FSC-A and forward scatter- height (FSC-H) to remove debris. Next, cells were gated for a negative response to the cell viability dye (Zombie Violet Fixable Viability Kit, BioLegend, Cat# 423113) (which permeates into dead cells, not live cells) for laser VL1. Then, cells were gated for a positive response to CD45 (CD45 APC eFluor770, Miltenyi Biotec, Cat# 130-110-635) for laser RL3. The remaining cells were then assessed in a series of cross-gates for expression of CD16 (CD16 Monoclonal Antibody (eBioCB16(CB16)), ThermoFisher Scientific/Invitrogen, Cat# 69-0168-42) for laser VL2 and CD41/CD61 (CD41/CD61 Monoclonal Antibody (PAC-1), ThermoFisher Scientific/Invitrogen, Cat# MA5-44123) for laser BL1, then for CD38 (Anti-human CD38 PE-Cy7, ThermoFisher Scientific/Invitrogen, Cat# 25-0388-42) for laser BL4 and CD7 (CD7 Monoclonal Antibody (4H9) eBioscience, ThermoFisher Scientific/Invitrogen, Cat# 46-0078-42) for laser BL3, then for CD34 (CD34-APC, Miltenyi Biotec, Cat# 130-113-176) for laser RL1, and finally for CD45RA (CD45RA Monoclonal Antibody (HI100), ThermoFisher Scientific/Invitrogen, Cat# 63-0458-42) for laser VL3 and CD90 (CD90 AlexaFluor 700, ThermoFisher Scientific/Invitrogen, Cat# 56-0909-42) for laser RL2.

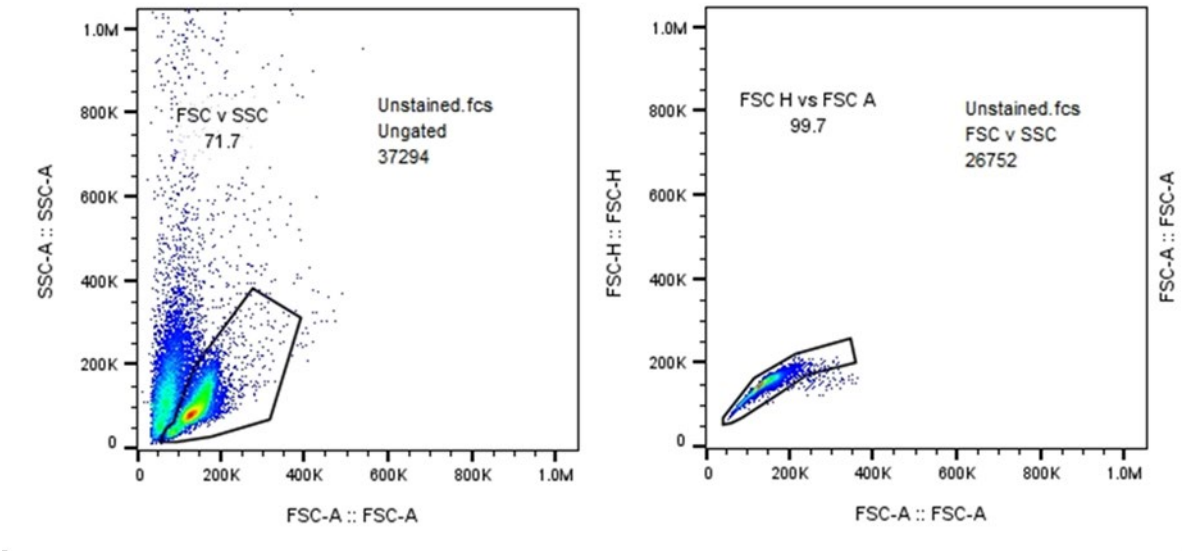

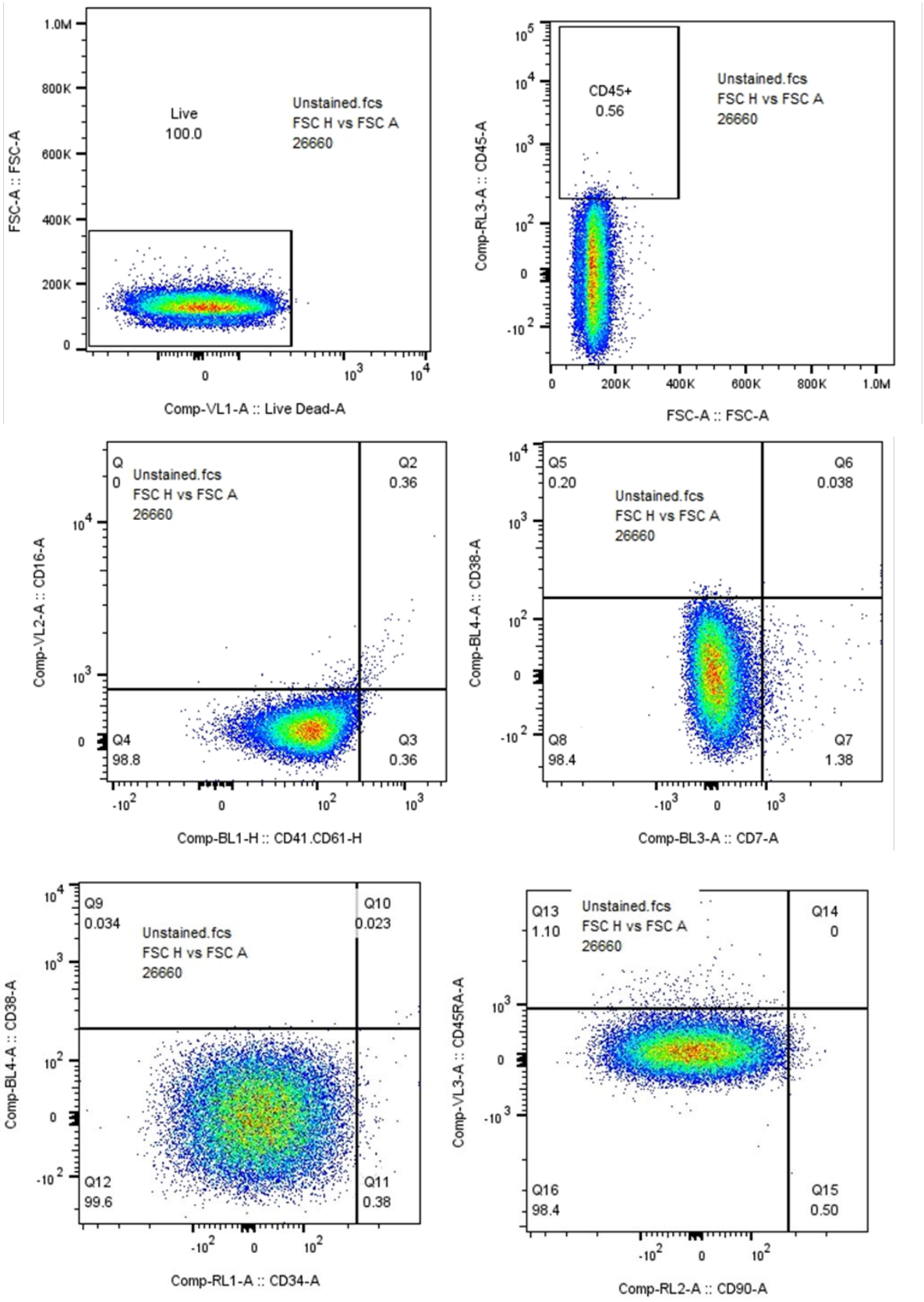

Figure 10. CD34+ Flow Gating strategy for Figure 28. HSC flow cytometry panel using an unstained control. FSC – Forward scatter, SSC – Side scatter A – area, H – height. Cells gated to remove debris, multiplets, negative gating for viability dye, negative marker mix and CD38, positive gate for CD45 and CD34. Zombie violet is used as the viability dye.

2.8 Nanoindentation

Experiments were performed, and data sets cleaned and analysed using the protocol established by Ciccone *et al*. in 2022 for the Chiaro nanoindentor (Ciccone et al., 2022). The probe was selected with the following specifications: Geo Factor in air 2.99, 3000 nm radius, 0.47 Nm^{-1} elastic constant (OpticsID life, Cat#P240253M). Samples were attached to the surface of a culture dish using MP Biomedicals™ Fixogum Rubber Cement (FisherScientific, Cat# 11430456) and submerged in DPBS++ (Gibco, Cat#14040133). A matrix scan of 20 points (5X and 4Y) was performed on each sample, with a distance between points (dx) of 6nm (the width of the probe, so measurements do not overlap).

2.9 LTC-IC

Colony-forming assays were designed and analysed using the protocols 'Human Colony-Forming Unit (CFU) Assays Using Methocult™ (and 'Human Long-Term Culture-Initiating Cell (LTC-IC) Assays' by Stemcell Technologies™ (Stemcell technologies, 2019). S1/S1 and M2-10B4 fibroblasts were seeded onto collagen-coated 6-well plates, and the day before the experiment, treated with Mitomycin-C (Biotechne, Cat# 74142) to halt proliferation. The HSCs were resuspended in Human Long-term Culture Medium (Myelocult™ H5100) (Stemcell technologies, Cat# 05150) supplemented with 1 μM Hydrocortisone hemisuccinate (Stemcell technologies, Cat# 74142) and added on top of the fibroblast feeder layer. Half of the media changes were performed once per week for 5 weeks, and then the CD34+s were removed and resuspended in Methocult™ H4435 (Stemcell technologies, Cat# 4435) growth medium. They were seeded in fresh plates and allowed to colonise for 14 days before colony counting. Colonies were categorised into CFU-E, BFU-E, CFU-GM and CFU-GEM **(see Figure 22).**

2.10 Experimental time-point set-up

During initial experiments, the day of cell encapsulation is categorised as day 0 (D0). This was consistent throughout this thesis. However, MSCs were aggregated two days before seeding as spheroids. As MSCs were characterised pre-aggregation and again on day 0 - to determine effects of aggregation as well as encapsulation - a day minus 2 (day-2) timepoint was introduced to avoid confusion and maintained throughout.

2.11 Statistical methods

In general, experiments were carried out in triplicate, and as three data points are not enough to justify an assumption of normality, and to minimise assumptions, non-parametric statistical tests were used. Further, data sets were independent and possessed similar variance. Therefore, Mann-Whitney U tests were used to measure statistical differences between individual data sets.

Assuming normality in data with limited replicates is not uncommon. By considering the central limit theorem, which says that as the number (N) of observations increases, a distribution must approach normality. Therefore, for many data sets, assuming normality is justified. However, due to the nature of cells and the limited three data points (from different biological replicates/donors) per data set, this is not suitable for most of the data presented in this work.
From a mathematical standpoint, GraphPad offers 4 different tests for normality: the D'Agostino & Pearson test, the Anderson-Darling test, the Shapiro-Wilk test and the Kolmogorov-Smirnov test (GraphPad Prism 10 Statistics Guide - Choosing a Normality Test, n.d.). All but the Shapiro-Wilk test say N=3 is too small to assess normal distribution, and therefore not to assume normality.

From an observational standpoint, as each replicate is a different donor, it cannot be assumed that they are behaviourally similar. As examples, many MSC donors were deemed not suitable for this work because they failed to aggregate into spheroids and/or demonstrated decreasing surface marker expression during culture/lost it entirely. While these criteria were met before a donor was used for experiments, it cannot be guaranteed that donor variability would not lead to different results based on the experimental conditions. For example, inconsistent surface marker expression between donors when aggregated could lead to variable results, but be due to donor variability, rather than experimental technique. However, this data would still be expected to approach a normal distribution over time. More importantly, as explained during the introduction, within a seemingly homogenous stem cell population, several potential subpopulations exist instead. Therefore, it is probable that with enough replicates, data points would cluster into groups based on common traits rather than exhibiting a normal distribution encompassing all of them. This variability is particularly apparent for HSPCs, which, due to needing to be used

immediately without any culture (other than overnight thawing if frozen), did not undergo any observation or screening other than the CD34 magnetic cell sorting as part of the isolation process. Therefore, as is presented later in this work, the cells do indeed exist in subpopulations with different properties, and therefore, assessing them collectively would be incorrect, as data would likely cluster based on the weighting of the subpopulations. It is therefore more useful to compare the donors individually.

The exceptions are for **figures 30, 31 and 32. Figures 30 and 31** were carried out with the same cell donor and represent three experimental replicates. In this case, as conditions and the donor were both constant, it is more reasonable to assume normality, as behavioural features should be consistent. For **Figure 32**, the donor was irrelevant, as the cell/spheroid number was consistent between each other, and the donor would not impact the properties of the gel. With this, all variables were controlled, and sub-populations and clustering would be unlikely. Therefore, a normal distribution can be assumed.
To compare the means of the **figures 30, 31 and 32** data sets, t-tests were performed. While the starting cell gel population is the same, the same gel is not measured at both time points, and so the data sets are unpaired. While it is likely that with increasing N, the standard deviations of each population would trend to a similar value, the populations do not have equal standard deviations; therefore, Welch’s correction was applied.

Chapter 3. Single Cell Encapsulation

3.1 Introduction

Reports of alginate used for cell encapsulation were first published at the end of the 70's when pancreatic islets were encapsulated and cultured at 37 °C for up to 4 months, maintaining their morphology and functionality (Zimmerberg et al., 1980). Since then, this use has been recorded for a variety of cell types; however, this is usually under the pretence of culture at 37 °C (Eleftheriadou et al., 2022; Sarker et al., 2015; Swioklo et al., 2016; Wright et al., 2012). Further, when used for adherent cell types, the gel is usually customised to contain RGD binding sites (Bonani et al., 2020; Sarker et al., 2015). Aside from culture, alginate encapsulation is also used as a delivery system, with cell-laden bead implantation used to enable controlled release from therapeutic cells or to enhance engraftment (Bhujbal et al., 2014; Kavand et al., 2024).

Use as a protectant under hypothermic or cryogenic temperatures, however, is usually due to a non-functionalised alginate. Although even at 37 °C, encapsulated myoblasts cultured for a week remain rounded and enter quiescence (Hejbøl et al., 2017). Encapsulation within alginate not only helps to induce a reduced metabolic state; it acts like biological bubble wrap. Its porosity enables nutrients and toxins to enter and disperse from the cell, while also stabilising the membrane, which is disrupted as temperatures decrease. However, hypothermic storage is not commonplace, as covered in **Section 1.4**. In fact, other than Chen *et al.*'s 2013 study, where MSCs were stored at 20 °C for 5 days and retained ~80% viability, most work has been performed by Atelerix and Newcastle University (B. Chen et al., 2013). They have demonstrated hypothermic cell storage, typically for a few days (Atelerix, 2022). Further, the exact storage temperature is variable, with the optimal being from 4 °C to 25 °C. However, while information at the start of the project indicated that 15 °C-25 °C is optimal for 2 to 3 weeks, this has since been amended to be specifically at 15 °C, and 14 days for A-MSCs and 7 days for BM MSCs (Atelerix, 2022; Swioklo et al., 2016). This chapter intends to validate these findings and investigate surface marker expression during the encapsulation process.

It was difficult to find examples of HSCs being encapsulated in alginate for storage purposes, with them instead being cultured in or on gels, such as for *In vitro* culture of hematopoietic stem cell niche using angiopoietin-1-coupled

alginate hydrogel, and *in vitro* expansion of hematopoietic stem cells in a porous hydrogel-based 3D culture system (Lee et al., 2022; Liu et al., 2023). This chapter intends to develop an understanding of HSC encapsulation in alginate and whether there are potential applications.

3.1.1 Aims and objectives

As Atelerix have the storage conditions for MSCs defined, the encapsulation technique should be validated by replicating their data. It was also necessary to start testing conditions that will likely be used for CD34+s and spheroid encapsulation further in the study. This chapter aims to determine if conditions optimal for MSC storage were matched by CD34+s by testing viability temperatures and whether serum-free media supplementation was beneficial to the HSCs. If it were not, then this would drastically reduce the cost of encapsulation. This will be carried out using viability staining and surface marker analysis using flow cytometry.

The base hypotheses were that BM-MSCs would be viable under encapsulation (favouring 15 ºC) and that quiescence-capable HSPCs would also be viable under the same conditions.

3.2 Results

3.2.1 MSC viability - temperature

To confirm that MSCs remained viable within the gels up to 21 days at 15 ºC, as stated by the manufacturer, some preliminary work was undertaken to confirm this **(Figure 11)**; these were only performed with one biological replicate. Viability of MSCs encapsulated at 4 ºC was poor, falling to 62% after a single day, 20% after a week and with no viable cells after 21 days, **see Figure 11a**. For 15 ºC, however, viability was 82% on day 1 and fell to 67% after 14 days. There was a more substantial drop over the final 7 days to 53%. Therefore, there was a 15% difference in viability from 15 to 4 ºC after just a single day, falling to 72% by day 7. **Figure 11b** shows starting viabilities around 94, 94 and 95% for 15, 20 and 37 ºC, respectively. A different donor was used for this experiment, and so differences between both 15ºC results were expected. By Day 21 at 37 ˚C, the gels had degraded; however, after 7 days, viability was at 56% (a 42% decrease) and at 39% (a 59% decrease) by day 14. By day 14, 20 ˚C gels had fallen to 45% viability (a 53% decrease) compared to 68% (a 29% decrease) for those at 15 ˚C.

While viability was 68% (a 28% decrease) and 45% (a 52% decrease) for 15 ºC and 20ºC respectively. Therefore, by day 14, there was a 34% difference between 15 ˚C and 20 ˚C; however, as the only two temperature conditions with viable populations after 21 days, these two conditions were progressed.

3.2.2 MSC culture in IMDM and DMEM

As HSCs require IMDM, studies were undertaken to determine the effects of media on encapsulated MSCs. Initially, the aim was to determine if priming the MSCs by transitioning to the alternate media would affect the cells **(Figures 12 and 13)**; in particular, changes from day 1 to day 7 for each media. For CD29, 105 and 73 (**Figure 12a, c and e),** DMEM saw greater expression intensity relative to IMDM at both day 1 and day 7.

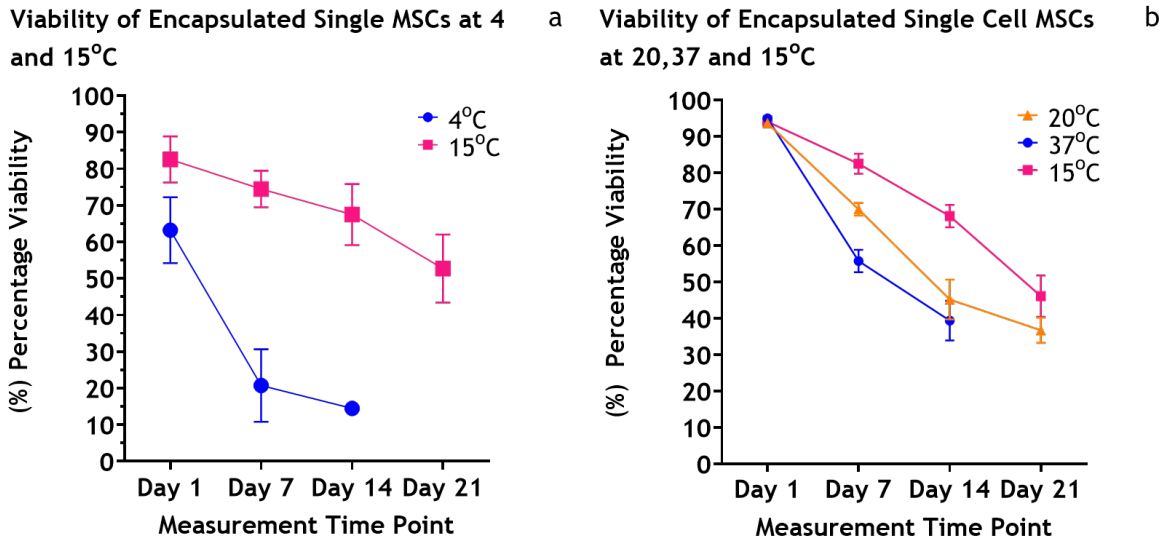

Figure 11. MSCs encapsulated within alginate hydrogels.

N=1 study to replicate the literature and consolidate the experimental technique (Swioklo et al., 2016). No statistics performed due to N=1. Error bars display mean +/- one standard deviation of 9 technical replicates.

Percentage viability of MSCs encapsulated in alginate hydrogel beads for 21 days.

a) Viability of MSCs encapsulated at 15 ˚C and 4 ˚C to compare with traditional non-frozen storage conditions.

b) Viability of MSCs encapsulated at 15, 20 and 37 ºC for 21 days to compare with room temperature and body temperature.

21 Day timepoint was not recorded for 37 ˚C as gels had degraded.

This trend was less apparent for CD90 and CD166 (**Figure 12d and f),** where expression at day 7 was the same between media types. CD146 (**Figure 12b)** was the only marker to show increased expression in IMDM relative to DMEM at day 14. All marker expression was upregulated at day 7 relative to day 1.
However, replicate variability was particularly noticeable when plotting the data sets separately **(Figure 13)**. For example, CD146 **(Figure 13b)** was upregulated far more at day 7 for biological replicate 3 than the other two replicates. Whilst for CD73 **(Figure 13e),** biological replicate 1 exhibited a noticeable increase at day 7, whereas other donors remained in line with day 1 results. Further, biological replicate 1 for CD166 **(Figure 13f)** displayed day 7 IMDM expression greater than day 7 DMEM – in contrast to trends throughout the rest of the data. However, error bars for this value are large, and so with additional experimental replicates, this could have fallen back within the general trend.
For biological replicate 1, the intensity of expression was higher for DMEM at day 0 for all markers, but by day 7, the intensity of expression under IMDM was greater than DMEM for CD29, CD146, CD90 and CD166 **(Figures 13a, b and f)**. However, the intensity did increase from day 0 to day 7 for all markers, independent of media type. For replicate 2, DMEM was greater than IMDM for CD29, CD105, CD90 and CD166 **(Figures 13a, c, d and f)** at both day 1 and day 7. DMEM intensity was higher at day 1 for CD146 **(Figure 13b)**, but IMDM was then higher at day 7. In contrast, IMDM was higher at day 1 for CD73 **(Figure 13e)**, but DMEM was then higher at day 7. For replicate 3, day 7 intensity was higher than day 1 intensity for both DMEM and IMDM, and DMEM was greater than IMDM at both day 1 and day 7 for CD29, 105, CD90, CD73 and CD166 **(Figure 13a, c, d, e, f)**.
Analysing the gating strategy by graphing the percentage of population gated as positive for each marker showed no significant difference between the population percentages with negative CD45 expression, nor between the CD34 negative populations **(see Figures 14 and 15).** However, it was noted that the graphs for all markers **(Figures 14c-h and 15c-h)** were nearly identical to the CD34 gated graph **(Figure 14b and 15b)**, except for the biological replicate 1, CD146 expressing population **(Figure 14d and 15d)**.
When analysing the donors individually, the percentage of cells expressing

(Figure 15) for IMDM is much lower than for DMEM for replicate 1 on day 1, but after 7 days, it recovers back to a percentage higher than DMEM. Biological replicate 2 shows a greater percentage for DMEM compared to IMDM at both day 1 and day 7 for all markers **(Figure 15)**. However, the percentage of cells expressing at day 7 decreases relative to day 1 for both media types. Lastly, replicate 3 displays an increase in percentage at day 7 compared to day 1 for each media type. However, while the percentage of expression at day 7 is roughly the same for both media types, at day 1, IMDM has more cells expressing than DMEM for all surface markers.

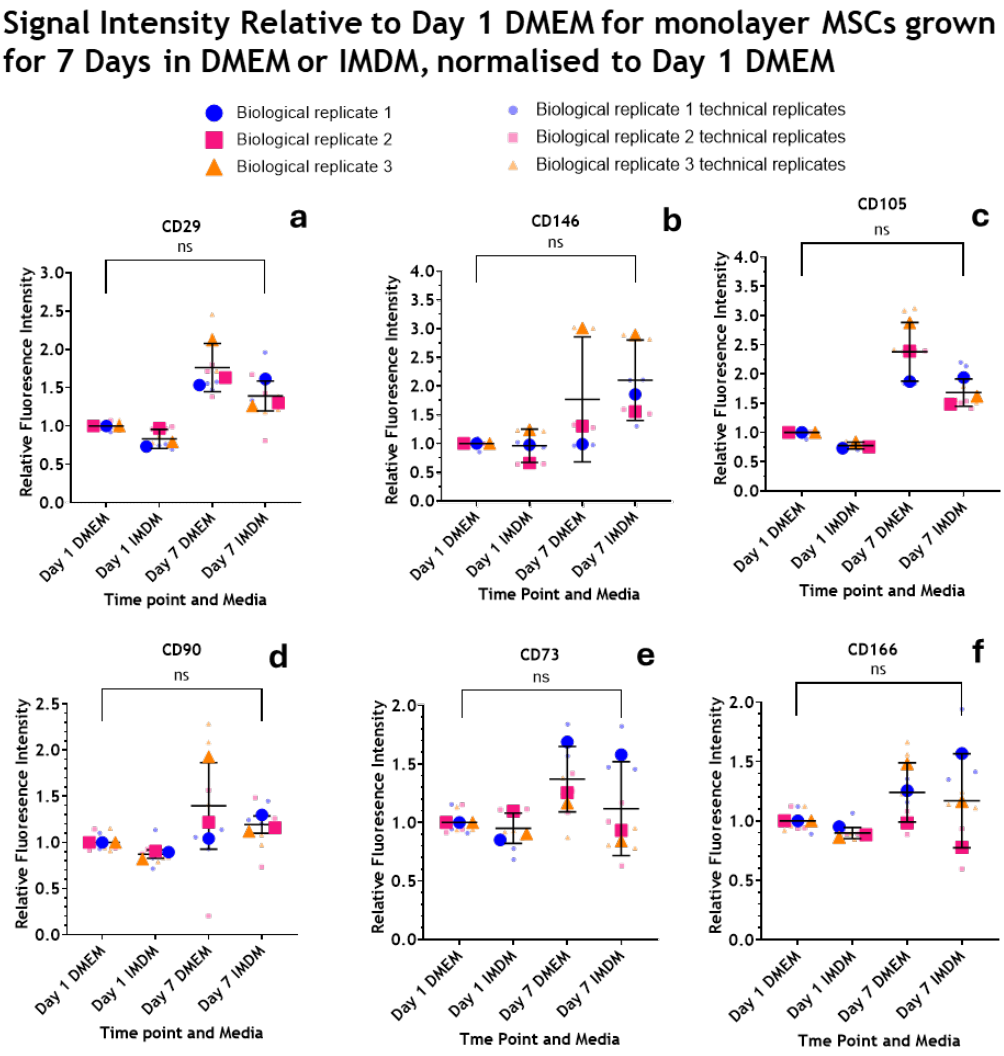

Figure 12. Fluorescence intensity geometric mean measured by flow cytometry of monolayer MSCs 1 and 7 days after seeding in either IMDM or DMEM, normalised to the day 1 DMEM condition.

Super plots depict expression of the following markers a) CD29, b) CD146, c) CD105, d) CD90, e) CD73, f) CD166 in the live, CD45- and CD34- gated data sets.

Error bars indicate the mean +/- one standard deviation of biological replicate data points. Brighter, larger points depict the mean value for that biological replicate, while the paler colours indicate the technical replicates.

Significance was calculated for comparison of data from the same media type and same measurement time point by using the Mann-Whitney U test with bounds of non-significance p>0.05.

Signal Intensity Relative to Day 1 DMEM for monolayer MSCs grown for 7 Days in DMEM or IMDM, normalised to Day 1 DMEM, with biological replicates separated.

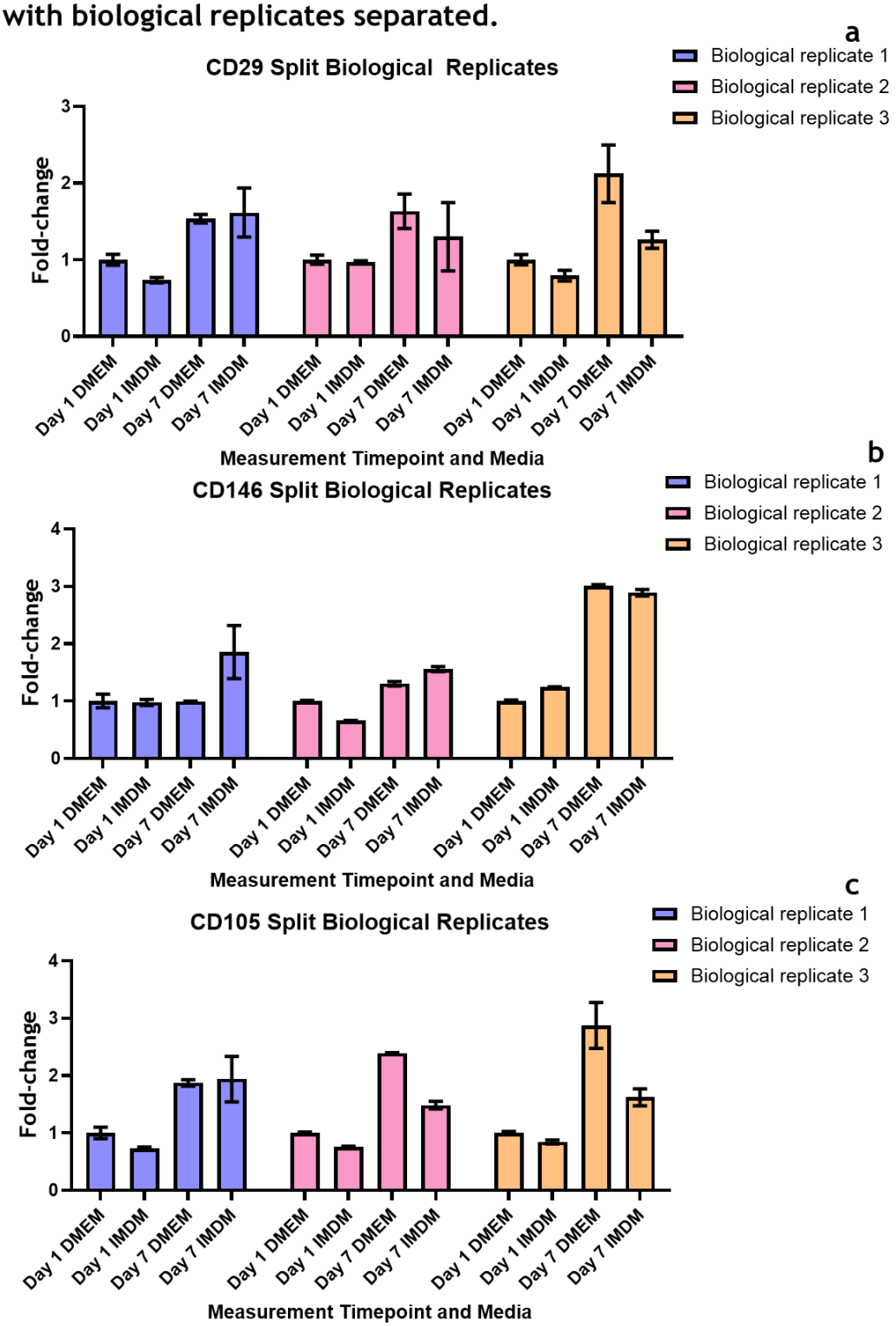

Signal Intensity Relative to Day 1 DMEM for monolayer MSCs grown for 7 Days in DMEM or IMDM, normalised to Day 1 DMEM, with biological replicates separated.

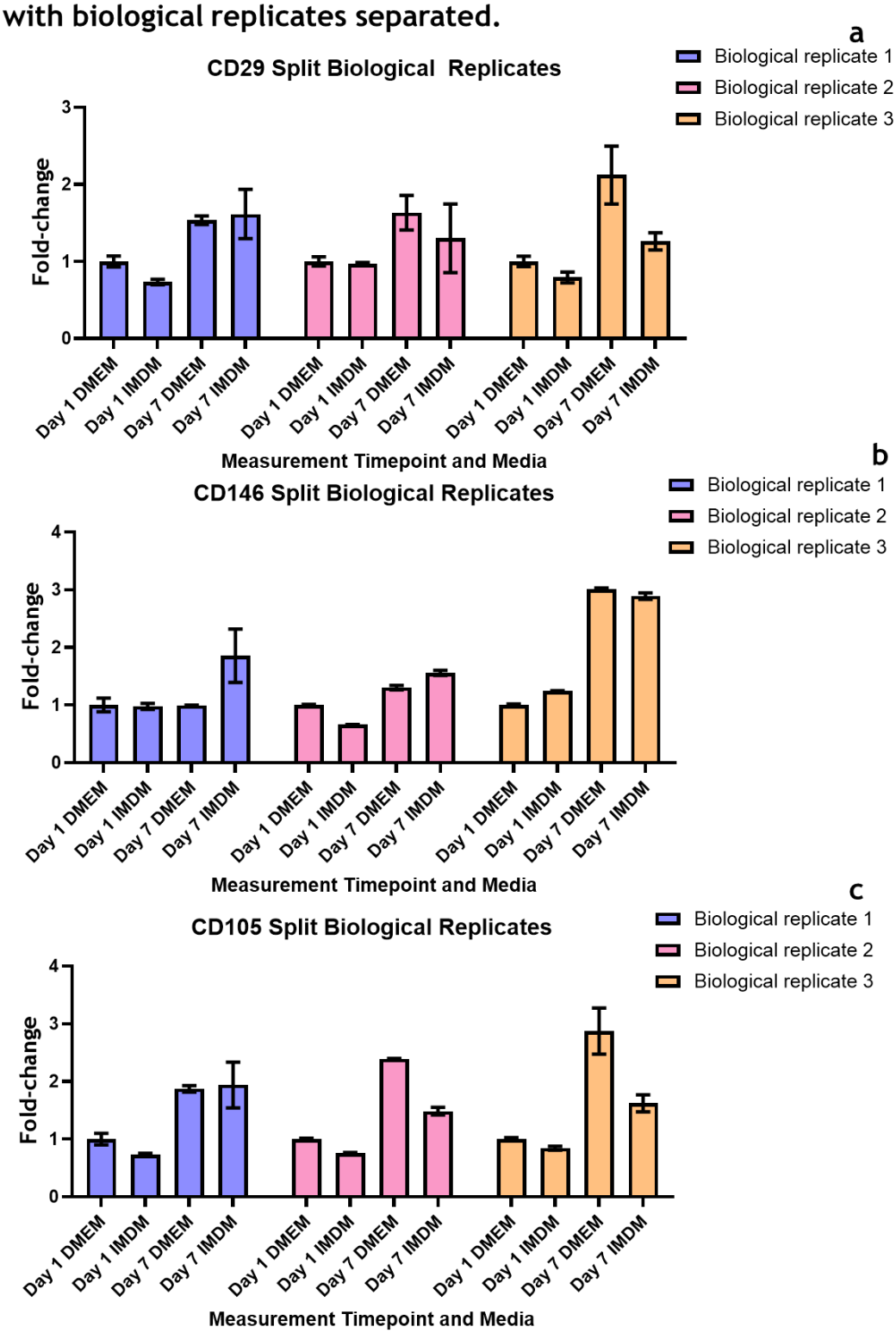

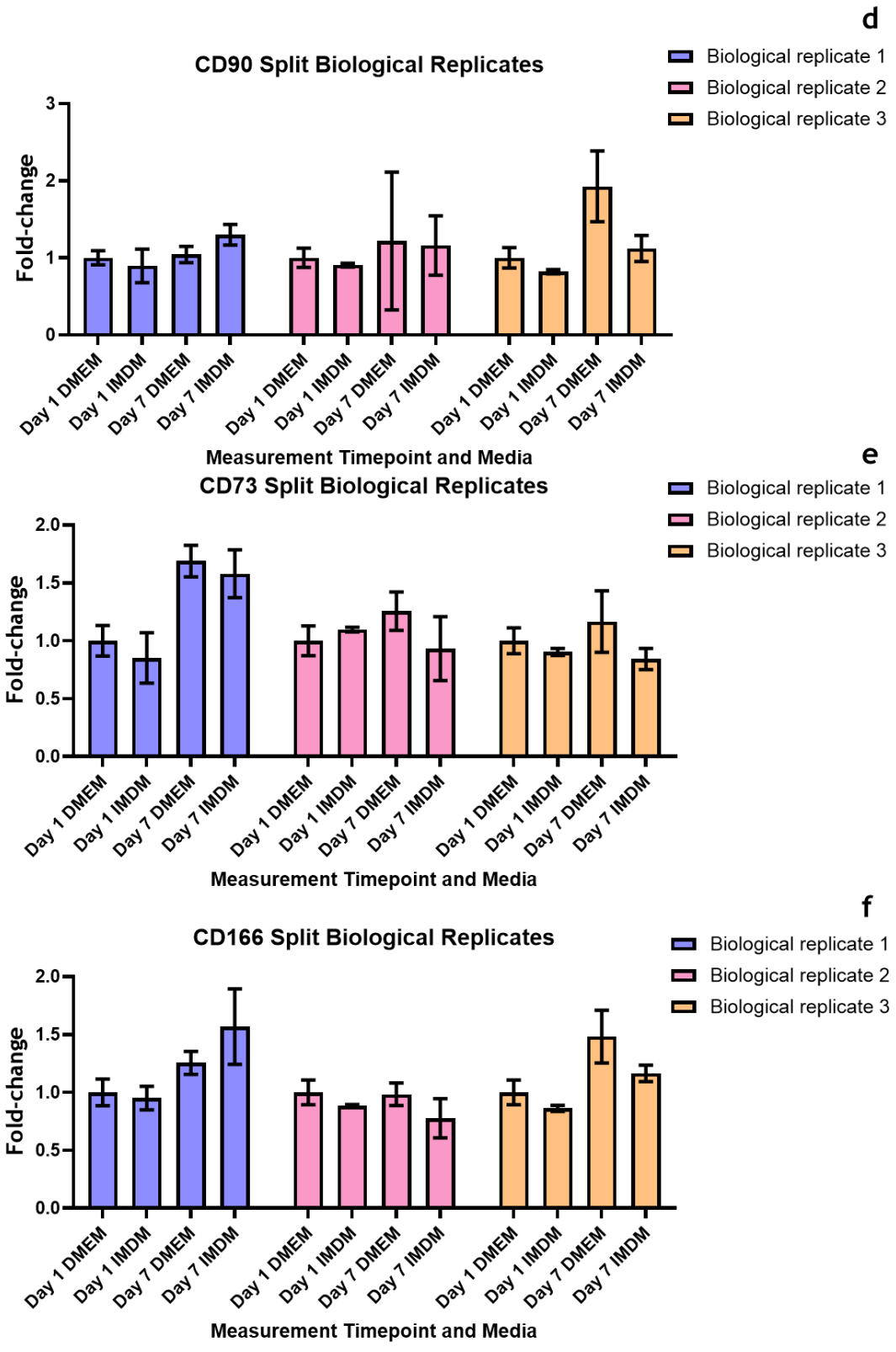

Figure 13. Fluorescence intensity geometric mean measured by flow cytometry of monolayer MSCs 1 and 7 days after seeding in either IMDM or DMEM, normalised to the day 1 DMEM condition. Biological replicates separated for graphs a-f in Figure 12 and replotted for a) CD29, b) CD146, c) CD105, d) CD90, e) CD73, f) CD166 in the live, CD45- and CD34- gated data sets. Graphs show the mean +/- one standard deviation; they are N=1, so no significance is calculated.

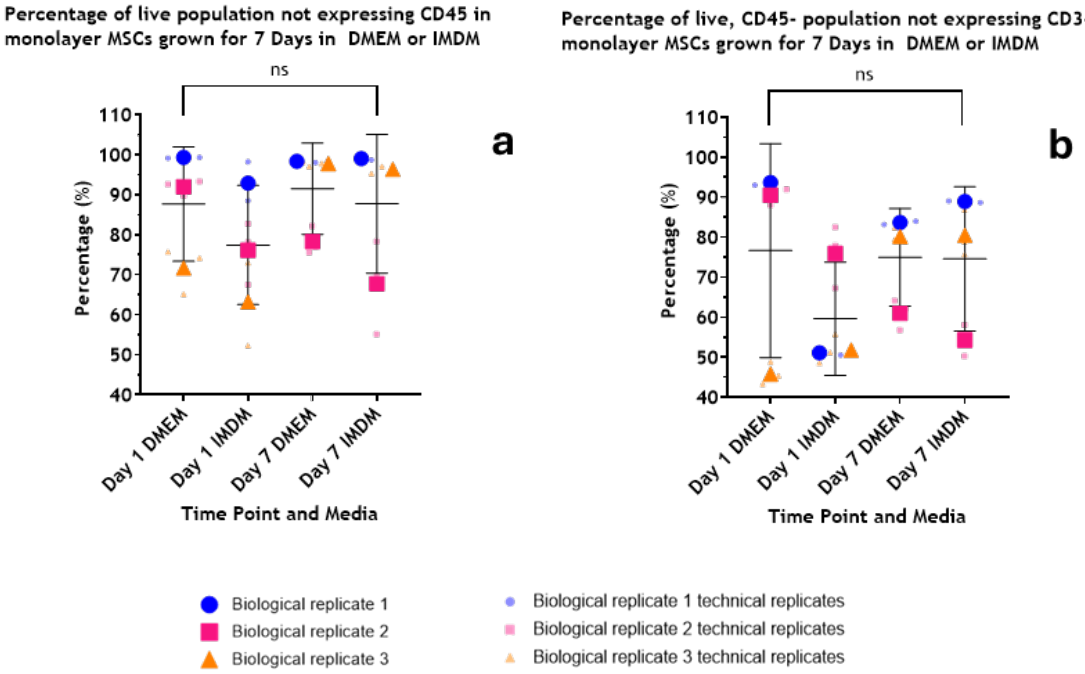

Percentage of Live, CD45-, CD34- cells with positive expression of specified surface marker in monolayer MSCs grown for 7 Days in DMEM or IMDM

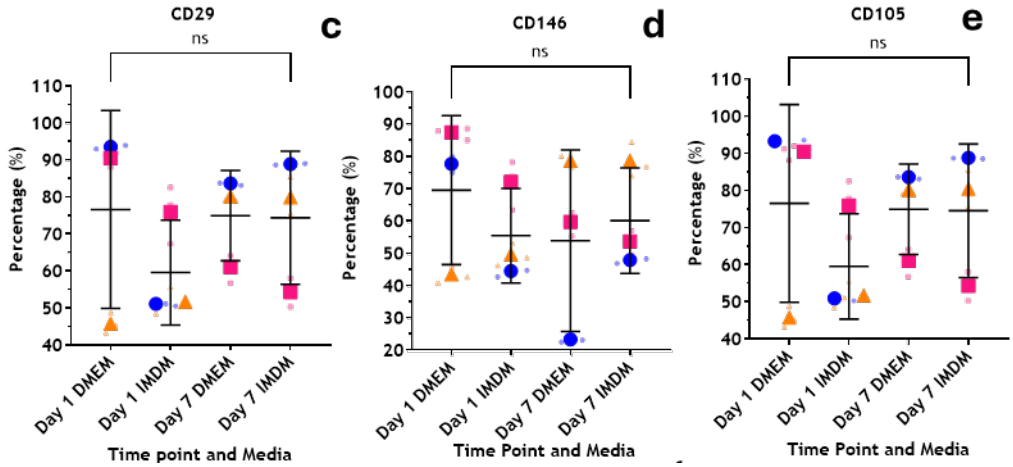

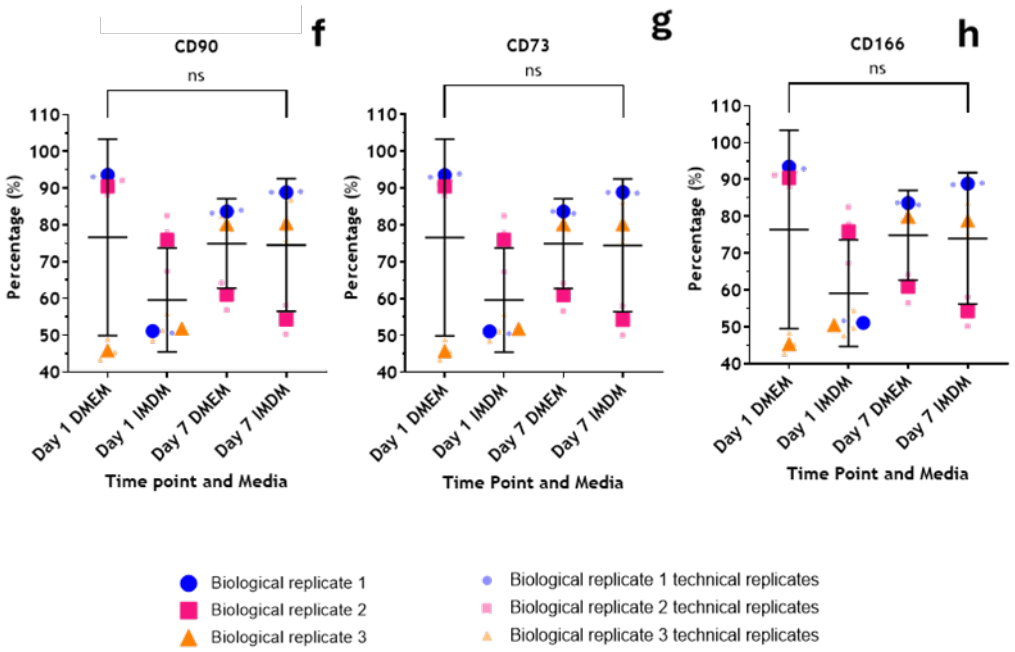

Figure 14. Percentage of monolayer MSC population expressing the specified marker 1 and 7 days after seeding in DMEM or IMDM, measured by flow cytometry. Super plots for the following markers: a) CD45 gated for live cells, b) CD34 gated for live cells and CD45-, c) CD29, d) CD146, e) CD105, f) CD90, g) CD73, h) CD166 gated for live, CD45- CD34- cell populations.

Error bars indicate the mean +/- one standard deviation for pooled data points.

Brighter, larger points depict the mean value for that biological replicate, while the paler colours indicate the technical replicates.

Significance was calculated for comparison of data from the same media type and the same measurement time point by using the Mann-Whitney U test with bounds of non-significance $p>0.05$.

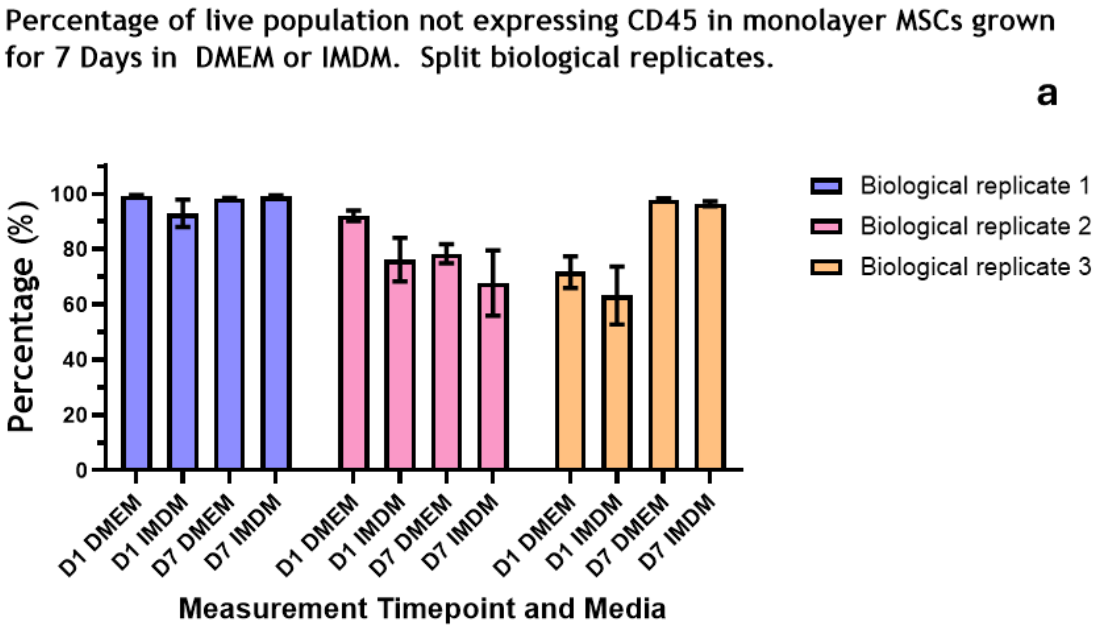

Percentage of live, CD45- population not expressing CD34 in monolayer MSCs grown for 7 Days in DMEM or IMDM. Split biological replicates.

b

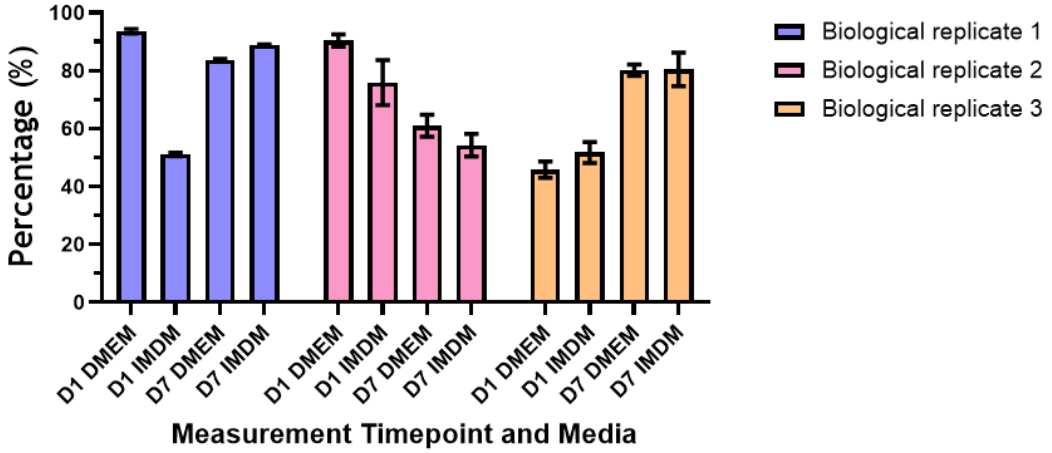

Percentage of Live, CD45-, CD34- cells with positive expression of specified surface marker in monolayer MSCs grown for 7 Days in DMEM or IMDM

c

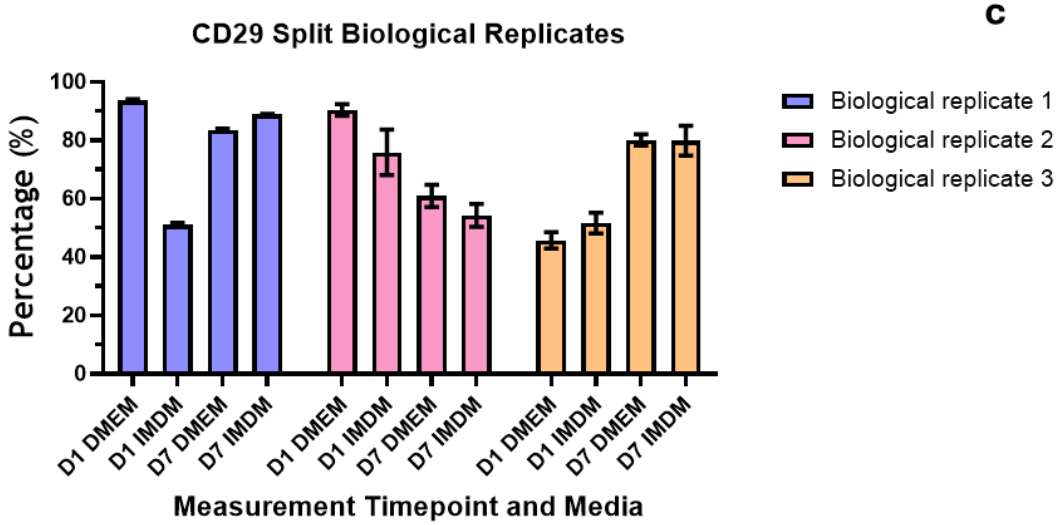

d

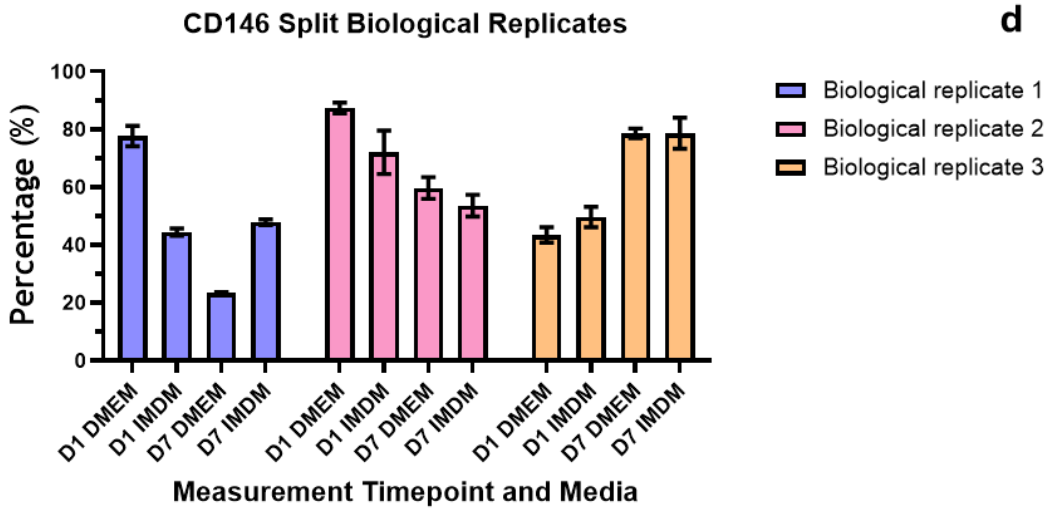

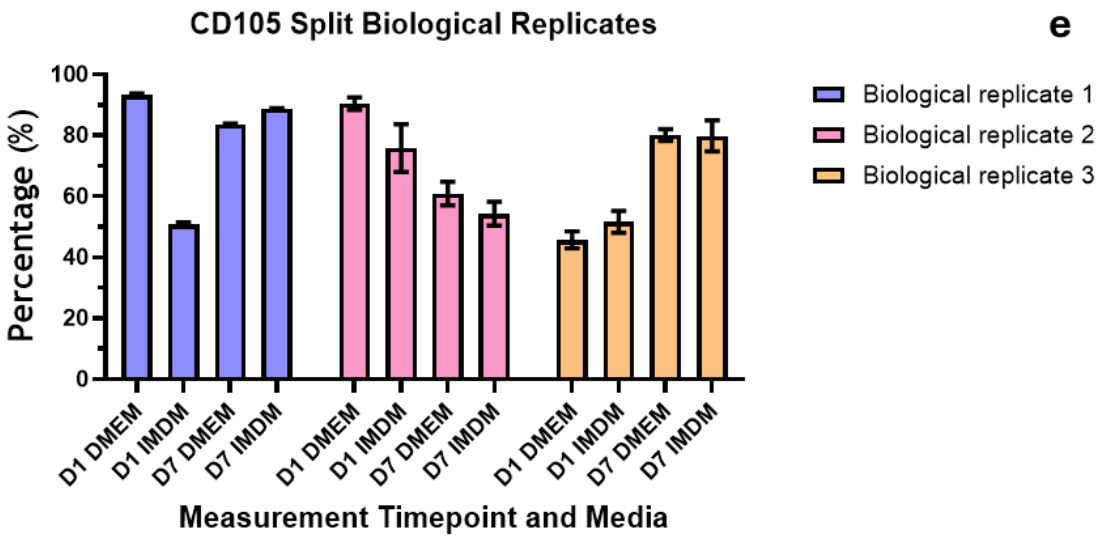
CD105 Split Biological Replicates
e
Percentage (%)
0
20
40
60
80
100
D1 DMEM
D1 IMDM
D7 DMEM
D7 IMDM
Measurement Timepoint and Media
Biological replicate 1
Biological replicate 2
Biological replicate 3

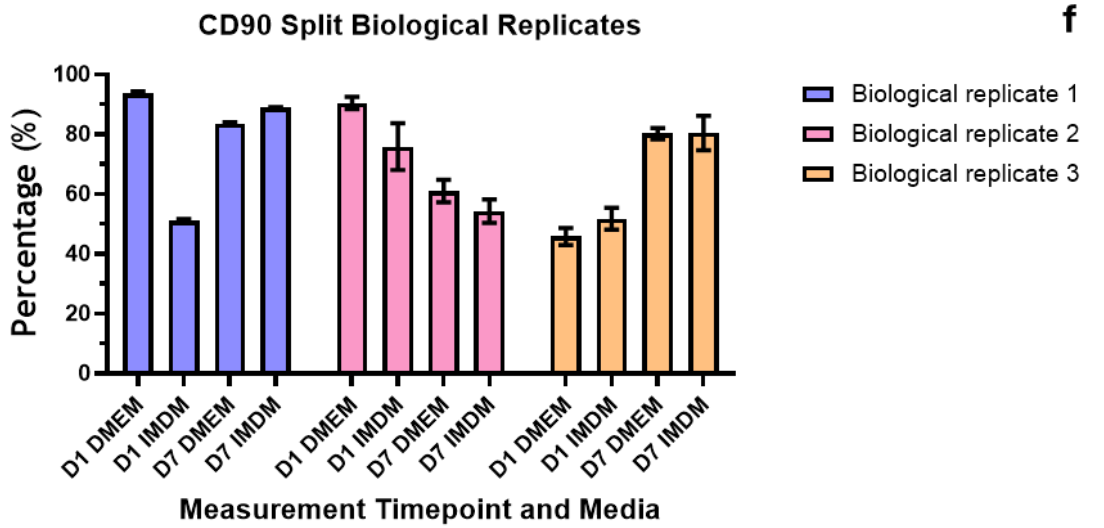
CD90 Split Biological Replicates
f
Percentage (%)
0
20
40
60
80
100
D1 DMEM
D1 IMDM
D7 DMEM
D7 IMDM
Measurement Timepoint and Media
Biological replicate 1
Biological replicate 2
Biological replicate 3

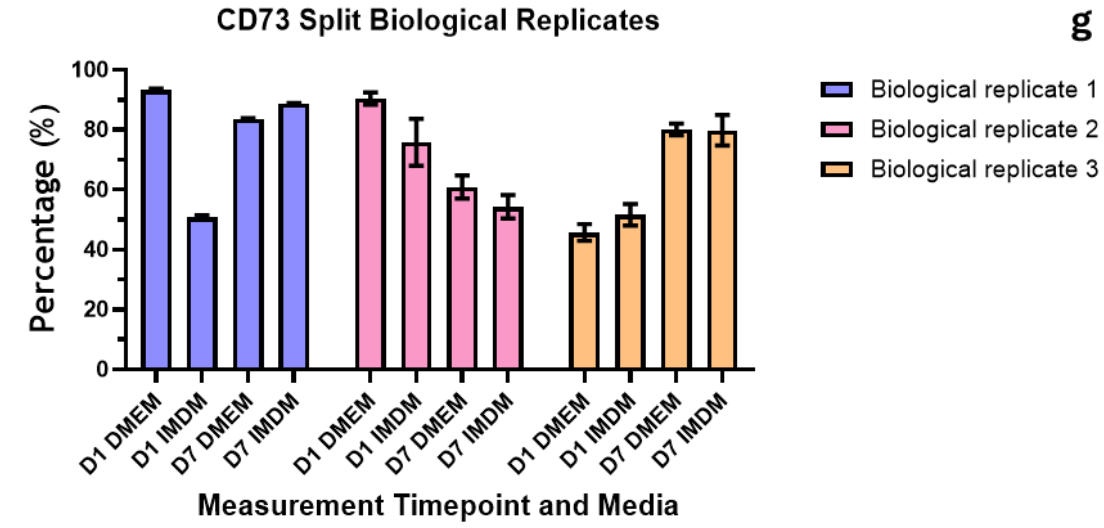
CD73 Split Biological Replicates
g
Percentage (%)
0
20
40
60
80
100
D1 DMEM
D1 IMDM
D7 DMEM
D7 IMDM
Measurement Timepoint and Media
Biological replicate 1
Biological replicate 2
Biological replicate 3

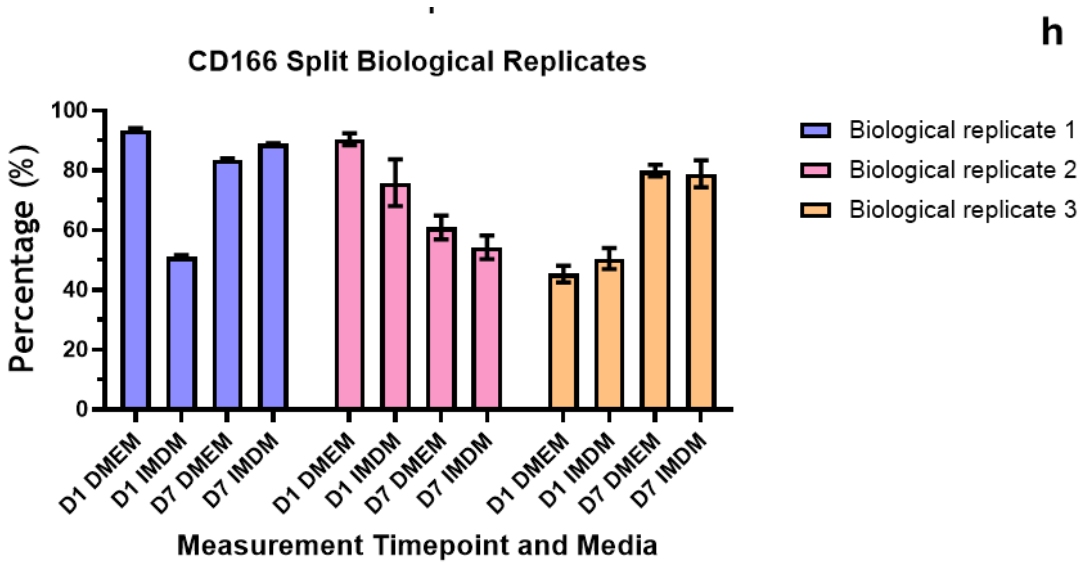

Figure 15. **Percentage of monolayer MSC population expressing the specified marker 1 and 7 days after seeding in DMEM or IMDM, measured by flow cytometry. Biological replicates separated for graphs a-h in Figure 14 and replotted for a) CD45 gated for live cells, b) CD34 gated for live cells and CD45-, c) CD29, d) CD146, e) CD105, f) CD90, g) CD73, h) CD166 gated for live, CD45- CD34- cell populations. Graphs show the mean +/- one standard deviation; they are N=1, so no significance is calculated.**

3.2.3 MSC encapsulation media comparison

When investigating the effects of single MSC encapsulation, the effects of DMEM and IMDM on cell viability **(see Figure 16)** were compared first. Whilst a greater decrease in viability for biological replicate 3 was observed, the results trended the same way, independent of media type. Percentage decrease from day 1 to day 14 was: biological replicate 1: DMEM 9% and IMDM 6%, biological replicate 2: DMEM 11% and IMDM 14%, biological replicate 3: DMEM 47% and IMDM 43%.

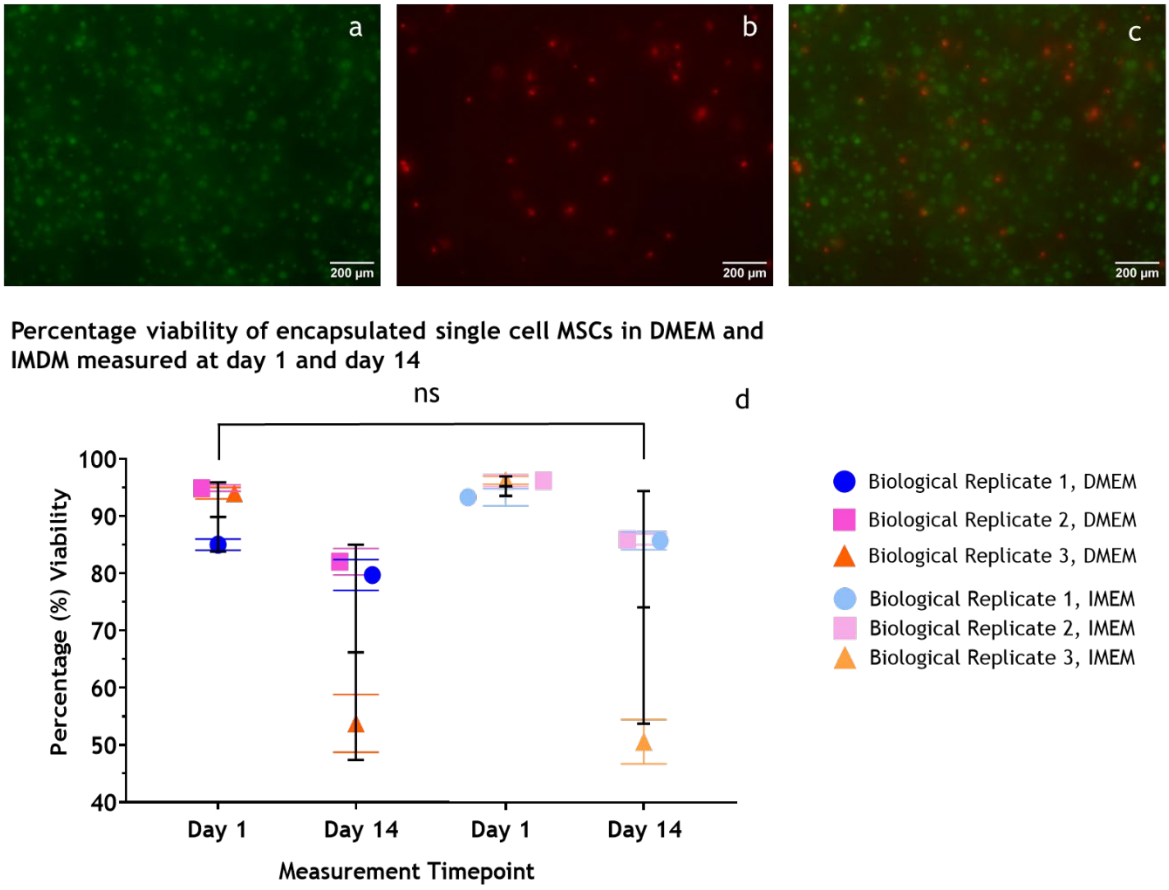

Figure 16. Single cell MSC viability comparing IMDM and DMEM media on encapsulated samples. Images depict Day 1 IMDM samples that are a) green (alive), b) red (dead), c) merged channel stain, while graph d) shows the percentage viability of 3 donors encapsulated MSCs in DMEM and IMDM-based gels for 14 days. N=3 biological/experimental replicates, N=9 technical replicates (9 z-stacks analysed per condition). Significance was calculated for comparison of data from the same media type and the same measurement time point using the Mann-Whitney U test with bounds of non-significance p>0.05.

3.2.4 Monolayer and encapsulated MSCs

This experiment was carried out to determine if encapsulation impacted surface marker expression. Firstly, the percentage of the population gated as positively expressing was plotted **(Figure 17)**. Based on the averages from the merged graphs, one observes that the number of cells expressing was slightly higher for the day 12 monolayer for CD29, CD105 and CD73 (**Figures 17a, c and d)** compared to day -2. For CD29 and CD73 **(Figures 17a and d)**, the number of expressing cells increased for encapsulated cells, but not as highly as the monolayer, whilst for CD105 (**Figure 17b),** there was a decrease; however, this was only small at around 10%. CD146 **(Figure 17c)** showed a similar decrease for both day 12 conditions compared to day -2, and finally CD166 **(Figure 17e)** showed an increase for both.

There was a large variability between donors, which is better visualised by plotting the replicates separately **(Figure 18)**. Replicate one has a greater number of cells expressing at day 12 monolayer than at day -2, and a lower number expressing when encapsulated compared to day -2 for CD29, CD105 and CD73 **(Figures 18a, b and d)**. For CD146, there are fewer cells at day 12 encapsulated compared to day -2 as well, but the day 12 monolayer then decreases further. Replicate 2 has fewer expressing cells for day 12 encapsulated than day 12 monolayer for all surface markers; however, for CD29, CD73 and CD166, both are higher than day -2 levels. In contrast, for CD105 and CD146, day -2 has the largest number of positive cells, followed by the day 12 monolayer and then the day 12 encapsulated. Biological replicate 3 has more encapsulated cells expressing relative to both monolayers for CD29, CD73 and CD166 (**Figures 18 a, d and e)**, but the opposite for CD105 and CD146 **(Figures 18 b and c)**.

Relative peak fluorescence intensity was then plotted **(see Figure 19)** for this data set. There was an increased trend for day 12 monolayer compared to day -2 for CD29, CD105, CD73 and CD166 (**Figures 19a, b, d and e).** Further, the day 12 encapsulated cells showed decreased intensity compared to the day 12 monolayer for all donors, although this decrease was more noticeable for CD105 and CD146. Whilst this was the case, encapsulated expression only decreased relative to the day -2 condition for CD105 and CD146, and it increased for the other markers.

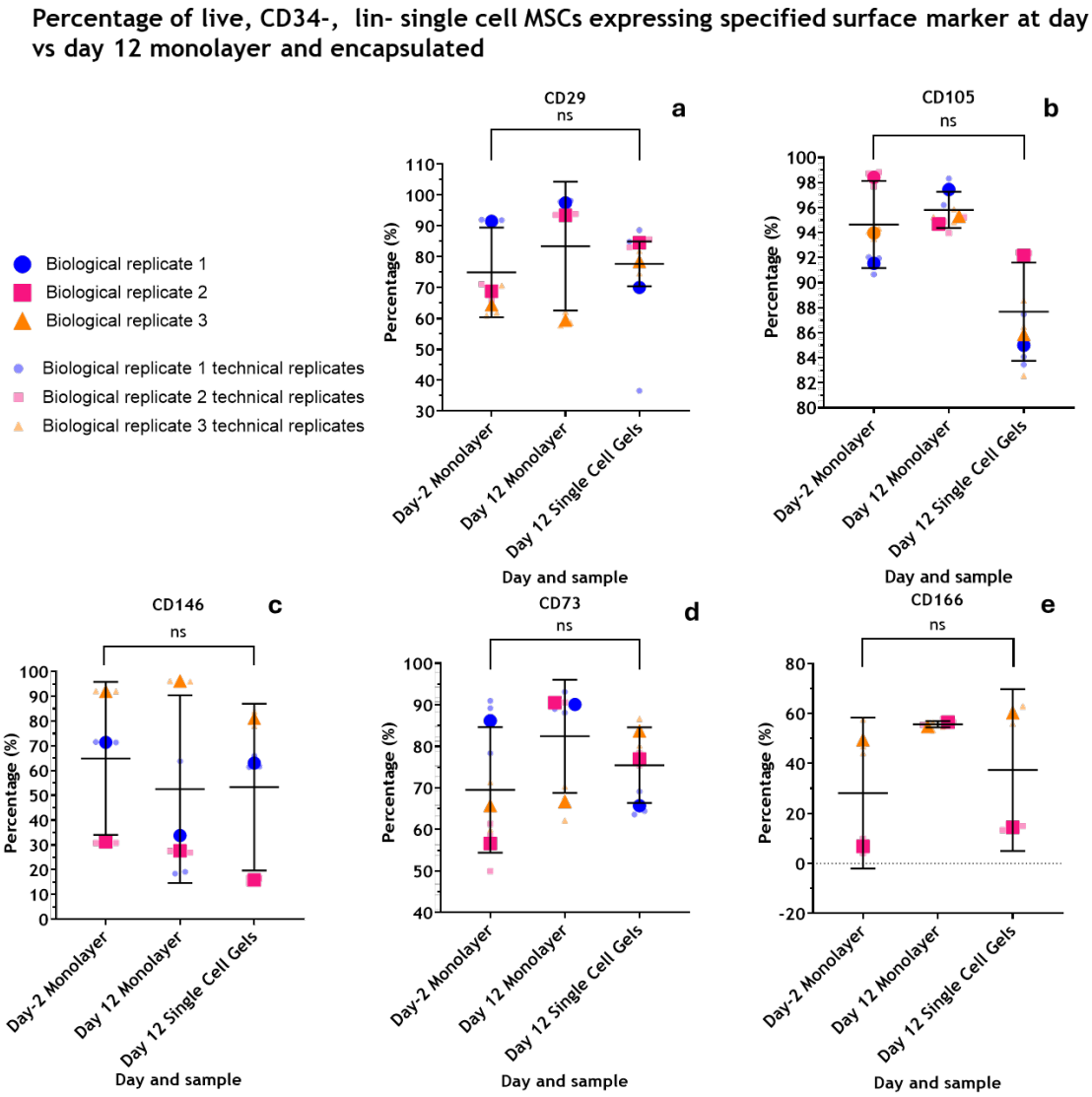

Figure 17. Percentage of MSC population expressing the specified marker on day of seeding and after 14 days of culture in a monolayer or encapsulated, measured by flow cytometry. Super plots for the following markers a) CD29, b) CD105, c) CD146, d) CD73, e) CD166 gated for live, CD45- CD34- cell populations.

Error bars indicate the mean +/- one standard deviation for biological replicate data points. Brighter, larger points depict the mean value for that biological replicate, while the paler colours indicate the technical replicates.

Significance was calculated for comparison of data from the same media type and the same measurement time point using the Mann-Whitney U test with bounds of non -significance $p<0.05$.

Relative to day -2, replicate 1 displayed decreased intensity by day 12 monolayers and a further decrease by day 12 encapsulated cells for all measured markers **(Figure 20)**. In contrast, replicate 2 showed increased intensity for day 12 monolayers compared to day -2, and was higher than encapsulated cells for all markers. However, for CD29, CD73 and CD166, the intensity of encapsulated cells also increased relative to day -2, whereas for CD105 and CD146 it decreased. Replicate 3 showed increased intensity by day 12 monolayers compared to day -2 for all markers except CD146, which decreased. However, for CD29 and CD73, encapsulated cells had greater intensity than both monolayers. Although for CD105 an CD146 encapsulated cells had the lowest intensity.

Percentage of live, CD34-, lin- single cell MSCs at day -2 vs day 12 monolayer and encapsulated expressing specified surface marker with biological replicates split.

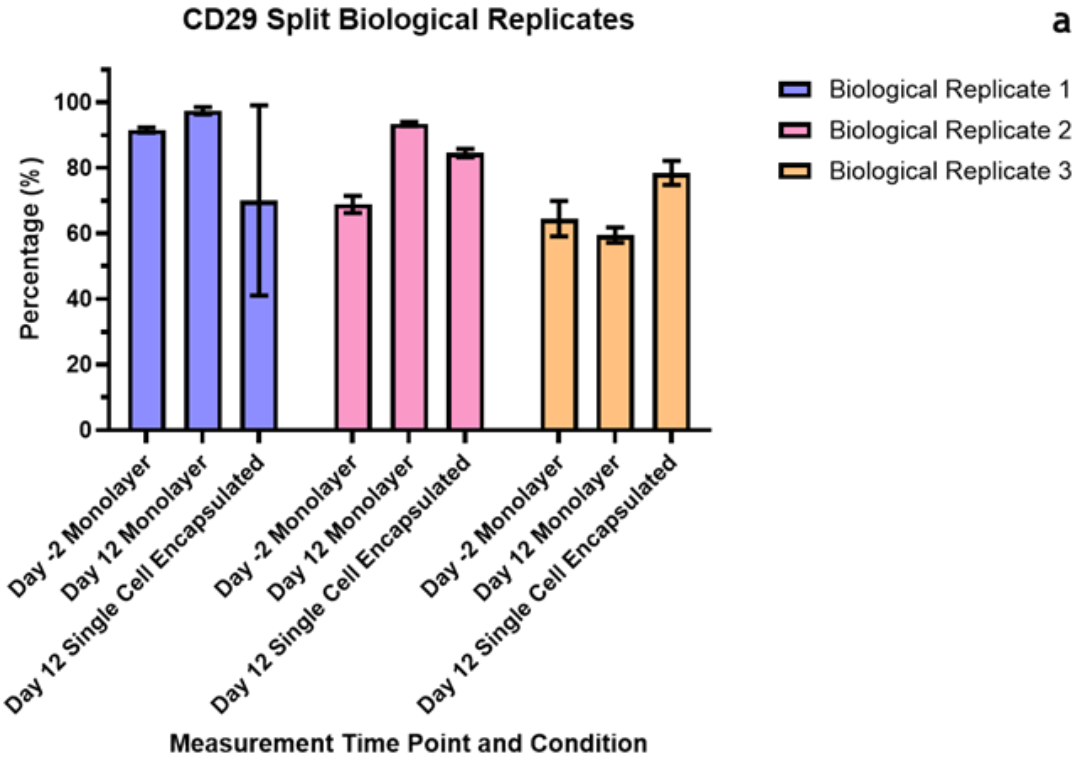

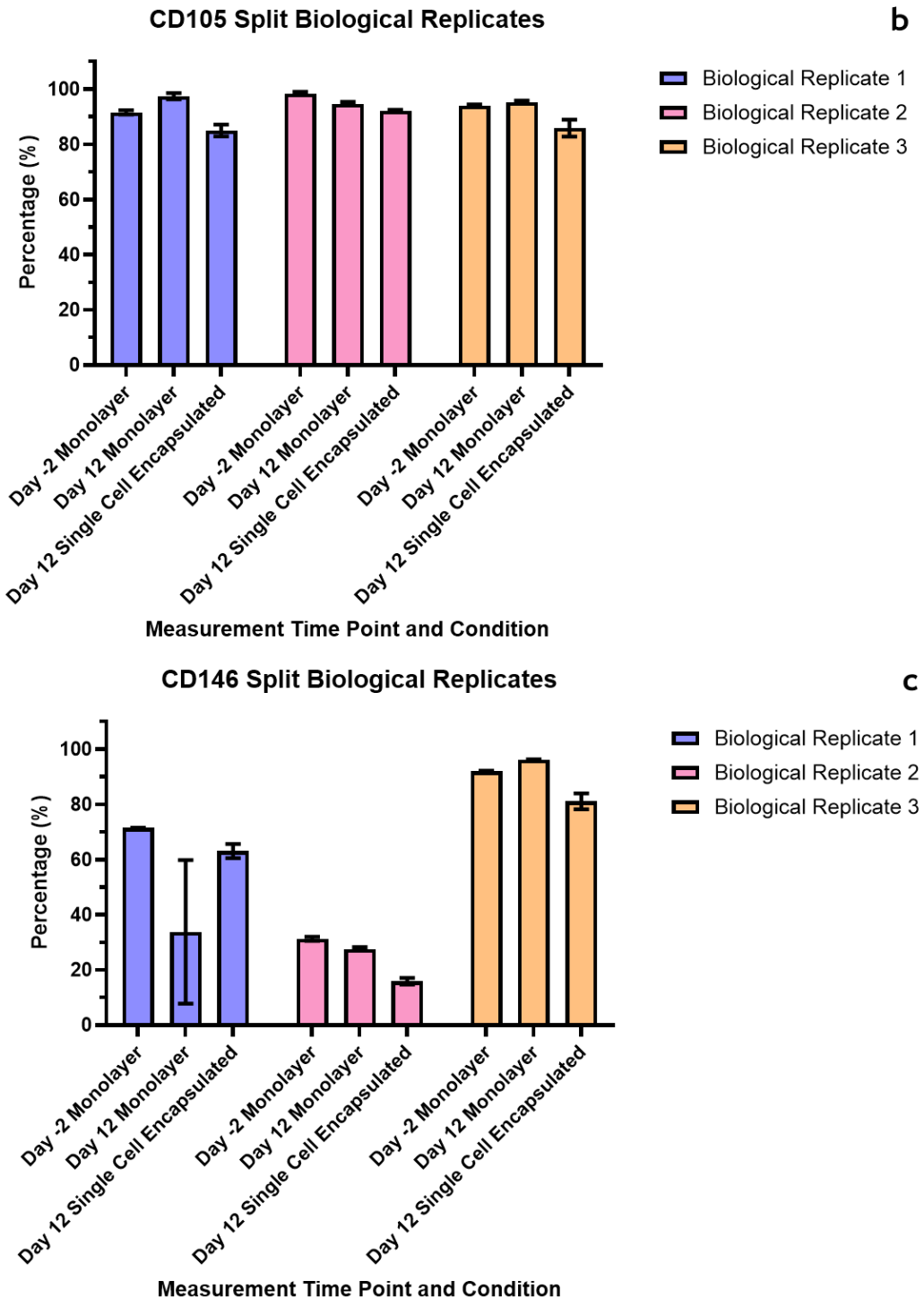
CD105 Split Biological Replicates
b
Biological Replicate 1
Biological Replicate 2
Biological Replicate 3
Percentage (%)
0
20
40
60
80
100
Day -2 Monolayer
Day 12 Monolayer
Day 12 Single Cell Encapsulated
Measurement Time Point and Condition
CD146 Split Biological Replicates
c
Biological Replicate 1
Biological Replicate 2
Biological Replicate 3
Percentage (%)
0
20
40
60
80
100
Day -2 Monolayer
Day 12 Monolayer
Day 12 Single Cell Encapsulated
Measurement Time Point and Condition

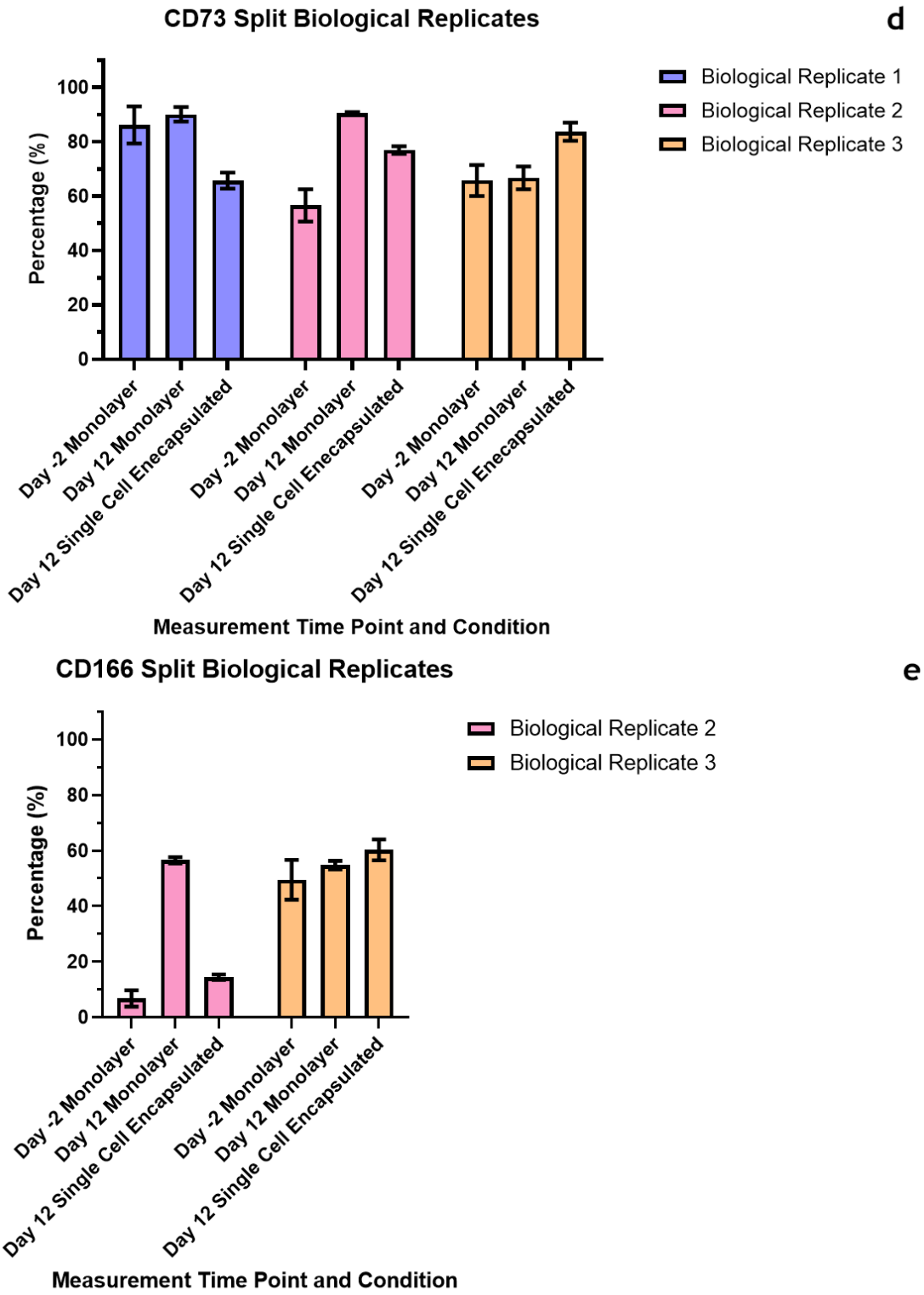

Figure 18. Percentage of MSC population expressing the specified marker on day of seeding and after 14 days of culture in a monolayer or encapsulated, measured by flow cytometry. Biological replicates separated for graphs a-e in Figure 17 and replotted for a) CD29, b) CD105, c) CD146, d) CD73, e) CD166 gated for live, CD45- CD34- cell populations. Graphs show the mean +/- one standard deviation; they are N=1, so no significance is calculated.

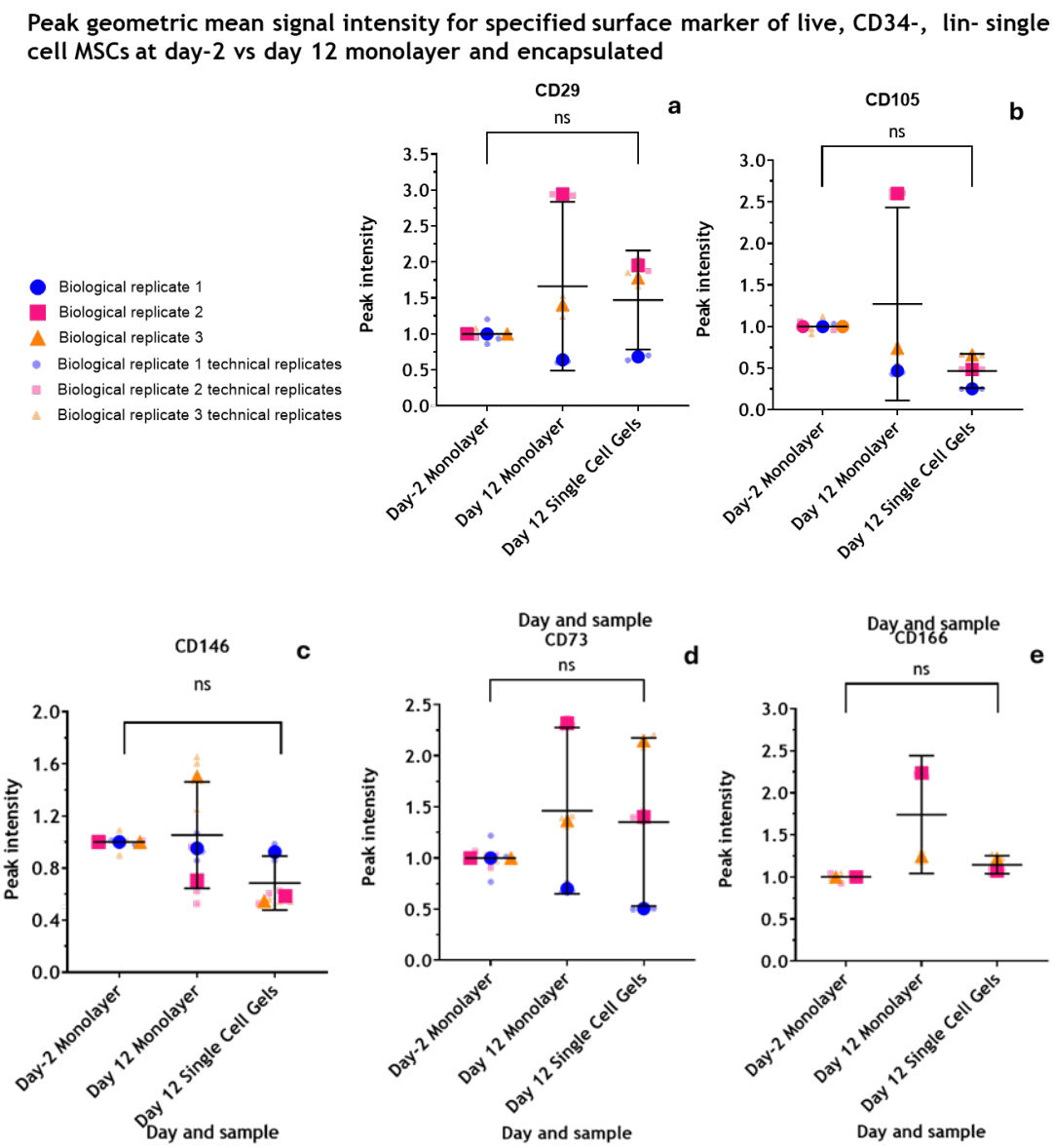

Figure 19. Fluorescence intensity geometric mean measured by flow cytometry of MSCs on the day of seeding and after 14 days of culture in a monolayer or encapsulated, normalised to the day-2 monolayer condition.

Super plots for the following markers a) CD29, b) CD105, c) CD146, d) CD73, e) CD166 gated for live, CD45- CD34- cell populations.

Error bars indicate the mean +/- one standard deviation for biological replicates.

Brighter, larger points depict the mean value for that biological replicate, while the paler colours indicate the technical replicates.

Significance was calculated for comparison of data from the same media type and the same measurement time point using the Mann-Whitney U test with bounds of non-significance $p>0.05$.

Peak geometric mean signal intensity for specified surface marker of live, CD34-, lin- single cell MSCs at day-2 vs day 12 monolayer and encapsulated. Biological replicates are separated.

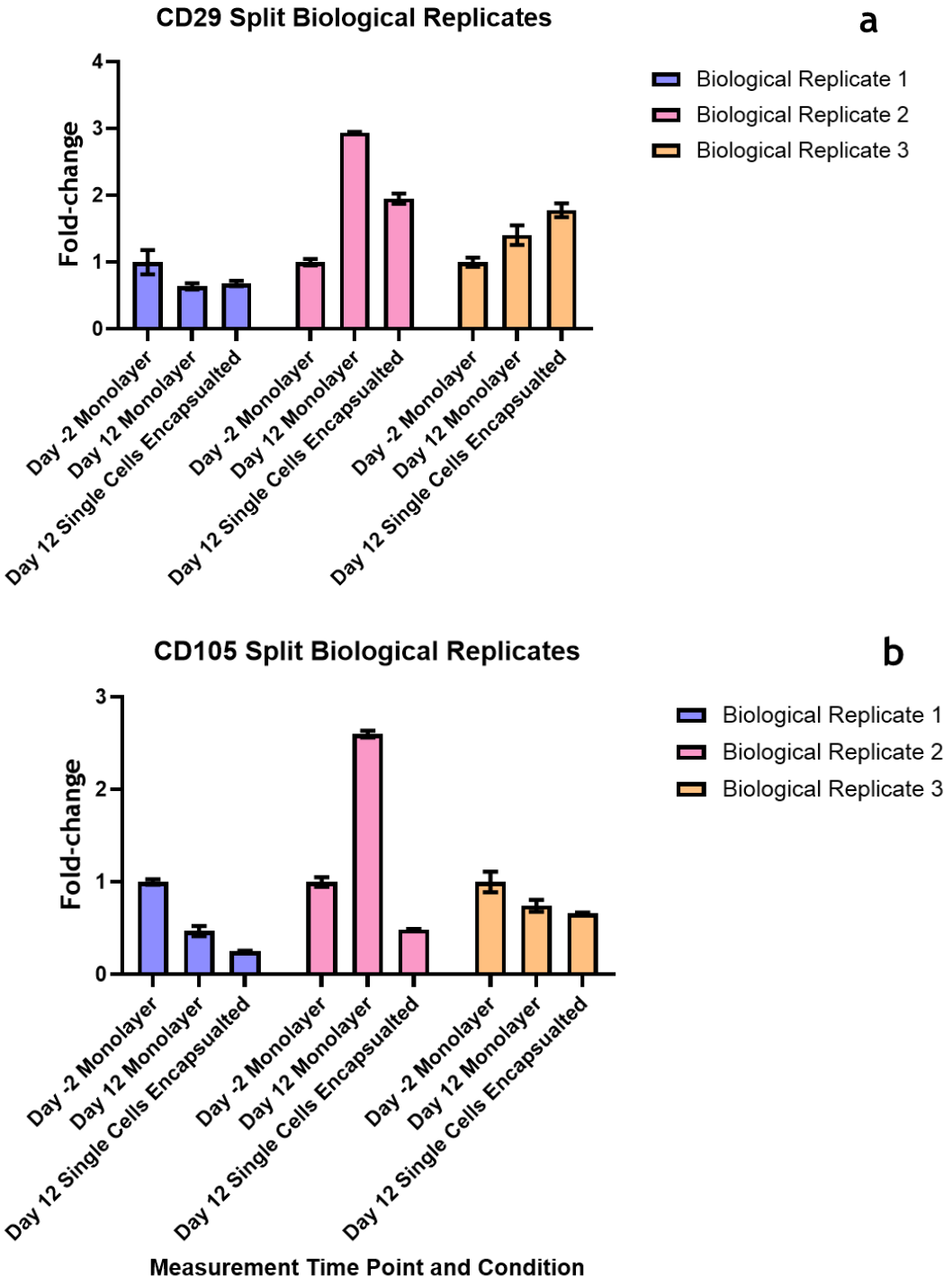

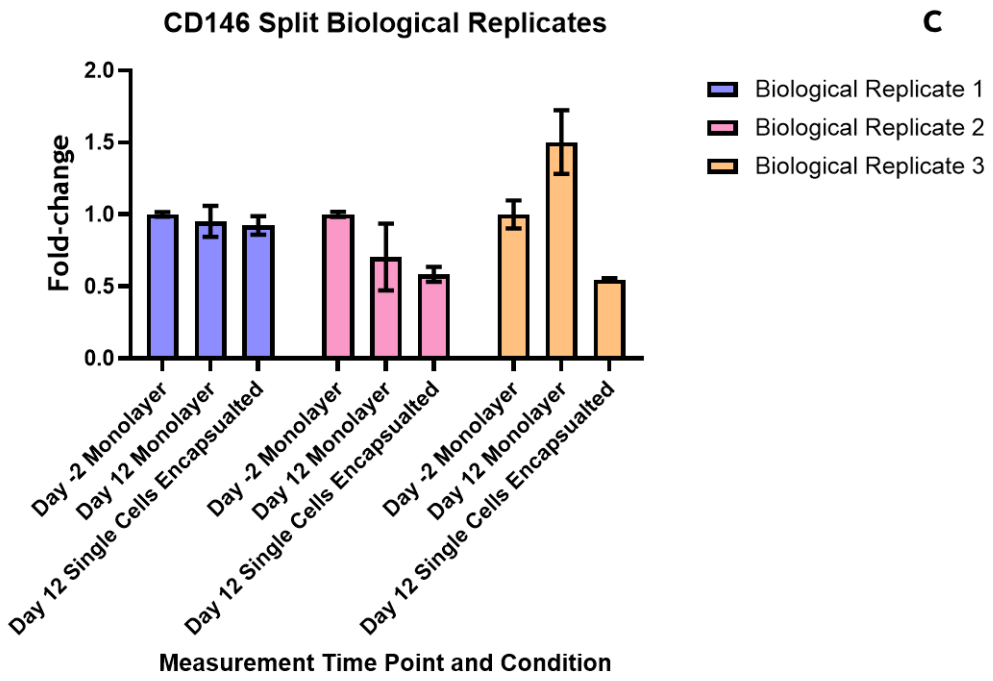
CD146 Split Biological Replicates
c
Biological Replicate 1
Biological Replicate 2
Biological Replicate 3
Fold-change
2.0
1.5
1.0
0.5
0.0
Day -2 Monolayer
Day 12 Monolayer
Day 12 Single Cells Encapsualted
Measurement Time Point and Condition

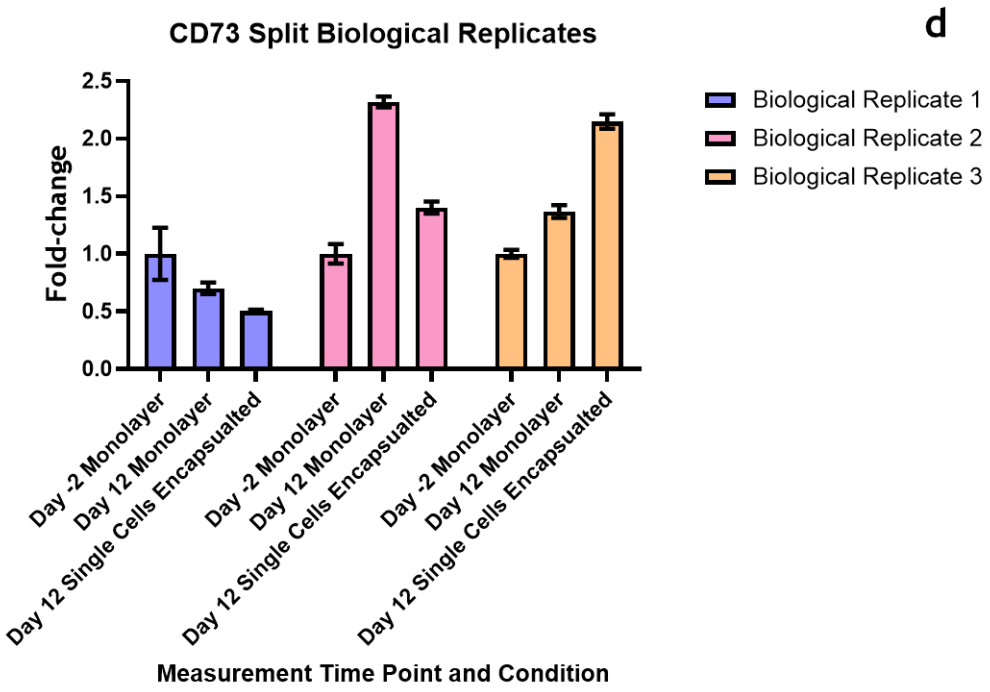
CD73 Split Biological Replicates
d
Biological Replicate 1
Biological Replicate 2
Biological Replicate 3
Fold-change
2.5
2.0
1.5
1.0
0.5
0.0
Day -2 Monolayer
Day 12 Monolayer
Day 12 Single Cells Encapsualted
Measurement Time Point and Condition

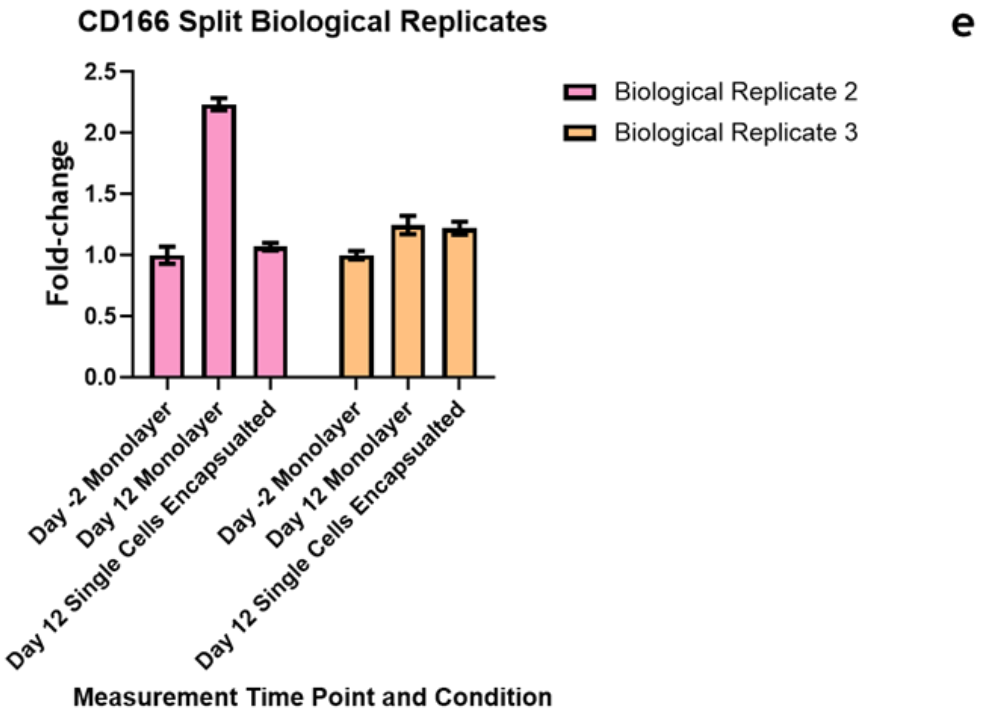

Figure 20. Fluorescence intensity geometric mean measured by flow cytometry of MSCs on the day of seeding and after 14 days of culture in a monolayer or encapsulated, normalised to the day-2 monolayer condition. Biological replicates for graphs a-e in Figure 19 are separated and replotted for a) CD29, b) CD105, c) CD146, d) CD73, e) CD166 gated for live, CD45- CD34- cell populations. Graphs show the mean +/- one standard deviation; they are N=1, so no significance is calculated.

3.2.5 Single CD34+ encapsulation

Initial plans were to replicate the single-cell MSC studies with CD34+s. However, as CD34+s cannot be grown under 'standard' culture conditions without proliferation of progenitors and dilution of the original sample, non-encapsulated controls were not possible. Viability of cells at 37 °C was 0 by day 7, so this condition was ruled out **(See Figure 21)**. 15 and 20 °C saw decreases in viability of roughly 40% over 14 days, with 20 being slightly worse.

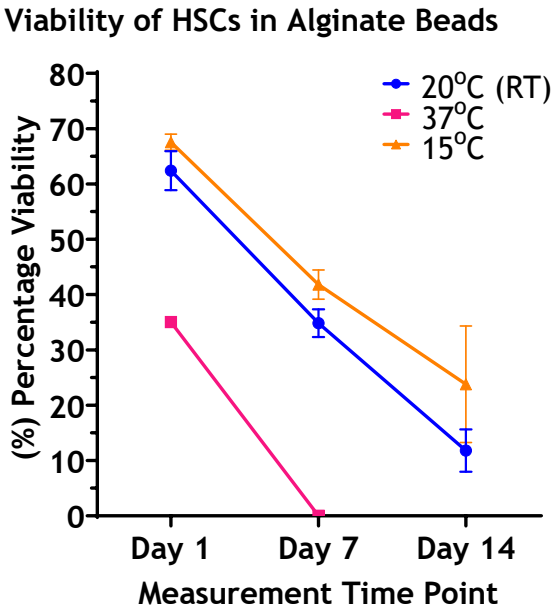

Figure 21. Proof of concept percentage viability of CD34+s cells encapsulated in alginate beads over 14 days at 20 °C (Controlled room temperature), 15 °C, 37 °C.
N=1, so no statistical analysis was carried out.
Error bars display mean +/- one standard deviation for 9 technical replicates.

Following this, the next experiment aimed to establish the surface marker expression of the population pre-encapsulation and post-encapsulation at 15 °C or 20 °C, with or without (+/-) cytokine supplementation **(Figure 22)**. The data was gated based on the gating strategy presented in **Figure 9**. The population was gated to split the group into four sub-populations using CD34 and CD38, which signify distinct phenotypes **(see Figure 1)**. It is worth noting that CD34+ donors 1 and 2 were encapsulated fresh and without cryopreservation. However, due to a lack of donors, CD34+ donor 3 was a cryopreserved sample. Donor 3 showed different results from the other replicates, showing a decreased population percentage in the CD34+CD38+ sub-population **(Figure 22a)** at day 14 for all conditions and a far greater population percentage in the CD34-CD38- sub-population **(Figure 22b)** at day 14 for all conditions. This is unexpected, as no mononuclear HSPC sub-population exists as CD34-CD38-, which would therefore suggest an error in the staining or imaging procedure. It was also the only donor which exhibited a decrease in the percentage of CD34+CD38- cells **(Figure 22d)**. This is shown more clearly in **Figure 22f**, where the data is normalised, and whilst donors 1 and 2 show similar increased trends, donor 3 shows the opposite. As would be expected with such varied data, there was no difference between the CD34+CD38- data when plotted together **(Figure 22e)**.

Number of cells in specified CD34+ sub-population as a percentage, relative to the total number of cells analysed, at day 0 and at day 14 while encapsulated at 15 or 20 °C, with or without cytokine supplementation.

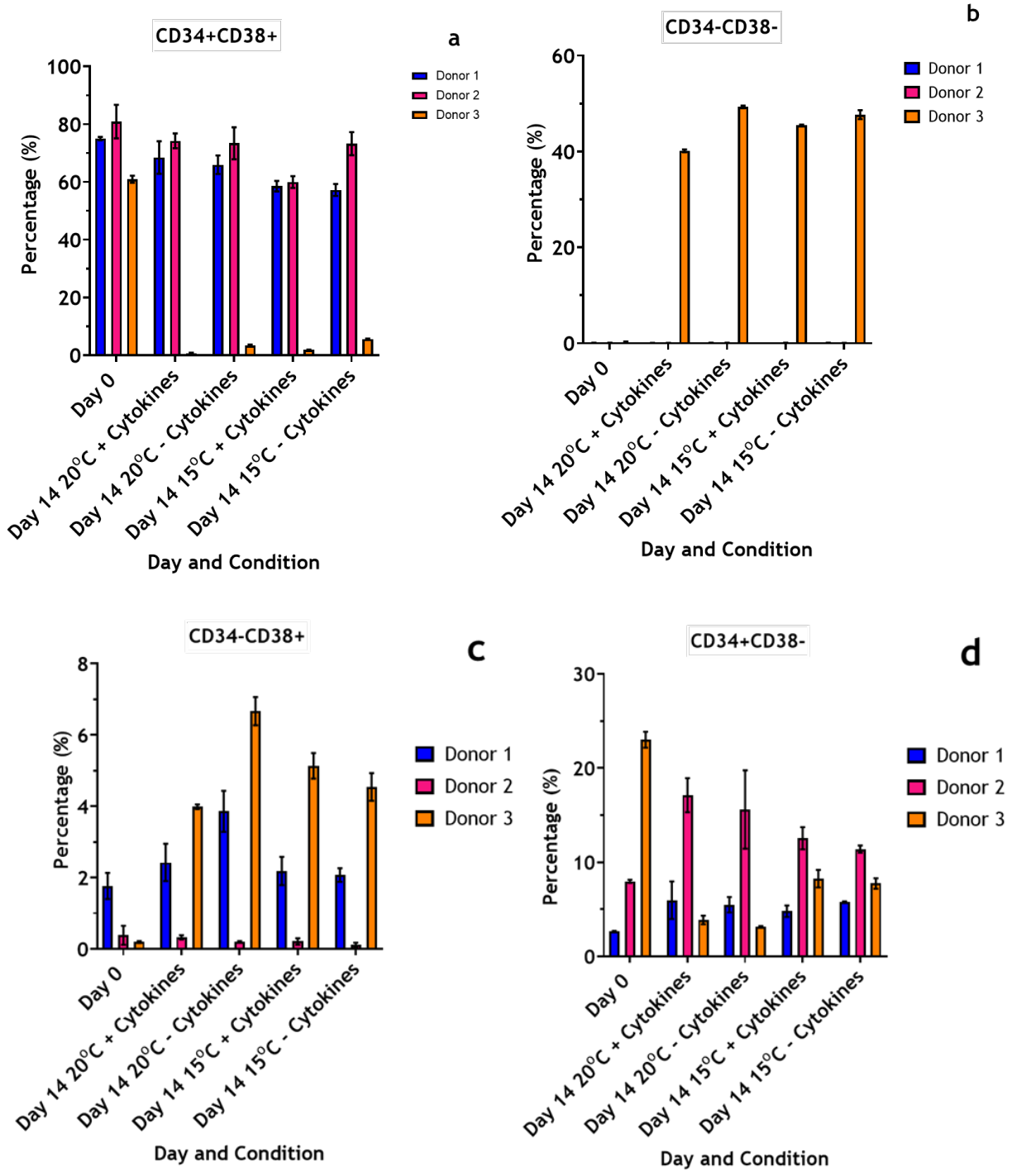

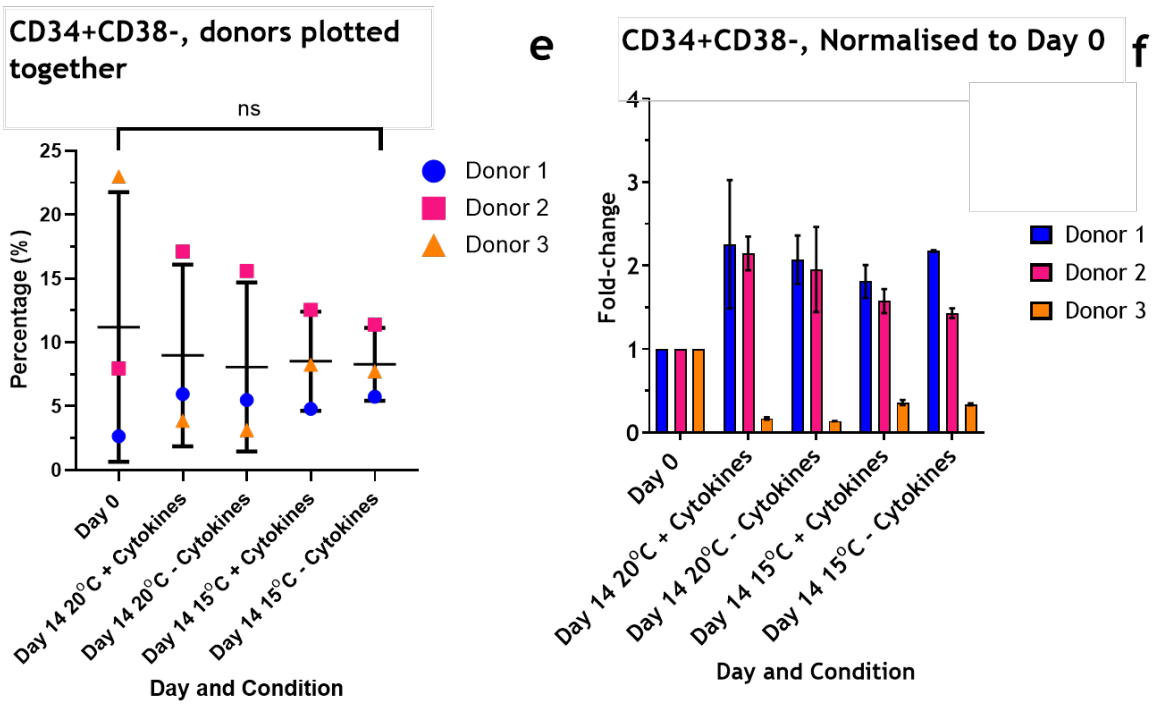

Figure 22. Flow cytometry data of CD34+s pre and post 14-day encapsulation. Samples were split into 4 conditions: 15 and 20 °C (RT), with or without cytokine supplementation. Samples were then analysed after 14 days encapsulated under these storage conditions for CD34 and CD38 expression, and plotted as sub-populations into graphs a-d. Biological replicates are plotted separately for graphs a), b), c), d), and f).

Graphs show the mean +/- one standard deviation and indicate the percentage of live, lineage marker -, CD45+ population separated by donor for a) CD34+ CD38+, b) CD34- CD38-, c) CD34- CD38+ and d) CD34+ CD38-. Graph e) is a pooled data set to determine any statistical significance between the conditions, and f) represents fold change in % of population expressing CD34+CD38- relative to day 0.

Significance for e) was calculated for comparison of data from the same media type and the same measurement time point using the Mann-Whitney U test with bounds of non-significance $p>0.05$. For the rest, as they are separated donors, they are N=1, so no significance is calculated.

3.3 Discussion

3.3.1 MSC viability

The optimal temperature for gel-encapsulated MSC storage in the literature lies at 15 °C, in line with observations from **Figure 11**. A 2018 study demonstrated that multipotent progenitor cells were viable after encapsulation for 72 hours at 4 °C and 15 °C and able to enhance corneal wound healing (Al-Jaibaji et al., 2018). Encapsulated limbus-derived MSCs (l-MSC) were shown to be 76.9% viable after 5 days stored at room temperature (Damala et al., 2019). More specifically, A-MSCs encapsulated at $2x10^6$ cells ml^{-1} at 4 and 15 °C after 72 hours had 65% and 86% viability, respectively (Swioklo et al., 2016). These results are comparable to what was observed after 1 day in **Figure 11a**; however, by day 7, a greater decrease was observed, suggesting the cells may last a short period of time before viability decreases more significantly. Further, this study does not provide an initial viability as a control, and therefore, the decrease relative to post-encapsulation viability may in fact be comparable to that observed in this study (Swioklo et al., 2016). In extension to this, A-MSCs were then stored for 7 days in 3D printed constructs at 15 °C and then cultured for 14 days at 37 °C with seemingly no negative effects (Kostenko et al., 2023).

3.3.2 Gel stability at different temperatures

Once gelated, alginate stability is sensitive to changes in both ion concentration and temperature. They are degraded by polar solvents, changes in ion concentration that occur during artificial nutrient exchange - media change or a dynamic system - or *in vivo*. Resultant ion-exchange in a water-based solution with an ion concentration lower than that of the gel results in the degradation (Barceló et al., 2022). This process renders the gels structurally compromised and is the core principle as to how alginate hydrogels are absorbed by the body when used in medical practices (Cunniffe et al., 2015).

Serp *et al*. theorised that increases in temperature result in increased crosslinking, ion mobility, chain rotation and subsequent re-organisation of the ionic network (Serp et al., 2002). This re-organisation decreased bead diameter and porosity and increased mechanical resistance. This was then confirmed by SEM, where they observed highly variant pore sizes in unheated alginate compared to the dense, highly uniform pore sizes in heated gels. A different study also showed that alginate gels increase in stiffness by 10% from 23 to 37 °C (Ganachaud et al., 2013).

This temperature effect is the opposite trend to that observed in **Figure 11b**, where enhanced temperature resulted in gel degradation. It's believed that degradation was a result of the cells remaining active at 37 ^{o}C and degrading the gel, as opposed to the temperature. This is a similar observation to Hunt in 1988, who encapsulated and cultured fibroblasts in 2% and 5% w/v alginate (Hunt, 1988). They saw a reduction in loss modulus by 95 and 97%, respectively, and in storage modulus over 99% across 28 days. The degradation rate was significantly increased with the presence of cells for both gels, indicating that cell secretions enhance the dissociation of metal ions from the network.

3.3.3 MSC priming

The compositions of IMDM and DMEM are very similar, with the only differences being some amino acids and buffer salts (Gong, 2023). However, DMEM has been the recommended medium for MSC growth since the 2000s (Sotiropoulou et al., 2006; Wang et al., 2009). Follow-up studies assessed common traits such as morphology, proliferation, surface marker retention and differentiation capacity (Bidarra et al., 2011; Pieri et al., 2011). There is a slight disagreement as to whether IMDM can support MSC culture at all, or whether it can cause an initial proliferative boost before surface marker loss. For example, Pieri showed that over the first passage, IMDM cultured cells were more proliferative (Pieri et al., 2011). However, they also showed IMDM culture decreased expression of CD73, 105, 90, 166, 29 and 44.

The expected observations of this experiment were that surface marker expression would be better for DMEM rather than IMDM; however, within media types, expression could increase over 7 days. This is due to the cells recovering from the trypsinisation and reseeding process, which can damage cell membrane proteins (Nowak-Terpiłowska et al., 2021). To avoid this damage before flow analysis, the cells were dissociated with TryplE which is a gentler method of detaching cells from cultureware. However, more commonplace Trypsin-EDTA was used during the seeding of cells at the start of the experiment and could result in reduced surface marker expression initially.

For replicate 1, the increase in signal intensity **(Figure 13)** generally increased over 7 days in culture; however, the number of cells expressing **(Figure 15)** remained consistent for DMEM but increased for IMDM between the two timepoints. Yet, by day 7, the number of expressing cells for the two media

types was similar. This would suggest that IMDM was less effective at recovering any marker expression in cells initially, to give a lower number of cells expressing at day 1, but between day 1 and day 7, it was able to recover a similar number of cells, and, like DMEM, enhance their marker expression. In fact, IMDM resulted in a slightly higher number of both cells recovered and their intensity, at day 7, compared to DMEM for CD29, CD105, CD90 and CD166 **(Figures 13a, c, d and f and Figures 15c, d, f and h)**.

Like replicate 1, all markers displayed increased intensity at day 7 compared to day 1 for replicate 2. In contrast, for replicate 2, DMEM gave increased intensity and percentage of cells for DMEM compared to IMDM at both timepoints for CD29, CD105, CD90 and CD166 **(Figures 13a, c, d and f and Figures 15c, d, f and h)**. Further, while the number of cells expressing was higher for DMEM compared to IMDM at both time points, the numbers decreased from day 1 to day 7. In this instance, while there was a high number of cells expressing markers at day 1, the average intensity was low. As cells with lower marker expression lost expression over time, the cells in the decreased population then had a higher average intensity. However, at both time points, DMEM had a larger number of cells and a greater average signal intensity than IMDM. Therefore, this donor exhibited better cell recovery than replicate 1 under IMDM conditions, but had decreased longevity of the whole population, with only cells with strong marker expression lasting till day 7.

Replicate 3, like the other two, displays increased signal intensity at day 7 relative to day 1, with DMEM intensity higher than IMDM for all but CD146. Furthermore, the percentage of cells expressing increases for day 7 compared to day 1 as well, showing that this replicate was slower to recover from re-seeding, but was able to recover equally for both IMDM and DMEM. The primary difference between IMDM and DMEM is therefore the intensity, with DMEM being preferential.

Overall, the intensity of marker expression was consistently higher for DMEM compared to IMDM at both time points, and increased from day 1 to day 7, suggesting that time in culture was encouraging the recovery of surface markers and subsequently more natural MSC properties. The percentage of cells positive for each marker showed less consistency, and shows how replicate variability can result in cell populations that recover at different rates, and maintain surface marker expression for different lengths of time. Further, while the intensity of

expression and the percentage of cells expressing correlated for replicate 3, it did not for the other two replicates, showing that the number of cells expressing may not be indicative of the abundance of a surface marker.

3.3.4 MSC encapsulation media comparison

Investigation of the viability of encapsulated single cell MSCs **(Figure 16)** showed considerable donor variability; however, the trends were generally in line with those observed in **Figure 11,** where viability decreased by 18% over 14 days of encapsulation. In fact, two biological replicates with less than 15% decrease would suggest that if the donor cells are suitable, alginate-encapsulated BM-MSCs are viable for twice the 7-day length stated by Atelerix (Atelerix, 2022). In addition, while DMEM showed benefits for maintaining cell expression and behaviour compared to IMDM under culture conditions, this is not the same once encapsulated. The lack of difference between IMDM and DMEM viabilities suggests that media nutrients are no longer required, indicating the cells have entered the reduced metabolic state of quiescence (Swioklo et al., 2016).

3.3.5 Monolayer and encapsulated MSC surface marker expression

It was expected that being encapsulated in a gel without binding domains would result in altered cellular surface marker expression due to the lack of physical interaction with its environment, as demonstrated on A-MSCs in 2016 (Swioklo et al., 2016)

Replicate 1 shows a greater number of cells expressing **(Figure 18)**, but with decreased expression intensity **(Figure 20)**, for day 12 monolayer cells compared to day -2 monolayer across all markers except CD146, contradicting observations from **3.3.3**. However, there were then fewer positive encapsulated cells than at day -2 for all surface markers, which correlated with decreased expression intensity compared to both monolayer conditions. So, whilst day 12 monolayers did not maintain earlier trends, the anticipated impact of encapsulation did occur.

Replicate 2 showed considerable correlation between signal intensity and the percentage of cells expressing. For example, for CD29, CD73 and CD166 **(Figures 18a, d and e)**, day 12 monolayer had the largest number of expressing cells, followed by day 12 encapsulated cells and then day-2 cells, which correlated the signal intensity being highest for day 12 monolayer, followed by encapsulated

cells and then day -2 cells for the same markers **(Figures 20a, d and e)**. This correlation between percentage and intensity existed for CD146 as well, albeit with a slight decrease from day -2 to day 12 monolayer to day 12 encapsulated. The exception was CD105, which displayed intensity that trended the same as CD29, CD73 and CD166, but the percentage of cells expressing decreased slightly from day -2 to day 12 monolayer to day 12 encapsulated, like CD146.
However, a theme throughout this replicates data was that day 12 monolayer cells had a larger percentage and intensity compared to day 12 encapsulated cells for all surface markers, with the exception of percentage expression for CD105 and for both intensity and percentage for CD146. This observation as a whole would suggest that rather than diminishing surface marker expression when encapsulated, it simply prevents recovery to the same degree as under monolayer culture, which is logical, as a reduced metabolic state would prevent the synthesis of new proteins, and in turn surface markers (Markides et al., 2019).
Whilst the expected trend of an increased percentage of cells expressing at day 12 monolayer and a decrease for day 12 encapsulated cells was observed for CD105 and CD146 **(Figures 18b and c)** for replicate 3, this trend was only matched in the intensity for CD146 **(Figure 20c)**. Further, more encapsulated cells expressed CD29, CD73 and CD166 (**Figures 18a, d and e)** than both monolayer conditions, and this was replicated in intensity for CD29 and CD73 **(Figures 20a and d)**. However, replicate 3 did show increased intensity by day 12 monolayers compared to day -2 for all markers except CD146, which decreased. As a result of these observations, only CD146 was impacted in the anticipated way by encapsulation and time in culture. All other surface markers showed intensities and percentages of expressing cells that would suggest there is no negative impact from encapsulation.

Therefore, unlike **Figure 12,** there was not a consistent increase in longer-term monolayer surface marker expression compared to day -2 for this experiment; however, variability in the percentage of cells expressing seemed to correlate with the intensity of expression for replicates 2 and 3. There was also more variability in the percentages of expression, suggesting less dependence on the gating criteria used compared to **Figures 12-**15. Some interesting similarities occurred between the replicates for CD29 and CD73, which showed matching

trends for all donors for both percentage and intensity **(Figures18a and d, Figures 20a and d),** suggesting that there may be some relationship between the two. This similarity did not exist between any other replicates.

3.3.6 HSPC viability

CD34+ encapsulation in alginate has occurred minimally; instead, hydrogels are typically used as a substrate or with CD34+s cultured on top (covered in **Section 1.4.2**). Further, these cultures are at 37 ºC, and CD34+s can migrate in and out of the gel. In this model, the CD34+s are immobilised within the gels and do not migrate out.

The viability being poor in **Figure 21** is likely a result of the heterogeneous cell population. Isolating haematopoietic mononuclear cells by CD34+ results in a population with cell types in varying levels of metabolic activity, and only some of those populations will be able to enter a quiescent state **(see Figure 1)**. Further, at 37 °C, immature cells were unable to enter quiescence, while a lack of nutrients and oxygen prevented growth, resulting in no viable cells after 7 days.

3.3.7 CD34 Flow

Evidence for **3.3.5**'s observations could be reinforced using flow cytometry to characterise the CD34 population. By gating for live cells, lin- and CD45 positive expression, CD34 v CD38 **(Figure 9)** expression pairings can be plotted (**Figure 22a, b, c, d)**. If the hypothesis were true, relative to the total live cell population, an increase in cell number in the HSPC population and a decrease in the number of CD34+CD38+ would be anticipated.

The data in **Figure 22** is inconclusive, as while for two donors an increase in HSPC/ decrease in the CD34+CD38+ **(Figure 22a and d)** population is observed, for donor 3, both populations decrease, and instead a CD34-CD38- population arises **(Figure 22b)**. Interestingly, donors 1 and 2 were the only CD34s used fresh from harvesting without cryopreservation – something which was initially intended before the supply of cells became irregular. It is possible, then, that the profiles of the cells are altered upon freeze/thaw and should be investigated further. The trend for donors 1 and 2 also indicates that room temperature better maintains both the HSPC **(Figure 22d)** and the CD34+CD38+ **(Figure 22a)** population; however, for donor 3, 15 ºC is better.

3.3.7.1 Cytokine supplementation

Cytokines expressed by MSCs that facilitate HSC culture were highlighted in **1.2.1;** however, their role in that sort of system does not necessarily translate to mine. Subsequently, the effect of these cytokines and, in extension, MSCs on encapsulated HSCs should be considered. For example, some, like Ang-1, CXCL12 and THPO, maintain the quiescent phenotype in HSCs (Arai et al., 2004; Nie et al., 2008; Yoshihara et al., 2007). Therefore, one should consider whether their presence, as a supplement or from co-encapsulated MSCs, would improve the ability of the system to induce quiescence or be redundant if the gel and temperature do this effectively on their own. While others, such as SCF, FLT-3, IL-3 and IL-6, stimulate or facilitate HSCs to produce progenitors and CFUs (Broudy, 1997; Dorronsoro et al., 2020; Mirantes et al., 2014; O'Shea et al., 2019; Stirewalt & Radich, 2003). A function that is not necessary if cells are quiescent, and certainly not something that should be stimulated when the goal is to maintain immature phenotypes. **Figure 22a** shows a slight trend that suggests cytokine-supplemented media is better than without; however, this cytokine mix is that used in 'gold-standard' HSC maintenance culture, not targeting quiescent HSCs specifically. Therefore, with increased optimisation or perhaps with live MSCs rather than supplementation, this impact could be made more effective.

3.4 Summary

There is a negative impact of IMDM on MSCs in culture **(Figures 12, 13, 14 and 15)** but not when encapsulated **(Figure 16d)**, which would indicate that the metabolic rate of the cells is indeed slow, as the nutrient uptake required during culture is no longer necessary. This metabolic rate decrease is paired with a trend towards decreased expression, or perhaps the inhibition of surface marker recovery, when encapsulated **(Figures 17, 18, 19 and 20)** – a phenomenon touched upon in literature but with limited investigation. The percentage of cells expressing specific MSC markers in **Figures 14 and 15** was seemingly dictated by the gating strategy, which would suggest fairly homogenous populations that, after passing the gating criteria, were then positive for every surface marker. In contrast, **Figures 17 and 18** exhibit less consistency between the percentage of cells expressing each marker, which would in turn indicate a more mixed population of cells, with some expressing certain markers and not others. This brings into question the applicability of this as a metric for analysing

flow cytometry data, especially when presented alone. Different conclusions can be made by comparing this information to the intensity of expression. For example, replicate one shows that an increased number of cells being positive for expression does not correlate with those cells expressing intensely, and therefore, the number of surface marker antigens on the cell is fewer.
Also of interest was that after 7 days in monoculture, independent of the media, the percentage of cells and the signal intensity showed a strong correlation, indicating that the expression of the cells increased over the culture time **(Figures 13 and 15)** (Nowak-Terpiłowska et al., 2021). However, this consistency was not present for the 14-day experiments **(Figures 18 and 20),** which suggests that expression is changing, and this may correlate to functional/phenotypical changes of some/all cells in the population – potentially towards osteogenic or adipogenic lineages. A consideration is that this could also be due to donor variability and, therefore, should be monitored going forward.

For CD34+s, a survival bias appears to be present when encapsulated towards the immature phenotypes **(Figure 22)**, which could provide useful secondary applications of the system to refine the most primitive population. This helps to explain the poor viability as more mature cells die, while immature cells were able to enter quiescence and survive **(Figure 21)**.
Difficulties arose in the study due to cell access. Fresh CD34+s are not consistently available in the numbers required in this lab, and therefore, frozen will be used from here on. However, it's possible that fresh vs frozen/thawed could negatively impact the feasibility of this study. Based on initial data, the fresh samples display better population maintenance compared to the frozen sample **(Figure 22)**. As the dual aim of this would be to encapsulate CD34+'s fresh to use as storage but also be able to use them from frozen as a bone marrow model, it is important to determine what differences there are. Further, there also seems to be large donor variability, and therefore, the optimal conditions are inconclusive. To rectify this, much larger technical and donor replicate numbers are required. While it varies based on experimental conditions such as number of experimental replicates, analytical replicates, number of cells measured, etc, it is generally agreed that 6-12 provide more robust statistical conclusions and should be used where biological/donor variance is large.

Unfortunately, that would be outside the financial and time scope of this study, and so a lack of statistical significance is to be expected.
In conclusion, following the hypotheses in **3.1.**1, encapsulation is a viable option for BM-MSCs, but with reduced surface marker expression when encapsulated. Contrastingly, with a mixed CD34+ population, this system is not viable. However, it appears that more primitive subpopulations of CD34+ cells have potential for use in this system, but a more stringent purification procedure to isolate them could yield better overall results.

Chapter 4. Culture and storage of MSC spheroids

4.1 Introduction

As mentioned, 2D monolayer cell culture techniques are not an effective way to mimic the *in vivo* cell environment. A simple and well-reported way to combat this is to use cell types with self-assembling ability and instigating the formation of cellular aggregates known as spheroids, as mentioned in section 1.4.1.1 (Kouroupis & Correa, 2021; Lin & Chang, 2008). One such cell type is MSC spheroids, with methods for their spheroid formation well-reported (Baraniak & McDevitt, 2012; Bartosh et al., 2010b; Frith et al., 2010; Vu et al., 2020).
In addition, as mentioned in **3.1,** single MSCs have a viable encapsulated period of 7 days (Atelerix, 2022). 7 days is not a sufficient time period for use as a ready-made drug testing platform. Subsequently, as an alternate and more resilient form of MSCs, spheroids may provide additional advantages to simple *in vivo* comparability. Whether MSC spheroids can be maintained whilst encapsulated in alginate, like single-cell MSCs, will be investigated in this chapter.

4.1.1 MSC spheroid culture

Techniques generally use the lack of a binding surface to encourage cell-cell adherence and vary in culture length suitability. For example, the 'hanging-drop' method and microwell plates utilise gravity to cluster cells and induce aggregation; however, neither is suitable for long-term culture (Baraniak & McDevitt, 2012; Bartosh et al., 2010). Whereas long-term culture is ideal in the constant mixing of a bioreactor or spinner flask (Bhang et al., 2011; Frith et al., 2010).
Compared to a monolayer of cells grown on a stiff substrate with limited cell-cell contact, spheroids are a cadherin and integrin, cell-cell interaction dominant environment with stiffness more like that of native tissue and morphologically different (Cesarz & Tamama, 2016; Lin et al., 2006). For example, Baraniak et al. showed in spheroids 600 cells in size, the stiffness was below 0.1 kPa, a Figure in line with the stiffness of BM (Baraniak et al., 2012).

4.1.2 Spheroid size

The number of cells used to form the spheroid is directly related to its size and is also integral to the properties it displays (Xie et al., 2021). Smaller spheroids have adequate nutrient and oxygen exchange to all cells within them, median-

sized spheroids display three distinct cell regions – a hypoxic core, a quiescent/senescent layer and a normoxic proliferative outer layer- while larger spheroids see a transition from a hypoxic to a necrotic core (**see Figure 23)** (Rovere et al., 2023). There is, however, a lack of consistency throughout the literature as to what these cutoff points are for MSC spheroids. With sizes for hypoxic core formation ranging from as few as 250 cells to as many as 250,000 cells (Kaitlin C. Murphy et al., 2017; Schmitz et al., 2021; Vu et al., 2020). Defining core formation criteria is important as it is the core that results in upregulation of hypoxic-related factors (Hazrati et al., 2022). Studies on spheroids often give variable results based on differences in spheroid size, and therefore, it is important to make conclusions on data with this in mind.

4.1.3 Advantages of spheroids

The spheroid hypoxic core cells show enhanced angiogenic potential with expression of numerous molecules like CXCL12, HIF1-a and IL6(Hazrati et al., 2022). While various studies have shown aggregated human A-MSCs have increased secretion of angiogenic factors such as hepatocyte growth factor (HGF), vascular endothelial growth factor (VEGF) and fibroblast growth factor 2 (FGF2) in spheroids 100-350 μm in diameter (Bhang et al., 2011; Cho et al., 2017; Shanbhag et al., 2020).

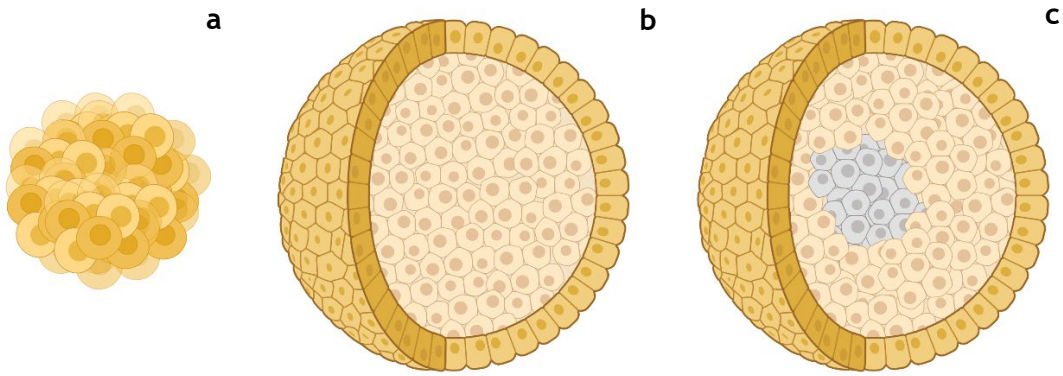

Figure 23. Representative figures of a) a small spheroid with a mixture of ~ 200 live and dead cells, b) a medium spheroid of ~ 10,000 cells with a hypoxic core and proliferative layer, c) a large spheroid of ~ 250,000 cells with a necrotic core, hypoxic layer and proliferative layer. Figures not to scale. Created in biorender.com

MSCs have also shown anti-inflammatory and immunomodulatory properties, with these enhanced when aggregated; spheroid MSCs secrete tumour necrosis factor–inducible gene 6 protein (TSG-6), stanniocalcin 1 (STC-1) and leukaemia inhibitory factor (LIF) at higher concentrations than monolayer MSCs, and this expression remains elevated after dissociation (Bartosh et al., 2010a; Zimmerman & Mcdevitt, 2014). This has been translated to a mouse model where TNF-α expression and secretion in macrophages were significantly decreased in the presence of spheroid MSCs compared to monolayer MSCs. In Xie *et al.'s* study, prostaglandin E2 (PGE2) was shown to increase 40-fold in 400 μm diameter spheroids compared to monolayer MSCs, a gene associated with tuning pro-inflammatory M1 macrophages into an anti-inflammatory M2 phenotype, preventing the activation of lymphocytes and suppressing the proliferation of T-cells (Najar et al., 2010; Vasandan et al., 2016; Xie et al., 2021; Ylöstalo et al., 2012). They also demonstrated that larger spheroids exhibited enhanced T-cell suppression and macrophage tuning to M2 than smaller ones, a theme matching that reported by Bhang *et al.*, who saw increased expression of angiogenic factors as spheroid size increased from 200 to 400μm.(Bhang et al., 2012) Upregulation of PGE2 has been documented by many, including Zimmerman *et al.*, who also showed upregulation in other immunomodulatory cytokines such as TGF-ß and IL-6 (Zimmermann & Mcdevitt, 2014).

Pluripotency markers sex determining region Y-box2 (SOX2), Octamer-binding transcription factor 4 (Oct-4), and NANOG are significantly upregulated in 150-200 μm diameter MSC spheroids, which then demonstrate enhanced osteogenic and adipogenic differentiation capability (Baraniak & McDevitt, 2012; Shanbhag et al., 2020).

More recent exploration has revealed that spheroid MSCs show enhanced survivability compared to 2D-grown cells. Specifically, they show resilience during the engraftment process and respond better to oxidative, hypoxic and inflammatory environments. This is postulated to be due to reduced apoptosis through ROS suppression and autophagy induction (Bhang et al., 2012; Regmi et al., 2020). It is also possible to recover senescent MSCs by aggregating them (Krasnova et al., 2023). Subsequently, aggregated spheroids provide a more resilient alternative to single-cell MSCs for several applications.

4.1.4 Clinical applications

Much of the modern clinical research with MSC spheroids aims to use and improve core discoveries covered in section **1.1.1.1 r**egarding single cell MSCs**,** utilising their regenerative, immunomodulatory and homing abilities (Griffin et al., 2022). For example, compared to single cells, spheroids result in denser bone mineral formation upon implantation into defects, can better help glucose level control in diabetes models and lead to faster remission in rat adjuvant rheumatoid arthritis models (Findeisen et al., 2021; Lee et al., 2021; Miranda et al., 2019). In addition, transplanted spheroids were found in greater numbers than single cells in the peri-infarcted area in a rat experimental myocardial infarction (heart attack) model, where they were incorporated into newly formed vessels (Wang et al., 2009). The vessels formed were of greater density and resulted in reduced infarct size and superior heart function. Similar trends were found when transplanting spheroids and single cells into the kidneys of rats with ischemia-reperfusion-induced acute kidney injury. Spheroids gave enhanced protection against apoptosis, promotion of vascularisation and recovery of renal function compared to their single counterparts (Xu et al., 2016).

4.1.5 Spheroid encapsulation

When MSC spheroids are encapsulated in gels, the aim is usually to improve the culture conditions. In Matrigel, cells migrate out of the spheroids to connect with others within 24 hours, and there is full spheroid migration to form clusters within 72 hours (Kim et al., 2022). When using alginate, the gel is usually functionalised with RGD binding domains. MSC spheroid culture in encapsulated alginate without functionalisation will exhibit significant cell death after 5 days, but in functionalized alginate, they exhibit loss of aggregation, increased migration and elongation, and better viability (Gionet-Gonzales & Leach, 2018; Ho et al., 2016). Further, while remaining viable, disaggregation and migration will not occur after 5 days in alginate gels with slow viscoelastic relaxation times, but extensive migration and disaggregation will occur in fast-relaxing gels (Wu et al., 2023).

4.1.6 Material characterisation of alginate beads

As covered in **3.4.2,** there are various factors that can result in the mechanical properties of alginate changing. Also to consider are differences in local and bulk properties, as well as the inherent differences in the mechanical properties of

3D shapes. For example, the physical properties of spheres are isotropic and therefore not comparable to any other shape. A general rule for material characterising equipment is that the surface being measured needs to be flat, which renders measurements of beads complicated. Subsequently, the method of nanoindentation was chosen, as at the micro-level the surface of a sphere can be considered flat, and this allows for measurements to be taken without altering the 3D shape, and therefore properties, of the gel.

4.1.7 CFU cell/colony types

A common way to assess the functionality and phenotype of haematopoietic cells is to perform CFU assays, while to assess the immaturity of HSPCs, an extended form coupled with LTC-IC can be undertaken (Lessard & Hoang, 2016; Pamphilon et al., 2013).

CFU assays use semi-solid methylcellulose medium, which encourages colony formation and cell growth, allowing assessment of the multilineage capacity of cells within the population. By visually discriminating between colony types based on cell morphology, colour, granularity, and colony size, lineage bias and functionality can be assessed. This establishes the samples' ability for full recapitulation and, therefore, if the sample is healthy (if direct from the patient) or remains *in vivo* comparable (if the sample has been under experimental conditions). The common breakdown of cell types is based on a hierarchy shown in **Figure 24,** and at the top lie LT-HSCs.

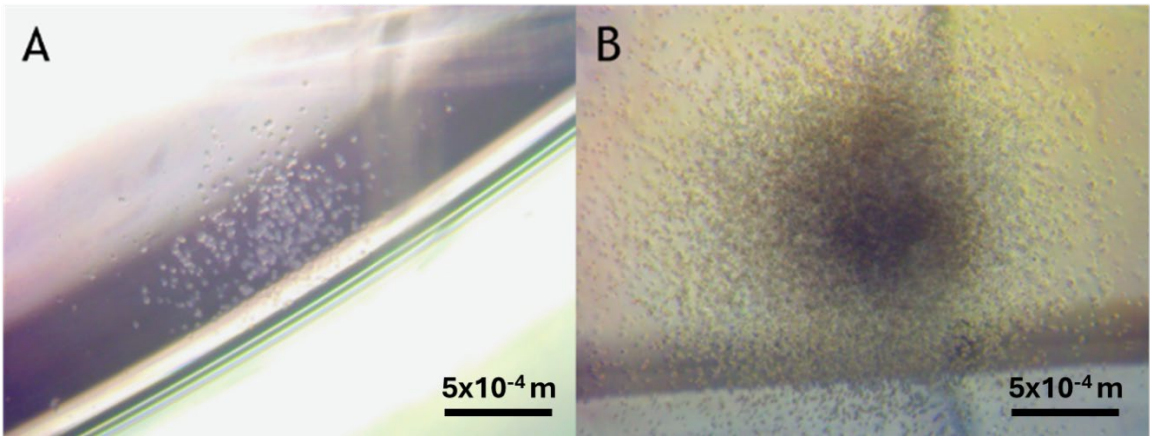

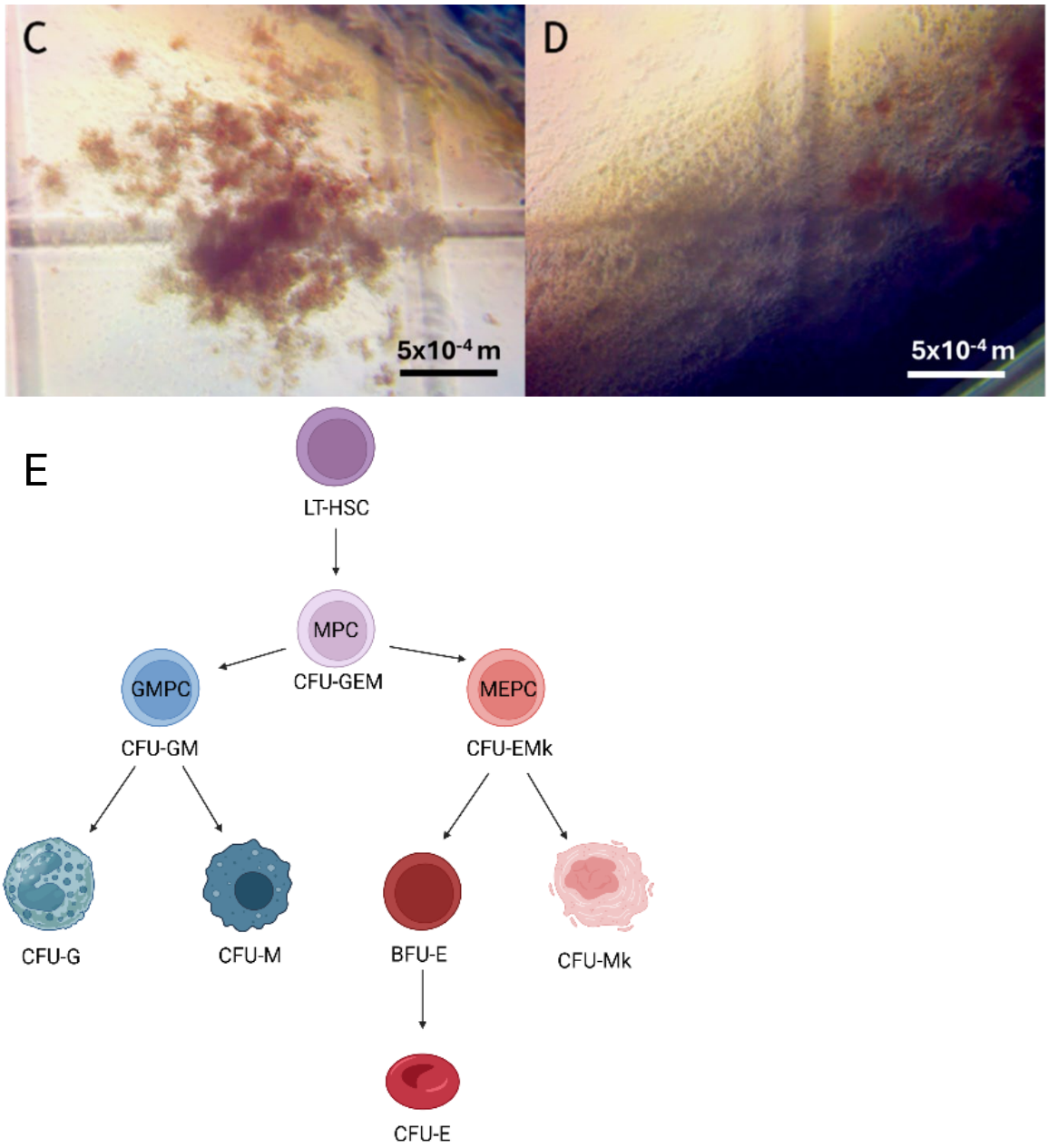

Figure 24. Examples of different colony types: a) CFU-E, b) CFU-GM, c) BFU-E, d) CFU-GEM. e) Simplified HSC Hierarchy specifying which cells give rise to which CFU colony type. LT-HSC Long-term HSC, CFU - Colony Forming Unit, BFU - Burst Forming Unit, GEM - Granulocyte/Erythroid/Macrophage/Megakaryocyte, MPC - Myeloid progenitor cell, GM - Granulocyte/Macrophage, GMPC - Granulocyte/ Macrophage progenitor cell, G -Granulocyte, M - Macrophage, EMk - Erythroid/Megakaryocyte, MEPC - Megakaryocyte/ Erythrocyte progenitor cell, E-Erythroid, Mk - Megakaryocyte

However, culture medium induces differentiation and expansion into CMPs – the most immature colony-forming cell type assessed in CFUs - resulting in the formation of CFU-GEM (Granulocyte/Erythroid/Macrophage/Megakaryocyte) **(Figure 24d).** This population is multipotent and highly proliferative, producing numerous large colonies with multiple different cell types.
GMPs produce CFU-GM (Granulocyte/Macrophage) **(Figure 24b),** which are large colonies of granulocytes and macrophages. While typically counted as one, this population can be broken down further into CFU-G or CFU-M.
MEPs produce CFU-Mk, which are not formed unless specific methylcellulose formulations are used, and BFU-E (Burst-forming unit – Erythroid). Called 'burst' forming because of the large colonies formed, BFU-E cells will, in turn, produce CFU-E colonies **(Figure 24c)**. CFU-E are the most mature colonies and have limited proliferative ability **(Figure 24a)** (Schippel & Sharma, 2023).
LTC-IC is performed before CFU and uses a proliferative media composition that encourages mature cells to expand, and their population dies out, while maintaining immature phenotype cells with long-term recapitulation capabilities (Ponchio et al., 2000).

4.1.8 Aims and objectives

This chapter will comprise two parts. The first will assess the viability of MSC spheroids when encapsulated in alginate beads. The type of media and temperature were characterised using viability staining. Once the preferred conditions were selected, the surface marker expression of MSC spheroids was to be analysed and compared to that of cells grown in a monolayer. Next, the stability of the gels was to be assessed using nanoindentation. Surface stiffness of beads without cells, single cells, spheroids, and spheroids and single cells was to be measured on day 1 and day 14 to ensure that there were no changes during the encapsulation period.
Secondly, the functional ability of CD34+s pre- and post-encapsulation would be assessed using LTC-IC and CFU assays and flow cytometry and compared to the results from **Chapter 3.** This should determine if there were any effects of freezing on the behaviour and/or composition of the HSPC populations and whether refinement of the population would give insight into the previously gathered data.

Hypotheses for spheroids were that they would have worse surface marker retention compared to monolayers, as suggested by the literature, but improved viability compared to monolayer cells, and be more resilient to temperature changes (Kim & Adachi, 2021). For HSPCs, it was anticipated that more primitive HSC phenotypes would have greater survivability under encapsulation compared to less primitive HSPC subpopulations due to their greater ability to enter quiescence. Further, it was hypothesised that the fresh samples would be less stressed, and therefore more likely to remain viable under encapsulation.

4.2 Results

4.2.1 Viability and radius

MSC spheroids encapsulated in IMDM and DMEM showed trends between comparative timepoints and media (**Figure 25h)**. Data was normalised to controls, which were kept in the spheroid plate culture rather than encapsulated. The percentage change for day 1 DMEM, day 1 IMDM, day 14 DMEM and day 14 IMDM was 5% decrease, 16% increase, 37% decrease and 14% decrease, respectively. Day 14 control spheroids lacked structural integrity, and only those for donor 2 remained intact after the staining process and transfer from the spheroid plate into a dish for imaging. Fluorescence of live cells was greater for IMDM at both day 1 and day 14, and therefore, IMDM was chosen to move forward.

Viability of spheroids in IMDM at 15 and 20 °C showed a decrease between day 1 and day 14, but no difference between 15 and 20 °C **(Figure 25i)**. The percentage change relative to day 1 for 15 °C was a 32% decrease, and a 31% decrease for 20 °C, indicating viability changes were independent of temperature.

The radius of spheroids (**Figure 25g)** was calculated by measuring the circumference of each spheroid stained for viability in **Figure 25h**. Radius decreases were observed from the control to the other conditions; similarly, DMEM spheroids were smaller than those in IMDM. However, there was no difference between day 1 and day 14 DMEM spheroids nor between day 1 and day 14 IMDM spheroids, indicating that spheroid size is maintained during the encapsulation process.

Figure 25j, k and l show the relative fluorescence intensity as the two individual channels, showing how the decreased viability ratio observed for **Figure 25h** is a result of increasing red intensity and decreasing green at day 14 relative to day 1. The main outlier was donor 1, which saw day 14 DMEM with a far greater increase in red intensity than the other two donors for that condition.

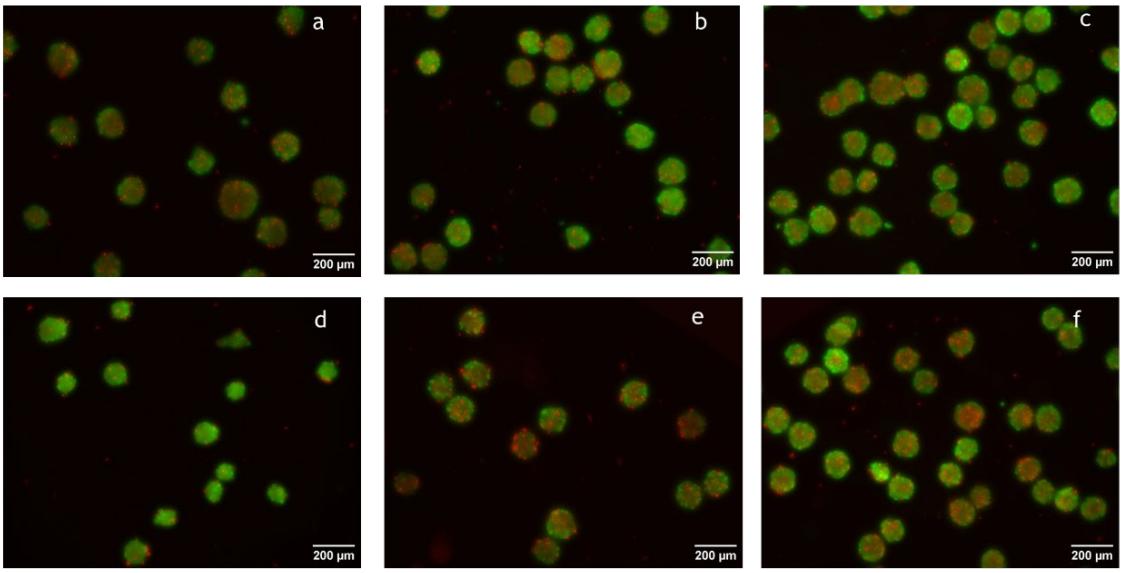

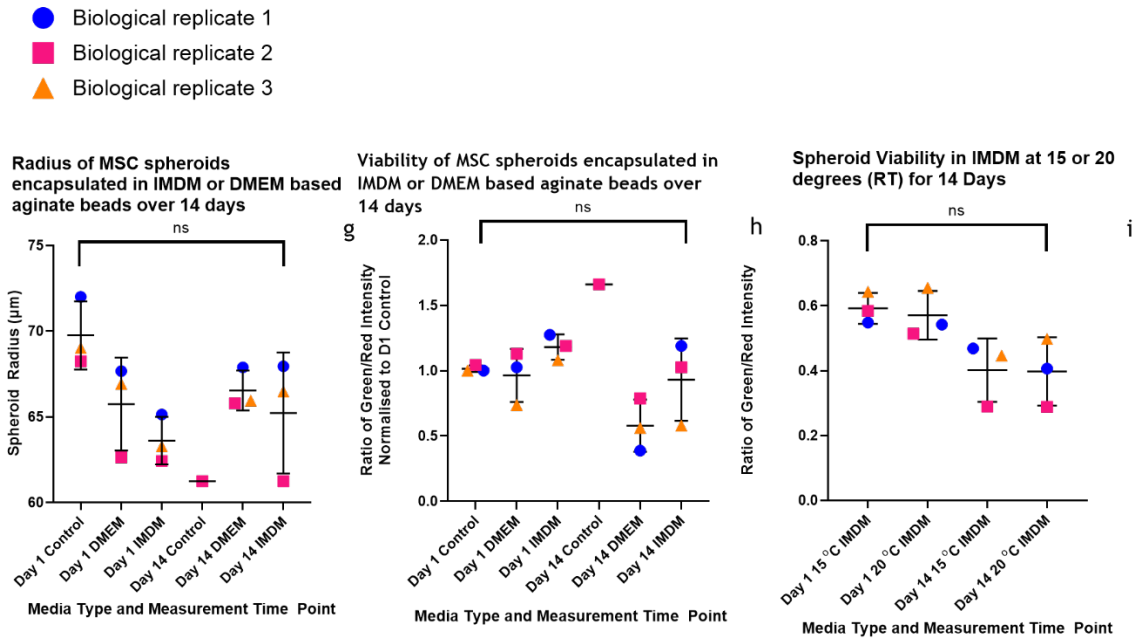

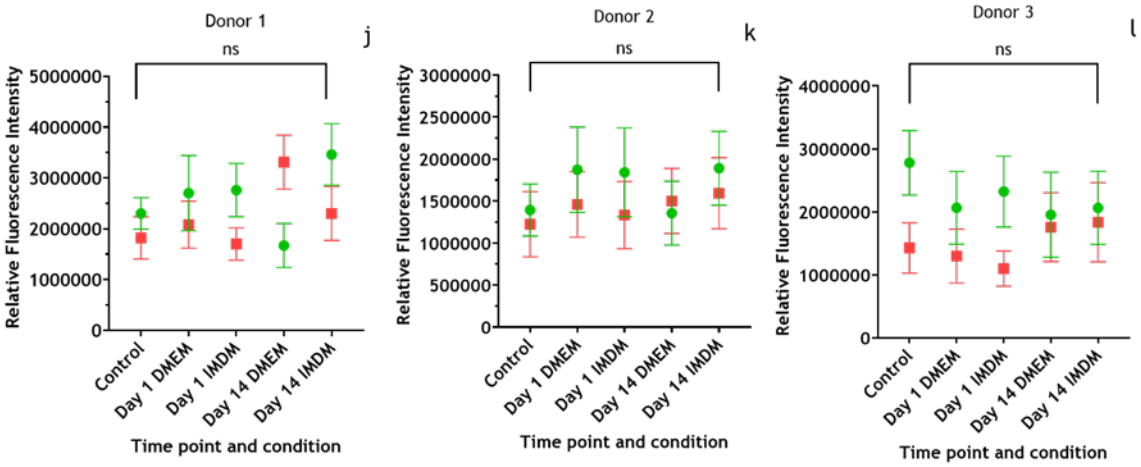

Figure 25. Viability analysis of encapsulated spheroids. Example z-stack images of spheroids from the following conditions: a) D1 Control, b) D1 DMEM, c) D1 IMDM, d) D14 Control, e) D14 DMEM, f) D14 IMDM

g) Radius in micrometres (μm) of MSC spheroids one day and fourteen days post encapsulation in IMDM or DMEM-based alginate beads, normalised to Day1 control spheroids (not encapsulated).

h) Viability of MSC spheroids one day and fourteen days post encapsulation in IMDM or DMEM-based alginate beads, normalised to Day 1 control spheroids (not encapsulated)

i) Viability of MSC spheroids one day and fourteen days post-encapsulation in IMDM-based alginate beads at 15 or 20 °C.

j,k,l) Separate green and red intensity for spheroids plotted in g) and h)

Any pairing not displayed statistically was non-significant. Error bars indicate the mean value +/- one standard deviation for the merged data set.

Significance calculated using the Mann-Whitney U test with bounds of non-significance $p>0.05$.

4.2.2 Flow cytometry

As in **figures 19 and 20**, mean fluorescence peak intensity was normalised to the day-2 monolayer to assess fold change. Fold changes in expression intensity were plotted into a heatmap **(Figure 26a),** which demonstrated that spheroid conditions resulted in reduced surface marker expression, particularly for CD146 and CD105. This data was then plotted graphically to show significance **(Figure 26b-f)**. Biological replicate 3, day-14 monolayer data sets were increased relative to other donors for all surface markers, most noticeably for day 14 monolayers. While this could be an error from antibody concentration or instrument settings, it seems unlikely given that the same master mix was used for day 14 spheroids. CD29 (**Figure 26b)** displayed no significant changes, although spheroid expression did generally trend lower than the comparative monolayer. The data sets seemed to trend slightly down from the day-2 monolayer. This was, however, skewed due to two outlying data points, biological replicate 2 on day 0 monolayer and biological replicate 3 on day 14 monolayer, which drastically increased the mean for their data sets. The same pattern arose for CD166 (**Figure 26f)**; expression generally trended downwards for spheroid conditions. CD73 (**Figure 26d)** had changes in intensity that were less clear; however, the trend of monolayers showing higher expression than the spheroids was retained, although the comparison was more evident at day 0 and less so by day 14. CD105 showed the clearest decrease in signal for spheroids compared to the monolayer at both time points. While the monolayer conditions remained consistent across all time points (**Figure 26c)**. The same pattern was observed for CD146 (**Figure 26d)**, with a decrease for spheroids relative to day -2 and their comparative timepoint monolayer.

When analysing trends of specific replicates **(Figure 27)**, replicate one exhibited a slight decrease in expression intensity of monolayers over time, but the comparative spheroid condition was lower. In particular, CD105 **(Figure 27b)** had nearly no expression at all by day 14. CD146 **(Figure 27c)** showed quite a large decrease in expression for day 14 spheroids compared to the monolayer, but not to the same extent. CD29 and CD73 **(Figures 27a and d)** intensity decreased, but it was less substantial than for the other markers. Control spheroid intensity was higher than day 14 encapsulated for CD105 and CD146, but the opposite for CD29 and CD73.

Replicate 2 showed a decrease for day 14 monolayers compared to day -2 for CD29, CD73 and CD166, but an increase for CD105 and CD146. However, the day 0 monolayer intensity was higher than both for CD29, CD105, CD73 and CD166. Once again, spheroids were less intense than the respective monolayer, other than for day 14 CD166. In addition, the expression of spheroids decreased from day 0 to day 14 for CD29, CD105 and CD73, but increased for CD146 and CD166. Replicate 3 showed increased intensity for the day 14 monolayer relative to day -2 for all markers; however, for CD105 and CD146, the day monolayer decreased relative to day -2, although the error bars were large and may follow the trend of CD29, CD73 and CD166, with it being higher if additional replicates were performed. Spheroid intensity was lower than the respective monolayer for all markers other than day 0 CD29, where it was the opposite. Further, the expression for spheroids increased from day 0 control to day 14 encapsulated for CD29, CD146, CD73 and CD166, but decreased for CD105.

The percentage of cells expressing showed a slight decrease in spheroid conditions relative to day -2 for all markers **(Figures 28a-e)**. Further, the number of day 14 spheroids was lower than that of day 0 spheroids for all markers except CD166. The number of monolayer cells expressing increased for CD29 and CD73 **(Figures 20a and d)** for day 0 relative to day -2 but decreased slightly from day 0 to day 14. The number stayed consistent for CD105 **(Figure 20b)**, and for CD146 **(Figure 20c)** decreased for day 0 and then increased slightly for day 14. For CD166 **(Figure 20e)**, the day 14 monolayer increases to day 0 and again for day 14.

For replicate 1, more spheroids were positive at day 0 than the monolayer for CD105 and CD146, and the opposite for CD29 and CD73. Whereas at day 14, more spheroids were positive than monolayers for CD29 and CD73, and the opposite for CD105 and CD146. Monolayer expression of CD29 and CD73 increased slightly, but was higher at day 0 than at day 14. While it increased at day 14 relative to day -2 for CD105, it decreased for day 0. Similarly, expression decreased at day 0 for CD146 monolayers, and while it increased for day 14, it remained lower than day -2. Spheroid expression was higher than monolayer at day 0 for CD105 and CD146, but both were lower than day -2. By day 14, the monolayer was higher than the spheroids; however, CD146 did not recover to day-2 levels, whilst CD105 did. In contrast, for CD29 and CD73, fewer cells were positive at day 0 spheroids

than day -2 and day 0 monolayer; however, by day 14, more cells were expressing for spheroids than monolayer.

For replicate 2, the monolayer cells show an increased percentage of positive cells compared to the corresponding spheroid condition for all markers. However, day 14 monolayer numbers for CD29 and CD73 are lower than those at day -2, which in turn are lower than those at day 0, whilst spheroids both stay below day-2. For CD105, the numbers for monolayers are consistent, and the numbers for spheroids decrease from day 0 to day 14. For CD146, spheroids show so few cells expressing that they're not visible on the graph. Day 14 monolayers have similar numbers of cells expressing as at day-2, but the number decreased for day 0.
Replicate 3 monolayers show increased numbers of cells expressing from day -2 to day 0 to day 14 for CD29, CD146, CD73 and CD166, but for CD105, the number remains consistent for day 0 and increases slightly for day 14. Spheroids at day 0 have more cells expressing than day -2 and day 0 monolayers for CD29, CD105, and CD73. For CD29 and CD73 at day 14, whilst spheroids were now higher than both day 0 conditions, the day 14 monolayer was now higher than spheroids. CD146 displayed spheroid numbers that decreased relative to day -2, and then decreased further by day 14. CD166 also saw a decrease for day 0 spheroids compared to day -2, but the numbers then increased for day 14 spheroids relative to day 0.

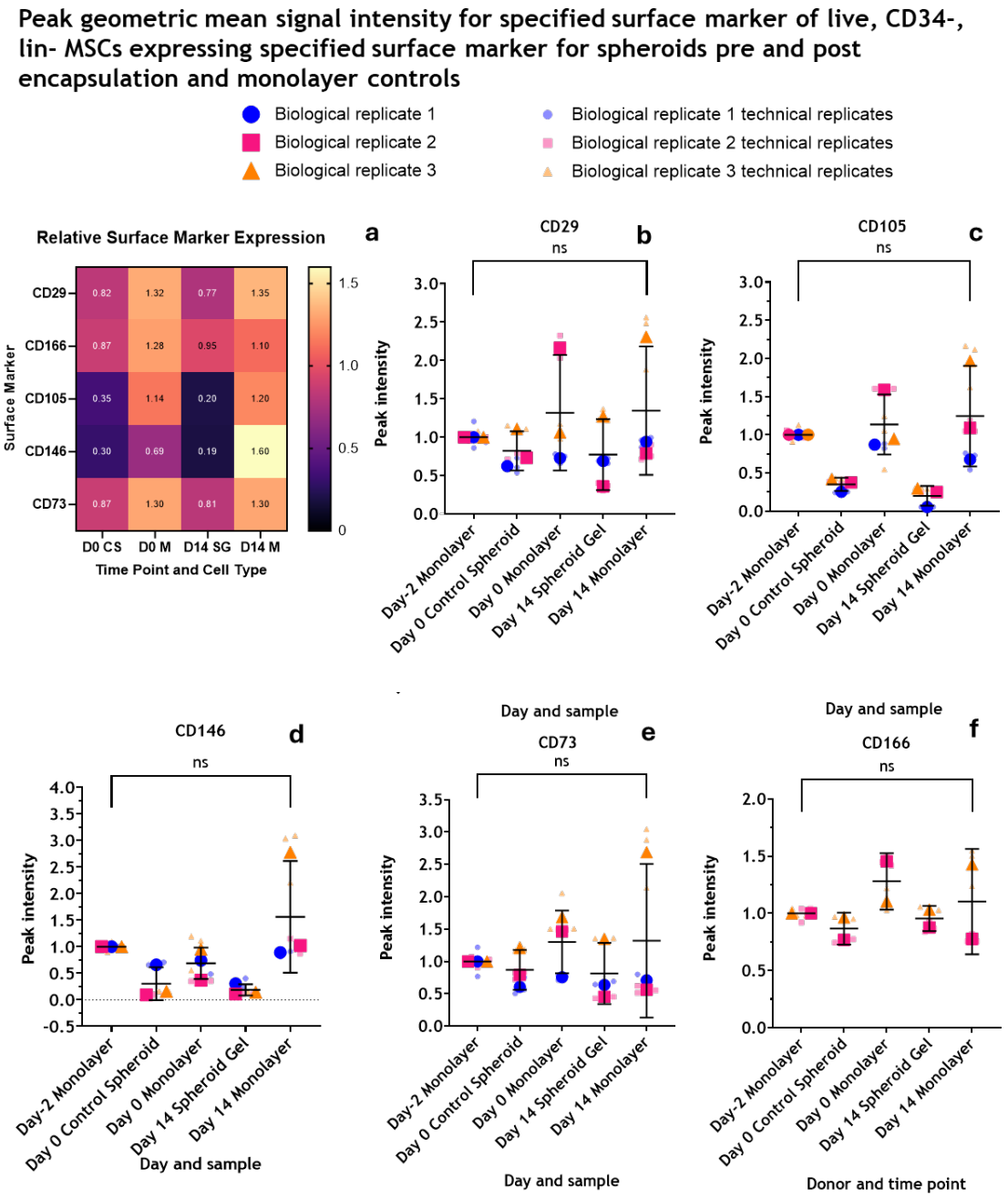

Figure 26. Fluorescence intensity geometric mean measured by flow cytometry on day of seeding, on day of spheroid encapsulation and 14 days post-encapsulation, normalised to day-2 monolayer control.

a) heatmap displaying fold change relative to D-2 monolayer. CS Control spheroid, M Monolayer, SD Spheroid Gels. Super plots for the following markers b) CD29, c) CD105, d) CD146, e) CD73, f) CD166 gated for live, CD45- CD34- cell populations.

Error bars indicate the mean +/- one standard deviation for pooled data points.

Brighter points depict the mean value for that data set, while the paler colours indicate the individual values themselves.

Significance was calculated for comparison of data from the same media type and same measurement time point by the Mann-Whitney U test with bounds of non-significance $p>0.05$.

Peak geometric mean signal intensity for specified surface marker of live, CD34-, lin- MSCs expressing specified surface marker for spheroids pre and post encapsulation and monolayer controls. Split biological replicates.

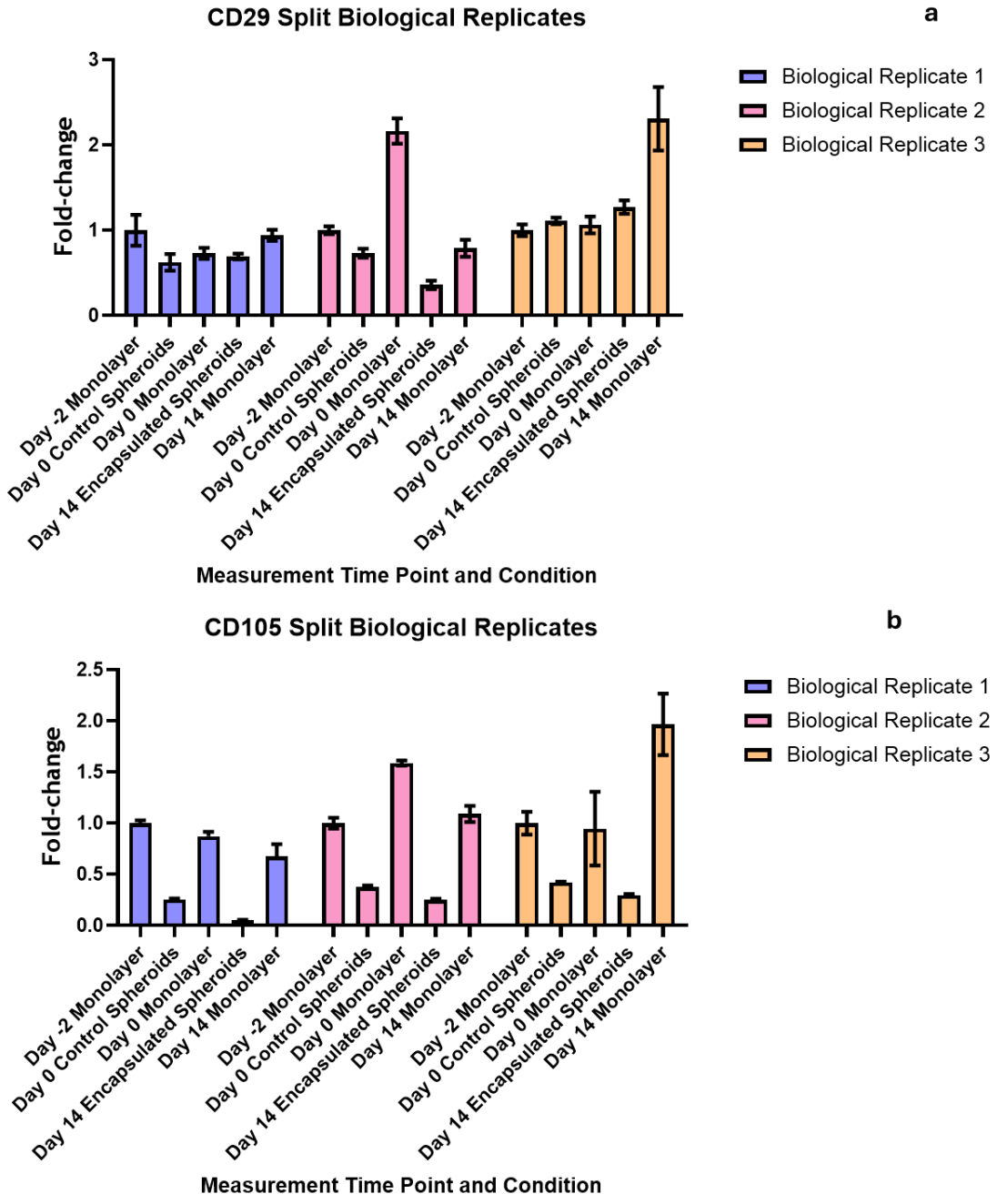

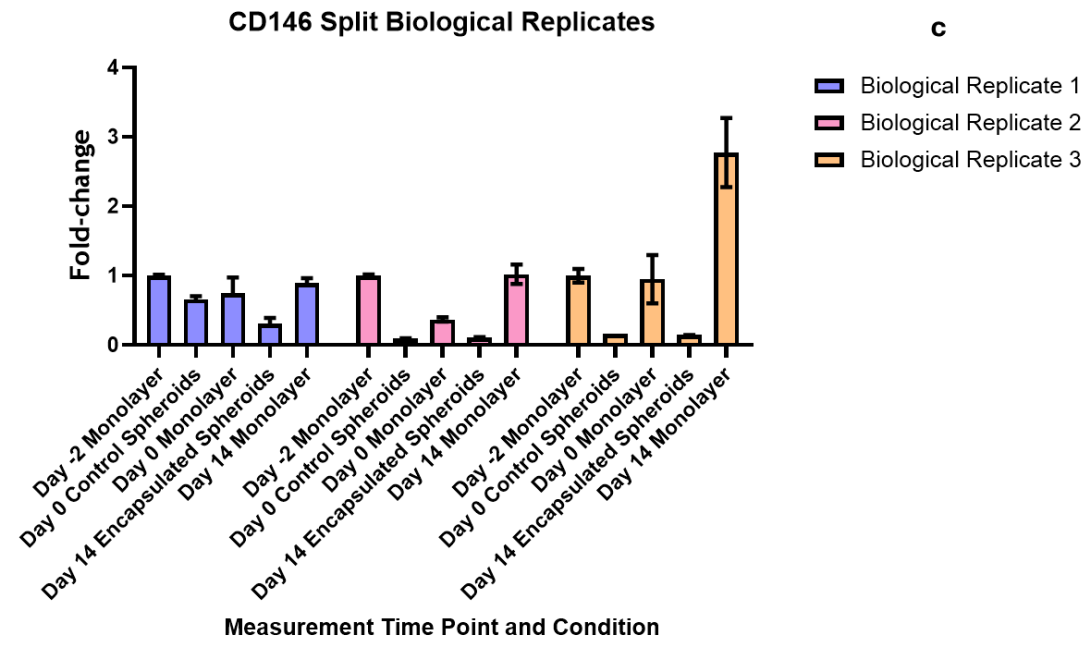
CD146 Split Biological Replicates
c
Biological Replicate 1
Biological Replicate 2
Biological Replicate 3
Fold-change
0
1
2
3
4
Day -2 Monolayer
Day 0 Control Spheroids
Day 0 Monolayer
Day 14 Encapsulated Spheroids
Day 14 Monolayer
Measurement Time Point and Condition

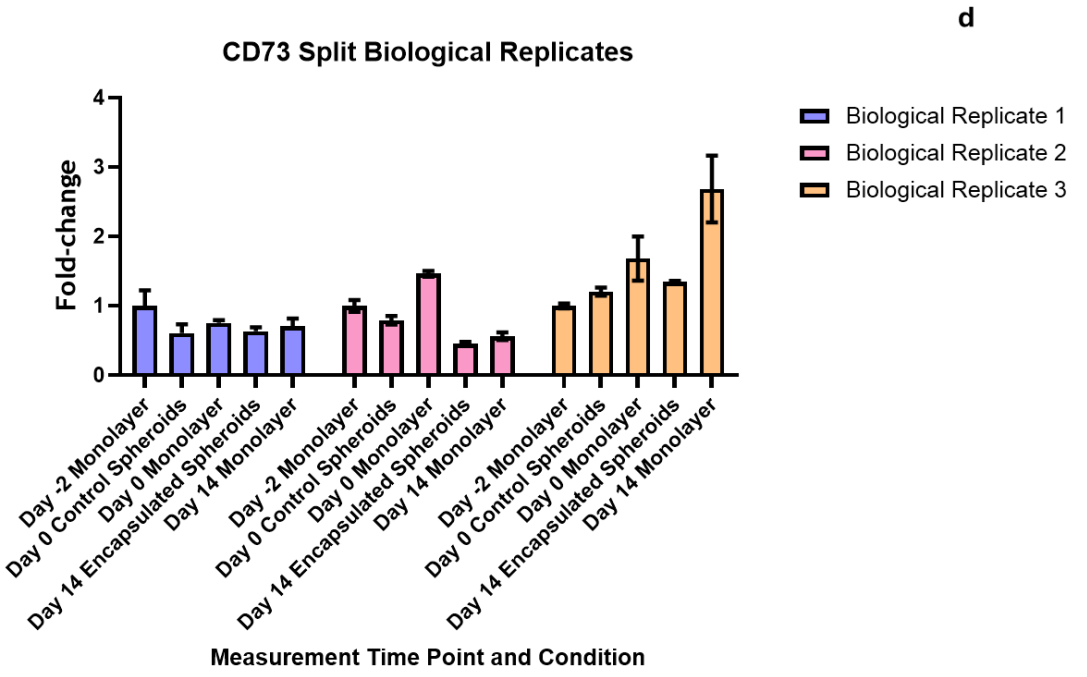
CD73 Split Biological Replicates
d
Biological Replicate 1
Biological Replicate 2
Biological Replicate 3
Fold-change
0
1
2
3
4
Day -2 Monolayer
Day 0 Control Spheroids
Day 0 Monolayer
Day 14 Encapsulated Spheroids
Day 14 Monolayer
Measurement Time Point and Condition

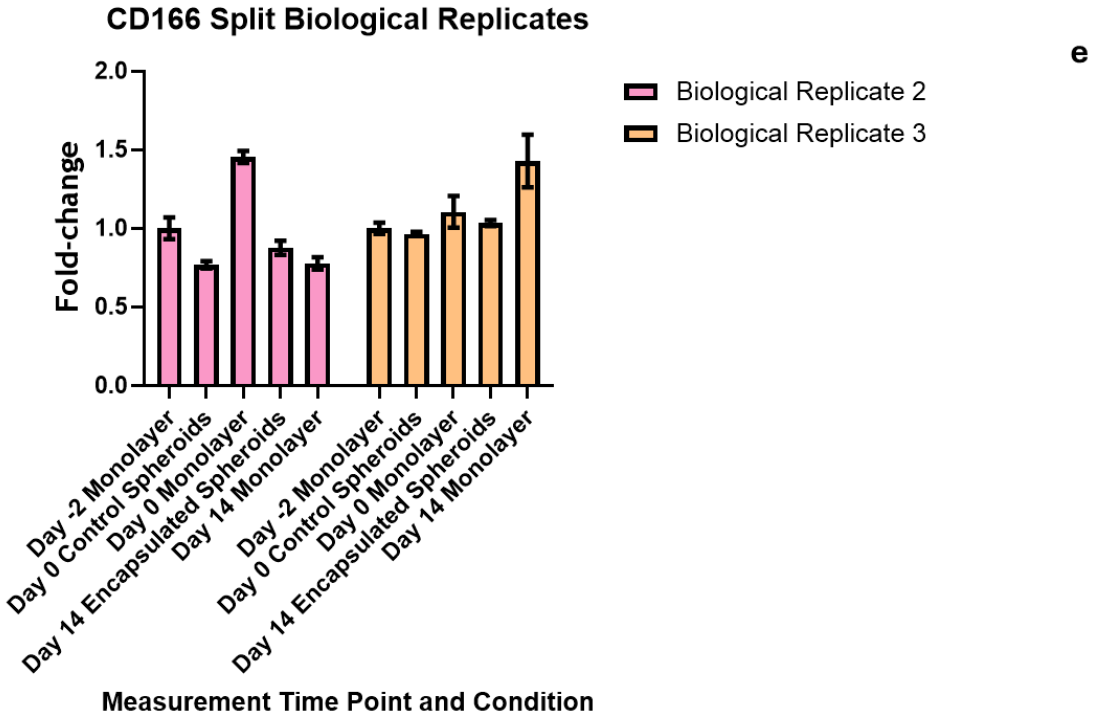

Figure 27. Fluorescence intensity geometric mean measured by flow cytometry on day of seeding, on day of spheroid encapsulation and 14 days post-encapsulation, normalised to day-2 monolayer control. Biological replicates separated for graphs a-e in Figure 26 and replotted for a) CD29, b) CD105, c) CD146, d) CD73, e) CD166 gated for live, CD45- CD34- cell populations. Graphs show the mean +/- one standard deviation; they are N=1, so no significance is calculated.

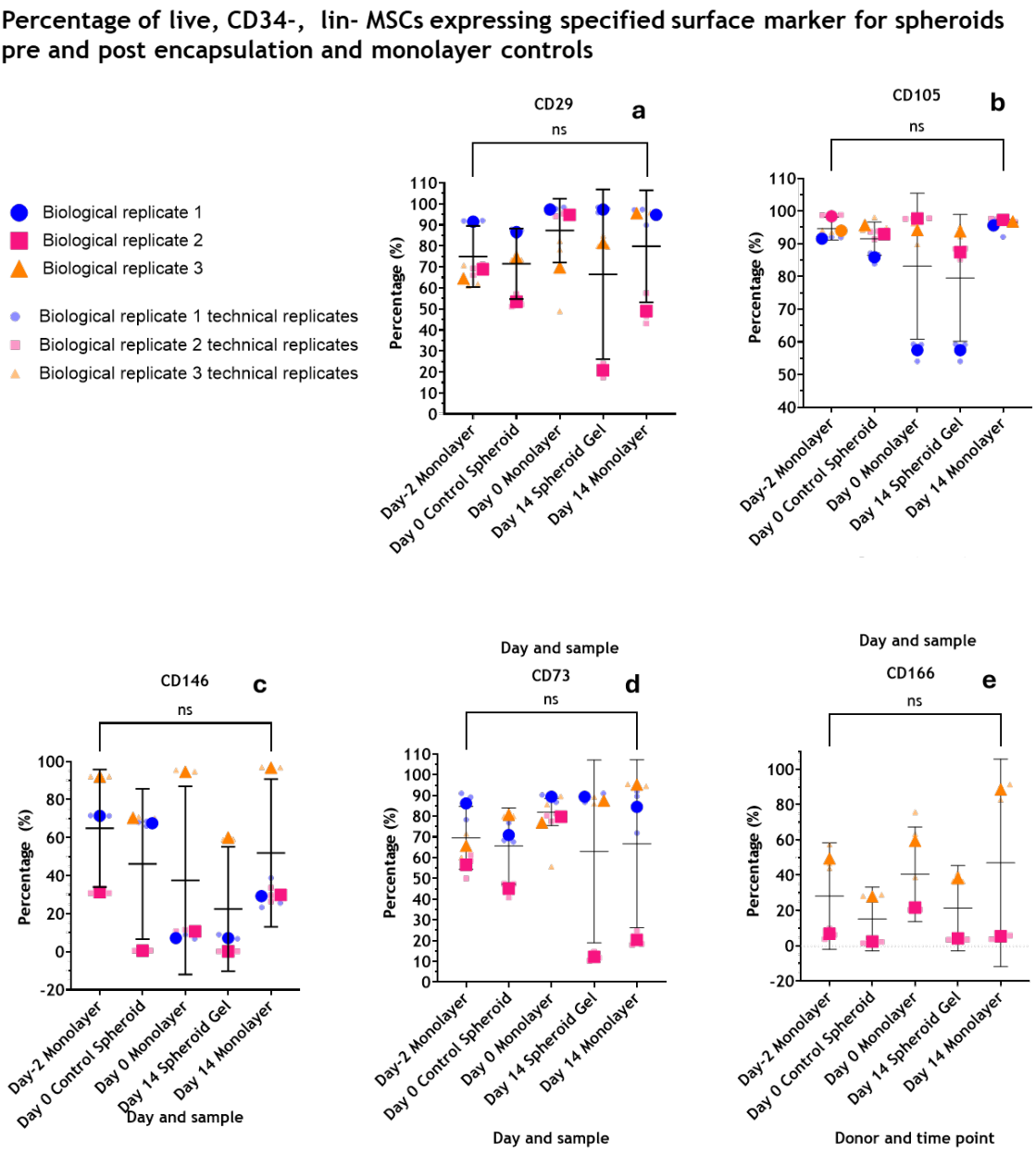

Figure 28. Percentage of MSC population expressing the specified marker measured by flow cytometry on the day of seeding, on the day of spheroid encapsulation and 14 days post-encapsulation.

Super plots for the following markers a) CD29, b) CD105, c) CD146, d) CD73, e) CD166 gated for live, CD45- CD34- cell populations.

Error bars indicate the mean +/- one standard deviation for pooled data points.

Brighter points depict the mean value for that data set, while the paler colours indicate the individual values themselves.

Significance was calculated for comparison of data from the same media type and the same measurement time point by using the Mann-Whitney U test with bounds of non-significance $p>0.05$.

Percentage of live, CD34-, lin- MSCs expressing specified surface marker for spheroids pre and post encapsulation and monolayer controls. Biological replicates are split.

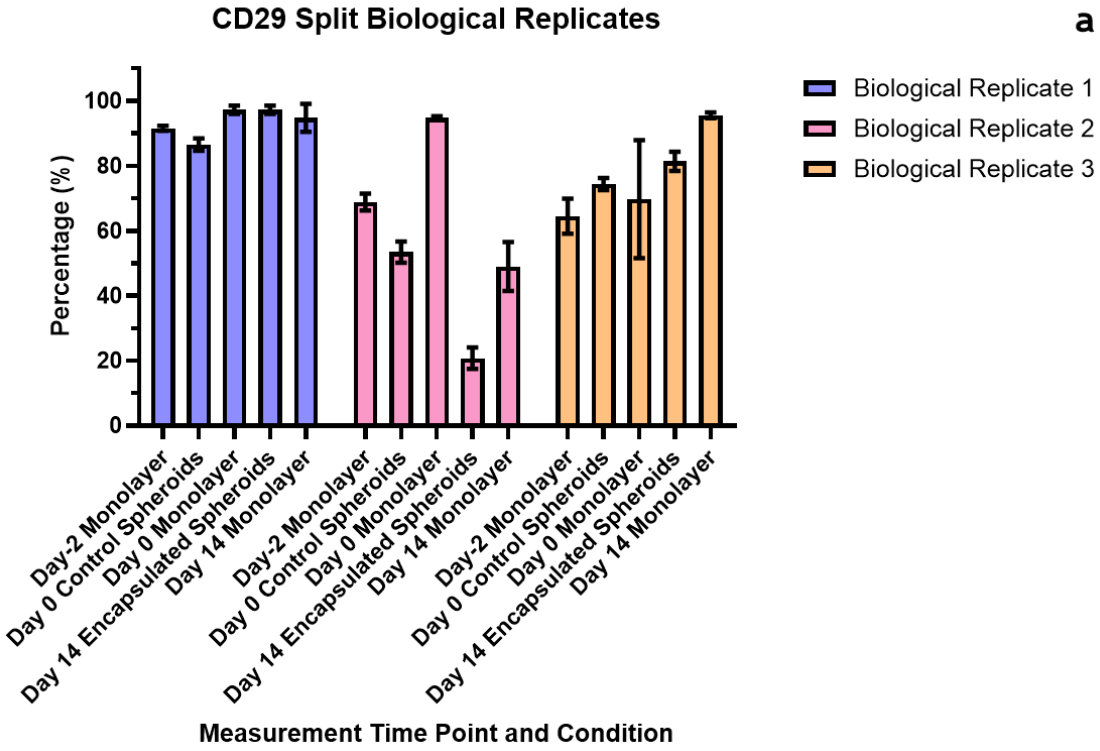

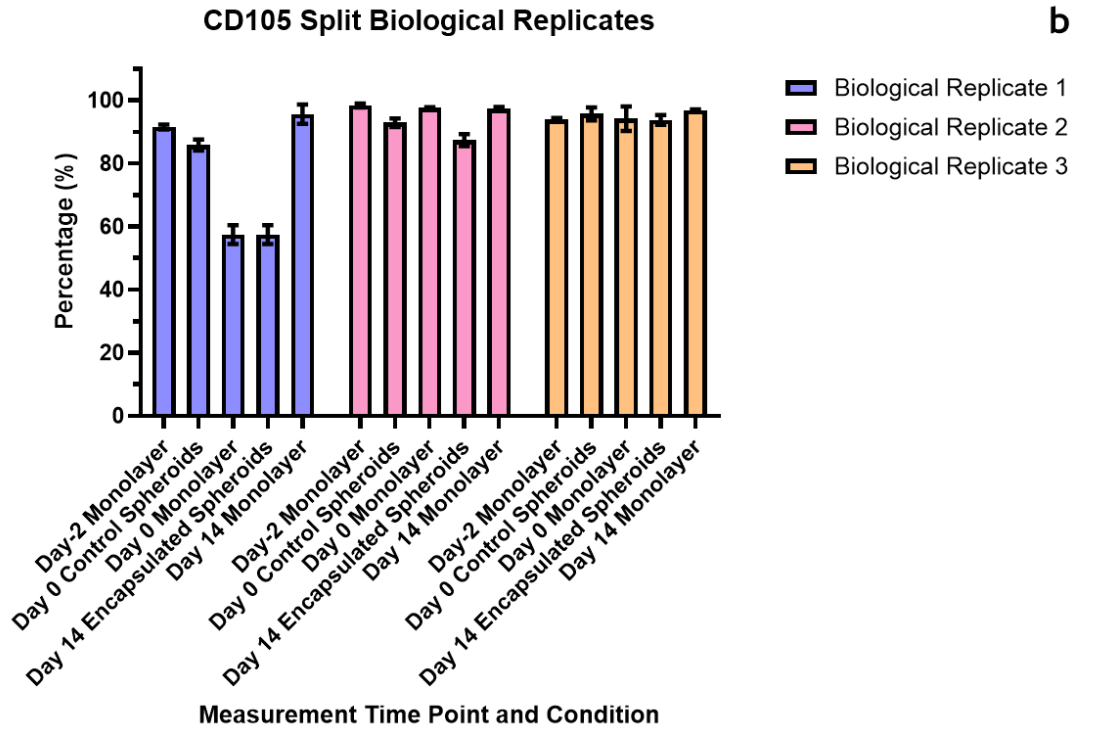

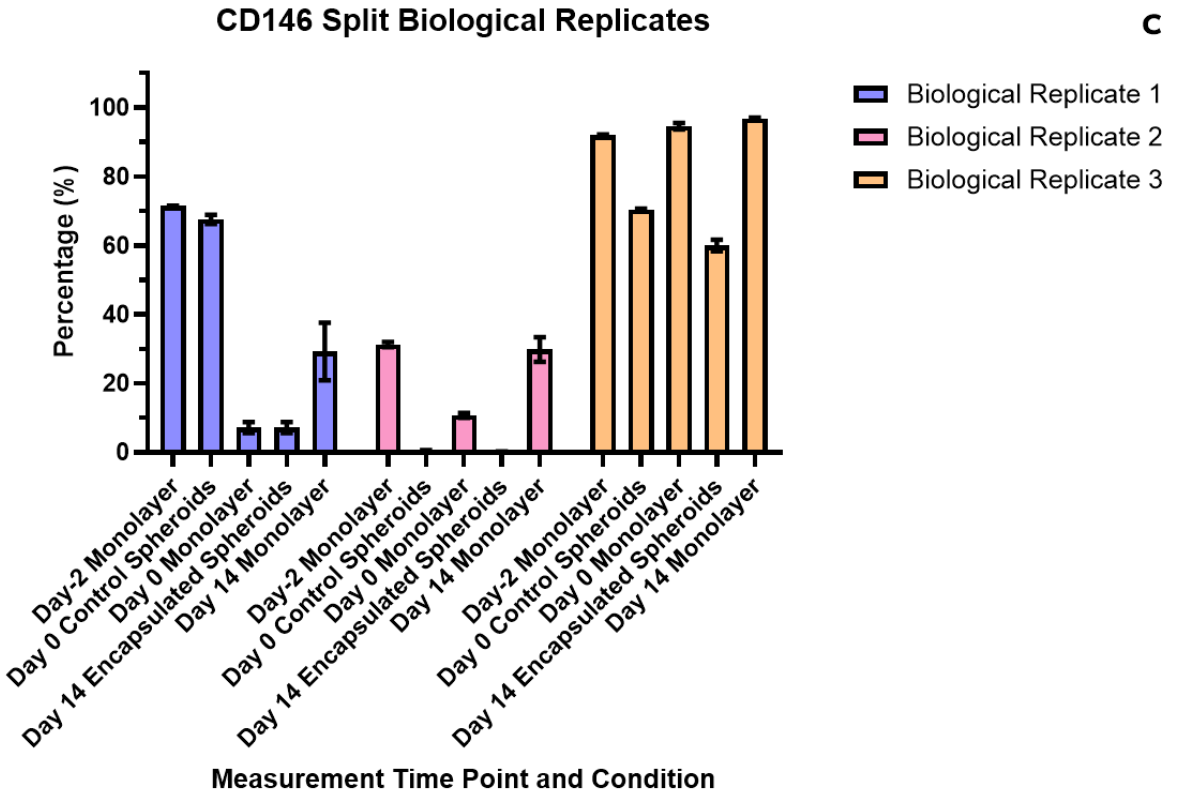
CD146 Split Biological Replicates
c
Biological Replicate 1
Biological Replicate 2
Biological Replicate 3
Percentage (%)
0
20
40
60
80
100
Day-2 Monolayer
Day 0 Control Spheroids
Day 0 Monolayer
Day 14 Encapsulated Spheroids
Day 14 Monolayer
Measurement Time Point and Condition

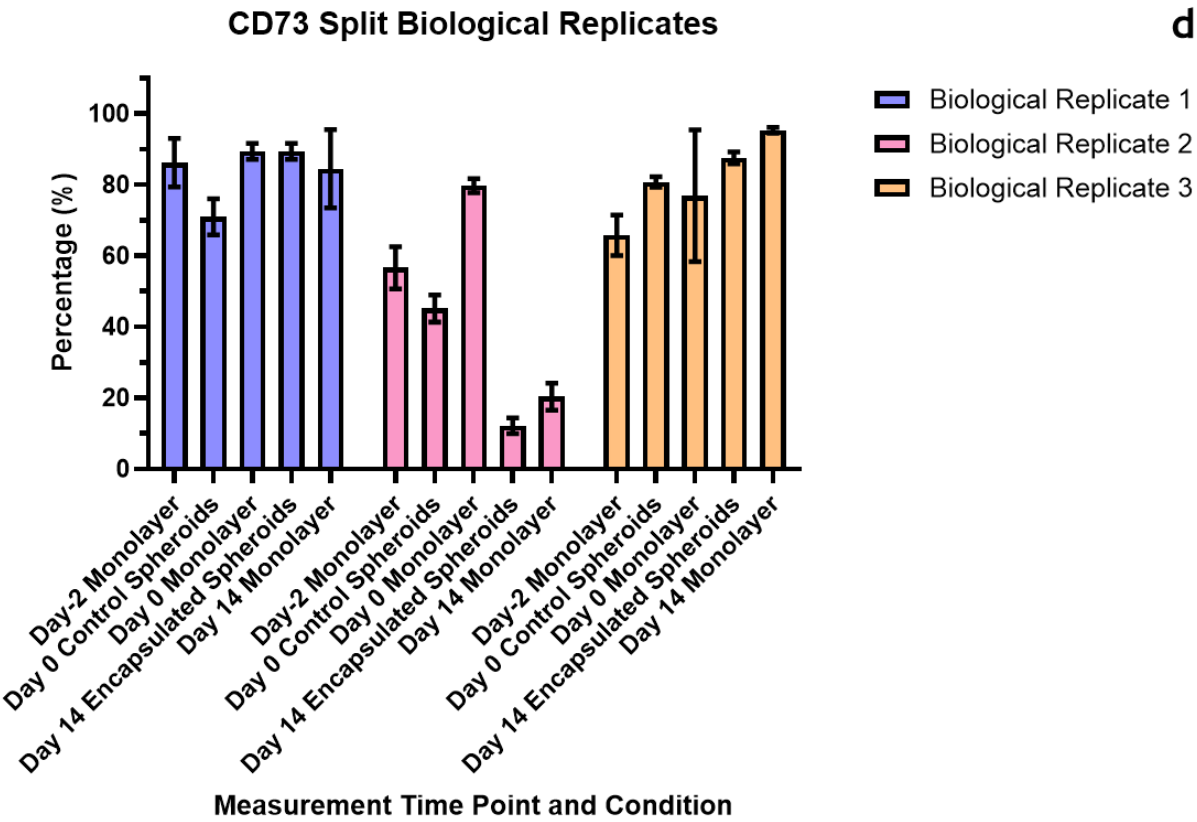
CD73 Split Biological Replicates
d
Biological Replicate 1
Biological Replicate 2
Biological Replicate 3
Percentage (%)
0
20
40
60
80
100
Day-2 Monolayer
Day 0 Control Spheroids
Day 0 Monolayer
Day 14 Encapsulated Spheroids
Day 14 Monolayer
Measurement Time Point and Condition

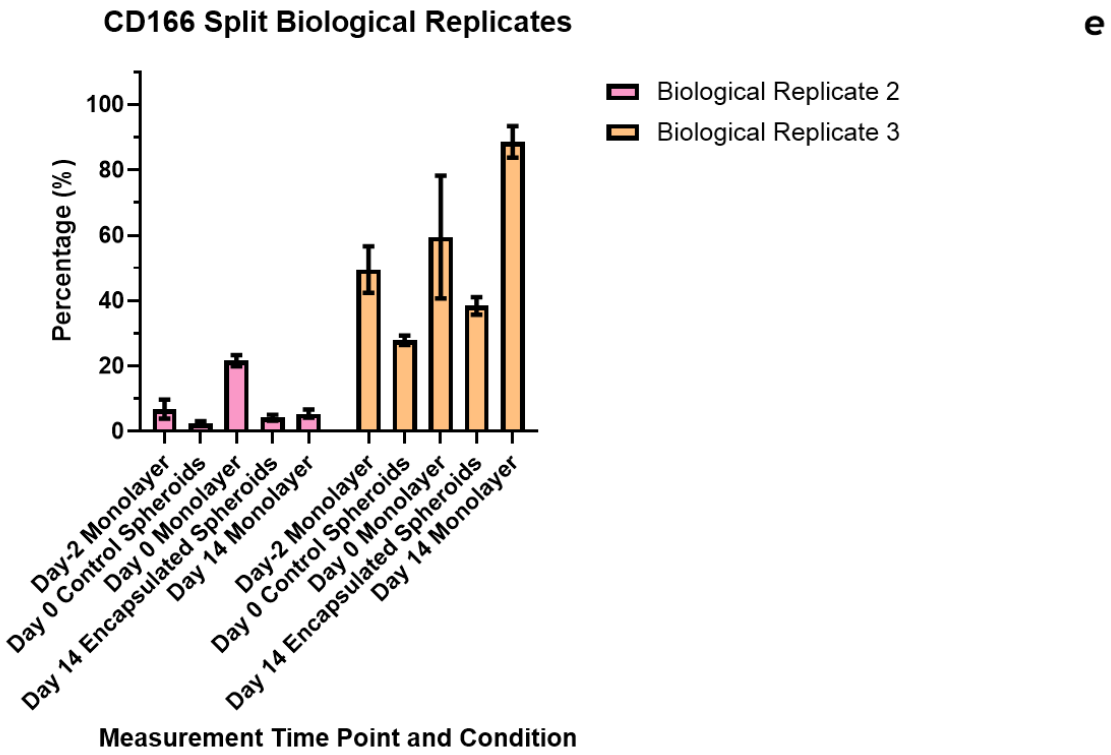

Figure 29. Percentage of MSC population expressing the specified marker measured by flow cytometry on the day of seeding, on the day of spheroid encapsulation and 14 days post-encapsulation. Biological replicates separated for graphs a-e in Figure 28 and replotted for a) CD29, b) CD105, c) CD146, d) CD73, e) CD166 gated for live, CD45- CD34- cell populations. Graphs show the mean +/- one standard deviation; they are N=1, so no significance is calculated.

4.2.3 MSC spheroid flow - experimental replicate

Flow analysis of surface marker expression on day-2 monolayer control vs day 14 encapsulated spheroids was performed in **Figures 30 and 31**. While the percentage of cells generally decreased **(Figure 30)**, there was no significant difference for CD29, CD34, CD90, CD146, CD166 and CD271. There was a significant difference for CD44, with expression decreasing close to 0, although the expression for replicates 2 and 3 was nearly 0 at day -2 already. The decrease in CD105 was less than 10%, and this was the same for CD73, except for replicate 1. CD271 had low lying expression, which fell to roughly 0 by day 14, while expression of CD34 was 0 for replicates 2 and 3, but increased substantially by day 14. In previous experiments, CD34 was used to negatively gate the samples, but because at day-14 such large numbers of cells were

positively expressing, it was instead included as a condition for analysis **(Figure 30h)**.

Replicate 1 showed an increase in the percentage of cells expressing from day-2 to day 14 for CD29, CD90 and CD105 **(Figures 30a, d, and f)**. It's worth noting that the range of change is within 5% and would therefore be less impactful compared to markers CD73, CD44, CD146 and CD166, which matched the decreasing trend for other donors but with a far greater decrease of 50%, 75%, 70% and 95%, respectively. In contrast, replicates 2 and 3 showed a decreased number of cells expressing at day 14 for CD29, CD73, CD90, CD146, CD105, and CD166 **(Figures 30a, b, d, e, f and g)**; however, the decrease for CD29 and CD73 was small **(Figures 30a and b)**. Expression for all replicates for CD271 **(Figure 30i)** was near 0 at day 2 and was 0 by day 14 (albeit higher at day -2 for replicate 1), and this was the same for CD44 **(Figure 30c)**.

The fluorescence intensity of positive-expressing cells significantly increased for CD44 **(Figure 31c).** Intensity decreased for all other markers - CD29, 73, 90, 146 and 105 **(Figure 31a, b, d, e and f),** with decreases in intensity by 66%, 37%, 80%, 55% and 90%, respectively. Replicates showed matching trends for all markers, although replicate 2 had the highest day -2 intensity for CD29, CD73 and CD90.

Percentage of MSCs with positive expression of specified surface marker after encapsulation as MSC spheroids for 14 days compared to day-2 monolayer.

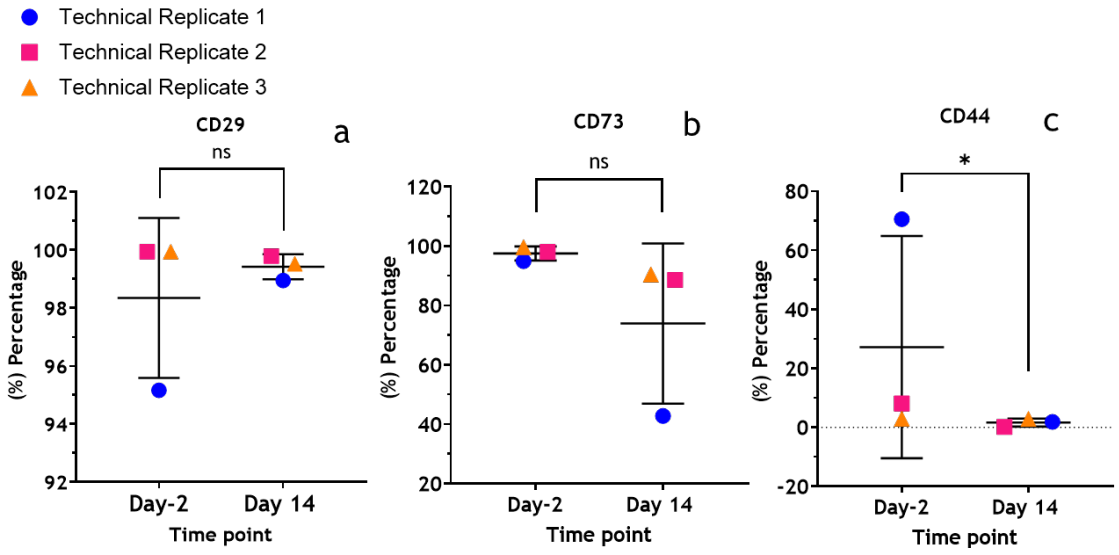

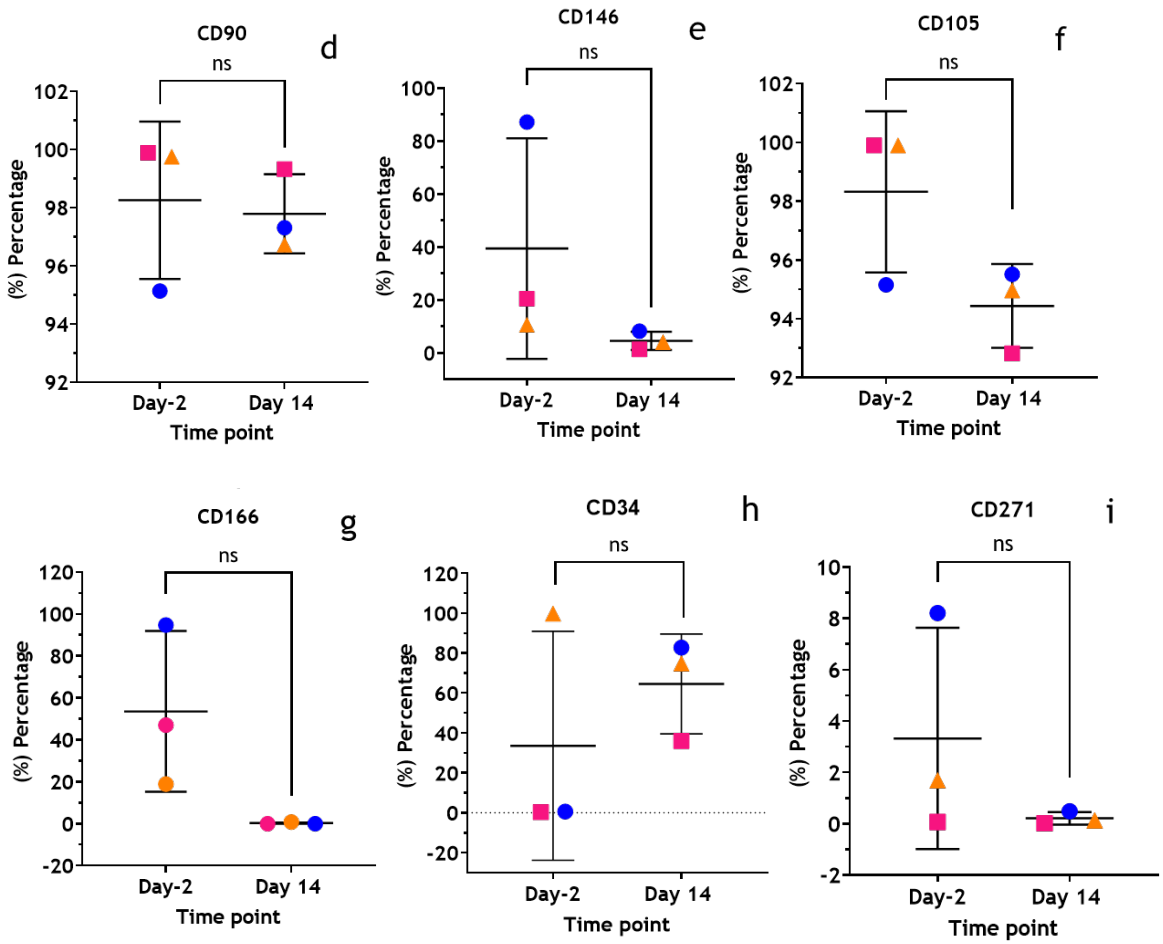

Figure 30. **Percentage of MSC population expressing the specified marker measured by flow cytometry on the day of seeding and 14 days post-encapsulation.**

Data points plotted depict technical replicates as individual data points, superimposed by the biological replicate - the mean of these points - and finally with error bars displaying the mean +/- one standard deviation of the pooled experimental replicates.

Super plots for the following markers: a) CD29, b) CD73, c) CD44, d) CD90, e) CD146, f) CD105, g) CD166, h) CD34, i) CD271, gated for live, negative marker cocktail - cell populations. Significance was calculated using Welch's t-test with bounds of ns $p>0.05$, * $p<0.05$.

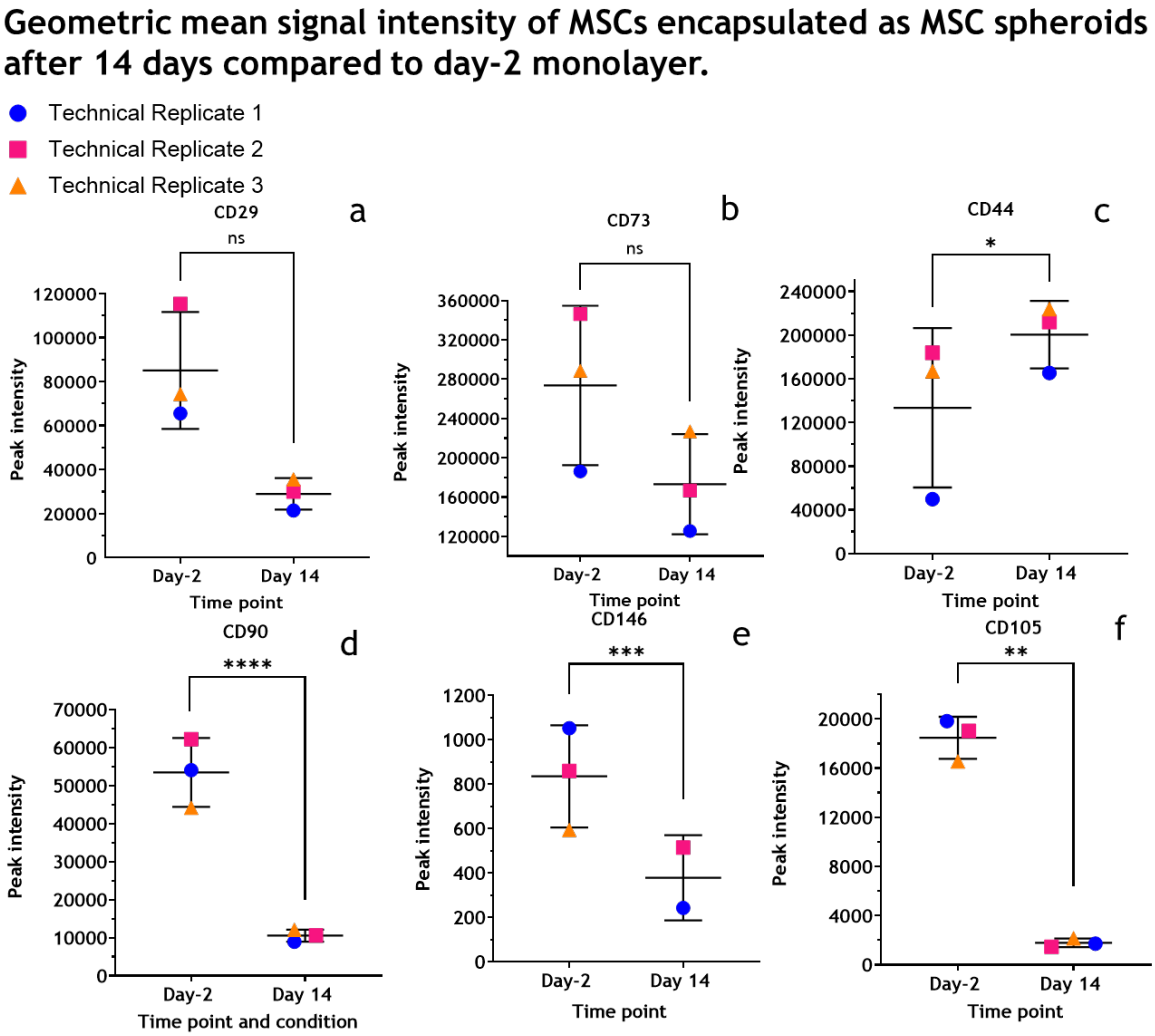

Figure 31. **MSC fluorescence intensity geometric mean measured by flow cytometry on the day of seeding and 14 days post-encapsulation as spheroids.**

Data points plotted depict technical replicates as individual data points, superimposed by the experimental replicate - the mean of these points - and finally with error bars displaying the mean +/- one standard deviation of the pooled experimental replicates.

Super plots for the following markers: a) CD29, b) CD73, c) CD44, d) CD90, e) CD146, f) CD105, gated for live, negative marker mix negative cell populations.

Significance was calculated using Welch's t-test with bounds of: ns $p>0.05$, * $p<0.05$, ** $p<0.005$, *** $p<0.0005$, **** $p<0.00005$

4.2.4 Nanoindentation

To assess the physical properties of the gels during the encapsulation process, the stiffness of the gels without cells with single cells, spheroids, or single and spheroid cells **(Figure 32)**. Single-cell gels saw a decrease in stiffness, while the other three conditions saw a slight increase. There was one potential outlier noticeable in this data; replicate 1 for mixed single cells and spheroids, day 14. The day 1 stiffness of all conditions shows a large range with highly variable results. While spheroids were slightly softer and no cell gels were slightly stiffer, there was no significance. Accounting for this result, gel stiffness is likely between 12 and 16 kPa, and additional replicates should be undertaken to determine differences between cell conditions.

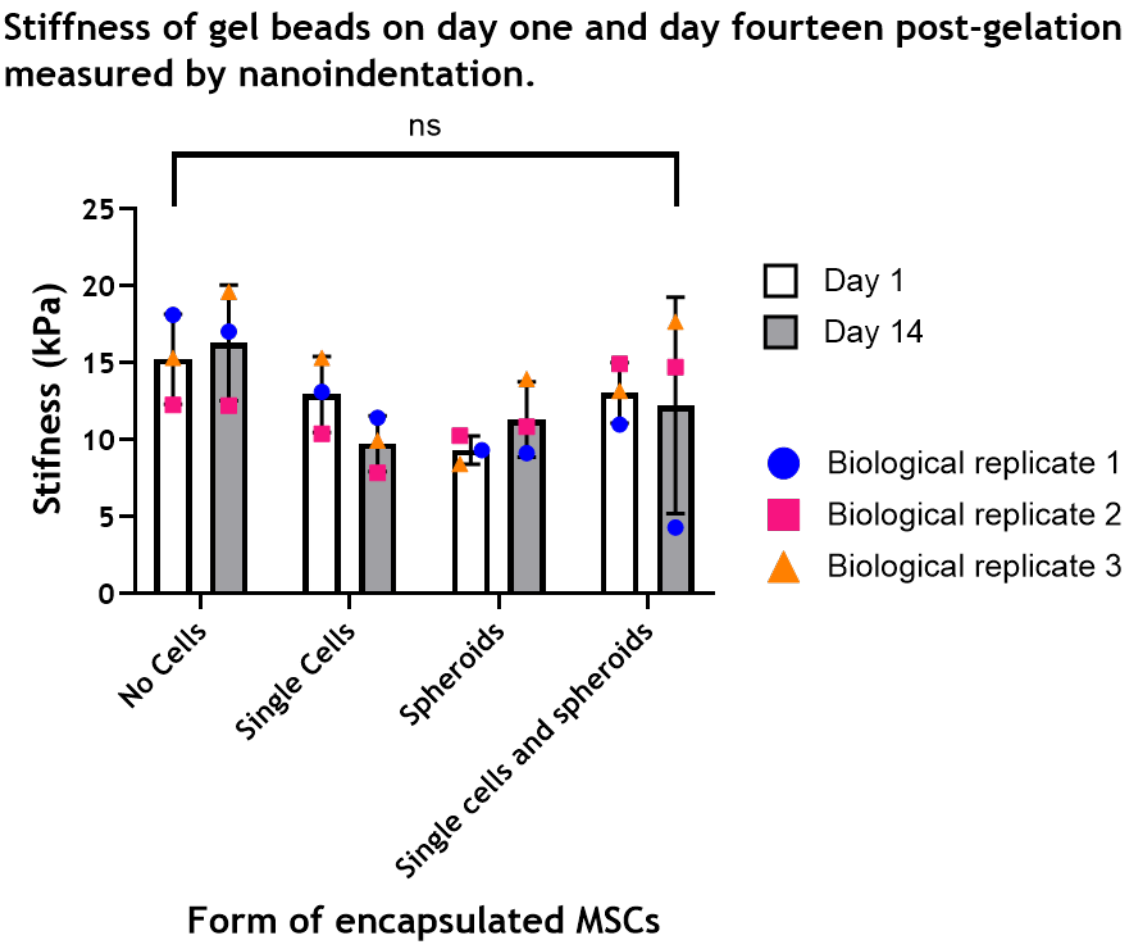

Figure 32. Average surface stiffness of gel beads one and fourteen-days post-gelation. Values calculated using nanoindentation.
N of 3 biological replicates plotted with individual colours. Error bars indicate the mean value +/- one standard deviation. Significance was calculated by the Welch's t-test with bounds of non-significance p>0.05.

4.2.5 CD34+ phenotype (Flow)

Three new donors were used for this chapter compared to those in Chapter **3.** However, as the original 3 donors were utilised to give an N=6 for some experiments in this chapter, the new donors were assigned their own colour and a black outline to their symbol to assist in distinguishing them.

HSPC recovery ranged from 1 to 7%, as seen in **Table 3.** Donor 6 having poor recovery was not surprising, as the overnight recovery period showed a decrease of over twice that of Donors 4 and 5, **see Table 2.**

Table 2. Numbers of viable cells recorded post-thawing of the CD34+ vial and after an overnight recovery period at 37 °C.

	D-1 Thawing viable cell number	D0 Encapsulation viable cell number	Overnight viable cell number decrease (%)
Donor 4	$3.975x10^6$	$3.12x10^6$	21.51
Donor 5	$4.0x10^6$	$3.0x10^6$	25.00
Donor 6	$3.15x10^6$	$1.4x10^6$	55.56

Table 3. Number of viable CD34+ cells pre- and post-encapsulation for 14 days at 15 °C.

	Cells encapsulated	Cells recovered	Percent (%) Recovery
Donor 4	$1.1x10^6$	$4.75x10^4$	4.75
Donor 5	$1.4x10^6$	$4.24x10^4$	7.14
Donor 6	$6.0x10^5$	$6.0x10^3$	1.00

This data was gated using the strategy presented in **Figure 10, and d**ue to poor cell recovery, day 14 flow was not performed on donors 4 and 6. However, day 0 composition was performed for all three donors. There was no significant difference between the samples; however, the number of CD34+s (**Figure 28a)** in the live cell population matched the trend for LT-HSC (**Figure 28 b)** cell number, but this was only 1-5%. The percentage of HSPCs that were LT-HSCs was roughly between 38% and 43% (**Figure 28c)**.

Plotting the donors from the initial single cell flow in **3.3.4.** alongside those from this experiment, we can see that the number of HSPCs within the CD34+ population is around 5-10% (**Figure 28d)**.

Donor 5 had sufficient cells to perform flow, and the number of HSPCs in the live population post-encapsulation rose from roughly 8.6% to 32.4% (**Figure 28e**). Interestingly, though, the LT-HSC population relative to HSPCs decreased from 41.6% to 25.3% (**Figure 28e**). The number of LT-HSCs as part of the total live cell population also did not follow the size of the trend of the HSPC population.

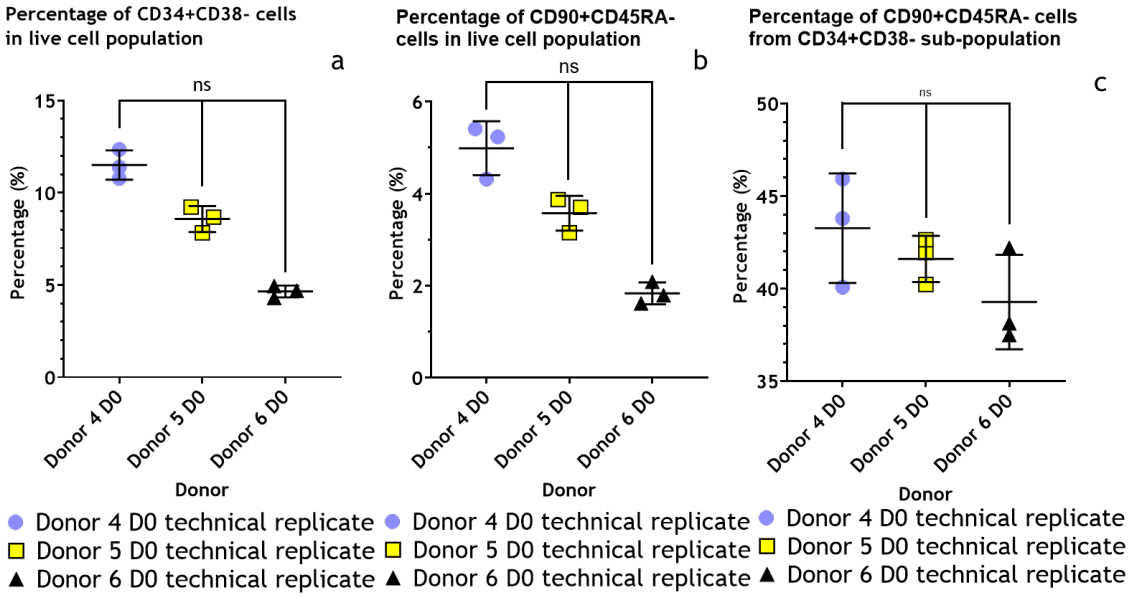

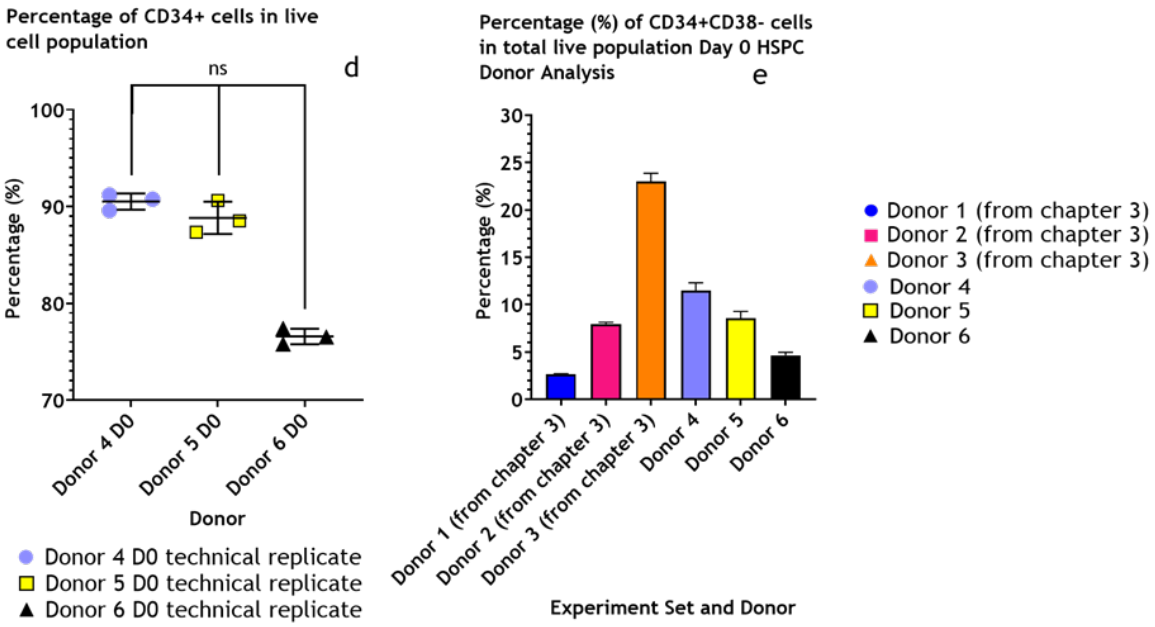

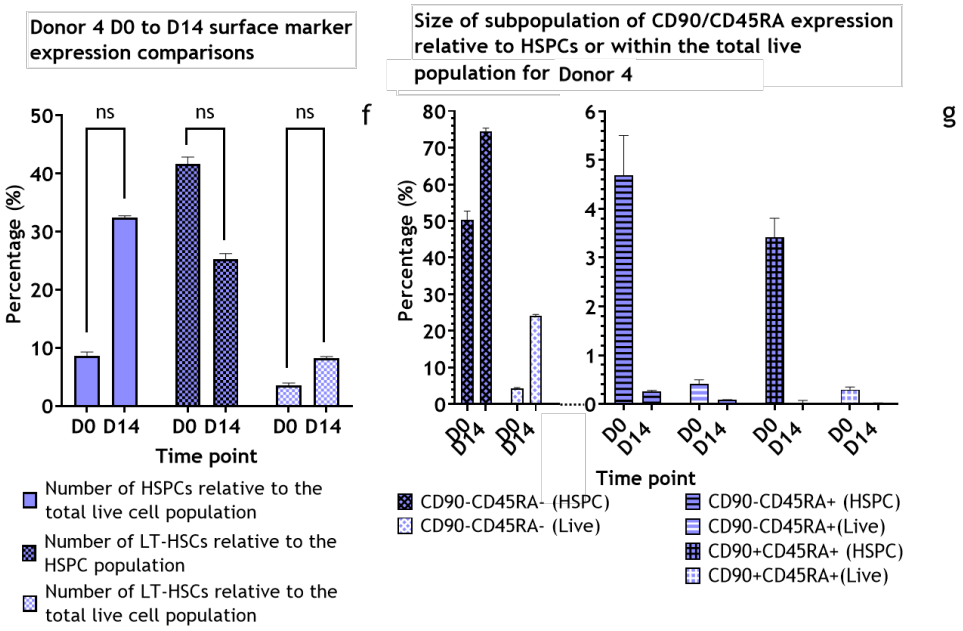

Figure 33. Graphs of CD34+ flow cytometry data.

a) Number of CD34+CD38- (HSPC) cells in the live and CD45+ population as a percentage, b) Number of CD90+CD45-, CD34+CD38- cells (LT-HSCs) in the total live population as a percentage, c) Number of CD90+CD45RA- cells in the CD34+CD38- population as a percentage d) number of CD34+ cells in the total live population e) Number of cells that are CD34+CD38- (HSPCs) in the full donor population at D0 for all HSPC donors used in chapter 3, figure 22 - denoted as Exp 1 (experiment 1) - and chapter 5 - denoted as Exp 2 (experiment 2) - 5 f) Number of Donor 2 CD34+CD38- cells (HSPCs) relative to the live and CD45+ population as a percentage, number of CD90+CD45RA-, CD34+CD38- cells (LT-HSCs) relative to the live and CD45+ population as a percentage, and the number of CD90+CD45RA- (LT-HSCs) and CD34+CD38- cells relative to CD34+CD38- (HSPC) population. g) size of CD90/CD45RA subpopulation for donor 4 at D0 and D14 relative to the live and HSPC populations.

Error bars indicate the mean +/- one standard deviation.

Significance was calculated for comparison of data from the same media type and the same measurement time point by using the Mann-Whitney U test with bounds of non-significance $p>0.05$.

Table 4 shows that of the cells expressing CD34+CD38- at day 0, 11.4% of them survived to day 14. Further, it shows how of the cells that would be deemed the most primitive in the population – CD90+CD45RA-, only 6.9% of them survived to day 14. Therefore, the populations that were assumed to enter quiescence more preferably had a worse recovery than the CD34+CD38- population that were initially thought to enter quiescence less preferably.

Table 4. Number of cells expressing specified markers at day 0 and day 14 for donor 4.

	Average percentage of cells expressing marker (%)	Number of cells counted	Number of cells that are expressing the marker	% of expressing cells that survived to D14
34+38- day 0	8.577375333	1400000	120083.2547	11.4260607
34+38- day 14	32.36034333	42400	13720.78557	
90+45RA- day 0	3.572958333	1400000	50021.41667	6.936663367
90+45RA- day 14	8.183531333	42400	3469.817285	

4.2.6 CD34+ CFU

Colonies counted for donor 4 day 0 were on average 1.3, 1.6, 12.3 and 0.3 for CFU-E, BFU-E, CFU-GM and CFU-GEM, respectively **(See figure 29)**. Colonies for other conditions were not viable at the analysis timepoint due to a lack of water in the incubator, drying the colonies the week before analysis.

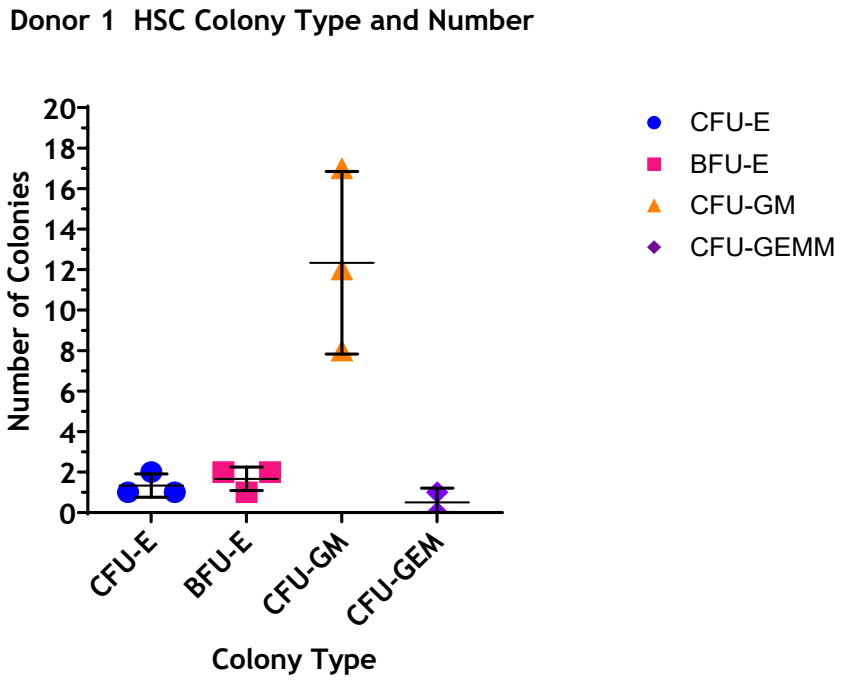

Figure 34. Graph of the number of colonies counted for donor 1 day 0 CD34+ CFU. The graph depicts 3 technical replicates with error bars showing the mean +/- one standard deviation. CFU - Colony Forming Unit, BFU - Burst Forming Unit, GEM - Granulocyte/Erythroid/Macrophage/Megakaryocyte, GM - Granulocyte/Macrophage, E- Erythroid.

4.3 Discussion

4.3.1 Viability

The control spheroids used were not encapsulated and left for a further day within the AggreWell™ plate. Subsequently, it's anticipated that the cells in the control spheroids would be more metabolically active than those encapsulated at hypothermic temperatures. To become fluorescent, Calcein AM must permeate the membrane and be hydrolysed into its fluorescent form. Subsequently, one would expect that once encapsulated, the green intensity would decrease and would do so further over time, while the red intensity should stay fairly stable if cells were remaining viable **Figure 25.** A non-encapsulated control was used for the IMDM vs DMEM test to observe this behaviour (**Figure 25a)**. That overall trend was not observed. Instead, the intensity of the dead signal increased between day 1 and day 14 for all three biological replicates for both media types **(Figure 25j, k and l).** This would suggest that increased apoptosis is occurring, and that viability is not completely maintained over 14 days of encapsulation. In comparison, the expected trend did occur for biological replicate 3 with a decrease in green intensity in all encapsulated conditions; however, biological replicates 1 and 2 instead trended the other direction, with both day 1 and day 14 IMDM conditions seeing an increase in green intensity. This would indicate increased activity and does not align with the expected reduced activity state of spheroids and encapsulated cells.

The difference from day 1 to day 14 for DMEM and IMDM (**Figure 25a**) was a 68% decrease and 70% decrease, respectively, suggesting that while the IMDM viability was higher, the decrease over time was similar, and therefore, there was no benefit to either media. This agrees with observations from **Figure 11d,** where we previously established that media composition does not impact the viability of single-cell MSCs. In contrast, the optimal encapsulation temperature of 15 °C for single cell MSCs in **3.3.4.** was not replicated in **Figure 25b**. Instead, there was only 1% difference between 15 and 20 °C, and therefore these temperatures do not have an observable impact on spheroids. This is not unexpected, as resistance to temperature changes has resulted in a few recent publications. In 2024, Trufanova *et al.* demonstrated that A-MSCs could be stored up to 7 days at 22 °C without a negative impact on functionality (Trufanova et al., 2024). Similarly, BM-MSCs and E-MSCs (embryonic) are viable after 7 days

across a range of temperatures from 10-37ºC thanks to decreased metabolism and proliferation (YS et al., 2016). Most drastically, Qiu *et al*. 2024 study demonstrated that MSC spheroids can be stored for 7 days at 12 °C, with greater viability and differentiation capacity relative to single cell MSCs (Qiu et al., 2024). Overall, the encapsulated spheroids display little difference in different media compositions or temperatures, and therefore, the condition optimisation can be flexible for future work.

4.3.2 Size and morphology

The spheroids held their spherical shape (**Figure 25a-f**) with no evidence of cell spreading and therefore interaction with the scaffold, in consolidation with work by Ho *et al*. in 2016 and 2017 (Ho et al., 2016, 2017).

In addition, in my own study, there was constriction of the spheroids upon encapsulation relative to the control **(Figure 25g)**. This phenomenon was also observed in Wu *et al.'s* 2023 paper, where they postulated that additional contraction occurred due to the viscoelasticity of the gel (Wu et al., 2023).

Based on **Figure 25g,** the diameter of spheroids used was typically 100-160 µm. No necrotic core formation was observed; instead, the spheroids were formed of both live and dead cells dispersed evenly throughout, except for day 14 controls (**Figure 25d**), which seemed to lose dead cells from the spheroid exterior/constrict to create a tight core of live cells. This is in line with the literature, which, while seemingly inconclusive on the minimum threshold on size and cell number for core formation, suggests that the minimums are above what was used in my study. Specifically, Vu et al demonstrated that while the hypoxic core was not formed for spheroids of 250 cells, it was present in spheroids of 500 and 1000 cells (Vu et al., 2020). Whereas Rovere et al showed that in spheroids of 1000 cells around 200 µm in diameter, the hypoxic core was not formed, but was present in spheroids of 2600 cells and 300 µm in diameter, with 200 µm being the generally agreed threshold (Rovere et al., 2023). Finally, Däster *et al*. showed that a diameter of 500 µm with multiple thousands of cells is required to have an observable necrotic core, an observation seconded by Murphy *et al*. in 2022 (Däster et al., 2016; Murphy et al., 2022). Although not before they'd presented data in 2016 showing 500 µm diameter and 30,000 cells is not sufficient, and instead 250,000 cells and 800 µm diameter are required to form a necrotic core (Murphy, Hung, et al., 2017).

Spheroids are renowned for their resilience to external stresses, which, in theory, makes them ideal for use within the model. However, with the increase in Calcein fluorescence intensity after encapsulation observed in 2 of 3 donors (**Figures 25j and k),** it's possible that quiescence is not being induced in all cells within the spheroid and instead only a certain population. As a result, metabolically active cells are unable to survive – evidence being the increase in red fluorescence. This could be consolidated by measuring marker expression with more frequent timepoints during encapsulation. In doing so, any changes over time would indicate cell activity.

4.3.3 MSC flow cytometry

There are case studies that indicate that MSC aggregation results in a decrease in surface marker expression; however, properties can then be recovered upon seeding back into a monolayer (Kim & Adachi, 2021; Santos et al., 2015). It is also indicated through literature and **Chapter 3** that encapsulation in alginate may inhibit surface marker recovery or reduce surface marker expression in MSCs (Swioklo et al., 2016).

Intensity of marker expression (**Figures 26 and 27)** shows that for monolayers, replicate 2 recovered marker expression quickly, whereas replicate 3 required longer, and replicate 1 did not recover at all. However, overall, the relationship between conditions is relatively consistent between biological replicates, even when the trends are more exaggerated, such as replicate 1 showing less variance in results compared to replicates 2 and 3 for CD146 and CD73 (**Figures 27c and d)**. The decrease in intensity of spheroids expression compared to monolayers for CD105 and CD146 **(Figures 26c and d and 27b and c)** was distinctly greater than that of other markers. More widely, the impact of encapsulation was replicate-dependent, but generally caused a decrease in marker expression for at least 2 of 3 replicates. In comparison to single cells, in **Figure 20**, CD105 and CD146 decrease, but not to the same extent as for aggregated cells in **Figure 27**. This suggests that both markers are strongly impacted by aggregation.

There was no consistent trend to determine the impact of encapsulation on surface marker expression of aggregated cells in **Figure 27**; however, the surface marker expression was typically reduced for spheroids compared to monolayers before encapsulation, which suggests that the impacts on the surface markers is dictated by the aggregation, and therefore, encapsulation doesn't have much

impact. The exception was CD105, which was decreased for all surface markers for day 14 encapsulated spheroids compared to day 0 controls, which suggest for this marker specifically, encapsulation reduced expression further than that caused by aggregation.

For replicate 2, the day 0 monolayer being higher than day -2 for CD29 and CD73 would suggest replicate 2 recovers these markers' expression quickly, but it then diminishes over time, explained by the lower day 14 numbers. This is also observed with the peak intensity for replicate 2, showing a strong correlation between the percentage of cells expressing and their intensity for these markers for replicate 2. Similarly, there is a strong correlation for the CD146 expression and intensity; in contrast, CD105 expression is fairly consistent across all conditions, but the intensity is far more variable, indicating that while a low level of expression is maintained, the intensity of expression is strongest for monolayers, particularly on day 0. Whilst replicate 2 shows a good correlation between the percentage of cells expressing and their intensity, this is not the case for replicates 1 and 3, which show very little correlation, in contrast to observations of **Figures 17-20,** where two of the three donors showed correlation. However, there were similarities in that the percentage of cells expressing was less uniform and therefore less dictated by the gating criteria. Of note is that, unlike in single-cell experiments **(Figures 17-20)**, the act of encapsulation does not seem to result in changed expression in MSC spheroids as it did for single cells. Potentially, the effect of the gel is being overshadowed by the aggregation and the resultant lack of interaction with the environment expected with spheroids. Another observation from **Chapter 3** was the correlation between CD29 and CD73. Whilst that correlation existed for the percentage of cells expressing for all replicates, only replicates one and two showed a correlation for the signal intensity.

Overall, this data failed to maintain the correlation between the percentage of cells expressing and their intensity; however, generally the spheroids showed decreased percentage of cells expressing and reduced intensity, but this was induced by aggregation rather than encapsulation, which would suggest that the process of aggregation also reduces cell metabolism. This could result in their viability being more consistent **(Figure 25)** as the cells are already in a low metabolic, resilient state before encapsulation.

4.3.4 MSC Flow cytometry repeat with one biological replicate

Starting numbers of cells expressing for replicate 1 were different to replicates 2 and 3 for CD29, CD44, CD90, CD146, CD105, CD166 and CD271, but by day 14, the number of cells expressing for these markers was now similar between donors. For CD73, expression on day -2 was in line with replicates 2 and 3, but by day 14 had decreased further. For CD34, expression for replicate 1 was in line with replicate 2, and by day 14, all donors were similar. The convergence of data for day 14 (excluding CD73) suggests that regardless of the starting number of cells expressing a marker, the aggregation and encapsulation seem to normalise it. As each replicate is cells from the same donor, results were expected to be more consistent than in **Figures 26-29**; this was not the case for day -2 results. It could be that the surface marker variations at day -2 are due to inconsistency in culture, resulting in different behavioural and marker expression. For example, if cells recovered from freezing more quickly and reached a higher confluency, then this could impact marker expression as MSCs at over 80%, or even 100%, confluency are typically more susceptible to differentiation, or will at least show decreased growth rates and increased cell-cell interaction markers due to their close proximity (Abo-Aziza & Zaki, 2017). However, as the cells were all the same, the baseline expression would theoretically be consistent, resulting in uniformity at day 14 for intensity, and the convergence of percentages for all but CD73 **(Figures 30 and 31)**.

Expression of CD34 being so high for replicate 3 would suggest an error in the cytometer setup, as these MSCs were tested and are not CD34+. This is therefore incorrect. Further, a large number of cells for all three replicates being positive for CD34 at day 14 was surprising. CD34 expression is found on *in vivo* BM-MSCs, specifically pericytes, and is also not unheard of for its expression to increase in MSCs upon aggregation (Lin et al., 2012; Frith et al., 2010). It is also possible to utilise ECs and growth factors such as insulin-like growth factor 1 (IGF-1) to induce the expression of CD34 on MSC spheroids, as demonstrated by Bellagamba *et al*. (Bellagamba et al., 2018). While IGF-1 can be expressed by OBs and chondrocytes, it is not expressed by HSCs or MSCs, and therefore, this will b occurring through different means.

While the number of cells expressing CD29, CD73, CD90 and CD105 **(Figures 30a, b, d, f)** was relatively unchanged over 14 days, the intensity of expression for all

(Figures 31a, b, d, f) decreased, which was expected based on the literature (Frith et al., 2010)**.** CD44 expression was already low for this replicate **(Figure 30c)**, and its expression has been observed to both increase and decrease on aggregation (Frith et al., 2010; Valente et al., 2021). Therefore, the lack of cells measured makes any conclusions on the intensity drawn from **Figure 31c** hard to trust.

As covered in **1.1.1.1,** CD271 is not a commonly expressed marker on BM-MSCs, and therefore, low values measured in the experiment are not unusual. It is also a commonly lost marker, and therefore, this is not an unexpected result. However, the loss of expressing cells for CD271, CD146 and CD166 **(Figure 30i, e and g)** combined suggests movement away from a primitive phenotype, in line with observations of **Figure 28**.

This experiment did not show consistency between the percentage of cells expressing and the intensity of the expression, as was observed in **Chapter 3**, in line with **4.3.3.** Another trend observed in earlier sections regarding CD29 and CD73 **(Figures 30 and 31 a and b)** was not apparent in this experiment. While the data showed the same trend, the changes between replicates were not consistent, as was the case earlier. Further,

4.3.5 Flow cytometry surface marker analysis

4.3.5.1 CD105

5 of the 6 papers presented in **Table 5** presented a decrease in CD105 expression on aggregation, with which the presented data agrees **(Figure 26c, 28b and 30f, 31f).** It showed the largest change in signal intensity for measured markers in both experiments, and the percentage of cells expressing remained fairly consistent for both, indicating that this was a consistent decrease across the population to a low-lying expression.

Ho *et al.*'s study explored protein expression in spheroids in alginate relative to RGD-modified alginate, and the total concentration was around 30% lower for those in unmodified alginate, indicating that this study's spheroids are likely to have a greatly reduced protein concentration (Ho et al., 2016). Their 2017 study also demonstrated that the non-adherent environment favoured osteogenesis (Ho et al., 2017). The favouring of osteogenesis is the same observation made in single MSCs with decreased CD105 expression (Anderson et al., 2013; Jin et al., 2009; Yang et al., 2019). However, the lack of difference between day 1 and day

14 spheroid conditions **(Figure 26c and Figure 28b)** indicates that it was the aggregation that caused loss of marker expression, and that the encapsulation then had no additional impact. Therefore, spheroid aggregation may direct an osteogenic phenotype.

Table 5. Lead author, cell type and findings summary for papers describing flow cytometry surface marker expression during aggregation of MSCs.

Lead Author and Publishing Year	**Cell Type**	**Observed effect of MSC aggregation on surface marker expression.**
Bartosh *et al.* 2010	Unspecified human MSCs	CD73 expression is maintained relative to adherent cells, but CD90, CD105, CD146 and CD166 are reduced, while CD82 and CD49b expression is increased (Bartosh et al., 2010).
Burand *et al.* 2020	hBM-MSC	Reduction in CD73 expression and ability to suppress T cells (Burand et al., 2020).
Frith *et al.* 2010	hBM-MSC	Decrease in CD29, CD44, CD73, CD90, CD105 and an increase in CD34 and CD45 relative to monolayer (Frith et al., 2010).
Kamprom *et al.* 2024	hAMSC	A-MSCs and observed a slight decrease in CD73 and CD90 expression and a significant reduction in CD105, which was almost lost completely (Kamprom et al., 2024).
Santos *et al.* 2015	hUC-MSC	Decrease in CD90 and CD105, although it was restored when reseeded into a monolayer (Santos et al., 2015).
Valente *et al.* 2021	hVW-MSC	CD44 was highly expressed, but CD105 and CD90 were only expressed lowly in vascular wall MSCs spheroids (VW-MSCs) (Valente et al., 2021).

The second observation of CD105 is that decreased expression trends with enhanced immunosuppressive abilities, the occurrence of which was covered in **1.1.1.1** (Pham et al., 2019). However, while data suggest that MSCs maintain their immunomodulatory ability upon osteo-lineage differentiation, there is conflicting information suggesting it is enhanced. Chao *et al.* osteogenically differentiated rat BM-MSCs and observed enhanced IL-6 and PGE-2 expression and maintained TGFß1 and IL-10 expression (Liu & Sun, 2019). Feng *et al.* demonstrated that osteogenically differentiated MSCs had enhanced IL-8 secretion and elevated T cell migration (Ye et al., 2022). And yet, Montespan *et al.*, Niemeyer *et al.,* and Schubert *et al.* used human, human and pig MSCs, respectively and found no changes in immunomodulatory profile (Montespan et al., 2014; Niemeyer et al., 2007; Schubert et al., 2011). Therefore, it seems that the enhanced immunomodulatory properties of spheroids are not entirely related to osteo-lineage priming and must be, at least in part, the result of another property. To assess immunomodulatory properties, the assessment of cytokines mentioned in **1.1.4.2** could be measured, such as IL-6. Overall, while CD105 is a suitable marker to indicate successful aggregation and therefore activation of enhanced spheroid properties, it is not certainly indicative of the osteogenic commitment of MSCs upon aggregation, and instead, an osteo-like phenotype is adopted, and the impact of encapsulation on CD105 expression observed in single cell MSCs is not observed when aggregated.

4.3.5.2 CD146

Aggregation also resulted in reduced signal intensity for CD146, which correlated with the reduction in the number of expressing cells **(Figure 26d, 28c, 30e and 31e).** As covered in **section 1.1.1.1,** CD146 expression in BM-MSCs is correlated to increased immunomodulatory ability, such as increased IL-6 and VEGF secretion, as well as improved differentiation capacity (Bikorimana et al., 2022; Wang et al., 2020; Wu et al., 2016). However, Coa *et al.* showed that if CD146-positive BM-MSCs undergo osteogenic differentiation, this expression is lost while CD73 and CD90 are maintained (Cao et al., 2024).

Therefore, loss of CD146 expression when aggregated could indicate that the spheroids undergo priming towards osteo-lineage. However, as with CD105, the

encapsulation has no additional impact on CD146 expression, and therefore, the aggregation is again outweighing any impact of the gel.

4.3.5.3 CD166

Whilst expression of CD166 was lost entirely in **Figures 30g and 31g,** for **Figures 26f, 27f, 28e and 29d,** by day 14, intensity was in line with day-2 control, and the percentage of cells was either in line with day -2, or in line with day 14 monolayer. It is well documented that CD166 is highly expressed in osteoblasts, is not lost during differentiation, and is an indicator of multilineage capacity in MSCs (Chitteti et al., 2013, 2014; Hooker et al., 2015). Further, Cho *et al*. presented findings in 2023 showing that CD166 is a related ligand for CD6 receptors on T-cells (Cho et al., 2023). This interaction enables MSC T-cell suppression, and therefore, CD166 is directly responsible for MSC immunomodulatory ability. However, literature indicates that spheroids have enhanced immunomodulatory capacity, which means CD166 should be retained (Zimmermann & Mcdevitt, 2014). Whilst one experiment conforms with literature observations, the other does not. Therefore, another experimental replicate would be useful to clarify whether CD166 expression is maintained upon aggregation.

4.3.5.4 Other markers

Expression of CD29 and CD73 is maintained by osteoblasts, and therefore, no change should be detected if osteogenic differentiation is occurring. However, CD73 is primarily involved in immunosuppressive properties, and therefore, expression was expected to be maintained in spheroids. Whilst CD29 was expected to decrease for both single and aggregated cells due to its involvement in ECM interaction, which would not occur in a non-adherent environment, such as encapsulation in non-functionalised alginate. There was a decrease in intensity of CD73 expression for spheroids compared to monolayers (**Figures 26 and 27e),** which correlated with the number of cells expressing **(Figures 28d and 29d),** and this was matched by CD29 in **Figures 26b, 27a, 28a and 29a.** However, while the two continued to correlate, in **Figure 30,** the percentage of cells expressing remained relatively consistent between the monolayer and spheroids conditions, but **Figure 31** showed the signal intensity to drop substantially. This indicates that the low-expressing cells had not fallen below the gating criteria for **Figures 30 and 31** and were therefore still counted as

positive, even though the trend (decreased expression in spheroids) was otherwise consistent.

Whilst some record retention of CD29 is consistent with osteogenic direction, this was not shown by Frith (Bradaschia-Correa et al., 2017; Li et al., 2018; Frith et al., 2010). Frith *et al.* also showed a decrease in CD73 on aggregation (Frith et al., 2010). However, other papers have shown only a slight decrease or no decrease in CD73 (Bartosh et al., 2010a; Burand et al., 2020; Kamprom et al., 2024). However, whilst not its primary function, CD73 has also been shown to be involved in cell homing and migration (Ode et al., 2011). Therefore, as MSCs could not migrate in the gel, perhaps CD73 expression trended along with CD29 because of this. This suggests that CD73 is more critical for cell motility than previously thought. However, this raises the question of why the encapsulated single cells, **figures 18 and 19,** did not exhibit a reduction in CD29 or CD73. This would suggest that, rather than the gel, it was aggregation that induced a low-motility state in the cells and the subsequent decrease in CD29 and CD73 expression. Further, CD73 expression is associated with osteogenic differentiation capability, and the loss of the marker would indicate otherwise, which contradicts observations of CD146.

4.3.5.5 Marker summary

The decrease in expression for CD105 is logical considering the well-known immunomodulatory properties of spheroids. However, the reduction of CD29 and CD73 for spheroids but not for encapsulated single cells was not expected. It's possible that cell-cell interactions are more prevalent when aggregated compared to cell-ECM interactions, and therefore, cell-motility is reduced. The notion of an osteogenically primed state theorised in **3.4** could be argued based on the decrease in CD146, and maintenance of CD166. However, with the decrease of CD73 as well, it appears that it’s the wider differentiation capabilities of the cells that are decreasing upon aggregation – in contradiction to literature observations (Shanbhag et al., 2020). To confirm this, specific testing of osteogenesis could be carried out on a re-seeded spheroids and single cells to determine if marker expression changes again. It would also be interesting to do simple osteogenesis tests, such as staining for calcium or for osteogenic markers such as RUNX2 or ALP (Loebel et al., 2014; Meesuk et al., 2022).

4.3.6 Nanoindentation

As covered in **section 3.1**, gel stability should not be influenced as long as the temperature remains consistent, the vessel remains sealed, and cellular secretions do not disrupt ion concentration. As the gels are stored at 15 or 20 ºC, this is not a concern. Therefore, gels should remain stable during encapsulation. This was confirmed with the nanoindentation experiments **(Figure 32)** as stiffness measurements were consistent regardless of cell type, except for single cell gels, which show a decrease in stiffness. The other conditions showed a slight increase in stiffness, and therefore, additional replicates would be useful to solidify conclusions.

The stiffness measured for this experiment ranges from roughly 9.5 to 15 kPa on day 1 and 9-17 kPa on day 14; however, there is a large variance in the data. These surface stiffness measurements fall between those of the endosteal and perivascular regions of the bone marrow niche, in similar ranges to those of the adult heart (Handorf et al., 2015; Querceto et al., 2022). As bone lies in MPa ranges, it is counterintuitive to think softer environments would direct osteogenesis (Leipzig & Shoichet, 2009). However, work by Huebsch *et al.* and Chaudhuri *et al.* has demonstrated that when MSCs are encapsulated within a 3D matrix, stiffness of 2.5-9 kPa will direct adipogenesis and 11-30 kPa osteogenesis, both far below the ranges of their native tissues (Chaudhuri et al., 2016; Handorf et al., 2015; Huebsch et al., 2010). It is worth noting that, as mentioned in **1.4.2.3**, the surface stiffness of the beads is likely higher than that internally and local to the cells, as the outside of the beads will crosslink more. Therefore, it's possible the actual stiffness is lower than that measured.

Chu *et al.* provide evidence to show how cell encapsulation in hydrogels can alter the mechanical properties at both local and bulk scales (Chu et al., 2020). However, their use of PEG means the causes – cellular removal of gel precursors and free radical interference before and during crosslinking, respectively – result in reduced mechanical properties in gels with cells. In contrast, Jahangir *et al.* demonstrated that in alginate hydrogels, incorporated cells have no effect on the stiffness (Jahangir et al., 2020). Subsequently, it was expected that the stiffness of gels would be consistent. However, as can be seen from **Figure 32,** there was a slight decrease in the stiffness of the spheroid encapsulated gels. This, and the general variability of data points, is likely a result of two things.

Firstly, the incomplete mixing of the gel and cell suspension before cross-linking results in higher concentration gels forming some beads. Secondly, inaccuracy due to technical complications during the measurement of gel and cell solution during gel fabrication. Viscous gels used in small volumes resulted in wastage from gel retention in syringes or vessels. When centrifuging spheroids, a pellet is not formed from which media can be almost completely removed, as with single cells; instead, they form a loose pellet from which media cannot be fully removed. Subsequently, there is an inaccuracy in the volume of media the spheroids are resuspended in. The correlation between alginate concentration and stiffness is well documented (Ferjaoui et al., 2024; Jeong et al., 2020; Khavari et al., 2016). It is the variation in w/v% during the gel-making process that yields inconsistent gel stiffness. This could be minimised by upscaling gel production, so losses are negligible relative to the volumes used, or by ensuring that the residual media during spheroid pelleting is negligible relative to the volume used to resuspend. Due to limitations in cell number, this was not possible during this study. Subsequently, effects due to differing stiffness cannot be ruled out during this work.

4.3.7 Second CD34+ Flow

Following on from observations in **section 3.4.6,** all three donors from this second experiment were frozen/thawed, and in addition, donor 4 was purchased from StemCell Technologies, whereas donors 5 and 6 were isolated in-house. Plotting HSPC populations breakdown of donors from experiment two alongside those from experiment one in **Figure 33e**, shows how the fresh donors (donors 1 and 2) have population breakdowns like those of frozen. Donor 2 is similar to those in experiment two at around 8%, while donor 1 is the lowest of all at around 2.5%. Further, **Figure 33f** shows that for a frozen sample, the percentage of the population that were HSPCS after 14 days increased from 8% to 33%, which is the same trend observed for the fresh donors in **Figure 22**. Therefore, it is likely that donor 3's decrease in this population is not linked to the sample being frozen. So, it seems that at least from a population breakdown perspective, there is no trend between fresh and frozen or bought and self-isolated. However, all but donor 3 had HSPC population numbers in the anticipated range, with this sample being a substantial outlier.

Literature indicates that less than 10% of CD34+ BM cells are HSPCs (Civin et al.,

1996). **Figure 33a** shows HSPC numbers between 5 and 12% in a population in which 75-90% were CD34+ (**Figure 33d),** which is therefore in line with the literature**.** However, **Table 3** shows that around 5% of cells survive 14 days encapsulated; therefore, not all HSPCs survive encapsulation. However, by day 14, over 95% are CD34+ (**Figures 33f and g)**; therefore, very few non-CD34+ cells survive. Moreover, as seen in **Figure 33f,** by day 14, less than 35% of cells are HSPCS; therefore, a large number of cells that survive the process are of a mature cell type, which we would not expect to survive.

As mentioned in **section 1.4.4.1.** CD34+ thaw recovery is typically around 70% and data suggest the functionality of the population corresponds to its recovery (Lee et al., 2008). Therefore, regardless of storage, we would anticipate less than this Figure for all samples. The poorest in terms of HSPC population retention **(Figure 33a)** in experiment 2, being donor 6, is in line with that in **tables 2 and 3**, as this population had the poorest recovery post-thawing and the worst recovery yields post-encapsulation, which would make sense if the population itself is the least primitive. However, in contrast, donor 5 has far superior cell recovery post-encapsulation **(Table 3**) while displaying average HSPC population retention **(Figure 33a)**. It even sees a decrease in the LT-HSC population at day 14 relative to day 0 **(Figure 33f)**, indicating that post-thaw recovery is not a failsafe way of determining the quality of a sample.
As mentioned in **1.1.2** in BM LT-HSCs, cells should occupy 30±18% of the HSPC population. This is consistent with that observed across the three donors in **Figure 33c,** with values between 36 and 46%. Therefore, none of our samples were atypical and should be representative of most human BM-HSPC samples.
From my observation, a logical trend is also observed where the CD34+CD38- expression trends in the same way as CD90+CD45RA-, as the most primitive population should be in a constant ratio with the number of more mature cells in a system.
By utilising the cell numbers for donor 5 recorded in **Tables 2 and 3** and applying them to the percentages for donor 5 displayed in **Figure 33f,** it can be determined that of the HSPC population, 11.4% survived the encapsulation process, whereas only 6.9% of LT-HSCs survive **(Table 4)**. An area of uncertainty is whether the change in subpopulation size is due to one population being more viable than the other, or, as observed in **3.3.3,** the cells exhibit reduced or a loss

of expression of that marker. Assuming the latter, one could perform additional CD90 gating before encapsulation and measure if the expression is lost or not. Unfortunately, as the role of CD90 in HSCs remains unknown, it is difficult to speculate what may be occurring. With its main role being integrin and proteoglycan binding, the non-adherent environment may be influencing expression; however, HSCs are non-adherent and have minimal ECM interaction anyway (Anjos-Afonso & Bonnet, 2023). Its potential influence could instead be cytoskeletal alterations or even HSC activation, both of which occur in MSCs during encapsulation and are thus more promising avenues. Assuming the prior, it is not the most primitive population of CD34+ cells that survives. In fact, the subpopulation expected to fare best - LT-HSCs - under encapsulated conditions fared worse than the more mature MPP/ST-HSC CD90-CD45RA population **(displayed in Figure 33g)**. For this population, the number of cells present relative to the total live cell number, as well as the number of cells relative to the HSPC population, both increased over 14 days. Whereas, as previously stated, the LT-HSC population decreased relative to HSCPCs, **see Figure 33f**. This result supports the idea that some of the 90-45RA-subpopulation can enter quiescence, much like the LT-HSCs (Laurenti & Göttgens, 2018).

With supposedly all LT-HSC cells able to enter quiescence, and it is well established that later MPP2-4 populations in the HSPC population cannot, one would assume that the survival rate would be higher in the former. The fact that this is not the case would suggest that either the CD90+ cells are more sensitive to the conditions or the CD90- cells are less so. Considering that CD90+ reside deep within the niche in a highly regulated environment and are particularly sensitive to stimuli, whereas the ST-HSC/MPPs are known to circulate and reside in less confined areas within not just the marrow but the body, it is within reason that it is both. Additional gating to remove the MPP2-4 populations and leave purely quiescence-capable CD90- cells should, in theory, increase the relative recovery of this population without impacting changes in the CD90+ population, while seeding the MPP2-4 populations in CFU-assays should exhibit limited recapitulation ability.

An alternate consideration is that combined, the two populations capable of quiescence (**Figures 33f and g)** occupy roughly 8% of the live population at day 0 to roughly 32% by day 14. This indicates that the quiescent population do survive better than other HSPC subpopulations during encapsulation and storage, and if

additional sorting steps were undertaken before encapsulation based on CD38- and perhaps CD90 and CD49f, it could be viable to repeat the study with just these populations and observe much greater recoverable cell number.
Another population of interest was the CD34+CD38-CD90-CD45RA+ subpopulation of LPCs. Literature suggests that LPCs (also referred to as Common Lymphoid Progenitor/CLP and Multipotent Lymphoid Progenitors/MLPS) in adult BM can enter a quiescent state (Pelayo et al., 2006). However, while at day 0 roughly 4% of HSPCs were LPCs, by day 14 this number was down to 0.26% - essentially negligible. Therefore, my findings do not conform to those observed elsewhere regarding LPCs.

4.3.8 CD34+ CFU

From the initial CFU, these cells exhibit characteristics of cells with high G/M lineage priming. Observations of CB CD34+ cells by Gafaar *et al.* showed BFU-E to be roughly 6 times more prevalent than CFU-E and CFU-GM, with no observable CFU-GEM colonies (Gaafar et al., 2025). In contrast, during an optimisation study of this technique with PB-CD34+'s, G/M colonies were 10x more prevalent than CFU E or GEM in CD34+ cells (Thompson et al., 2023). This suggests that while there may be cell lineage bias depending on the cell source, neither had high numbers of the colony type produced by the most primitive of colony-forming cells, the MPC. This was, however, observed by Simsek *et al.*, who demonstrated that low mitochondrial potential (MP) BM cells (>80% LT-HSCs) display a colony composition of 1% BFU-E, 56% CFU-GEM and 43% CFU-GM. While the high MP cells display 6% BFU-E, 32% GEM and 62% GM (Simsek et al., 2010). This is a useful comparison to the prior studies, where only CD34+ cells were investigated. The subpopulations have very different colony-forming abilities, and the breakdown enables identification towards how primitive the population is. As the cells analysed in **Figure 34** compare more towards a CD34+ population (as is expected based on the purification method used in **section 2.3.4**, rather than LT-HSC, this shows that before encapsulation, these cells were likely not primarily LT-HSCs, instead being a more mature population with greater MP. As only around 3% of cells in this population were LT-HSCs **(Figure 33b),** this was indeed the case for this donor, and as the percentage of CD90+CD45RA- cells in the CD34+ population is relatively consistent **1.1.2** this should probably be the case for most CFU studies of healthy BM.

By day 14, it's expected that there would be a significant contrast in the colony composition due to the increased relative number of quiescent cells present compared to day 0. As displayed in **Figures 33f and 33g and covered in 4.3.5,** the cell population capable of quiescence (and the most primitive populations that correlate to the number of CFU-GEMs that arise during CFU assays) increases from 8% at day 0 to 32% by day 14. Subsequently, Its anticipated that should the other CFU assay for donor 2 survive, it would have had a significant increase in the number of GEM colonies formed.

4.4 Summary

The effects of encapsulation within unmodified alginate hydrogels at 1.2% w/v are independent of media composition (**Figure 25h)** at 15 or 20 °C (**Figure 25i)**. However, there is also a decrease in viable cells within the spheroid **(Figures25j, k and l)** and as spheroids are not maintained effectively in culture within AggreWell™ plates, there is a lack of a suitable control to determine if this decrease in viability is due to encapsulation. Further, the encapsulation process causes the spheroids to contract more than those in culture, although this new size is then maintained for a minimum of 14 days (**Figure 25g)**.

Over the period of the experiment, spheroids are maintained far better within the gels than outside, and initial thoughts were that this could provide a suitable storage and/or transport method for formed spheroids.

When assessing the surface marker of cells in spheroids relative to a monolayer (**Figures 26, 27, 28 and 29)**, there was a noticeable decrease of CD146, which would indicate loss of multilineage ability, particularly when coupled with the far greater decrease in signal intensity observed for CD29 and CD73 **(Figure 31)**. However, MSCs are known to retain full functionality upon dissociation. Analysis of **Figures 25 I, j and k** shows cells displayed increased metabolic activity via increased Calcein intensity – an indication of differentiation. However, cells are known to re-establish normal MSC behaviour if re-seeded, and so any loss in multipotency is not permanent. This marker expression loss is seemingly induced pre-encapsulation, and after 14 days of encapsulation, there is no noticeable change in expression, suggesting that the gel does not further influence this state.

Nanoindentation of gels showed surface stiffness values in ranges known to

induce osteogenic differentiation **(Figure 32)**, as well as quite a large variability in stiffness for both technical and biological replicates. However, the internal and local stiffness of the cells is likely softer than this, due to the decreased crosslinking further into the gel.

While characterisation of MSCs and their progenitors has become more detailed over the years, there still lacks uniformity across studies. It would be worthwhile to assess surface markers, RNA and behavioural characteristics of MSCs in depth in order to provide clearer criteria for identifying subtypes and their subsequent culture. Further, this would enhance the consistency of data across studies and provide conclusions with stronger foundations and greater reproducibility.

In relation to the hypothesis stated in **4.1.8,** encapsulation of spheroids results in a temperature-resilient method of storing MSCs, which is also independent of media type. Further, while encapsulation does not impact surface marker expression of aggregated MSCs, the act of aggregation does. This reduction of surface markers indicates that a less 'stem-like' state is adopted by the cells.

The functional ability of CD34+s observed via CFU assay **(Figure 34)** correlates with surface marker expression **(Figure 33)** in that there are very few LT-HSCs present, with the colony giving rise to very few GEM cells and marker expression showing few LT-HSCs.

Additionally, the post-thaw recovery and post-encapsulation recovery are strongly correlated **(Tables 2 and 3)**; however, this does not correlate directly to the primitivity of the cells **(Figure 33a and 33b), which** is in contradiction to the literature (Lee et al., 2008). Across 6 CD34+ primed donor samples **(Figure 33e),** roughly 7% (excluding potential outlier) or 12.4% (including potential outlier) are HSPCs, in line with expected values from the literature (Civin et al., 1996). Further, LT-HSCs then occupied roughly 40% of this population, again in line with literature **(Figure 33c) (**Majeti et al., 2007)**.** Therefore, the populations used were representative of the composition of *in vivo* BM and can be considered valid model cell types.

While recovery numbers post-encapsulation were generally disappointing, the hypothesis that cell populations too mature to enter quiescence were those that saw the greatest decrease in viability was maintained; however, this then resulted in the consideration of the MMP/ST-HSC subpopulation having

quiescence-capable cells. When both LT-HSC and MMP/ST-HSC populations were grouped, the substantial bias towards these cells surviving the encapsulation and storage process was evident. Therefore, it is hypothesised that with additional priming towards CD38- and even CD49f, the survivability of HSPCs in this system could be dramatically improved. In future developments, if the intended use of the system is to simply transport the total cell population, then adding additional purification before encapsulation would not be necessary. However, if for use as a testing platform, then it would be logical to investigate how well a purer population survives to truly assess applicability. It could also be beneficial to assess each subpopulation individually, from LT-HSCs to the different progenitors, as that would indicate specific cell types. This could be more viable if the mixed population remains impractical. Comparing data to the hypothesis in **4.1.8**, LT-HSCs are not more capable of surviving encapsulation than other quiescence-capable phenotypes; however, this mixed population is more viable than non-CD34+CD38- populations. Further, fresh or frozen samples showed no difference in their sub-population composition or survivability.

Chapter 5. Discussion

5.1 Project summary

As covered in **Chapter 1**, the primary goals of this project were to determine the impact of encapsulation and hypothermic storage on MSC spheroids and on HSCs. In addition, observations were made regarding the impact of aggregation on MSCs, and also the composition of CD34+ isolated cells from self-isolated and external, purchased sources.

Whilst viability of the entire CD34+ cell population after encapsulation and storage was low **(Figure 21)**, the HSPC sub-population number was in the anticipated range for both purchased and donated samples of around 10% **(Figure 22d, 33a),** and this was confirmed with a functional CFU-assay **(Figure 34)**. However, this raises the question of how suitable the CD34+ population is for use as 'HSCs' in other studies.

Based on these observations, it was theorised that the HSPC population would be maintained in this system while the non-HSPC CD34+s would not. Further, the LT-HSC subpopulation would be the most viable under encapsulated conditions. This is due to the stiffness of the gel favouring osteogenic phenotypes **(Figure 32)**, and therefore, as HSCs reside in the stiff, endosteal niche, this would similarly favour them. In addition, it's widely regarded that LT-HSCs reside primarily in the quiescent state while ST-HSCs/MPPs are more metabolically active. Therefore, a quiescence-inducing environment would be more favourable to LT-HSCs.

The first hypothesis was not correct – while HSPCs showed more favourable survivability **(Figure 22d, 33a)**, non-HSPC CD34+ cells still survived the process **(Figure 22a)**. For the second hypothesis, it was the ST-HSC/MPP subpopulation that was maintained more effectively than LT-HSCs **(Figure 33e and f)**. However, this validates findings that MPPs can enter quiescence alongside HSCs, even if they do not have long-term recapitulative capabilities, and this system does enable hypothermic, encapsulated storage of HSPCs.

The hypothesis for MSCs was that 15 °C would give the best viability, in line with the literature, and that encapsulation would impact surface marker expression of spheroids.

MSCs retain their surface marker expression, and therefore phenotype, more effectively when cultured in DMEM compared to IMDM **(Figures 12-15)**. The

optimal temperature for MSC encapsulation was confirmed as 15 °C, as stated by Atelerix **(Figure 11)**. However, the culture medium had no impact on the viability of encapsulated MSCs, indicating that the cells are no longer in a metabolically active state **(Figure 16)**.
Encapsulation of MSCs **(Figures 17-20)** resulted in the reduction of CD105 and CD146 expression compared to the starting control, with other markers unchanged. There was also an indication that some marker expression increased over the two weeks in culture.
Aggregated MSCs showed no change in viability due to temperature or media changes, demonstrating their documented increased resilience compared to MSCs. Interestingly, aggregation reduced surface marker expression in MSCs for more markers than encapsulation did. In fact, for spheroids, the encapsulation had no further impact on expression, suggesting that the effects of aggregation are more severe than those of encapsulation and explaining why viability was not impacted by encapsulation either. This would indicate a decreased multipotency and 'stem-like' phenotype of the cells, which explains the different properties of aggregated MSCs compared to single cells, if a phenotypical change is occurring.

5.1.1 Comparison to Atelerix

During this study, Atelerix have produced updated guidelines regarding potential encapsulation times for subpopulations of MSCs, namely BM-MSCs, and CD34+ HSCs; however, there is no information regarding the source of the CD34+ cells and whether they are actually HSCs or HSPCs (*Samples Preserved | Atelerix*, n.d.). For BM-MSCs, they suggest 15- 25 °C for 7 days, which is in contradiction to observations in Figure 11b, where 20 °C saw a decrease in viable cell number relative to 15 °C. For CD34+, they suggest 15- 25 °C for three days, which was in line with trends observed in Figure 21. and suggests that rather than a purified CD34+ population of HSCs, this was likely a population of HSPCs. This thesis indicates that by breaking HSPCs into subpopulations, different encapsulation times than those presented by Atelerix are probable. Move over; if the population being encapsulated is properly primed, longer times than 3 days are feasible. This work specifically encapsulated BM-HSPCs, which are distinctly different from cells from other sources, and should therefore be presented as

such, in line with their updated website, which does so with MSCs. Atelerix also have no specification for the encapsulation of MSC spheroids, which remain viable for 14 days; however, additional functional testing is necessary before being advertised for use.

5.2 Limitations of the study and troubleshooting

5.2.1 Cells

Due to limited availability, there was no ability to use specifically male or female donors, nor a specific age range. However, the donor samples were from femoral heads after hip replacements, over 90% of which occur in over 50's (*Patient Profile - NHS England Digital*, n.d.). Some studies have shown over 50's exhibit reduced regenerative ability in their stem cells, although findings are not consistent (Koudy Williams et al., 2017). Also, some studies show female BM-MSCs having reduced CFU-F capacity, differentiation capacity and surface marker expression under standard culture conditions, while others show no difference (Selle et al., 2022; Vogt et al., 2024). While unclear, attempts to replicate the work may choose to consider stricter controls over the age and gender of the donor samples. It would also be preferable to carry a group of donors through the entire study, rather than using different MSC donors for each experiment. This would make it easier to compare and draw results from different experiments.

Regardless of the behavioural characteristics of the cells in the gels, the recovery rate of cells over time periods relevant to their desired use is too poor to be a viable use for CD34s (**Section 4.2.5, Table 3)**. However, if only HSPCs were used – requiring additional purification based on CD38 – then these cells were more viable and would be of interest to investigate further (**Figure 22d, 33f)**. However, the number of rare cells required would then become limiting. For example, it is an unfeasible number to expect to retrieve from a donated sample, and therefore, single donors for studies would be hard to come by, resulting in donor pooling and greater uncertainty in results. However, it remains that if financially capable, another could repeat or expand this research using purchased HSCs.

Immortalised alternative cell types with similar size and adherence to HSCs, such as leukaemic lines THP-1, U-937, and K-562, were all tried as alternatives; however, due to their highly proliferative and mature phenotype, they were not

viable at hypothermic temperatures. This is likely the case for any immortalised lines, such as genetically modified hTERT-immortalised MSC lines, as modifications to ensure unlimited proliferative capacity are counteractive towards entering a low metabolic, quiescent state. As with HSCs, if finances allowed, MSCs could be purchased to repeat or expand on this work, with multiple vials from the same donor available.

Ideally, 6 biological replicates should be used for experiments to make assessments on normality and therefore use more conclusive statistical tests, with ≥3 experimental replicates each, each with ≥3 technical replicates. This provides the most robust data and can provide meaningful statistics.

5.2.2 HSPC Experiments

In **chapter 3,** while they weren't strictly measured, roughly 1million CD34+ cells for Donors 1, 2 and 3 were encapsulated for each condition. For flow cytometry, not all cells were stained and analysed; however, numbers analysed per condition were 64,000, 33,000 and 24,000 for donors 1,2 and 3, respectively. These numbers were roughly as expected based on the hypothesis that it was likely the HSPCs that were surviving the process, and at most 10% of CD34+ cells are HSPCs. Considering the cells analysed for flow were underestimates of the actual number, the number of cells encapsulated per condition was increased to 1.5 million in **Chapter 4**, with the expectation that this would give sufficient numbers to use 15000 of the surviving cells for triplicate CFUs and split the rest for flow and PCR. However, as was observed in **Table 3,** the number of cells recovered from the lone CD34+ cell gels was all below 50,000 in total. Further, while surface marker expression was not impacted by the cells being fresh or frozen, the frozen donor in chapter 3 – donor 3 – had the lowest number of analysed cells for flow. While only speculation, and remembering to consider the inaccuracy previously stated, all 3 donors in chapter 5 were frozen, and all had poor recovery, like donor 3. Therefore, it could be that while freeze/thaw doesn't impact phenotype, it does impact the hardiness of the cells and prevents them from being suitable for encapsulation. An easy way to test this would be to utilise more fresh samples, but this was not practical. However, if there were a method to store the HSCs for a few days without the need for freezing them, this would enable time to set up the experiment and prevent the need for freezing. In an ideal world, that product would be Atelerix hydrogels or a version

of it; perhaps a simple home-made alginate gel at similar concentrations could be used as a placeholder before using the actual thing. In extension, the products' short-term applications could therefore be tested. These studies were not carried out in this work due to the lack of access to cells. The final experiments were designed to be co-cultures with MSCs, and therefore required setup time and cells available when needed, because there were limited cells available, and the aim was to gather as much information from three experiments as possible. However, with more cells available, this slower, more methodical approach to validating the method would have been adopted.

5.2.3 MSC experiments

For MSC studies, something that should also be considered is that, based on the viability **(Figure 16)**, the number of dead cells increases during encapsulation. Therefore, there is a population of cells which were characterised initially, which are then not part of the day 14 analysis. This could mean that rather than the expression being lost or gained in a condition, this population always existed but was instead diluted by the additional population at day 0, which then no longer existed. This is possible for observably small changes; however, when substantial decreases in population are observed, it is unlikely to have a significant impact. It is also difficult to identify these subpopulations if they are exhibiting the same expression of the markers we are using as one another. The argument could be made for more complex panels; however, the flow cytometer used had only 12 channels. With the current advancements in spectral sorting enabling real-time morphological measurements and panels easily in excess of 50 colours, this technique could be possible and probably preferable for future work.

The flow cytometric experiments could be refined to improve the accuracy of the data. For example, the experiments could be carried out at the same time rather than concurrently, which would mean conditions were as consistent as possible. Further, increased numbers of technical, experimental and biological replicates would give more statistically robust data. The data could also be mirrored using alternative analytical methods, such as antibody staining for the assessed flow panel and measuring using fluorescence microscopy, or by analysing protein expression via a western blot or gene expression via PCR. The only thing to consider with protein analysis is that cells in a low metabolic state

will produce less protein, and so yields will be low. Further, additional RNA clean-up steps or specific columns will be required as the degraded alginate will leave residue, which may clog the columns without adequate sample preparation.

Additional differentiation experiments could be carried out to determine whether multipotency has been lost permanently due to aggregation, such as inducing adipogenesis and staining with oil red O solution to stain lipid droplets, or inducing osteogenesis and staining with alizarin red to stain calcium deposits (Bernar et al., 2023; Du et al., 2023). Alternatively, the cells could be stained without re-seeding them using immunofluorescence by stabilising the alginate using larger ions and imaged within the gel using confocal microscopy or another high-resolution technique (Lee & Mooney, 2012).

Nanoindentation gave stiffness values in line with those observed to induce osteogenic lineages. However, based on information presented in **1.4.2.3**, in beads of the size used in this study, the crosslinking is likely inconsistent – being more heavily crosslinked on the surface and less crosslinked towards the centre of the bead. As a result, the local stiffness experienced by the cells is not that which was measured on the surface using nanoindentation. Therefore, assessments on the impact of this stiffness on the cells must be taken with this caveat. To determine local effects of the gel stiffness, this experiment could be repeated with gels cut in half or sectioned, to enable stiffness measurements to be taken on the internal structure of the gel.

5.2.4 Gels

The primary technique for characterising hydrogels in the lab available is rheology, which is a useful technique when you have access to relatively large volumes of gel. However, each gel disc for measurement required a minimum of 1ml to be both wide and thick enough to be tested, which was beyond the scope of this work. Additionally, as mentioned in **4.1.6,** the material properties would not have been directly comparable to the beads.

Nano-indentation, on the other hand, allowed for a smaller volume of gel to be used and allowed direct comparison to the environment of the cells in my system. However, it did bring its own complications. As the sample must be submerged in liquid and ion concentration changes will alter the properties of the gel, PBS Ca++ Mg++ was used, and the time of measurements was limited to

15 minutes, after which the sample was discarded. If the sample is in solution for too long, it will soften, and measurements will not be taken accurately and/or the degrading gel will adhere to the cantilever, dampen measurements and potentially damage the probe. Other methods that could have been utilised were compression testing, where Young's modulus is measured by compressing the bulk material or SEM to measure the pore size of the gel, which correlates to the mechanical properties (Nafar Dastgerdi et al., 2021) (Santana et al., 2015). If another were to try to pursue this avenue of work without using Atelerix materials, elements of gel customisation may be beneficial. Such customisation could also be beneficial for analytical purposes. For example, gel degradation observed at 37 °C could be slowed by using more robust crosslinking, such as with Ba^{2+} or covalent crosslinking, as covered in **1.4.2.3** (Lee & Mooney, 2012). Ba^{2+} could also have been used to stabilise the gels before imaging – making them less susceptible to degrading during washing steps for immunofluorescence or viability staining. If using smaller cells, using smaller beads could also yield faster crosslinking and reduce processing times, as well as provide a more consistent pore size and crosslinking density throughout the gel, resulting in a more homogeneous environment.

5.3 Recommendations for future work

5.3.1 Alternative and complementary experiments

To assist in the analysis of cells, alternative experimental methods could have been used to assess the metabolic activity of the cells and, therefore, judge if quiescence is induced upon encapsulation. This is usually performed using colorimetric or fluorescent techniques. For example, one method to measure proliferation or viability utilises the reducing environment of cells to convert a non-coloured or non-fluorescent molecule into a coloured or fluorescent form, such as the resazurin-resorufin transition of Alamar blue (AlamarBlue Cell Proliferation Assay | BMG LABTECH, n.d.). Alternatively, staining can occur by the cellular uptake of a coloured/fluorescent molecule, which is either held within the cell or binds to something within the cell, such as BrdU (5-bromo-2'-deoxyuridine), which binds to new DNA fragments as they are synthesised (BrdU Labeling & Detection Protocol - UK, n.d.). Other targets include measuring oxidative phosphorylation, ATP synthesis or assessing glycolysis by measuring lactate and glucose (Glycolysis/OXPHOS Assay Kit G270 Manual | DOJINDO, n.d.).

Alternatively, one could stain for genes upregulated during quiescence, rather than those upregulated during metabolism/proliferation, such as P27 (Toyoshima & Hunter, 1994). These techniques are typically simple and inexpensive, and could give good consolidatory evidence to a project and provisional information prior to a larger experiment. Gene analysis using PCR or Fluidigm would give greater insight into the behaviour of the cells and potential phenotypical changes, along with offering a secondary method of analysing quiescence and metabolic markers other than with stains and microscopy, as common targets for staining are often regulated by a specific gene. By isolating RNA from cells, the number of genes that can be analysed is limited only by the quantity of RNA obtained, compared to the number of laser channels available to analyse co-stained samples for flow cytometry or microscopy. This enables a much larger picture of the workings of the cell population.

5.3.1.1 HSC gene expression

More mature subpopulations should exhibit increased expression of metabolic/respiratory genes than primitive cells. Similarly, it's expected that they would show decreased expression of cell cycle inhibitors and increased expression of the receptors. As covered in **1.1.2,** the MMP2-4 cells within the HSPC population exhibit no ability to self-renew or enter quiescence. In fact, this behaviour is only guaranteed in LT-HSCs, with only 1 in 4 CD90-CD45RA-s (MMP1/ST-HSCs) capable. This would mean strong expression of CDKs 1-4, CCND1, Ki67, ATP and Glut-1, while displaying poor expression of P16, 21, 27, 53, CDKN1A, as the gene expression of the few primitive cells is diluted by the more numerous mature cells (Engeland, 2022; Malumbres et al., 2004; Mende et al., 2015; Toyoshima & Hunter, 1994). This trend would continue for other primitive markers, such as seeing a relatively low expression of cytokine receptors c-MPL, CXCR4 and Tie-2, while seeing more activity of c-KIT (Arai et al., 2004; Broudy, 1997; Nie et al., 2008; Yoshihara et al., 2007). Additionally, one would expect to see relatively low expression of hypoxic genes such as HIF1-α, Notch1, TGFβ, CEBPα and stronger expression of HIF2-α, low expression of Bmi-1, YAP, TAZ, Tcf7 and finally activation of the canonical/inhibition of the non-canonical Wnt pathway (Heng et al., 2020; Hidalgo et al., 2022; Patel & Simon, 2008; Zeng et al., 2004).

In theory, comparing this expected day 0 expression to that at day 14 should give

significant changes. Populations that are encapsulated should see a reduction in metabolic/cell cycle genes compared to the day 0 cells in culture, as the decreased temperature and nutrient availability once encapsulated should

5.3.1.2 MSC gene expression

Gene analysis for MSCs should aim to investigate the difference in expression between monolayer MSCs and spheroid MSCs, the effect of encapsulation and co-encapsulation with HSCs. Genes of interest would be associated with hypoxia, quiescence/cell cycle/metabolism, 'stemness' and differentiation. For example, aggregation into MSC spheroids should show increased expression of hypoxia-related markers such as HIF1-α and VEG-F, angiogenic cytokines such as ANG-1 and upregulation of CXCR4 for homing abilities (Rovere et al., 2023; Zhang et al., 2012; Nai-Chen Cheng et al., 2013). However, these increases (except for ANG-1) would be less than in a larger spheroid with a necrotic core, as my 200-cell spheroids do not have one.

During maturation – which would be occurring if osteogenesis is also induced - cell activity typically increases and one would anticipate increasing expression of cell cycle receptors CDK1, CDK2, CDK4 as well as genes encoding ligands that complex during activity such as CCND1, and metabolic marker genes like Ki-67 (Rovere et al., 2023, Brugarolas et al., 1998, Malumbres et al., 2004). I'd also expect upregulation of the cell cycle inhibitor CEBPα and stemness markers NANOG, OCT4 and SOX2 (Kim & Adachi, 2021; Friedman, 2015; Imamura et al., 2020; Zhang et al., 2012; Nai-Chen Cheng et al., 2013).

Literature demonstrates contradictory osteogenic gene expression and functional behaviours of MSCs upon aggregation. For instance, one should expect little change or even a decrease in early osteogenic markers such as ALP or Col1α1 (Yamaguchi et al., 2014; Kim & Adachi, 2021). However, one should see clear upregulation in late osteogenic markers such as BMP-2, MSX and OSX (Yamaguchi et al., 2014), notch-1 signalling during osteogenesis (He & Zou, 2019).

If the expression of cell cycle inhibitors increased and cells that died under encapsulation did not enter quiescence, this should be observable by changes in proliferative and metabolic/respiratory genes such as Ki-67, glut-1 and ATP between day 0 and day 14 (Flood et al., 2023, Engeland, 2022, Arponen et al., 2022). In addition, I'd anticipate the original RNA to have reduced expression of inhibitors P16, P21, P27, and P53 relative to day 14.

The addition of HSCs to the MSCs, due to all being hypothesised to be in a metabolically inactive state, could result in no impact on one another. However, both cell types reside in low metabolic states in the BM and still exert a significant influence on neighbouring cells. Subsequently, it would be interesting to see if HSCs trigger a response in MSCs, perhaps upregulation of HSCs maintaining cytokines, and maybe enhanced expression of stemness markers.

5.3.1.3 Combined MSC spheroids and CD34+s

The interaction between spheroids and HSCs could have a variety of implications. One of the most likely outcomes of co-encapsulation is that the environment induces a low activity state in all cells, significantly reducing expression levels of cytokines in MSCs and the corresponding receptors on the HSCs. Subsequently, any observable trends in gene and surface marker expression from the homogeneous encapsulation should then be equally apparent in those encapsulated heterogeneously.

It is unlikely that any significant activation occurs in either cell type, as the conditions are harsh enough to induce and maintain a low metabolic state, regardless of the other cell. If one were to influence the other, it is expected that the background secretory profile of the cells would be the cause rather than an active response to the other. From this perspective it would be anticipated that MSCs expression profiles are consistent with or without HSCs, however the HSCs could then respond to this secretory profile with either; activity induced, subsequent viability decreases, and primitive population decrease as cells exit quiescence, are unable to survive and die; or it helps maintain the state of quiescence in the HSPC population, increasing the number of recoverable cells. For the former, this may correlate to increased c-KIT expression, along with potential canonical Wnt activation. For the prior, HSC gene expression would likely see changes similar to those expected between day 0 and day 14, but to a greater extent, particularly those of the cytokine receptors c-MPL, CXCR4 and Tie-2.

However, based on the SCF and CXCL12 expression observed in spheroids by Zhang *et al.,* this would result in the counteraction between HSC activation and quiescence; therefore, the expression of the cytokines could adjust when in proximity of HSCs to favour one outcome (Zhang et al., 2012). In which case, the

directed metabolic state would correlate to a change in expression of cytokine from the MSCs, unlike the passive interaction considered above.
If spheroids induce self-renewal, then the HSCs would temporarily have to enter the cell cycle to do so – therefore, the levels of CDKs 1-4, CCND1, Ki67, ATP and Glut-1 would not be as low (or as high for P16, 21, 27, 53, CDKN1A) as the lone-HSC condition. However, if no induction into self-renewal takes place, these genes should remain consistent, and if the HSC population maintenance is enhanced by the MSCs, then they would follow trends of the lone-encapsulation condition, but to a greater extent.
Analysing the surface marker expression would also be beneficial, as if the MSCs are supporting the wider HSPC population, then the recovery for all subpopulations should be greater. Further, if it is inducing any phenotypical changes, this would mean cell cycle activation with trends similar to that above, but this time a shift in surface marker expression would correlate to more mature sub-populations, with a decrease in CD90+CD45RA- or even CD34+CD38- numbers and an increase in others. In contrast, if the cell cycle is being activated to induce self-renewal, then the result is expected to be an increase in the expression of the primitive surface markers relative to the lone-encapsulated HSCs, while the mature subpopulation numbers would remain consistent.

If the CD34+s are simply being better maintained in the presence of MSCs, it is expected that an even larger disparity between day 0 and day 14 composition than that covered in **section 4.3.6.** would occur, as the subpopulations unable to enter quiescence at all would still experience the same fate, whereas some of those that were capable but unable would be supported by the MSCs, resulting in the quiescence-capable cells occupying more than 32%.
Finally, any eventuality that resulted in more widespread maintenance of HSPCs should then be functionally observed by colony composition more closely related to that observed at day 0, however, one would anticipate a greater number of colonies per cell, as the most mature cells, which were unable to form colonies, are highly unlikely to survive in the gel at all.
In comparison, much like the gene expression, if the quiescence-capable populations are even better maintained than in the lone-encapsulated

conditions, then the same trend would be observed, but with even greater emphasis on the number of GEM colonies that are formed relative to the others.

5.3.2 Short-term HSPC investigation

While viability over 14 days is poor enough to rule CD34+ cells out as an off-the-shelf product for drug testing, it may still be applicable for use as an alternative storage and transport method for HSPCs as long as the cells remain viable for a few days. Therefore, short-term testing should be undertaken (< 14 days). It would also be beneficial to use the HSPC population only by additional gating. The HSPC subpopulation is maintained more effectively after 14 days compared to the other cells in the CD34+ population **(Figure 28)**, and it's anticipated that this would be the case across all time points. Therefore, the maximum time of encapsulation that yields acceptable recovery (>80%) should be found.

5.3.3 Quiescent cell secretion

Investigation into HSPCs while encapsulated should use different supplementation and determine whether cytokine mix, MSC co-encapsulation or MSC spheroid co-encapsulation, if any, is most suited. Many of the cytokines added in solution are unstable at room temperature, and therefore, MSCs/spheroids could act as a supply during storage if they are expressed under low metabolic conditions. While literature is unclear regarding the level at which intercellular signalling occurs in quiescent cells, they exhibit clear upregulation in intercellular signalling genes (Maresca & Cheeseman, 2020). For example, quiescent fibroblasts have been observed with complex secretory profiles, highlighting the possibility that other cells may do the same (Chen, 2012; Bräuninger, 2021).

Atelerix does not indicate that seeding density is related to viability. However, as both direct cellular interaction and intercellular signalling are integral to the maintenance of quiescent cells, seeding density is likely to play a role in how well the cells survive encapsulation (Crippa, 2018). Subsequently, this should be investigated for HSPCs, MSCs and MSC spheroids. However, upper limits should be considered for when the physical properties of the gel are influenced by the cells.

5.3.4 Spheroid Size

Spheroids are formed and used with a wide range of cell numbers, which is directly correlated to their size (Xie et al., 2021). The maximum spheroid size

that can be encapsulated without detrimental impacts on the physical properties of the gel should be calculated before advertising for use. Further, the properties of spheroids vary based on size, and therefore, the spheroids of different sizes may behave differently (Bhang et al., 2012).
Once the maximum size of the spheroid that can be encapsulated with gel properties maintained is found, then spheroids within the size range can be assessed for their behaviour.

5.3.5 Validation

If used for spheroids as a storage/shipping method, then this process should be validated. At the very least, if shipping at 'room temperature', the temperature is likely to fluctuate, and if shipping aerially, there will be pressure changes. For example, Damala *et al.* demonstrated that L-MSCs transported across India at 18.6 ± 1.8 ^{o}C remained viable for use there, and similar case studies would be required before HSPC and/or spheroid encapsulation storage being advertised in specific areas (Damala, 2019).

5.3.6 Co-encapsulation

Once hypothermic encapsulation has been proved to work with both HSPCs and MSC spheroids, then co-encapsulation can be investigated through two avenues. First, they could be used as a dual testing platform to observe drug effects on both cell types at the same time, as well as the interaction they have with each other under those conditions. Secondly, spheroids could be used to enhance the survivability of the HSPCS. For instance, MSC spheroids can be used to supplement/replace media supplementation.

5.3.7 High throughput manufacturing

3D bioprinting of MSCs and MSC spheroids using alginate hydrogels is well established, and this could reduce the labour intensity of the encapsulation process (Datta et al., 2023; Sanchez-Rubio et al., 2025). However, there is not the same level of information regarding bioprinting and HSPCs. Therefore, ensuring a bioprinting process has no negative effects on HSPCs means a larger-scale production process could be used if this were to be an active product.

In order to decrease costs, decreasing the size of the gels, and therefore the number of HSCs, should be considered. The gels were produced at a specific size as per the protocol provided by Atelerix. However, smaller cell-laden alginate hydrogel beads more than 10 times smaller (50-200μm diameter) have been

produced in numerous studies, particularly by utilising microfluidics to do so at high throughput (Tan & Takeuchi, 2007; Utech et al., 2015; Enck et al., 2020). While these studies often use MSCs, one did utilise HSPCs. However, the beads were closer to 400μm in diameter – still an over 75% decrease in diameter compared to my own (Carreras et al., 2021). Utilising microfluidic techniques could therefore reduce the throughput of the process as well as provide more control over the number of cells in each gel and make them more consistent as a platform in potential applications.

5.3.8 Material properties

The protocol described by Atelerix suggests a gelation time of 10 minutes, with crosslinker in excess, and with beads roughly 2mm in diameter. Based on work by Ramdhan, the time taken for contraction – and therefore crosslinking – to plateau is upwards of 2 hours of gelation time (Ramdhan et al., 2019). Therefore, it is likely that the Atelerix gels are not fully crosslinked when moved to culture medium, and the gels will then continue to crosslink using cations from the medium until equilibrium is reached. It would be of interest to investigate more than surface stiffness, but whole-gel properties by compression or maybe take cross-sectional slices of the gel to examine both internal and external properties, perhaps using SEM (Santana et al., 2015). Per the Atelerix protocol, any media can be used for the storage and delayed crosslinking of the beads. However, with different media having differing ion concentrations, it can be assumed that the type of media would give different gelation times and potentially differing gel properties, so this should be assessed. A way to alleviate the delayed crosslinking is by using smaller beads to reduce gelation time and, therefore, give more consistent gel properties – something possible with microfluidics.

5.4 Prospective applications of hypothermic, alginate-encapsulated stem cells

5.4.1 MSC spheroids

Due to their maintained viability over 14 days, this system could be used as a storage/shipping method for MSC spheroids. This means that labs could purchase ready-to-use MSC spheroids without needing equipment to make them themselves. This longer time period would also enable more widespread

distribution of the cells to an international clientele. It also means that a ready-to-use drug testing/screening application is viable, particularly by utilising 3D-bioprinting to produce gels in a 96-well plate format. However, drug choice must be considered based on the pore size of the gel, as larger molecules would not permeate through. Further, the resilience of spheroids resulted in reduced susceptibility to temperature changes and, therefore, would be viable in a wider variety of climates and/or fluctuating temperatures.

5.4.2 CD34 and HSPCs

Encapsulation of the entire CD34+ population is not a viable use due to the poor viability of mature haematopoietic cell types in the system. However, encapsulation of HSPCs for short-term (< 7-day) studies remains feasible and should be investigated further. While the cells do not remain viable long enough to survive shipping as well as an assay, they could be used for one or the other. Therefore, for local delivery as an alternative to cryopreservation, this remains an option - requiring immediate use or cryopreservation upon receipt. It could be utilised as a transport method in areas without cold-chain infrastructure, such as that demonstrated by Damala *et al.,* to enable the use of SCT in more remote hospitals (Damala, 2019). It also removes the need for toxic cryoprotectants such as DMSO (Valentini, 2024).

Encapsulated HSPCs could also be used as an in-house drug testing platform independently of a storage/transport system. An *ex vivo* method for maintaining a quiescent phenotype could improve insights into how drug uptake is impacted by quiescence in HSPCs for investigating treatments of haematopoietic diseases, as well as off-target drug uptake.

5.4.3 Spheroids and HSPCs

As mentioned in **1.3.4.** The protective effect of MSCs on HSCs is something not widely considered in research, and yet it is critical to HSC response to stress and trauma (Mendez-Ferrer, 2020). There is also evidence that MSCs reduce the effectiveness of drugs on diseased cells (Méndez-Ferrer, 2021; Tang et al., 2018). Therefore, if drug testing on HSCs is to be carried out *in vitro,* it would be most biologically comparable in a co-culture system with MSCs present. This then applies to the presented work, which, if to be used as a drug testing/screening platform, should strive for *in vivo* comparability. Further, this system could provide insights into interactions between low-metabolic cells within BM,

expanding on existing work investigating cytokine expression and intercellular signalling (Chen, 2012; Bräuninger, 2021).

5.4.4 Alternate cells

It is not just MSCs and HSCs which can enter quiescence; other stem cells still require investigation. For example, it remains unclear whether active neural stem cells (NSCs) are a unique cell population from quiescent NSCs (Meng, 2024). Whilst muscle stem cells enter quiescence in methylcellulose medium, this is far from an optimal system for experiments, and viability starts falling after 3 days (Arora, 2017). Additionally, some mature cells have been shown to enter a quiescent state. The regenerative capabilities of the liver are a result of hepatocytes (Fabris, 2019; Berasain & Avila, 2015). They are highly potent and regenerative cells which primarily exist in a quiescent state and are activated upon injury, though they can become exhausted if long-term, persistent damage occurs. T cells enter the blood circulation from the thymus in a naïve, quiescent state and are maintained until stimulated to differentiate (Chapman, 2020). While fibroblasts can be induced to enter quiescence through serum starvation and contact-inhibition (Mitra, 2018). This system could also be used for investigating LSCs. A way to study which leukaemic cells can enter quiescence and further provide an *in vitro* method to test treatments and drugs on them could be of benefit. All aforementioned cell types are viable options for storage/transport using alginate hydrogels. Further, the lack of information regarding stem cell quiescence makes alginate encapsulation a potential platform for future research to determine if they are quiescence-capable.

5.5 Conclusion

Whilst the last 20 years have seen great advances in our understanding of stem cells within the BM niche, HSCs are reported inconsistently in the literature. This inconsistency hinders scientific progress with a cell type that is already a financial and practical challenge to use, complicated further by the societal emphasis of environmentally and ethically favourable alternatives to established practises. As a result, we lack adequate methods with which to maintain HSPCs *in vitro* to provide a platform for future testing and research. Without enabling research with this cell type, advancement rates will stumble, and so too will the treatment of haematopoietic diseases that remain some of the world’s greatest killers.

Simple, inexpensive methods of maintaining quiescent HSPCs that are ethically and environmentally considered will help future-proof advancements and not render costly research redundant before ever becoming established. This project was able to demonstrate the intricacies of HSPC subpopulations and how the ability of some HSPC cells to enter quiescence would enable them to be stored near room temperature for short periods of time. This would help address some of the above issues by improving access to the cells, as well as being a more environmentally friendly method of storing cells short-term than traditional methods. There is also potential for this encapsulation method to be used to maintain quiescent HSCPS *in vitro* and enable testing on a population which currently cannot be cultured in the lab.

MSCs are already widely established as a therapeutic tool, with potential avenues into osteo-regeneration. MSC spheroids are a newer form of MSC therapy which is hinted at offering benefits in alternative areas, or an improvement on current single-MSC therapies. This work has demonstrated that while single BM-MSCs show decreasing viability over 14 days, when aggregated as spheroids, their viability is stable and they are more resilient to external variables, making their transport using encapsulation a viable option.

References

Abkowitz, J. L., Catlin, S. N., McCallie, M. T., & Guttorp, P. (2002). Evidence that the number of hematopoietic stem cells per animal is conserved in mammals. Blood, 100(7), 2665–2667. https://doi.org/10.1182/BLOOD-2002-03-0822

Abo-Aziza, F. A. M., & Zaki, A. A. (2017). The Impact of Confluence on Bone Marrow Mesenchymal Stem (BMMSC) Proliferation and Osteogenic Differentiation. International Journal of Hematology-Oncology and Stem Cell Research, 11(2), 121. https://pmc.ncbi.nlm.nih.gov/articles/PMC5575725/

Atelerix. (2025). About Us. https://www.atelerix.co.uk/about-us/

LifeTimeCDT. (2025). About us. https://lifetime-cdt.org/about-us/

ABPI. (2025, September 16). The use of animals in pharmaceutical research. https://www.abpi.org.uk/r-d-manufacturing/the-use-of-animals-in-pharmaceutical-research/

Abu Shmeis, R. M. (2022). Nanotechnology in wastewater treatment. Comprehensive Analytical Chemistry, 99, 105–134. https://doi.org/10.1016/BS.COAC.2021.11.002

Aderibigbe, B. A., & Buyana, B. (2018). Alginate in Wound Dressings. Pharmaceutics, 10(2). https://doi.org/10.3390/PHARMACEUTICS10020042

Ahmad, N., Kiriako, G., Saliba, J., Abla, K., El-Sabban, M., & Mhanna, R. (2024). Engineering a 3D Biomimetic Peptides Functionalized-Polyethylene Glycol Hydrogel Model Cocultured with Endothelial Cells and Astrocytes: Enhancing In Vitro Blood-Brain Barrier Biomimicry. Molecular Pharmaceutics, 21(9), 4664–4672. https://doi.org/10.1021/ACS.MOLPHARMACEUT.4C00599/SUPPL_FILE/MP4C00599_SI_001.PDF

Akbarzadeh Solbu, A., Koernig, A., Kjesbu, J. S., Zaytseva-Zotova, D., Sletmoen, M., & Strand, B. L. (2022). High resolution imaging of soft alginate hydrogels by atomic force microscopy. Carbohydrate Polymers, 276, 118804. https://doi.org/10.1016/J.CARBPOL.2021.118804

Akira, S., Taga, T., & Kishimoto, T. (1993). Interleukin-6 in Biology and Medicine. Advances in Immunology, 54, 1–78. https://doi.org/10.1016/S0065-2776(08)60532-5

Al Hamed, R., Bazarbachi, A. H., Malard, F., Harousseau, J. L., & Mohty, M. (2019). Current status of autologous stem cell transplantation for multiple myeloma. Blood Cancer Journal, 9(4), 1–10. https://doi.org/10.1038/S41408-019-0205-9;SUBJMETA=1541,1542,1990,532,631,67,692,699,804;KWRD=HAEMATOPOIETIC+STEM+CELLS,MYELOMA

AlamarBlue cell proliferation assay | BMG LABTECH. (n.d.). Retrieved January 22, 2026, from https://www.bmglabtech.com/en/application-notes/alamarblue-assay-for-assessment-of-cell-proliferation-using-a-bmg-labtech-microplate-reader/

Alberts, B., Johnson, A., Lewis, J., Raff, M., Roberts, K., & Walter, P. (2002). The Extracellular Matrix of Animals. https://www.ncbi.nlm.nih.gov/books/NBK26810/

Aleman, J., George, S. K., Herberg, S., Devarasetty, M., Porada, C. D., Skardal, A., & Almeida-Porada, G. (2019). Deconstructed Microfluidic Bone Marrow On-A-Chip to Study Normal and Malignant Hemopoietic Cell-Niche Interactions. Small (Weinheim an Der Bergstrasse, Germany), 15(43). https://doi.org/10.1002/SMLL.201902971

Algisite M Calcium Alginate Dressing - MedicalDressings. (n.d.). Retrieved January 7, 2026, from https://medicaldressings.co.uk/algisite-m-calcium-alginate-dressing/

Aljagthmi, A. A., & Abdel-Aziz, A. K. (2025). Hematopoietic stem cells: Understanding the mechanisms to unleash the therapeutic potential of hematopoietic stem cell transplantation. Stem Cell Research & Therapy 2025 16:1, 16(1), 1–11. https://doi.org/10.1186/S13287-024-04126-Z

Al-Jaibaji, O., Swioklo, S., Gijbels, K., Vaes, B., Figueiredo, F. C., & Connon, C. J. (2018). Alginate encapsulated multipotent adult progenitor cells promote corneal stromal cell activation via release of soluble factors. PLOS ONE, 13(9), e0202118. https://doi.org/10.1371/JOURNAL.PONE.0202118

Álvarez-Viejo, M., Menéndez-Menéndez, Y., Otero-Hernández, J., & Roma, de. (2015). CD271 as a marker to identify mesenchymal stem cells from diverse sources before culture. World Journal of Stem Cells, 7(2), 470. https://doi.org/10.4252/WJSC.V7.I2.470

Andersen, T., Auk-Emblem, P., & Dornish, M. (2015). 3D Cell Culture in Alginate Hydrogels. Microarrays 2015, Vol. 4, Pages 133-161, 4(2), 133–161. https://doi.org/10.3390/MICROARRAYS4020133

Anderson, P., Carrillo-Gálvez, A. B., García-Pérez, A., Cobo, M., & Martín, F. (2013). CD105 (Endoglin)-Negative Murine Mesenchymal Stromal Cells Define a New Multipotent Subpopulation with Distinct Differentiation and Immunomodulatory Capacities. PLOS ONE, 8(10), e76979. https://doi.org/10.1371/JOURNAL.PONE.0076979

Anjos-Afonso, F., & Bonnet, D. (2023). Human CD34+ hematopoietic stem cell hierarchy: how far are we with its delineation at the most primitive level? Blood, 142(6), 509. https://doi.org/10.1182/BLOOD.2022018071

Anne Turner, B. M., Lin, N. L., Issarachai, S., & Lyman, S. D. (n.d.). FLT3 Receptor Expression on the Surface of Normal and Malignant Human Hematopoietic Cells. Retrieved April 24, 2025, from http://ashpublications.org/blood/article-pdf/88/9/3383/623261/3383.pdf

Antoine, E. E., Vlachos, P. P., & Rylander, M. N. (2014). Review of Collagen I Hydrogels for Bioengineered Tissue Microenvironments: Characterization of Mechanics, Structure, and Transport. Tissue Engineering. Part B, Reviews, 20(6), 683. https://doi.org/10.1089/TEN.TEB.2014.0086

Antoine, E. E., Vlachos, P. P., & Rylander, M. N. (2015). Tunable Collagen I Hydrogels for Engineered Physiological Tissue Micro-Environments. PLOS ONE, 10(3), e0122500. https://doi.org/10.1371/JOURNAL.PONE.0122500

Aoki, K., Kurashige, M., Ichii, M., Higaki, K., Sugiyama, T., Kaito, T., Ando, W., Sugano, N., Sakai, T., Shibayama, H., Takaori-Kondo, A., Morii, E., Kanakura, Y., & Nagasawa, T. (2021). Identification of CXCL12-abundant reticular cells in human adult bone marrow. British Journal of Haematology, 193(3), 659–668. https://doi.org/10.1111/BJH.17396

Arai, F., Hirao, A., Ohmura, M., Sato, H., Matsuoka, S., Takubo, K., Ito, K., Koh, G. Y., & Suda, T. (2004). Tie2/Angiopoietin-1 Signaling Regulates Hematopoietic Stem Cell Quiescence in the Bone Marrow Niche. Cell, 118(2), 149–161. https://doi.org/10.1016/J.CELL.2004.07.004

Arch, R., Wirth, K., Hofmann, M., Ponta, H., Matzku, S., Herrlich, P., & Zöller, M. (1992). Participation in normal immune responses of a metastasis-inducing splice variant of CD44. Science (New York, N.Y.), 257(5070), 682–685. https://doi.org/10.1126/SCIENCE.1496383

Ashok, A., Brison, M., & LeTallec, Y. (2017). Improving cold chain systems: Challenges and solutions. Vaccine, 35(17), 2217–2223. https://doi.org/10.1016/J.VACCINE.2016.08.045

Aswathy, S. H., Narendrakumar, U., & Manjubala, I. (2020). Commercial hydrogels for biomedical applications. Heliyon, 6(4). https://doi.org/10.1016/J.HELIYON.2020.E03719

Atelerix. (2022). Atelerix testing guidelines. https://www.atelerix.co.uk/guidelines-for-testing-conditions/

Atelerix. (2026). Atelerix: Innovative Cell Preservation. https://www.atelerix.co.uk/

Aterlerix. (n.d.). BR-MNS Preservation of Cells Suspended in Gel Beads.

Bahsoun, S., Coopman, K., & Akam, E. C. (2019). The impact of cryopreservation on bone marrow-derived mesenchymal stem cells: a systematic review. Journal of Translational Medicine, 17(1), 397. https://doi.org/10.1186/S12967-019-02136-7

Bandzerewicz, A., & Gadomska-Gajadhur, A. (2022). Into the Tissues: Extracellular Matrix and Its Artificial Substitutes: Cell Signalling Mechanisms. Cells, 11(5), 914. https://doi.org/10.3390/CELLS11050914

Banu, N., Deng, B., Lyman, S. D., & Avraham, H. (1999). MODULATION OF HAEMATOPOIETIC PROGENITOR DEVELOPMENT BY FLT-3 LIGAND. Cytokine, 11(9), 679–688. https://doi.org/10.1006/CYTO.1998.0477

Baraniak, P. R., Cooke, M. T., Saeed, R., Kinney, M. A., Fridley, K. M., & McDevitt, T. C. (2012). Stiffening of Human Mesenchymal Stem Cell Spheroid Microenvironments Induced by Incorporation of Gelatin Microparticles. Journal of the Mechanical Behavior of Biomedical Materials, 11, 63. https://doi.org/10.1016/J.JMBBM.2012.02.018

Baraniak, P. R., & McDevitt, T. C. (2012). Scaffold-free culture of mesenchymal stem cell spheroids in suspension preserves multilineage potential. Cell and Tissue Research, 347(3), 701–711. https://doi.org/10.1007/S00441-011-1215-5/FIGURES/9

Barceló, X., Eichholz, K. F., Garcia, O., & Kelly, D. J. (2022). Tuning the Degradation Rate of Alginate-Based Bioinks for Bioprinting Functional Cartilage Tissue. Biomedicines, 10(7), 1621. https://doi.org/10.3390/BIOMEDICINES10071621/S1

Bartenstein, M., & Deeg, H. J. (2010). Hematopoietic Stem Cell Transplantation for MDS. Hematology/Oncology Clinics of North America, 24(2), 407. https://doi.org/10.1016/J.HOC.2010.02.003

Bartosh, T. J., Ylöstalo, J. H., Mohammadipoor, A., Bazhanov, N., Coble, K., Claypool, K., Lee, R. H., Choi, H., & Prockop, D. J. (2010a). Aggregation of human mesenchymal stromal cells (MSCs) into 3D spheroids enhances their antiinflammatory properties. Proceedings of the National Academy of Sciences of the United States of America, 107(31), 13724–13729. https://doi.org/10.1073/PNAS.1008117107/-/DCSUPPLEMENTAL

Bartosh, T. J., Ylöstalo, J. H., Mohammadipoor, A., Bazhanov, N., Coble, K., Claypool, K., Lee, R. H., Choi, H., & Prockop, D. J. (2010b). Aggregation of human mesenchymal stromal cells (MSCs) into 3D spheroids enhances their antiinflammatory properties. Proceedings of the National Academy of Sciences of the United States of America, 107(31), 13724–13729. https://doi.org/10.1073/PNAS.1008117107/SUPPL_FILE/PNAS.201008117SI.PDF

Batsali, A. K., Georgopoulou, A., Mavroudi, I., Matheakakis, A., Pontikoglou, C. G., & Papadaki, H. A. (2020). The Role of Bone Marrow Mesenchymal Stem Cell Derived Extracellular Vesicles (MSC-EVs) in Normal and Abnormal Hematopoiesis and Their Therapeutic Potential. Journal of Clinical Medicine, 9(3), 856. https://doi.org/10.3390/JCM9030856

Bellagamba, B. C., Grudzinski, P. B., Ely, P. B., Nader, P. D. J. H., Nardi, N. B., & Da Silva Meirelles, L. (2018). Induction of Expression of CD271 and CD34 in Mesenchymal Stromal Cells Cultured as Spheroids. Stem Cells International, 2018(1), 7357213. https://doi.org/10.1155/2018/7357213

Bentley, S. A. (1981). Close range cell:cell interaction required for stem cell maintenance in continuous bone marrow culture. Experimental Hematology, 9(3), 308–312.

Bernar, A., Gebetsberger, J. V., Bauer, M., Streif, W., & Schirmer, M. (2023). Optimization of the Alizarin Red S Assay by Enhancing Mineralization of Osteoblasts. International Journal of Molecular Sciences, 24(1), 723. https://doi.org/10.3390/IJMS24010723/S1

Bernstein, I., Andrews, R., & Zsebo, K. (1991). Recombinant Human Stem Cell Factor Enhances the Formation of Colonies by CD34+ and CD34+lin- Cells, and the Generation of Colony-Forming Cell Progeny From CD34+lin- Cells Cultured With Interleukin-3, Granulocyte Colony-Stimulating Factor, or Granulocyte-Macrophage Colony-Stimulating Factor. Blood, 77(11), 2316–2321. https://doi.org/10.1182/BLOOD.V77.11.2316.2316

Berz, D., McCormack, E. M., Winer, E. S., Colvin, G. A., & Quesenberry, P. J. (2007). Cryopreservation of Hematopoietic Stem Cells. American Journal of Hematology, 82(6), 463. https://doi.org/10.1002/AJH.20707

Bhang, S. H., Cho, S. W., La, W. G., Lee, T. J., Yang, H. S., Sun, A. Y., Baek, S. H., Rhie, J. W., & Kim, B. S. (2011). Angiogenesis in ischemic tissue produced by spheroid grafting of human adipose-derived stromal cells. Biomaterials, 32(11), 2734–2747. https://doi.org/10.1016/J.BIOMATERIALS.2010.12.035

Bhang, S. H., Lee, S., Shin, J. Y., Lee, T. J., & Kim, B. S. (2012). Transplantation of Cord Blood Mesenchymal Stem Cells as Spheroids Enhances Vascularization. Https://Home.Liebertpub.Com/Tea, 18(19–20), 2138–2147. https://doi.org/10.1089/TEN.TEA.2011.0640

Bhujbal, S. V., de Vos, P., & Niclou, S. P. (2014). Drug and cell encapsulation: Alternative delivery options for the treatment of malignant brain tumors. Advanced Drug Delivery Reviews, 67–68, 142–153. https://doi.org/10.1016/J.ADDR.2014.01.010

Bian, X. H., Zhou, G. Y., Wang, L. N., Ma, J. F., Fan, Q. L., Liu, N., Bai, Y., Guo, W., Wang, Y. Q., Sun, G. P., He, P., Yang, X., Su, X. S., Du, F., Zhao, G. F., Miao, J. N., Ma, L., Zheng, L. Q., Li, D. T., & Feng, J. M. (2013). The role of CD44-hyaluronic acid interaction in exogenous mesenchymal stem cells homing to rat remnant kidney. Kidney & Blood Pressure Research, 38(1), 11–20. https://doi.org/10.1159/000355749

Bidarra, S. J., Barrias, C. C., Barbosa, M. A., Soares, R., Amédée, J., & Granja, P. L. (2011). Phenotypic and proliferative modulation of human mesenchymal stem cells via crosstalk with endothelial cells. Stem Cell Research, 7(3), 186–197. https://doi.org/10.1016/J.SCR.2011.05.006

Bikorimana, J. P., Saad, W., Abusarah, J., Lahrichi, M., Talbot, S., Shammaa, R., & Rafei, M. (2022). CD146 Defines a Mesenchymal Stromal Cell Subpopulation with Enhanced Suppressive Properties. Cells, 11(15), 2263. https://doi.org/10.3390/CELLS11152263/S1

Boateng, J. S., Matthews, K. H., Stevens, H. N. E., & Eccleston, G. M. (2008). Wound healing dressings and drug delivery systems: A review. Journal of Pharmaceutical Sciences, 97(8), 2892–2923. https://doi.org/10.1002/jps.21210

Bolan, C. D., Childs, R. W., Procter, J. L., Barrett, A. J., & Leitman, S. F. (2001). Massive immune haemolysis after allogeneic peripheral blood stem cell transplantation with minor ABO incompatibility. British Journal of Haematology, 112(3), 787–795. https://doi.org/10.1046/J.1365-2141.2001.02587.X

Bonani, W., Cagol, N., & Maniglio, D. (2020). Alginate Hydrogels: A Tool for 3D Cell Encapsulation, Tissue Engineering, and Biofabrication. Advances in Experimental Medicine and Biology, 1250, 49–61. https://doi.org/10.1007/978-981-15-3262-7_4/TABLES/1

Boudjadi, S., Carrier, J. C., Groulx, J. F., & Beaulieu, J. F. (2015). Integrin α1β1 expression is controlled by c-MYC in colorectal cancer cells. Oncogene 2016 35:13, 35(13), 1671–1678. https://doi.org/10.1038/onc.2015.231

Bowlin, G. L., Demitri, C., Piuzzi, E., Kefallinou, D., Grigoriou, M., Boumpas, D. T., & Tserepi, A. (2024). Mesenchymal Stem Cell and Hematopoietic Stem and Progenitor Cell Co-Culture in a Bone-Marrow-on-a-Chip Device toward the Generation and Maintenance of the Hematopoietic Niche. Bioengineering 2024, Vol. 11, Page 748, 11(8), 748. https://doi.org/10.3390/BIOENGINEERING11080748

Bowman, T. V., & Zon, L. I. (2009). Lessons from the niche for generation and expansion of hematopoietic stem cells. Drug Discovery Today: Therapeutic Strategies, 6(4), 135–140. https://doi.org/10.1016/J.DDSTR.2009.06.003

Boyle, C., Lansdorp, P. M., & Edelstein-Keshet, L. (2023). Predicting the number of lifetime divisions for hematopoietic stem cells from telomere length measurements. IScience, 26(7), 107053. https://doi.org/10.1016/J.ISCI.2023.107053

Bradaschia-Correa, V., Josephson, A. M., Egol, A. J., Mizrahi, M. M., Leclerc, K., Huo, J., Cronstein, B. N., & Leucht, P. (2017). Ecto-5′-nucleotidase (CD73) regulates bone formation and remodeling during intramembranous bone repair in aging mice. Tissue and Cell, 49(5), 545–551. https://doi.org/10.1016/J.TICE.2017.07.001

Braham, M. V. J., Ahlfeld, T., Akkineni, A. R., Minnema, M. C., Dhert, W. J. A., Öner, F. C., Robin, C., Lode, A., Gelinsky, M., & Alblas, J. (2018). Endosteal and Perivascular Subniches in a 3D Bone Marrow Model for Multiple Myeloma. Tissue Engineering. Part C, Methods, 24(5), 300–312. https://doi.org/10.1089/TEN.TEC.2017.0467

Branco, A., Rayabaram, J., Miranda, C. C., Fernandes-Platzgummer, A., Fernandes, T. G., Sajja, S., da Silva, C. L., & Vemuri, M. C. (2024). Advances in ex vivo expansion of hematopoietic stem and progenitor cells for clinical applications. Frontiers in Bioengineering and Biotechnology, 12, 1380950. https://doi.org/10.3389/FBIOE.2024.1380950/PDF

Branco, A., Tiago, A. L., Laranjeira, P., Carreira, M. C., Milhano, J. C., Santos, F. Dos, Cabral, J. M. S., Paiva, A., Da Silva, C. L., & Fernandes-Platzgummer, A. (2022). Hypothermic Preservation of Adipose-Derived Mesenchymal Stromal Cells as a Viable Solution for the Storage and Distribution of Cell Therapy Products. https://doi.org/10.3390/bioengineering9120805

Brashem-Stein, C., Flowers, D. A., & Bernstein, I. D. (1996). Regulation of colony forming cell generation by flt-3 ligand. British Journal of Haematology, 94(1), 17–22. https://doi.org/10.1046/J.1365-2141.1996.D01-1773.X

BrdU Labeling & Detection Protocol - UK. (n.d.). Retrieved January 21, 2026, from https://www.thermofisher.com/uk/en/home/references/protocols/cell-and-tissue-analysis/protocols/brdu-labeling-and-detection-protocol.html

Brenez, D., Devriendt, J., Lenclud, C., & Schmerber, J. (1990). Acute nonlymphocytic leukemia following chemotherapy with cisplatin and etoposide for non-small-cell carcinoma of the lung: case report. Cancer Chemotherapy and Pharmacology, 26(3), 235–236. https://doi.org/10.1007/BF02897207

Broudy, V. C. (1997). Stem Cell Factor and Hematopoiesis. Blood, 90(4), 1345–1364. https://doi.org/10.1182/BLOOD.V90.4.1345

Broxmeyer, H. E., Kohli, L., Kim, C. H., Lee, Y., Mantel, C., Cooper, S., Hangoc, G., Shaheen, M., Li, X., & Clapp, D. W. (2003). Stromal cell-derived factor-1/CXCL12 directly enhances survival/antiapoptosis of myeloid progenitor cells through CXCR4 and Gαi proteins and enhances engraftment of competitive, repopulating stem cells. Journal of Leukocyte Biology, 73(5), 630–638. https://doi.org/10.1189/JLB.1002495

Broxmeyer, H. E., Lu, L., Cooper, S., Ruggieri, L., Li, Z. H., & Lyman, S. D. (1995). Flt3 ligand stimulates/costimulates the growth of myeloid stem/progenitor cells. Experimental Hematology, 23(10), 1121–1129. https://europepmc.org/article/med/7544740

Bruns, I., Lucas, D., Pinho, S., Ahmed, J., Lambert, M. P., Kunisaki, Y., Scheiermann, C., Schiff, L., Poncz, M., Bergman, A., & Frenette, P. S. (2014). Megakaryocytes regulate hematopoietic stem cell quiescence through CXCL4 secretion. Nature Medicine 2014 20:11, 20(11), 1315–1320. https://doi.org/10.1038/nm.3707

Bryder, D., & Jacobsen, S. E. W. (2000). Interleukin-3 supports expansion of long-term multilineage repopulating activity after multiple stem cell divisions in vitro. Blood, 96(5), 1748–1755. https://doi.org/10.1182/BLOOD.V96.5.1748

Bucar, S., Branco, A. D. de M., Mata, M. F., Milhano, J. C., Caramalho, Í., Cabral, J. M. S., Fernandes-Platzgummer, A., & da Silva, C. L. (2021). Influence of the mesenchymal stromal cell source on the hematopoietic supportive capacity of umbilical cord blood-derived CD34+-enriched cells. Stem Cell Research and Therapy, 12(1), 1–16. https://doi.org/10.1186/S13287-021-02474-8/FIGURES/6

Budgude, P., Kale, V., & Vaidya, A. (2025). Microvesicles and exosomes isolated from murine bone marrow-derived mesenchymal stromal cells primed with p38MAPK inhibitor differentially regulate hematopoietic stem cell function. Artificial Cells, Nanomedicine, and Biotechnology, 53(1), 122–137. https://doi.org/10.1080/21691401.2025.2475095

Burand, A. J., Di, L., Boland, L. K., Boyt, D. T., Schrodt, M. V., Santillan, D. A., & Ankrum, J. A. (2020). Aggregation of Human Mesenchymal Stromal Cells Eliminates Their Ability to Suppress Human T Cells. Frontiers in Immunology, 11. https://doi.org/10.3389/FIMMU.2020.00143/PDF

Butler, J. T., Abdelhamed, S., & Kurre, P. (2018). Extracellular vesicles in the hematopoietic microenvironment. Haematologica, 103(3), 382–394. https://doi.org/10.3324/HAEMATOL.2017.183335

Cacciamali, A., Villa, R., & Dotti, S. (2022). 3D Cell Cultures: Evolution of an Ancient Tool for New Applications. Frontiers in Physiology, 13. https://doi.org/10.3389/FPHYS.2022.836480

Caixia, S., Stewart, S., Wayner, E., Carter, W., & Wilkins, J. (1991). Antibodies to different members of the beta 1 (CD29) integrins induce homotypic and heterotypic cellular aggregation. Cellular Immunology, 138(1), 216–228. https://doi.org/10.1016/0008-8749(91)90146-3

Caliari, S. R., & Burdick, J. A. (2016). A practical guide to hydrogels for cell culture. Nature Methods 2016 13:5, 13(5), 405–414. https://doi.org/10.1038/nmeth.3839

Camilleri, E. T., Gustafson, M. P., Dudakovic, A., Riester, S. M., Garces, C. G., Paradise, C. R., Takai, H., Karperien, M., Cool, S., Sampen, H. J. I., Larson, A. N., Qu, W., Smith, J., Dietz, A. B., & Van Wijnen, A. J. (2016). Identification and validation of multiple cell surface markers of clinical-grade adipose-derived mesenchymal stromal cells as novel release criteria for good manufacturing practice-compliant production. Stem Cell Research and Therapy, 7(1), 1–16. https://doi.org/10.1186/S13287-016-0370-8/TABLES/2

Cao, Y., Boss, A. L., Bolam, S. M., Munro, J. T., Crawford, H., Dalbeth, N., Poulsen, R. C., & Matthews, B. G. (2024). In Vitro Cell Surface Marker Expression on Mesenchymal Stem Cell Cultures does not Reflect Their Ex Vivo Phenotype. Stem Cell Reviews and Reports, 20(6), 1656–1666. https://doi.org/10.1007/S12015-024-10743-1/FIGURES/3

Catlin, S. N., Busque, L., Gale, R. E., Guttorp, P., & Abkowitz, J. L. (2011). The replication rate of human hematopoietic stem cells in vivo. Blood, 117(17), 4460. https://doi.org/10.1182/BLOOD-2010-08-303537

Cesarz, Z., & Tamama, K. (2016). Spheroid Culture of Mesenchymal Stem Cells. Stem Cells International, 2016. https://doi.org/10.1155/2016/9176357

Chan, E. S., Lim, T. K., Voo, W. P., Pogaku, R., Tey, B. T., & Zhang, Z. (2011). Effect of formulation of alginate beads on their mechanical behavior and stiffness. Particuology, 9(3), 228–234. https://doi.org/10.1016/J.PARTIC.2010.12.002

Chandanala, S., Mohan, G., Manukonda, D. L., Kumar, A., & Prasanna, J. (2024). A novel role of CD73-IFNγ signalling axis in human mesenchymal stromal cell mediated inflammatory macrophage suppression. Regenerative Therapy, 26, 89–101. https://doi.org/10.1016/J.RETH.2024.05.011

Chang, T., & Zhao, G. (2021). Ice Inhibition for Cryopreservation: Materials, Strategies, and Challenges. Advanced Science, 8(6), 2002425. https://doi.org/10.1002/ADVS.202002425

Chatterjee, C., Schertl, P., Frommer, M., Ludwig-Husemann, A., Mohra, A., Dilger, N., Naolou, T., Meermeyer, S., Bergmann, T. C., Alonso Calleja, A., & Lee-Thedieck, C. (2021). Rebuilding the hematopoietic stem cell niche: Recent developments and future prospects. Acta Biomaterialia, 132, 129–148. https://doi.org/10.1016/J.ACTBIO.2021.03.061

Chaudhuri, O., Gu, L., Klumpers, D., Darnell, M., Bencherif, S. A., Weaver, J. C., Huebsch, N., Lee, H.-P., Lippens, E., Duda, G. N., & Mooney, D. J. (2016). Hydrogels with tunable stress relaxation regulate stem cell fate and activity. https://doi.org/10.1038/NMAT4489

Cheifetz, S., Bellón, T., Calés, C., Vera, S., Bernabeu, C., Massagué, J., & Letarte, M. (1992). Endoglin is a component of the transforming growth factor-beta receptor system in human endothelial cells. Journal of Biological Chemistry, 267(27), 19027–19030. https://doi.org/10.1016/S0021-9258(18)41732-2

Chen, B., Wright, B., Sahoo, R., & Connon, C. J. (2013). A novel alternative to cryopreservation for the short-term storage of stem cells for use in cell therapy using alginate encapsulation.

Tissue Engineering - Part C: Methods, 19(7), 568–576. https://doi.org/10.1089/TEN.TEC.2012.0489/SUPPL_FILE/SUPP_FIG3.PDF

Chen, J., Yang, G., Guo, Jie, Liu, Y., Guo, Jinchen, Suo, J., & Yu, H. (2021). The Expression of Angiopoietin-1 and −2 in the Osteogenesis of Mesenchymal Stem Cells. BioRxiv, 2021.04.15.440087. https://doi.org/10.1101/2021.04.15.440087

Chen, W., Kim, J. H., Zhang, D., Lee, K. H., Cangelosi, G. A., Soelberg, S. D., Furlong, C. E., Chung, J. H., & Shen, A. Q. (2013). Microfluidic one-step synthesis of alginate microspheres immobilized with antibodies. Journal of the Royal Society Interface, 10(88), 20130566. https://doi.org/10.1098/RSIF.2013.0566

Cheng, H., Zheng, Z., & Cheng, T. (2020). New paradigms on hematopoietic stem cell differentiation. Protein and Cell, 11(1), 34–44. https://doi.org/10.1007/S13238-019-0633-0/FIGURES/4

Cheng, T., & Scadden, D. T. (2009). Cell Cycle Regulators in Adult Stem Cells. Essentials of Stem Cell Biology, Second Edition, 81–87. https://doi.org/10.1016/B978-0-12-374729-7.00009-3

Chitteti, B. R., Cheng, Y. H., Kacena, M. A., & Srour, E. F. (2013). HIERARCHICAL ORGANIZATION OF OSTEOBLASTS REVEALS THE SIGNIFICANT ROLE OF CD166 IN HEMATOPOIETIC STEM CELL MAINTANANCE AND FUNCTION. Bone, 54(1), 58. https://doi.org/10.1016/J.BONE.2013.01.038

Chitteti, B. R., Kobayashi, M., Cheng, Y., Zhang, H., Poteat, B. A., Broxmeyer, H. E., Pelus, L. M., Hanenberg, H., Zollman, A., Kamocka, M. M., Carlesso, N., Cardoso, A. A., Kacena, M. A., & Srour, E. F. (2014). CD166 regulates human and murine hematopoietic stem cells and the hematopoietic niche. Blood, 124(4), 519–529. https://doi.org/10.1182/BLOOD-2014-03-565721

Cho, R. J., Kim, Y. S., Kim, J. Y., & Oh, Y. M. (2017). Human adipose-derived mesenchymal stem cell spheroids improve recovery in a mouse model of elastase-induced emphysema. BMB Reports, 50(2), 79. https://doi.org/10.5483/BMBREP.2017.50.2.101

Cho, W. K. J., Mittal, S. K., & Chauhan, S. K. (2023). Mesenchymal Stromal Cells Suppress T-Cell-Mediated Delayed-Type Hypersensitivity via ALCAM-CD6 Interaction. Stem Cells Translational Medicine, 12(4), 221–233. https://doi.org/10.1093/STCLTM/SZAD012

Chu, S., Maples, M. M., & Bryant, S. J. (2020). Cell encapsulation spatially alters crosslink density of poly(ethylene glycol) hydrogels formed from free-radical polymerizations. Acta Biomaterialia, 109, 37. https://doi.org/10.1016/J.ACTBIO.2020.03.033

Ciccone, G., Azevedo Gonzalez Oliva, M., Antonovaite, N., Lüchtefeld, I., Salmeron-Sanchez, M., & Vassalli, M. (2022). Experimental and Data Analysis Workflow for Soft Matter Nanoindentation. Journal of Visualized Experiments, (179). https://doi.org/10.3791/63401

Cisplatin Monograph for Professionals - Drugs.com. (n.d.). Retrieved March 5, 2024, from https://www.drugs.com/monograph/cisplatin.html

Civin, C. I., Almeida-Porada, G., Lee, M. J., Olweus, J., Terstappen, L. W. M. M., & Zanjani, E. D. (1996). Sustained, Retransplantable, Multilineage Engraftment of Highly Purified Adult Human Bone Marrow Stem Cells In Vivo. Blood, 88(11), 4102–4109. https://doi.org/10.1182/BLOOD.V88.11.4102.4102

Cleary, M. A., Narcisi, R., Focke, K., van der Linden, R., Brama, P. A. J., & van Osch, G. J. V. M. (2016). Expression of CD105 on expanded mesenchymal stem cells does not predict their

chondrogenic potential. Osteoarthritis and Cartilage, 24(5), 868–872. https://doi.org/10.1016/J.JOCA.2015.11.018

Cohen, S., Bambace, N., Ahmad, I., Roy, J., Tang, X., Zhang, M. J., Burns, L., Barabé, F., Bernard, L., Delisle, J. S., Kiss, T., Lachance, S., Roy, D. C., Veilleux, O., & Sauvageau, G. (2023). Improved outcomes of UM171–expanded cord blood transplantation compared with other graft sources: real-world evidence. Blood Advances, 7(19), 5717–5726. https://doi.org/10.1182/BLOODADVANCES.2023010599/2064735/BLOODADVANCES.2023010599.PDF

Colgan, S. P., Eltzschig, H. K., Eckle, T., & Thompson, L. F. (2006). Physiological roles for ecto-5'-nucleotidase (CD73). Purinergic Signalling, 2(2), 351–360. https://doi.org/10.1007/S11302-005-5302-5/FIGURES/1

Coppack, S. W. (2001). Pro-inflammatory cytokines and adipose tissue. The Proceedings of the Nutrition Society, 60(3), 349–356. https://doi.org/10.1079/PNS2001110

Costa, M. H. G., de Soure, A. M., Cabral, J. M. S., Ferreira, F. C., & da Silva, C. L. (2018). Hematopoietic Niche – Exploring Biomimetic Cues to Improve the Functionality of Hematopoietic Stem/Progenitor Cells. Biotechnology Journal, 13(2), 1700088. https://doi.org/10.1002/BIOT.201700088

Cottle, C., Porter, A. P., Lipat, A., Turner-Lyles, C., Nguyen, J., Moll, G., & Chinnadurai, R. (2022). Impact of Cryopreservation and Freeze-Thawing on Therapeutic Properties of Mesenchymal Stromal/Stem Cells and Other Common Cellular Therapeutics. Current Stem Cell Reports, 8(2), 72–92. https://doi.org/10.1007/S40778-022-00212-1/FIGURES/4

Crisan, M., Yap, S., Casteilla, L., Chen, C. W., Corselli, M., Park, T. S., Andriolo, G., Sun, B., Zheng, B., Zhang, L., Norotte, C., Teng, P. N., Traas, J., Schugar, R., Deasy, B. M., Badylak, S., Buhring, H. J., Giacobino, J. P., Lazzari, L., … Péault, B. (2008). A Perivascular Origin for Mesenchymal Stem Cells in Multiple Human Organs. Cell Stem Cell, 3(3), 301–313. https://doi.org/10.1016/j.stem.2008.07.003

Cummings, C. L., Gawlitta, D., Nerem, R. M., & Stegemann, J. P. (2004). Properties of engineered vascular constructs made from collagen, fibrin, and collagen–fibrin mixtures. Biomaterials, 25(17), 3699–3706. https://doi.org/10.1016/J.BIOMATERIALS.2003.10.073

Cunniffe, G. M., Vinardell, T., Thompson, E. M., Daly, A. C., Matsiko, A., O'Brien, F. J., & Kelly, D. J. (2015). Chondrogenically primed mesenchymal stem cell-seeded alginate hydrogels promote early bone formation in critically-sized defects. European Polymer Journal, 72, 464–472. https://doi.org/10.1016/J.EURPOLYMJ.2015.07.021

da Silva Meirelles, L., Chagastelles, P. C., & Nardi, N. B. (2006). Mesenchymal stem cells reside in virtually all post-natal organs and tissues. Journal of Cell Science, 119(11), 2204–2213. https://doi.org/10.1242/JCS.02932

Dallas, S. L., Chen, Q., & Sivakumar, P. (2006). Dynamics of Assembly and Reorganization of Extracellular Matrix Proteins. Current Topics in Developmental Biology, 75, 1–24. https://doi.org/10.1016/S0070-2153(06)75001-3

Damala, M., Swioklo, S., Koduri, M. A., Mitragotri, N. S., Basu, S., Connon, C. J., & Singh, V. (2019). Encapsulation of human limbus-derived stromal/mesenchymal stem cells for biological preservation and transportation in extreme Indian conditions for clinical use. Scientific Reports 2019 9:1, 9(1), 1–11. https://doi.org/10.1038/s41598-019-53315-x

Damas, P., Ledoux, D., Nys, M., Vrindts, Y., De Groote, D., Franchimont, P., & Lamy, M. (1992). Cytokine serum level during severe sepsis in human IL-6 as a marker of severity. Annals of Surgery, 215(4), 356. https://doi.org/10.1097/00000658-199204000-00009

Darrabie, M. D., Kendall, W. F., & Opara, E. C. (2006). Effect of alginate composition and gelling cation on micro-bead swelling. Journal of Microencapsulation, 23(1), 29–37. https://doi.org/10.1080/02652040500286144

Dasari, S., & Bernard Tchounwou, P. (2014). Cisplatin in cancer therapy: Molecular mechanisms of action. European Journal of Pharmacology, 740, 364–378. https://doi.org/10.1016/j.ejphar.2014.07.025

Däster, S., Amatruda, N., Calabrese, D., Ivanek, R., Turrini, E., Droeser, R. A., Zajac, P., Fimognari, C., Spagnoli, G. C., Iezzi, G., Mele, V., & Muraro, M. G. (2016). Induction of hypoxia and necrosis in multicellular tumor spheroids is associated with resistance to chemotherapy treatment. Oncotarget, 8(1), 1725. https://doi.org/10.18632/ONCOTARGET.13857

de Graaf, C. A., Kauppi, M., Baldwin, T., D. Hyland, C., Metcalf, D., Willson, T. A., Carpinelli, M. R., Smyth, G. K., Alexander, W. S., & Hilton, D. J. (2010). Regulation of hematopoietic stem cells by their mature progeny. Proceedings of the National Academy of Sciences, 107(50), 21689–21694. https://doi.org/10.1073/pnas.1016166108

De Graaf, C. A., & Metcalf, D. (2011). Thrombopoietin and hematopoietic stem cells. Cell Cycle, 10(10), 1582. https://doi.org/10.4161/CC.10.10.15619

de Lima, M., McMannis, J., Gee, A., Komanduri, K., Couriel, D., Andersson, B. S., Hosing, C., Khouri, I., Jones, R., Champlin, R., Karandish, S., Sadeghi, T., Peled, T., Grynspan, F., Daniely, Y., Nagler, A., & Shpall, E. J. (2008). Transplantation of ex vivo expanded cord blood cells using the copper chelator tetraethylenepentamine: a phase I/II clinical trial. Bone Marrow Transplantation 2008 41:9, 41(9), 771–778. https://doi.org/10.1038/sj.bmt.1705979

de Lima, M., McNiece, I., Robinson, S. N., Munsell, M., Eapen, M., Horowitz, M., Alousi, A., Saliba, R., McMannis, J. D., Kaur, I., Kebriaei, P., Parmar, S., Popat, U., Hosing, C., Champlin, R., Bollard, C., Molldrem, J. J., Jones, R. B., Nieto, Y., … Shpall, E. J. (2012). Cord-Blood Engraftment with Ex Vivo Mesenchymal-Cell Coculture. New England Journal of Medicine, 367(24), 2305–2315. https://doi.org/10.1056/NEJMOA1207285/SUPPL_FILE/NEJMOA1207285_DISCLOSURES.PDF

de Morree, A., & Rando, T. A. (2023). Regulation of adult stem cell quiescence and its functions in the maintenance of tissue integrity. Nature Reviews Molecular Cell Biology 2023 24:5, 24(5), 334–354. https://doi.org/10.1038/s41580-022-00568-6

De Souza, L. E. B., Malta, T. M., Kashima Haddad, S., & Covas, D. T. (2016). Mesenchymal Stem Cells and Pericytes: To What Extent Are They Related? Stem Cells and Development, 25(24), 1843–1852. https://doi.org/10.1089/SCD.2016.0109

Decker, M., Leslie, J., Liu, Q., & Ding, L. (2018). Hepatic thrombopoietin is required for bone marrow hematopoietic stem cell maintenance. Science (New York, N.Y.), 360(6384), 106–110. https://doi.org/10.1126/SCIENCE.AAP8861

Derkus, B., Okesola, B. O., Barrett, D. W., D'Este, M., Chowdhury, T. T., Eglin, D., & Mata, A. (2020). Multicomponent hydrogels for the formation of vascularized bone-like constructs in vitro. Acta Biomaterialia, 109, 82–94. https://doi.org/10.1016/J.ACTBIO.2020.03.025

Di, G., Wang, J., Liu, M., Wu, C. T., Han, Y., & Duan, H. (2012). Development and evaluation of a trehalose-contained solution formula to preserve hUC-MSCs at 4°C. Journal of Cellular Physiology, 227(3), 879–884. https://doi.org/10.1002/JCP.23066,

DiGiusto, D. L., Cannon, P. M., Holmes, M. C., Li, L., Rao, A., Wang, J., Lee, G., Gregory, P. D., Kim, K. A., Hayward, S. B., Meyer, K., Exline, C., Lopez, E., Henley, J., Gonzalez, N., Bedell, V., Stan, R., & Zaia, J. A. (2016). Preclinical development and qualification of ZFN-mediated CCR5 disruption in human hematopoietic stem/progenitor cells. Molecular Therapy Methods and Clinical Development, 3, 16067. https://doi.org/10.1038/mtm.2016.67

Ding, L., & Morrison, S. J. (2013). Haematopoietic stem cells and early lymphoid progenitors occupy distinct bone marrow niches. Nature 2013 495:7440, 495(7440), 231–235. https://doi.org/10.1038/nature11885

Ding, L., Saunders, T. L., Enikolopov, G., & Morrison, S. J. (2012). Endothelial and perivascular cells maintain haematopoietic stem cells. Nature 2012 481:7382, 481(7382), 457–462. https://doi.org/10.1038/nature10783

Domen, J., & Weissman, I. L. (2000). Hematopoietic Stem Cells Need Two Signals to Prevent Apoptosis; Bcl-2 Can Provide One of These, Kitl/C-KIT Signaling the Other. Journal of Experimental Medicine, 192(12), 1707–1718. https://doi.org/10.1084/JEM.192.12.1707

Dominici, M., Le Blanc, K., Mueller, I., Slaper-Cortenbach, I., Marini, F. C., Krause, D. S., Deans, R. J., Keating, A., Prockop, D. J., & Horwitz, E. M. (2006). Minimal criteria for defining multipotent mesenchymal stromal cells. The International Society for Cellular Therapy position statement. Cytotherapy, 8(4), 315–317. https://doi.org/10.1080/14653240600855905

Dong, Y., Shi, O., Zeng, Q., Lu, X., Wang, W., Li, Y., Wang, Q., Wang, Q., & Wang, Q. (2020). Leukemia incidence trends at the global, regional, and national level between 1990 and 2017. Experimental Hematology and Oncology, 9(1), 1–11. https://doi.org/10.1186/S40164-020-00170-6/FIGURES/5

Dorronsoro, A., Lang, V., Ferrin, I., Fernández-Rueda, J., Zabaleta, L., Pérez-Ruiz, E., Sepúlveda, P., & Trigueros, C. (2020). Intracellular role of IL-6 in mesenchymal stromal cell immunosuppression and proliferation. Scientific Reports, 10(1), 1–12. https://doi.org/10.1038/S41598-020-78864-4;SUBJMETA=127,250,256,631,641,80,86;KWRD=CELL+DIVISION,CELL+SIGNALLING,CYTOKINES,INFLAMMATION

Dovedytis, M., Liu, Z. J., & Bartlett, S. (2020). Hyaluronic acid and its biomedical applications: A review. Engineered Regeneration, 1, 102–113. https://doi.org/10.1016/J.ENGREG.2020.10.001

Dowden, H., & Munro, J. (2019). Trends in clinical success rates and therapeutic focus. Nature Reviews. Drug Discovery, 18(7), 495–496. https://doi.org/10.1038/D41573-019-00074-Z

Draget, K. I., & Taylor, C. (2011). Chemical, physical and biological properties of alginates and their biomedical implications. Food Hydrocolloids, 25(2), 251–256. https://doi.org/10.1016/J.FOODHYD.2009.10.007

Drageta, K. I., GåserØd, O., Aunea, I., Andersen, P. O., Storbakken, B., Stokke, B. T., & SmidsrØd, O. (2001). Effects of molecular weight and elastic segment flexibility on syneresis in Ca-alginate gels. Food Hydrocolloids, 15(4–6), 485–490. https://doi.org/10.1016/S0268-005X(01)00046-7

Drobek, C., Meyer, J., Mau, R., Wolff, A., Peters, K., & Seitz, H. (2023). Volumetric mass density measurements of mesenchymal stem cells in suspension using a density meter. IScience, 26(1), 105796. https://doi.org/10.1016/J.ISCI.2022.105796

Du, J., Zhao, L., Kang, Q., He, Y., & Bi, Y. (2023). An optimized method for Oil Red O staining with the salicylic acid ethanol solution. Adipocyte, 12(1), 2179334. https://doi.org/10.1080/21623945.2023.2179334

Eleftheriadou, D., Evans, R. E., Atkinson, E., Abdalla, A., Gavins, F. K. H., Boyd, A. S., Williams, G. R., Knowles, J. C., Roberton, V. H., & Phillips, J. B. (2022). An alginate-based encapsulation system for delivery of therapeutic cells to the CNS. RSC Advances, 12(7), 4005–4015. https://doi.org/10.1039/D1RA08563H

Elliott, J. A. W. (2013). Intracellular Ice Formation: The Enigmatic Role of Cell-Cell Junctions. Biophysical Journal, 105(9), 1935. https://doi.org/10.1016/J.BPJ.2013.10.001

Engeland, K. (2022). Cell cycle regulation: p53-p21-RB signaling. https://doi.org/10.1038/s41418-022-00988-z

Erdal, S., Sivrikaya, S. K., Ozdelikara, A., & Murray, J. (2023). Hematopoietic Stem Cell Transplantation. Medical Nursing, 85–90. https://doi.org/10.5339/qmj.2007.2.7

Espagnolle, N., Guilloton, F., Deschaseaux, F., Gadelorge, M., Sensébé, L., & Bourin, P. (2014). CD146 expression on mesenchymal stem cells is associated with their vascular smooth muscle commitment. Journal of Cellular and Molecular Medicine, 18(1), 104–114. https://doi.org/10.1111/JCMM.12168

Ezoe, S. (2012). Secondary Leukemia Associated with the Anti-Cancer Agent, Etoposide, a Topoisomerase II Inhibitor. International Journal of Environmental Research and Public Health, 9(7), 2444. https://doi.org/10.3390/IJERPH9072444

Fekete, N., Béland, A. V., Campbell, K., Clark, S. L., & Hoesli, C. A. (2018). Bags versus flasks: a comparison of cell culture systems for the production of dendritic cell–based immunotherapies. Transfusion, 58(7), 1800–1813. https://doi.org/10.1111/TRF.14621

Fereydani, N. M., Galehdari, H., Hoveizi, E., Alghasi, A., & Ajami, M. (2024). Ex vivo expansion of hematopoietic stem cells in two/ three-dimensional co-cultures with various source of stromal cells. Tissue and Cell, 87, 102331. https://doi.org/10.1016/J.TICE.2024.102331

Ferjaoui, Z., López-Muñoz, R., Akbari, S., Chandad, F., Mantovani, D., Rouabhia, M., & D. Fanganiello, R. (2024). Design of Alginate/Gelatin Hydrogels for Biomedical Applications: Fine-Tuning Osteogenesis in Dental Pulp Stem Cells While Preserving Other Cell Behaviors. Biomedicines, 12(7), 1510. https://doi.org/10.3390/BIOMEDICINES12071510/S1

Fernández-Francos, S., Eiro, N., Costa, L. A., Escudero-Cernuda, S., Fernández-Sánchez, M. L., & Vizoso, F. J. (2021). Mesenchymal Stem Cells as a Cornerstone in a Galaxy of Intercellular Signals: Basis for a New Era of Medicine. International Journal of Molecular Sciences 2021, Vol. 22, Page 3576, 22(7), 3576. https://doi.org/10.3390/IJMS22073576

Ferragut, F., Vachetta, V. S., Troncoso, M. F., Rabinovich, G. A., & Elola, M. T. (2021). ALCAM/CD166: A pleiotropic mediator of cell adhesion, stemness and cancer progression. Cytokine & Growth Factor Reviews, 61, 27–37. https://doi.org/10.1016/J.CYTOGFR.2021.07.001

Fielding, A. K., Richards, S. M., Chopra, R., Lazarus, H. M., Litzow, M. R., Buck, G., Durrant, I. J., Luger, S. M., Marks, D. I., Franklin, I. M., McMillan, A. K., Tallman, M. S., Rowe, J. M., &

Goldstone, A. H. (2007). Outcome of 609 adults after relapse of acute lymphoblastic leukemia (ALL); an MRC UKALL12/ECOG 2993 study. Blood, 109(3), 944–950. https://doi.org/10.1182/BLOOD-2006-05-018192

Filipp, F. V., Li, C., & Boiko, A. D. (2019). CD271 is a molecular switch with divergent roles in melanoma and melanocyte development. Scientific Reports 2019 9:1, 9(1), 1–11. https://doi.org/10.1038/s41598-019-42773-y

Findeisen, L., Bolte, J., Vater, C., Petzold, C., Quade, M., Müller, L., Goodman, S. B., & Zwingenberger, S. (2021). Cell spheroids are as effective as single cells suspensions in the treatment of critical-sized bone defects. BMC Musculoskeletal Disorders, 22(1), 1–11. https://doi.org/10.1186/S12891-021-04264-Y/FIGURES/5

Fink, T., & Zachar, V. (2011). Adipogenic Differentiation of Human Mesenchymal Stem Cells. Methods in Molecular Biology, 698, 243–251. https://doi.org/10.1007/978-1-60761-999-4_19/FIGURES/1_19

Flores-Guzman, P., Fernandez-Sanchez, V., Valencia-Plata, I., Arriaga-Pizano, L., Alarcon-Santos, G., & Mayani, H. (2013). Comparative in vitro analysis of different hematopoietic cell populations from human cord blood: in search of the best option for clinically oriented ex vivo cell expansion. Transfusion, 53(3), 668–678. https://doi.org/10.1111/J.1537-2995.2012.03799.X

Fonseca, L. N., Bolívar-Moná, S., Agudelo, T., Beltrán, L. D., Camargo, D., Correa, N., Del Castillo, M. A., Fernández de Castro, S., Fula, V., García, G., Guarnizo, N., Lugo, V., Martínez, L. M., Melgar, V., Peña, M. C., Pérez, W. A., Rodríguez, N., Pinzón, A., Albarracín, S. L., … Gutiérrez-Gómez, M. L. (2023). Cell surface markers for mesenchymal stem cells related to the skeletal system: A scoping review. Heliyon, 9(2), e13464. https://doi.org/10.1016/J.HELIYON.2023.E13464

Fox, N., Priestley, G., Papayannopoulou, T., & Kaushansky, K. (2002). Thrombopoietin expands hematopoietic stem cells after transplantation. Journal of Clinical Investigation, 110(3), 389–394. https://doi.org/10.1172/JCI15430

Frantz, C., Stewart, K. M., & Weaver, V. M. (2010). The extracellular matrix at a glance. Journal of Cell Science, 123(24), 4195–4200. https://doi.org/10.1242/JCS.023820

Fratzl, P. (2008). Collagen: Structure and Mechanics, an Introduction. Collagen: Structure and Mechanics, 1–13. https://doi.org/10.1007/978-0-387-73906-9_1

Frith, J. E., Thomson, B., & Genever, P. G. (2010). Dynamic three-dimensional culture methods enhance mesenchymal stem cell properties and increase therapeutic potential. Tissue Engineering. Part C, Methods, 16(4), 735–749. https://doi.org/10.1089/TEN.TEC.2009.0432

Fry, L. J., Giner, S. Q., Gomez, S. G., Green, M., Anderson, S., Horder, J., McArdle, S., Rees, R., & Madrigal, J. A. (2013). Avoiding room temperature storage and delayed cryopreservation provide better postthaw potency in hematopoietic progenitor cell grafts. Transfusion, 53(8), 1834–1842. https://doi.org/10.1111/TRF.12006,

Gaafar, A., Hamza, F. N., Yousif, R., Shinwari, Z., Alotaibi, A. G., Iqniebi, A., Al-Hussein, K., Al-Mazrou, A., Manogaran, P. S., Elhassan, T., Marquez-Méndez, M., Aljurf, M., Al-Humaidan, H., & Alaiya, A. (2025). Distinct Phenotypic and Molecular Characteristics of CD34− and CD34+ Hematopoietic Stem/Progenitor Cell Subsets in Cord Blood and Bone Marrow Samples: Implications for Clinical Applications. Diagnostics, 15(4), 447. https://doi.org/10.3390/DIAGNOSTICS15040447/S1

Galgaro, B. C., Beckenkamp, L. R., van den M. Nunnenkamp, M., Korb, V. G., Naasani, L. I. S., Roszek, K., & Wink, M. R. (2021). The adenosinergic pathway in mesenchymal stem cell fate and functions. Medicinal Research Reviews, 41(4), 2316–2349. https://doi.org/10.1002/MED.21796

Gálvez, P., Martín, M. J., Calpena, A. C., Tamayo, J. A., Ruiz, M. A., & Clares, B. (2014). Enhancing effect of glucose microspheres in the viability of human mesenchymal stem cell suspensions for clinical administration. Pharmaceutical Research, 31(12), 3515–3528. https://doi.org/10.1007/S11095-014-1438-8,

Gálvez-Martín, P., Hmadcha, A., Soria, B., Calpena-Campmany, A. C., & Clares-Naveros, B. (2014). Study of the stability of packaging and storage conditions of human mesenchymal stem cell for intra-arterial clinical application in patient with critical limb ischemia. European Journal of Pharmaceutics and Biopharmaceutics, 86(3), 459–468. https://doi.org/10.1016/j.ejpb.2013.11.002

Ganachaud, C., Bernin, D., Isaksson, D., & Holmberg, K. (2013). An anomalous behavior of trypsin immobilized in alginate network. Applied Microbiology and Biotechnology, 97(10), 4403–4414. https://doi.org/10.1007/S00253-012-4333-4/FIGURES/8

Gang, E. J., Jeong, J. A., Hong, S. H., Hwang, S. H., Kim, S. W., Yang, I. H., Ahn, C., Han, H., & Kim, H. (2004). Skeletal myogenic differentiation of mesenchymal stem cells isolated from human umbilical cord blood. Stem Cells (Dayton, Ohio), 22(4), 617–624. https://doi.org/10.1634/STEMCELLS.22-4-617

Gao, D. Y., Chang, Q., Liu, C., Farris, K., Harvey, K., McGann, L. E., English, D., Jansen, J., & Critser, J. K. (1998). Fundamental Cryobiology of Human Hematopoietic Progenitor Cells I: Osmotic Characteristics and Volume Distribution. Cryobiology, 36(1), 40–48. https://doi.org/10.1006/cryo.1997.2060

Gao, X., Murphy, M. M., Peyer, J. G., Ni, Y., Yang, M., Zhang, Y., Guo, J., Kara, N., Embree, C., Tasdogan, A., Ubellacker, J. M., Crane, G. M., Fang, S., Zhao, Z., Shen, B., & Morrison, S. J. (2023). Leptin receptor+ cells promote bone marrow innervation and regeneration by synthesizing nerve growth factor. Nature Cell Biology 2023 25:12, 25(12), 1746–1757. https://doi.org/10.1038/s41556-023-01284-9

Ge, J., Guo, L., Wang, S., Zhang, Y., Cai, T., Zhao, R. C. H., & Wu, Y. (n.d.). The Size of Mesenchymal Stem Cells is a Significant Cause of Vascular Obstructions and Stroke. https://doi.org/10.1007/s12015-013-9492-x

Genovese, P., Schiroli, G., Escobar, G., Di Tomaso, T., Firrito, C., Calabria, A., Moi, D., Mazzieri, R., Bonini, C., Holmes, M. C., Gregory, P. D., Van Der Burg, M., Gentner, B., Montini, E., Lombardo, A., & Naldini, L. (2014). Targeted genome editing in human repopulating haematopoietic stem cells. Nature 2014 510:7504, 510(7504), 235–240. https://doi.org/10.1038/nature13420

Gionet-Gonzales, M. A., & Leach, J. K. (2018). Engineering principles for guiding spheroid function in the regeneration of bone, cartilage, and skin. Biomedical Materials, 13(3), 034109. https://doi.org/10.1088/1748-605X/AAB0B3

Glaser, D. E., Curtis, M. B., Sariano, P. A., Rollins, Z. A., Shergill, B. S., Anand, A., Deely, A. M., Shirure, V. S., Anderson, L., Lowen, J. M., Ng, N. R., Weilbaecher, K., Link, D. C., & George, S. C. (2022). Organ-on-a-chip model of vascularized human bone marrow niches. Biomaterials, 280, 121245. https://doi.org/10.1016/J.BIOMATERIALS.2021.121245

Gligor, D., Tan, A., & Nguyen, T. N. T. (2018). The obstacles to cold chain implementation in developing countries: insights from Vietnam. International Journal of Logistics Management, 29(3), 942–958. https://doi.org/10.1108/IJLM-02-2017-0026/FULL/XML

Glycolysis/OXPHOS Assay Kit G270 manual | DOJINDO. (n.d.). Retrieved January 22, 2026, from https://www.dojindo.com/manual/G270/

Goers, L., Freemont, P., & Polizzi, K. M. (2014). Co-culture systems and technologies: taking synthetic biology to the next level. Journal of the Royal Society Interface, 11(96). https://doi.org/10.1098/RSIF.2014.0065

Gokarn, A., Tembhare, P. R., Syed, H., Sanyal, I., Kumar, R., Parab, S., Khanka, T., Punatar, S., Kedia, S., Ghogale, S. G., Deshpande, N., Nikam, Y., Girase, K., Mirgh, S., Jindal, N., Bagal, B., Chichra, A., Nayak, L., Bonda, A., … Khattry, N. (2023). Long-Term Cryopreservation of Peripheral Blood Stem Cell Harvest Using Low Concentration (4.35%) Dimethyl Sulfoxide with Methyl Cellulose and Uncontrolled Rate Freezing at -80 °C: An Effective Option in Resource-Limited Settings. Transplantation and Cellular Therapy, 29, 777.e1-777.e8. https://doi.org/10.1016/j.jtct.2023.08.032

Gorodetsky, R., Levdansky, L., Gaberman, E., Gurevitch, O., Lubzens, E., & McBride, W. H. (2011). Fibrin microbeads loaded with mesenchymal cells support their long-term survival while sealed at room temperature. Tissue Engineering - Part C: Methods, 17(7), 745–755. https://doi.org/10.1089/TEN.TEC.2010.0644,

Gragert, L., Eapen, M., Williams, E., Freeman, J., Spellman, S., Baitty, R., Hartzman, R., Rizzo, J. D., Horowitz, M., Confer, D., & Maiers, M. (2014). HLA Match Likelihoods for Hematopoietic Stem-Cell Grafts in the U.S. Registry. New England Journal of Medicine, 371(4), 339–348. https://doi.org/10.1056/NEJMSA1311707/SUPPL_FILE/NEJMSA1311707_DISCLOSURES.PDF

GraphPad Prism 10 Statistics Guide - Choosing a normality test. (n.d.). Retrieved January 13, 2026, from https://www.graphpad.com/guides/prism/latest/statistics/stat_choosing_a_normality_test.htm

Griffin, K. H., Fok, S. W., & Kent Leach, J. (2022). Strategies to capitalize on cell spheroid therapeutic potential for tissue repair and disease modeling. Npj Regenerative Medicine 2022 7:1, 7(1), 1–13. https://doi.org/10.1038/s41536-022-00266-z

Grinenko, T., Arndt, K., Portz, M., Mende, N., Günther, M., Cosgun, K. N., Alexopoulou, D., Lakshmanaperumal, N., Henry, I., Dahl, A., & Waskow, C. (2014). Clonal expansion capacity defines two consecutive developmental stages of long-term hematopoietic stem cells. Journal of Experimental Medicine, 211(2), 209–215. https://doi.org/10.1084/JEM.20131115

Gryshkov, O., Pogozhykh, D., Hofmann, N., Pogozhykh, O., Mueller, T., & Glasmacher, B. (2014). Encapsulating Non-Human Primate Multipotent Stromal Cells in Alginate via High Voltage for Cell-Based Therapies and Cryopreservation. PLOS ONE, 9(9), e107911. https://doi.org/10.1371/JOURNAL.PONE.0107911

Guidi, N., Sacma, M., Ständker, L., Soller, K., Marka, G., Eiwen, K., Weiss, J. M., Kirchhoff, F., Weil, T., Cancelas, J. A., Florian, M. C., & Geiger, H. (2017). Osteopontin attenuates aging-associated phenotypes of hematopoietic stem cells. The EMBO Journal, 36(7), 840–853. https://doi.org/10.15252/EMBJ.201694969/SUPPL_FILE/EMBJ201694969-SUP-0004-MOVIEEV2.ZIP

Gunti, S., Hoke, A. T. K., Vu, K. P., & London, N. R. (2021). Organoid and Spheroid Tumor Models: Techniques and Applications. Cancers, 13(4), 1–18. https://doi.org/10.3390/CANCERS13040874

Guo, Q., He, Z., Jin, Y., Zhang, S., Wu, S., Bai, G., Xue, H., Liu, Z., Jin, S., Zhao, L., & Wang, J. (2018). Tuning Ice Nucleation and Propagation with Counterions on Multilayer Hydrogels. Langmuir, 34(40), 11986–11991. https://doi.org/10.1021/ACS.LANGMUIR.8B02106/ASSET/IMAGES/LARGE/LA-2018-02106S_0004.JPEG

Gurruchaga, H., Saenz del Burgo, L., Hernandez, R. M., Orive, G., Selden, C., Fuller, B., Ciriza, J., & Pedraz, J. L. (2018). Advances in the slow freezing cryopreservation of microencapsulated cells. Journal of Controlled Release, 281, 119–138. https://doi.org/10.1016/J.JCONREL.2018.05.016

Halfter, K., Hoffmann, O., Ditsch, N., Ahne, M., Arnold, F., Paepke, S., Grab, D., Bauerfeind, I., & Mayer, B. (2016). Testing chemotherapy efficacy in HER2 negative breast cancer using patient-derived spheroids. Journal of Translational Medicine, 14(1), 112. https://doi.org/10.1186/S12967-016-0855-3

Hancock, M. J., Piraino, F., Camci-Unal, G., Rasponi, M., & Khademhosseini, A. (2011). Anisotropic material synthesis by capillary flow in a fluid stripe. Biomaterials, 32(27), 6493–6504. https://doi.org/10.1016/J.BIOMATERIALS.2011.05.057

Handorf, A. M., Zhou, Y., Halanski, M. A., & Li, W. J. (2015). Tissue Stiffness Dictates Development, Homeostasis, and Disease Progression. Organogenesis, 11(1), 1. https://doi.org/10.1080/15476278.2015.1019687

Haynes, B. F., Telen, M. J., Hale, L. P., & Denning, S. M. (1989). CD44 - A molecule involved in leukocyte adherence and T-cell activation. Immunology Today, 10(12), 423–428. https://doi.org/10.1016/0167-5699(89)90040-6

Hazrati, A., Malekpour, K., Soudi, S., & Hashemi, S. M. (2022). Mesenchymal stromal/stem cells spheroid culture effect on the therapeutic efficacy of these cells and their exosomes: A new strategy to overcome cell therapy limitations. Biomedicine & Pharmacotherapy, 152, 113211. https://doi.org/10.1016/J.BIOPHA.2022.113211

He, S., Nakada, D., & Morrison, S. J. (2009). Mechanisms of stem cell self-renewal. Annual Review of Cell and Developmental Biology, 25, 377–406. https://doi.org/10.1146/ANNUREV.CELLBIO.042308.113248

He, Y., & Zou, L. (2019). Notch-1 inhibition reduces proliferation and promotes osteogenic differentiation of bone marrow mesenchymal stem cells. Experimental and Therapeutic Medicine, 18(3), 1884. https://doi.org/10.3892/ETM.2019.7765

He, Z., Wu, C., Hua, M., Wu, S., Wu, D., Zhu, X., Wang, J., & He, X. (2020). Bioinspired Multifunctional Anti-icing Hydrogel. Matter, 2(3), 723–734. https://doi.org/10.1016/J.MATT.2019.12.017

Healy, L., May, G., Gale, K., Grosveld, F., Greaves, M., & Enver, T. (1995). The stem cell antigen CD34 functions as a regulator of hemopoietic cell adhesion. Proceedings of the National Academy of Sciences, 92(26), 12240–12244. https://doi.org/10.1073/PNAS.92.26.12240

Heazlewood, S. Y., Neaves, R. J., Williams, B., Haylock, D. N., Adams, T. E., & Nilsson, S. K. (2013). Megakaryocytes co-localise with hemopoietic stem cells and release cytokines that up-

regulate stem cell proliferation. Stem Cell Research, 11(2), 782–792. https://doi.org/10.1016/J.SCR.2013.05.007

Hejbøl, E. K., Sellathurai, J., Nair, P. D., & Schrøder, H. D. (2017). Injectable scaffold materials differ in their cell instructive effects on primary human myoblasts. Journal of Tissue Engineering, 8. https://doi.org/10.1177/2041731417717677/ASSET/2F7A548A-E94C-4E9C-B405-97524F0C673E/ASSETS/IMAGES/LARGE/10.1177_2041731417717677-FIG4.JPG

Hemler, M. E. (1990). VLA proteins in the integrin family: structures, functions, and their role on leukocytes. Annual Review of Immunology, 8(1), 365–400. https://doi.org/10.1146/ANNUREV.IY.08.040190.002053

Heng, B. C., Zhang, X., Aubel, D., Bai, Y., Li, X., Wei, Y., Fussenegger, M., & Deng, X. (2020). Role of YAP/TAZ in Cell Lineage Fate Determination and Related Signaling Pathways. Frontiers in Cell and Developmental Biology, 8, 735. https://doi.org/10.3389/FCELL.2020.00735

Hermida-Gómez, T., Fuentes-Boquete, I., Gimeno-Longas, M. J., Muiños-López, E., Díaz-Prado, S., De Toro, F. J., & Blanco, F. J. (2011). Bone Marrow Cells Immunomagnetically Selected For CD271+ Antigen Promote In Vitro the Repair of Articular Cartilage Defects. Https://Home.Liebertpub.Com/Tea, 17(7–8), 1169–1179. https://doi.org/10.1089/TEN.TEA.2010.0346

Hidalgo, I., Wahlestedt, M., Yuan, O., Zhang, Q., Bryder, D., & Pronk, C. J. (2022). Bmi1 induction protects hematopoietic stem cells against pronounced long-term hematopoietic stress. Experimental Hematology, 109, 35–44. https://doi.org/10.1016/J.EXPHEM.2022.02.004

Ho, A. D., Haas, R., & Champlin, R. E. (2000). Hematopoietic Stem Cell Transplantation. Hematopoietic Stem Cell Transplantation, 1–604. https://doi.org/10.5339/qmj.2007.2.7

Ho, S. S., Keown, A. T., Addison, B., & Leach, J. K. (2017). Cell Migration and Bone Formation from Mesenchymal Stem Cell Spheroids in Alginate Hydrogels Are Regulated by Adhesive Ligand Density. Biomacromolecules, 18(12), 4331–4340. https://doi.org/10.1021/ACS.BIOMAC.7B01366/SUPPL_FILE/BM7B01366_SI_002.AVI

Ho, S. S., Murphy, K. C., Binder, B. Y. K., Vissers, C. B., & Leach, J. K. (2016). Increased Survival and Function of Mesenchymal Stem Cell Spheroids Entrapped in Instructive Alginate Hydrogels. Stem Cells Translational Medicine, 5(6), 773–781. https://doi.org/10.5966/SCTM.2015-0211

Ho, S. T. B., Cool, S. M., Hui, J. H., & Hutmacher, D. W. (2010). The influence of fibrin based hydrogels on the chondrogenic differentiation of human bone marrow stromal cells. Biomaterials, 31(1), 38–47. https://doi.org/10.1016/J.BIOMATERIALS.2009.09.021

Hoban, M. D., Cost, G. J., Mendel, M. C., Romero, Z., Kaufman, M. L., Joglekar, A. V., Ho, M., Lumaquin, D., Gray, D., Lill, G. R., Cooper, A. R., Urbinati, F., Senadheera, S., Zhu, A., Liu, P. Q., Paschon, D. E., Zhang, L., Rebar, E. J., Wilber, A., … Kohn, D. B. (2015). Correction of the sickle cell disease mutation in human hematopoietic stem/progenitor cells. Blood, 125(17), 2597–2604. https://doi.org/10.1182/BLOOD-2014-12-615948

Holyoake, T. L., Jiang, X., Jorgensen, H. G., Graham, S., Alcorn, M. J., Laird, C., Eaves, A. C., & Eaves, C. J. (2001). Primitive quiescent leukemic cells from patients with chronic myeloid leukemia spontaneously initiate factor-independent growth in vitro in association with up-regulation of expression of interleukin-3. Blood, 97(3), 720–728. https://doi.org/10.1182/blood.V97.3.720

Hooker, R. A., Chitteti, B. R., Egan, P. H., Cheng, Y. H., Himes, E. R., Meijome, T., Srour, E. F., Fuchs, R. K., & Kacena, M. A. (2015). Activated leukocyte cell adhesion molecule (ALCAM or CD166) modulates bone phenotype and hematopoiesis. Journal of Musculoskeletal & Neuronal Interactions, 15(1), 83. https://pmc.ncbi.nlm.nih.gov/articles/PMC4439374/

Hornberger, K., Yu, G., McKenna, D., & Hubel, A. (2019). Cryopreservation of Hematopoietic Stem Cells: Emerging Assays, Cryoprotectant Agents, and Technology to Improve Outcomes. Transfusion Medicine and Hemotherapy, 46(3), 188. https://doi.org/10.1159/000496068

Huang, W., Hickson, L. T. J., Eirin, A., Kirkland, J. L., & Lerman, L. O. (2022). Cellular senescence: the good, the bad and the unknown. Nature Reviews Nephrology 2022 18:10, 18(10), 611–627. https://doi.org/10.1038/s41581-022-00601-z

Hubrecht, R. C., & Carter, E. (2019). The 3Rs and Humane Experimental Technique: Implementing Change. Animals : An Open Access Journal from MDPI, 9(10). https://doi.org/10.3390/ANI9100754

Huebsch, N., Arany, P. R., Mao, A. S., Shvartsman, D., Ali, O. A., Bencherif, S. A., Rivera-Feliciano, J., & Mooney, D. J. (2010). Harnessing traction-mediated manipulation of the cell/matrix interface to control stem-cell fate. Nature Materials, 9(6), 518–526. https://doi.org/10.1038/NMAT2732,

Human Colony-Forming Unit (CFU) Assays Using MethoCult™. (n.d.). Retrieved January 17, 2025, from https://www.stemcell.com/media/files/manual/MA28404-Human_Colony_Forming_Unit_Assays_Using_MethoCult.pdf

Human Long-Term Culture-Initiating Cell (LTC-IC) Assays. (n.d.). Retrieved January 17, 2025, from https://cdn.stemcell.com/media/files/manual/10000005591-MAN_00.pdf

Hunt, L., Hacker, D. L., Grosjean, F., De Jesus, M., Uebersax, L., Jordan, M., & Wurm, F. M. (2005). Low-temperature pausing of cultivated mammalian cells. Biotechnology and Bioengineering, 89(2), 157–163. https://doi.org/10.1002/BIT.20320,

Hunt, N. (1988). An alginate hydrogel matrix for the localised delivery of a fibroblast/ keratinocyte co-culture to expedite wound healing.

Ikonomi, N., Kühlwein, S. D., Schwab, J. D., & Kestler, H. A. (2020). Awakening the HSC: Dynamic Modeling of HSC Maintenance Unravels Regulation of the TP53 Pathway and Quiescence. Frontiers in Physiology, 11, 557667. https://doi.org/10.3389/FPHYS.2020.00848/XML/NLM

Inaba, K. , Z. D. , Y. B. , V. I. , & S. A. M. (1996). Normalization of diabetes by xenotransplantation of cryopreserved microencapsulated pancreatic islets: Application of a new strategy in islet banking. Transplantation , 61(2), 175–178. https://journals.lww.com/transplantjournal/fulltext/1996/01270/NORMALIZATION_OF_DIABETES_BY_XENOTRANSPLANTATION.1.aspx

Iriuchishima, H., Takubo, K., Matsuoka, S., Onoyama, I., Nakayama, K. I., Nojima, Y., & Suda, T. (2011). Ex vivo maintenance of hematopoietic stem cells by quiescence induction through Fbxw7α overexpression. Blood, 117(8), 2373–2377. https://doi.org/10.1182/BLOOD-2010-07-294801

Isaacson, A., Swioklo, S., & Connon, C. J. (2018). 3D bioprinting of a corneal stroma equivalent. Experimental Eye Research, 173, 188–193. https://doi.org/10.1016/J.EXER.2018.05.010

Itkin, T., Gur-Cohen, S., Spencer, J. A., Schajnovitz, A., Ramasamy, S. K., Kusumbe, A. P., Ledergor, G., Jung, Y., Milo, I., Poulos, M. G., Kalinkovich, A., Ludin, A., Kollet, O., Shakhar, G., Butler, J.

M., Rafii, S., Adams, R. H., Scadden, D. T., Lin, C. P., & Lapidot, T. (2016). Distinct bone marrow blood vessels differentially regulate haematopoiesis. Nature 2016 532:7599, 532(7599), 323–328. https://doi.org/10.1038/nature17624

Jahandideh, B., Derakhshani, M., Abbaszadeh, H., Akbar Movassaghpour, A., Mehdizadeh, A., Talebi, M., & Yousefi, M. (2020). The pro-Inflammatory cytokines effects on mobilization, self-renewal and differentiation of hematopoietic stem cells. Human Immunology, 81(5), 206–217. https://doi.org/10.1016/J.HUMIMM.2020.01.004

Jahangir, S., Eglin, D., Pötter, N., Khozaei Ravari, M., Stoddart, M. J., Samadikuchaksaraei, A., Alini, M., Baghaban Eslaminejad, M., & Safa, M. (2020). Inhibition of hypertrophy and improving chondrocyte differentiation by MMP-13 inhibitor small molecule encapsulated in alginate-chondroitin sulfate-platelet lysate hydrogel. Stem Cell Research and Therapy, 11(1). https://doi.org/10.1186/S13287-020-01930-1,

Jain, M., Rajan, R., Hyon, S. H., & Matsumura, K. (2014). Hydrogelation of dextran-based polyampholytes with cryoprotective properties via click chemistry. Biomaterials Science, 2(3), 308–317. https://doi.org/10.1039/C3BM60261C

Jaiswal, S. (2020). Clonal hematopoiesis and nonhematologic disorders. Blood, 136(14), 1606. https://doi.org/10.1182/BLOOD.2019000989

Jaiswal, S., & Ebert, B. L. (2019). Clonal hematopoiesis in human aging and disease. Science, 366(6465). https://doi.org/10.1126/SCIENCE.AAN4673

Jaiswal, S., Fontanillas, P., Flannick, J., Manning, A., Grauman, P. V., Mar, B. G., Lindsley, R. C., Mermel, C. H., Burtt, N., Chavez, A., Higgins, J. M., Moltchanov, V., Kuo, F. C., Kluk, M. J., Henderson, B., Kinnunen, L., Koistinen, H. A., Ladenvall, C., Getz, G., … Ebert, B. L. (2014). Age-Related Clonal Hematopoiesis Associated with Adverse Outcomes. The New England Journal of Medicine, 371(26), 2488. https://doi.org/10.1056/NEJMOA1408617

Jalkanen, S. T., Bargatze, R. F., Herron, L. R., & Butcher, E. C. (1986). A lymphoid cell surface glycoprotein involved in endothelial cell recognition and lymphocyte homing in man. European Journal of Immunology, 16(10), 1195–1202. https://doi.org/10.1002/EJI.1830161003

Jeannet, R., Cai, Q., Liu, H., Vu, H., & Kuo, Y. H. (2013). Alcam Regulates Long-term Hematopoietic Stem Cell Engraftment and Self-Renewal. Stem Cells (Dayton, Ohio), 31(3), 10.1002/stem.1309. https://doi.org/10.1002/STEM.1309

Jeong, C., Kim, S., Lee, C., Cho, S., & Kim, S. B. (2020). Changes in the Physical Properties of Calcium Alginate Gel Beads under a Wide Range of Gelation Temperature Conditions. Foods, 9(2). https://doi.org/10.3390/FOODS9020180

Jin, D., Zhang, R., Chen, H., & Li, C. (2020). Aberrantly glycosylated integrin α3β1 is a unique urinary biomarker for the diagnosis of bladder cancer. Aging (Albany NY), 12(11), 10844. https://doi.org/10.18632/AGING.103297

Jin, H. J., Park, S. K., Oh, W., Yang, Y. S., Kim, S. W., & Choi, S. J. (2009). Down-regulation of CD105 is associated with multi-lineage differentiation in human umbilical cord blood-derived mesenchymal stem cells. Biochemical and Biophysical Research Communications, 381(4), 676–681. https://doi.org/10.1016/j.bbrc.2009.02.118

Jing, D., Fonseca, A. V., Alakel, N., Fierro, F. A., Muller, K., Bornhauser, M., Ehninger, G., Corbeil, D., & Ordemann, R. (2010). Hematopoietic stem cells in co-culture with mesenchymal stromal cells - modeling the niche compartments in vitro. Haematologica, 95(4), 542–550. https://doi.org/10.3324/HAEMATOL.2009.010736

Johannsen, H., Godthardt, K., Schreiner, C., Völkel, A., Noack, K., Jüngerkes, F., Barth, C., Mockel-Tenbrinck, N., Schult, S., Eckardt, D., Bosio, A., & Knöbel, S. (2016). An animal component-free, chemically defined media formulation for cryopreservation ensuring high cell recovery and viability.

Johnstone, B., Hering, T. M., Caplan, A. I., Goldberg, V. M., & Yoo, J. U. (1998). In vitro chondrogenesis of bone marrow-derived mesenchymal progenitor cells. Experimental Cell Research, 238(1), 265–272. https://doi.org/10.1006/EXCR.1997.3858

Johnstone, R. M., Adam, M., Hammond, J. R., Orr, L., & Turbide, C. (1987). Vesicle formation during reticulocyte maturation. Association of plasma membrane activities with released vesicles (exosomes). Journal of Biological Chemistry, 262(19), 9412–9420. https://doi.org/10.1016/s0021-9258(18)48095-7

Jones, E. A., Kinsey, S. E., English, A., Jones, R. A., Straszynski, L., Meredith, D. M., Markham, A. F., Jack, A., Emery, P., & McGonagle, D. (2002). Isolation and characterization of bone marrow multipotential mesenchymal progenitor cells. Arthritis & Rheumatism, 46(12), 3349–3360. https://doi.org/10.1002/ART.10696

Joshkon, A., Heim, X., Dubrou, C., Bachelier, R., Traboulsi, W., Stalin, J., Fayyad-Kazan, H., Badran, B., Foucault-Bertaud, A., Leroyer, A. S., Bardin, N., & Blot-Chabaud, M. (2020). Role of CD146 (MCAM) in Physiological and Pathological Angiogenesis—Contribution of New Antibodies for Therapy. Biomedicines, 8(12), 633. https://doi.org/10.3390/BIOMEDICINES8120633

Jung, Y., Wang, J., Schneider, A., Sun, Y. X., Koh-Paige, A. J., Osman, N. I., McCauley, L. K., & Taichman, R. S. (2006). Regulation of SDF-1 (CXCL12) production by osteoblasts; a possible mechanism for stem cell homing. Bone, 38(4), 497–508. https://doi.org/10.1016/J.BONE.2005.10.003

K., S., Y., L., H., W., T., L., M., F., F., S., HM., M., X., M., & Z., C. (2011). Ex vivo expansion of human umbilical cord blood hematopoietic stem/progenitor cells with support of microencapsulated rabbit mesenchymal stem cells in a rotating bioreactor. Tissue Engineering and Regenerative Medicine, 8, 334–345.

Kaltostat Sterile Alginate Haemostatic Dressing - MedicalDressings. (n.d.). Retrieved January 7, 2026, from https://medicaldressings.co.uk/kaltostat-sterile-alginate-haemostatic-dressing/

Kamprom, W., Tangporncharoen, R., Vongthaiwan, N., Tragoonlugkana, P., Phetfong, J., Pruksapong, C., & Supokawej, A. (2024). Enhanced potent immunosuppression of intracellular adipose tissue-derived stem cell extract by priming with three-dimensional spheroid formation. Scientific Reports, 14(1), 1–15. https://doi.org/10.1038/S41598-024-59910-X;SUBJMETA=250,532,631,80;KWRD=CELL+BIOLOGY,IMMUNOLOGY,STEM+CELLS

Kanczler, J. M., Ginty, P. J., White, L., Clarke, N. M. P., Howdle, S. M., Shakesheff, K. M., & Oreffo, R. O. C. (2010). The effect of the delivery of vascular endothelial growth factor and bone morphogenic protein-2 to osteoprogenitor cell populations on bone formation. Biomaterials, 31(6), 1242–1250. https://doi.org/10.1016/j.biomaterials.2009.10.059

Kapałczyńska, M., Kolenda, T., Przybyła, W., Zajączkowska, M., Teresiak, A., Filas, V., Ibbs, M., Bliźniak, R., Łuczewski, Ł., & Lamperska, K. (2016). 2D and 3D cell cultures – a comparison of

different types of cancer cell cultures. Archives of Medical Science : AMS, 14(4), 910. https://doi.org/10.5114/AOMS.2016.63743

Karsunky, H., Merad, M., Cozzio, A., Weissman, I. L., & Manz, M. G. (2003). Flt3 Ligand Regulates Dendritic Cell Development from Flt3+ Lymphoid and Myeloid-committed Progenitors to Flt3+ Dendritic Cells In Vivo. The Journal of Experimental Medicine, 198(2), 305. https://doi.org/10.1084/JEM.20030323

Kasow, K. A., Sims-Poston, L., Eldridge, P., & Hale, G. A. (2007). CD34+ Hematopoietic Progenitor Cell Selection of Bone Marrow Grafts for Autologous Transplantation in Pediatric Patients. Biology of Blood and Marrow Transplantation, 13(5), 608–614. https://doi.org/10.1016/j.bbmt.2007.01.074

Kaushansky, K. (2009). Thrombopoietin. Http://Dx.Doi.Org/10.1056/NEJM199809103391107, 339(11), 746–754. https://doi.org/10.1056/NEJM199809103391107

Kavand, A., Noverraz, F., & Gerber-Lemaire, S. (2024). Recent Advances in Alginate-Based Hydrogels for Cell Transplantation Applications. Pharmaceutics 2024, Vol. 16, Page 469, 16(4), 469. https://doi.org/10.3390/PHARMACEUTICS16040469

Key, J. A., & Ball, D. W. (2014). Introductory Chemistry- 1st Canadian Edition. https://ecampusontario.pressbooks.pub/introductorychemistry/chapter/electron-transfer-ionic-bonds-2/

Khaddour, K., Hana, C., & Mewawalla Prerna. (2023). Hematopoietic Stem Cell Transplantation. Scleroderma: From Pathogenesis to Comprehensive Management, 657–664. https://doi.org/10.1007/978-3-031-40658-4_43

Khaldoyanidi, S. K., Hindoyan, A., Stein, A., & Subklewe, M. (2022). Leukemic stem cells as a target for eliminating acute myeloid leukemia: Gaps in translational research. Critical Reviews in Oncology/Hematology, 175, 103710. https://doi.org/10.1016/J.CRITREVONC.2022.103710

Khavari, A., Nydén, M., Weitz, D. A., & Ehrlicher, A. J. (2016). Composite alginate gels for tunable cellular microenvironment mechanics. Scientific Reports, 6(1), 1–11. https://doi.org/10.1038/SREP30854;TECHMETA=14;SUBJMETA=2268,301,54,57,631,639;KWRD=BIOMATERIALS,BIOPOLYMERS+IN+VIVO

Kim, D., Kim, J., Yoon, J. H., Ghim, J., Yea, K., Song, P., Park, Soyeon, Lee, A., Hong, C. P., Jang, M. S., Kwon, Y., Park, Sehoon, Jang, M. H., Berggren, P. O., Suh, P. G., & Ryu, S. H. (2014). CXCL12 secreted from adipose tissue recruits macrophages and induces insulin resistance in mice. Diabetologia, 57(7), 1456–1465. https://doi.org/10.1007/S00125-014-3237-5

Kim, J., & Adachi, T. (2021). Cell-fate decision of mesenchymal stem cells toward osteocyte differentiation is committed by spheroid culture. Scientific Reports, 11(1), 1–11. https://doi.org/10.1038/S41598-021-92607-Z;SUBJMETA=1360,2074,2139,532,631;KWRD=MESENCHYMAL+STEM+CELLS,STEM-CELL+DIFFERENTIATION,STEM-CELL+NICHE

Kim, S. jeong, Byun, H., Lee, S., Kim, E., Lee, G. M., Huh, S. J., Joo, J., & Shin, H. (2022). Spatially arranged encapsulation of stem cell spheroids within hydrogels for the regulation of spheroid fusion and cell migration. Acta Biomaterialia, 142, 60–72. https://doi.org/10.1016/j.actbio.2022.01.047

King, K. Y., & Goodell, M. A. (2011). Inflammatory modulation of HSCs: viewing the HSC as a foundation for the immune response. Nature Reviews Immunology 2011 11:10, 11(10), 685–692. https://doi.org/10.1038/nri3062

King, K. Y., Huang, Y., Nakada, D., & Goodell, M. A. (2019). Environmental Influences on Clonal Hematopoiesis. Experimental Hematology, 83, 66. https://doi.org/10.1016/J.EXPHEM.2019.12.005

Kisselbach, L., Merges, M., Bossie, A., & Boyd, A. (2009). CD90 expression on human primary cells and elimination of contaminating fibroblasts from cell cultures. Cytotechnology, 59(1), 31–44. https://doi.org/10.1007/S10616-009-9190-3/TABLES/6

Kobayashi, H., Morikawa, T., Okinaga, A., Suematsu, M., Shimizu, T., & Correspondence, K. T. (2019). Environmental Optimization Enables Maintenance of Quiescent Hematopoietic Stem Cells Ex Vivo. Cell Reports, 28, 145–158. https://doi.org/10.1016/j.celrep.2019.06.008

Kostenko, A., Connon, C. J., & Swioklo, S. (2023). Storable Cell-Laden Alginate Based Bioinks for 3D Biofabrication. Bioengineering, 10(1), 23. https://doi.org/10.3390/BIOENGINEERING10010023/S1

Koudy Williams, J., Mariya, S., & Suparto, I. (2017). Gender, age and differences in stem cell expression and efficacy. Journal of Stem Cell Research & Therapeutics, Volume 3(Issue 2). https://doi.org/10.15406/JSRT.2017.03.00097

Kouroupis, D., & Correa, D. (2021). Increased Mesenchymal Stem Cell Functionalization in Three-Dimensional Manufacturing Settings for Enhanced Therapeutic Applications. Frontiers in Bioengineering and Biotechnology, 9, 621748. https://doi.org/10.3389/FBIOE.2021.621748

Krampera, M., Franchini, M., Pizzolo, G., & Aprili, G. (2007). Mesenchymal stem cells: from biology to clinical use. Blood Transfusion, 5(3), 120. https://doi.org/10.2450/2007.0029-07

Krasnova, O., Kovaleva, A., Saveleva, A., Kulakova, K., Bystrova, O., Martynova, M., Domnina, A., Sopova, J., & Neganova, I. (2023). Mesenchymal stem cells lose the senescent phenotype under 3D cultivation. Stem Cell Research and Therapy, 14(1), 1–19. https://doi.org/10.1186/S13287-023-03599-8/FIGURES/6

Krause, D. S., Fackler, M. J., Civin, C. I., & Stratford May, W. (1996). CD34: structure, biology, and clinical utility [see comments]. Blood, 87(1), 1–13. https://doi.org/10.1182/BLOOD.V87.1.1.1

Kristensen, J. H., & Karsdal, M. A. (2016). Elastin. Biochemistry of Collagens, Laminins and Elastin: Structure, Function and Biomarkers, 197–201. https://doi.org/10.1016/B978-0-12-809847-9.00030-1

Kruse, A., Abdel-Azim, N., Kim, H. N., Ruan, Y., Phan, V., Ogana, H., Wang, W., Lee, R., Gang, E. J., Khazal, S., & Kim, Y. M. (2020). Minimal Residual Disease Detection in Acute Lymphoblastic Leukemia. International Journal of Molecular Sciences, 21(3), 1054. https://doi.org/10.3390/IJMS21031054

Kuçi, S., Kuçi, Z., Kreyenberg, H., Deak, E., Pütsch, K., Huenecke, S., Amara, C., Koller, S., Rettinger, E., Grez, M., Koehl, U., Latifi-Pupovci, H., Henschler, R., Tonn, T., von Laer, D., Klingebiel, T., & Bader, P. (2010). CD271 antigen defines a subset of multipotent stromal cells with immunosuppressive and lymphohematopoietic engraftment-promoting properties. Haematologica, 95(4), 651. https://doi.org/10.3324/HAEMATOL.2009.015065

Kumar, M. A., Baba, S. K., Sadida, H. Q., Marzooqi, S. Al, Jerobin, J., Altemani, F. H., Algehainy, N., Alanazi, M. A., Abou-Samra, A. B., Kumar, R., Al-Shabeeb Akil, A. S., Macha, M. A., Mir, R., &

Bhat, A. A. (2024). Extracellular vesicles as tools and targets in therapy for diseases. Signal Transduction and Targeted Therapy 2024 9:1, 9(1), 1–41. https://doi.org/10.1038/s41392-024-01735-1

Kumar, S., & Geiger, H. (2017). HSC Niche Biology and HSC Expansion Ex Vivo. Trends in Molecular Medicine, 23(9), 799–819. https://doi.org/10.1016/J.MOLMED.2017.07.003/ASSET/163E58C1-169F-4D3F-8C98-A4AE58658228/MAIN.ASSETS/GR3.JPG

Kunisaki, Y., Bruns, I., Scheiermann, C., Ahmed, J., Pinho, S., Zhang, D., Mizoguchi, T., Wei, Q., Lucas, D., Ito, K., Mar, J. C., Bergman, A., & Frenette, P. S. (2013). Arteriolar niches maintain haematopoietic stem cell quiescence. Nature, 502(7473), 637–643. https://doi.org/10.1038/nature12612

Kuroda, Y., Kitada, M., Wakao, S., Nishikawa, K., Tanimura, Y., Makinoshima, H., Goda, M., Akashi, H., Inutsuka, A., Niwa, A., Shigemoto, T., Nabeshima, Y., Nakahata, T., Nabeshima, Y. I., Fujiyoshi, Y., & Dezawa, M. (2010). Unique multipotent cells in adult human mesenchymal cell populations. Proceedings of the National Academy of Sciences of the United States of America, 107(19), 8639–8643. https://doi.org/10.1073/PNAS.0911647107/SUPPL_FILE/PNAS.200911647SI.PDF

Labour-Party-manifesto-2024. (n.d.).

Lamanuzzi, A., Saltarella, I., Frassanito, M. A., Ribatti, D., Melaccio, A., Desantis, V., Solimando, A. G., Ria, R., & Vacca, A. (2021). Thrombopoietin Promotes Angiogenesis and Disease Progression in Patients with Multiple Myeloma. The American Journal of Pathology, 191(4), 748–758. https://doi.org/10.1016/J.AJPATH.2020.12.016

Laurenti, E., Frelin, C., Xie, S., Ferrari, R., Dunant, C. F., Zandi, S., Neumann, A., Plumb, I., Doulatov, S., Chen, J., April, C., Fan, J. B., Iscove, N., & Dick, J. E. (2015). CDK6 levels regulate quiescence exit in human hematopoietic stem cells. Cell Stem Cell, 16(3), 302–313. https://doi.org/10.1016/j.stem.2015.01.017

Laurenti, E., & Göttgens, B. (2018). From haematopoietic stem cells to complex differentiation landscapes. Nature, 553(7689), 418. https://doi.org/10.1038/NATURE25022

Lee, J. Y., & Hong, S. H. (2020). Hematopoietic Stem Cells and Their Roles in Tissue Regeneration. International Journal of Stem Cells, 13(1), 1. https://doi.org/10.15283/IJSC19127

Lee, K. Y., & Mooney, D. J. (2001). Hydrogels for tissue engineering. Chemical Reviews, 101(7), 1869–1879. https://doi.org/10.1021/CR000108X/ASSET/CR000108X.FP.PNG_V03

Lee, K. Y., & Mooney, D. J. (2012). Alginate: properties and biomedical applications. Progress in Polymer Science, 37(1), 106. https://doi.org/10.1016/J.PROGPOLYMSCI.2011.06.003

Lee, S., Kim, H. S., Min, B. H., Kim, B. G., Kim, S. A., Nam, H., Lee, M., Kim, M., Hwang, H. Y., Leesong, A. I., Leesong, M. M., Kim, J. H., & Shin, J. S. (2021). Enhancement of anti-inflammatory and immunomodulatory effects of adipose-derived human mesenchymal stem cells by making uniform spheroid on the new nano-patterned plates. Biochemical and Biophysical Research Communications, 552, 164–169. https://doi.org/10.1016/J.BBRC.2021.03.026

Lee, S., Kim, S., Kim, H., Baek, E. J., Jin, H., Kim, J., & Kim, H. O. (2008). Post-thaw viable CD34+ cell count is a valuable predictor of haematopoietic stem cell engraftment in autologous

peripheral blood stem cell transplantation. Vox Sanguinis, 94(2), 146–152. https://doi.org/10.1111/J.1423-0410.2007.01009.X,

Lee, S., Tong, X., & Yang, F. (2014). The effects of varying poly(ethylene glycol) hydrogel crosslinking density and the crosslinking mechanism on protein accumulation in three-dimensional hydrogels. Acta Biomaterialia, 10(10), 4167–4174. https://doi.org/10.1016/J.ACTBIO.2014.05.023

Lee-Six, H., Øbro, N. F., Shepherd, M. S., Grossmann, S., Dawson, K., Belmonte, M., Osborne, R. J., Huntly, B. J. P., Martincorena, I., Anderson, E., O'Neill, L., Stratton, M. R., Laurenti, E., Green, A. R., Kent, D. G., & Campbell, P. J. (2018). Population dynamics of normal human blood inferred from somatic mutations. Nature 2018 561:7724, 561(7724), 473–478. https://doi.org/10.1038/s41586-018-0497-0

Lee-Thedieck, C., Rauch, N., Fiammengo, R., Klein, G., & Spatz, J. P. (2012). Impact of substrate elasticity on human hematopoietic stem and progenitor cell adhesion and motility. Journal of Cell Science, 125(16), 3765–3775. https://doi.org/10.1242/JCS.095596/258417/AM/IMPACT-OF-SUBSTRATE-ELASTICITY-ON-HUMAN

Leipzig, N. D., & Shoichet, M. S. (2009). The effect of substrate stiffness on adult neural stem cell behavior. Biomaterials, 30(36), 6867–6878. https://doi.org/10.1016/J.BIOMATERIALS.2009.09.002

Leisten, I., Kramann, R., Ventura Ferreira, M. S., Bovi, M., Neuss, S., Ziegler, P., Wagner, W., Knüchel, R., & Schneider, R. K. (2012). 3D co-culture of hematopoietic stem and progenitor cells and mesenchymal stem cells in collagen scaffolds as a model of the hematopoietic niche. Biomaterials, 33(6), 1736–1747. https://doi.org/10.1016/J.BIOMATERIALS.2011.11.034

Lessard, J., & Hoang, T. (2016). Myelopoiesis. Encyclopedia of Immunobiology, 1, 26–37. https://doi.org/10.1016/B978-0-12-374279-7.01004-3

Levorson, E. J., Santoro, M., Kurtis Kasper, F., & Mikos, A. G. (2014). Direct and indirect co-culture of chondrocytes and mesenchymal stem cells for the generation of polymer/extracellular matrix hybrid constructs. Acta Biomaterialia, 10(5), 1824–1835. https://doi.org/10.1016/j.actbio.2013.12.026

Li, J., Carrillo García, C., Riedt, T., Brandes, M., Szczepanski, S., Brossart, P., Wagner, W., & Janzen, V. (2018). Murine hematopoietic stem cell reconstitution potential is maintained by osteopontin during aging. Scientific Reports 2018 8:1, 8(1), 1–9. https://doi.org/10.1038/s41598-018-21324-x

Li, T., Luo, C., Zhang, J., Wei, L., Sun, W., Xie, Q., Liu, Y., Zhao, Y., Xu, S., & Wang, L. (2021). Efficacy and safety of mesenchymal stem cells co-infusion in allogeneic hematopoietic stem cell transplantation: a systematic review and meta-analysis. Stem Cell Research and Therapy, 12(1), 1–22. https://doi.org/10.1186/S13287-021-02304-X/TABLES/6

Li, W., Wang, C., Zhang, M., Wu, J., Gu, Y., Deng, Y., Wang, J., Zhang, X., Feng, J., Chen, K., Zhu, J., Xie, J., & Zhang, J. (2018). Young and old adipocytes have differential influence on the development of osteoblasts. Obesity Research & Clinical Practice, 12(6), 520–527. https://doi.org/10.1016/J.ORCP.2018.06.006

Lim, H. I., & Cuker, A. (2022). Thrombocytopenia and liver disease: pathophysiology and periprocedural management. Hematology, 2022(1), 296–302. https://doi.org/10.1182/HEMATOLOGY.2022000408

Lin, C. C., & Anseth, K. S. (2008). PEG Hydrogels for the Controlled Release of Biomolecules in Regenerative Medicine. Pharmaceutical Research, 26(3), 631. https://doi.org/10.1007/S11095-008-9801-2

Lin, C. S., Ning, H., Lin, G., & Lue, T. F. (2012). Is CD34 Truly a Negative Marker for Mesenchymal Stem Cells? Cytotherapy, 14(10), 10.3109/14653249.2012.729817. https://doi.org/10.3109/14653249.2012.729817

Lin, M., Cao, H., & Li, J. (2023). Control strategies of ice nucleation, growth, and recrystallization for cryopreservation. Acta Biomaterialia, 155, 35–56. https://doi.org/10.1016/J.ACTBIO.2022.10.056

Lin, R. Z., & Chang, H. Y. (2008). Recent advances in three-dimensional multicellular spheroid culture for biomedical research. Biotechnology Journal, 3(9–10), 1172–1184. https://doi.org/10.1002/BIOT.200700228

Lin, R. Z., Chou, L. F., Chien, C. C. M., & Chang, H. Y. (2006). Dynamic analysis of hepatoma spheroid formation: roles of E-cadherin and beta1-integrin. Cell and Tissue Research, 324(3), 411–422. https://doi.org/10.1007/S00441-005-0148-2

Linnes, M. P., Ratner, B. D., & Giachelli, C. M. (2007). A fibrinogen-based precision microporous scaffold for tissue engineering. Biomaterials, 28(35), 5298–5306. https://doi.org/10.1016/J.BIOMATERIALS.2007.08.020

Lipreri, M. V., Baldini, N., Graziani, G., & Avnet, S. (2022). Perfused Platforms to Mimic Bone Microenvironment at the Macro/Milli/Microscale: Pros and Cons. Frontiers in Cell and Developmental Biology, 9, 760667. https://doi.org/10.3389/FCELL.2021.760667/PDF

Liu, C., & Sun, J. (2019). Osteogenically differentiated mesenchymal stem cells induced by hydrolyzed fish collagen maintain their immunomodulatory effects. Life Sciences, 238, 116970. https://doi.org/10.1016/J.LFS.2019.116970

Llames, S., García-Pérez, E., Meana, Á., Larcher, F., & Del Río, M. (2015). Feeder Layer Cell Actions and Applications. Tissue Engineering. Part B, Reviews, 21(4), 345–353. https://doi.org/10.1089/TEN.TEB.2014.0547

Loebel, C., Czekanska, E. M., Bruderer, M., Salzmann, G., Alini, M., & Stoddart, M. J. (2014). In Vitro Osteogenic Potential of Human Mesenchymal Stem Cells Is Predicted by Runx2/Sox9 Ratio. Tissue Engineering. Part A, 21(1–2), 115. https://doi.org/10.1089/TEN.TEA.2014.0096

Lonza Bioscience. (2025). Human Bone Marrow CD34+ Progenitor Cells | Lonza. https://bioscience.lonza.com/lonza_bs/GB/en/Primary-and-Stem-Cells/p/000000000000181987/Human-Bone-Marrow-CD34%2B-Progenitor-Cells%2C-Cryopreserved%2C-1-Million

Lv, F. J., Tuan, R. S., Cheung, K. M. C., & Leung, V. Y. L. (2014). Concise Review: The Surface Markers and Identity of Human Mesenchymal Stem Cells. Stem Cells, 32(6), 1408–1419. https://doi.org/10.1002/STEM.1681

Lv, H., Wang, H., Zhang, Z., Yang, W., Liu, W., Li, Y., & Li, L. (2017). Biomaterial stiffness determines stem cell fate. Life Sciences, 178, 42–48. https://doi.org/10.1016/J.LFS.2017.04.014

Ma, H. L., Hung, S. C., Lin, S. Y., Chen, Y. L., & Lo, W. H. (2003). Chondrogenesis of human mesenchymal stem cells encapsulated in alginate beads. Journal of Biomedical Materials Research. Part A, 64(2), 273–281. https://doi.org/10.1002/JBM.A.10370

Ma, L., Huang, Z., Wu, D., Kou, X., Mao, X., & Shi, S. (2021). CD146 controls the quality of clinical grade mesenchymal stem cells from human dental pulp. Stem Cell Research and Therapy, 12(1), 1–16. https://doi.org/10.1186/S13287-021-02559-4/FIGURES/7

Maan, Z. N., Hu, M. S., Rennert, R., Barrera, J. A., Duscher, D., Januszyk, M., Whittam, A., Padmanabhan, J., Vial, N., Ho, N., Fischer, L. H., Riegler, J., Wu, J. C., Longaker, M. T., & Gurtner, G. C. (2020). Endothelial CXCL12 regulates neovascularization during tissue repair and tumor progression. BioRxiv, 2020.05.24.113845. https://doi.org/10.1101/2020.05.24.113845

Majeti, R., Park, C. Y., & Weissman, I. L. (2007). Identification of a Hierarchy of Multipotent Hematopoietic Progenitors in Human Cord Blood. Cell Stem Cell, 1(6), 635. https://doi.org/10.1016/J.STEM.2007.10.001

Malara, A., Currao, M., Gruppi, C., Celesti, G., Viarengo, G., Buracchi, C., Laghi, L., Kaplan, D. L., & Balduini, A. (2014). Megakaryocytes contribute to the bone marrow-matrix environment by expressing fibronectin, type IV collagen, and laminin. Stem Cells (Dayton, Ohio), 32(4), 926–937. https://doi.org/10.1002/STEM.1626

Malpique, R., Osório, L. M., Ferreira, D. S., Ehrhart, F., Brito, C., Zimmermann, H., & Alves, P. M. (2010). Alginate Encapsulation as a Novel Strategy for the Cryopreservation of Neurospheres. Https://Home.Liebertpub.Com/Tec, 16(5), 965–977. https://doi.org/10.1089/TEN.TEC.2009.0660

Malumbres, M., Sotillo, R., Santamaría, D., Galán, J., Cerezo, A., Ortega, S., Dubus, P., & Barbacid, M. (2004). Mammalian cells cycle without the D-type cyclin-dependent kinases Cdk4 and Cdk6. Cell, 118(4), 493–504. https://doi.org/10.1016/j.cell.2004.08.002

Mann, Z., Sengar, M., Verma, Y. K., Rajalingam, R., & Raghav, P. K. (2022). Hematopoietic Stem Cell Factors: Their Functional Role in Self-Renewal and Clinical Aspects. Frontiers in Cell and Developmental Biology, 10, 664261. https://doi.org/10.3389/FCELL.2022.664261

Markides, H., El Haj, A. J., Webb, W. R., Chippendale, T., Coopman, K., Rafiq, Q., & Hewitt, C. J. (2019). Isolation of Mesenchymal Stem Cells From Bone Marrow Aspirate. Comprehensive Biotechnology, 137–148. https://doi.org/10.1016/B978-0-444-64046-8.00320-7

Mason, C., & Dunnill, P. (2008). A Brief Definition of Regenerative Medicine. Regenerative Medicine, 3(1), 1–5. https://doi.org/10.2217/17460751.3.1.1

Mazur, P., Leibo, S. P., & Chu, E. H. Y. (1972). A two-factor hypothesis of freezing injury: Evidence from Chinese hamster tissue-culture cells. Experimental Cell Research, 71(2), 345–355. https://doi.org/10.1016/0014-4827(72)90303-5

McKenna, H. J., Stocking, K. L., Miller, R. E., Brasel, K., De Smedt, T., Maraskovsky, E., Maliszewski, C. R., Lynch, D. H., Smith, J., Pulendran, B., Roux, E. R., Teepe, M., Lyman, S. D., & Peschon, J. J. (2000). Mice lacking flt3 ligand have deficient hematopoiesis affecting hematopoietic progenitor cells, dendritic cells, and natural killer cells. Blood, 95(11), 3489–3497. https://doi.org/10.1182/BLOOD.V95.11.3489

Mcniece, I. K., Briddell, R. A., Yan, X. Q., Hartley, C. A., Gringeri, A., Foote, M. A., & Andrews, R. G. (1994). The role of stem cell factor in mobilization of peripheral blood progenitor cells. Leukemia & Lymphoma, 15(5–6), 405–409. https://doi.org/10.3109/10428199409049743

Meesuk, L., Suwanprateeb, J., Thammarakcharoen, F., Tantrawatpan, C., Kheolamai, P., Palang, I., Tantikanlayaporn, D., & Manochantr, S. (2022). Osteogenic differentiation and proliferation

potentials of human bone marrow and umbilical cord-derived mesenchymal stem cells on the 3D-printed hydroxyapatite scaffolds. Scientific Reports, 12(1), 1–19. https://doi.org/10.1038/S41598-022-24160-2;SUBJMETA=337,532,631,80;KWRD=CELL+BIOLOGY,MOLECULAR+BIOLOGY,STEM+CELLS

Mehrasa, R., Vaziri, H., Oodi, A., Khorshidfar, M., Nikogoftar, M., Golpour, M., & Amirizadeh, N. (2014). Mesenchymal Stem Cells as a Feeder Layer Can Prevent Apoptosis of Expanded Hematopoietic Stem Cells Derived from Cord Blood. International Journal of Molecular and Cellular Medicine, 3(1), 1. https://pmc.ncbi.nlm.nih.gov/articles/PMC3927388/

Mende, N., Kuchen, E. E., Lesche, M., Grinenko, T., Kokkaliaris, K. D., Hanenberg, H., Lindemann, D., Dahl, A., Platz, A., Höfer, T., Calegari, F., & Waskow, C. (2015). CCND1–CDK4–mediated cell cycle progression provides a competitive advantage for human hematopoietic stem cells in vivo. Journal of Experimental Medicine, 212(8), 1171–1183. https://doi.org/10.1084/JEM.20150308

Mendez-Ferrer, S. (2021). How bone marrow stem cells can support Acute Myeloid Leukemia to escape chemotherapy treatment - Research and Development - NHS Blood and Transplant. https://www.nhsbt.nhs.uk/research-and-development/research-blogs/how-bone-marrow-stem-cells-can-support-acute-myeloid-leukemia-to-escape-chemotherapy-treatment/

Mendez-Ferrer, S. N. M. (2020). HSCs revive their niche after transplantation. Blood, 136(23), 2597–2598. https://doi.org/10.1182/BLOOD.2020008923

Meurer, S. K., & Weiskirchen, R. (2020). Endoglin: An “Accessory” Receptor Regulating Blood Cell Development and Inflammation. International Journal of Molecular Sciences, 21(23), 1–28. https://doi.org/10.3390/IJMS21239247

Miranda, J. P., Camões, S. P., Gaspar, M. M., Rodrigues, J. S., Carvalheiro, M., Bárcia, R. N., Cruz, P., Cruz, H., Simões, S., & Santos, J. M. (2019). The secretome derived from 3D-cultured umbilical cord tissue MSCS counteracts manifestations typifying rheumatoid arthritis. Frontiers in Immunology, 10(FEB), 425923. https://doi.org/10.3389/FIMMU.2019.00018/BIBTEX

Mirantes, C., Passegué, E., & Pietras, E. M. (2014). Pro-inflammatory cytokines: Emerging players regulating HSC function in normal and diseased hematopoiesis. Experimental Cell Research, 329(2), 248–254. https://doi.org/10.1016/J.YEXCR.2014.08.017

Mizuno, M., Katano, H., Mabuchi, Y., Ogata, Y., Ichinose, S., Fujii, S., Otabe, K., Komori, K., Ozeki, N., Koga, H., Tsuji, K., Akazawa, C., Muneta, T., & Sekiya, I. (2018). Specific markers and properties of synovial mesenchymal stem cells in the surface, stromal, and perivascular regions. Stem Cell Research and Therapy, 9(1), 1–11. https://doi.org/10.1186/S13287-018-0870-9/FIGURES/6

Mohyeldin, A., Garzón-Muvdi, T., & Quiñones-Hinojosa, A. (2010). Oxygen in stem cell biology: A critical component of the stem cell niche. Cell Stem Cell, 7(2), 150–161. https://doi.org/10.1016/J.STEM.2010.07.007/ASSET/04CC8242-3059-408B-8E52-52E7DD276784/MAIN.ASSETS/GR1.JPG

Montespan, F., Deschaseaux, F., Sensébé, L., Carosella, E. D., & Rouas-Freiss, N. (2014). Osteodifferentiated Mesenchymal Stem Cells from Bone Marrow and Adipose Tissue Express HLA-G and Display Immunomodulatory Properties in HLA-Mismatched Settings: Implications

in Bone Repair Therapy. Journal of Immunology Research, 2014(1), 230346. https://doi.org/10.1155/2014/230346

Moraes, D. A., Sibov, T. T., Pavon, L. F., Alvim, P. Q., Bonadio, R. S., Da Silva, J. R., Pic-Taylor, A., Toledo, O. A., Marti, L. C., Azevedo, R. B., & Oliveira, D. M. (2016). A reduction in CD90 (THY-1) expression results in increased differentiation of mesenchymal stromal cells. Stem Cell Research and Therapy, 7(1), 1–14. https://doi.org/10.1186/S13287-016-0359-3/FIGURES/8

Morandi, F., Airoldi, I., Marimpietri, D., Bracci, C., Faini, A. C., & Gramignoli, R. (2019). CD38, a Receptor with Multifunctional Activities: From Modulatory Functions on Regulatory Cell Subsets and Extracellular Vesicles, to a Target for Therapeutic Strategies. Cells, 8(12). https://doi.org/10.3390/CELLS8121527

Morgan, R. A., Gray, D., Lomova, A., & Kohn, D. B. (2017). Hematopoietic Stem Cell Gene Therapy – Progress and Lessons Learned. Cell Stem Cell, 21(5), 574. https://doi.org/10.1016/J.STEM.2017.10.010

Morris, C., De Wreede, L., Scholten, M., Brand, R., Van Biezen, A., Sureda, A., Dickmeiss, E., Trneny, M., Apperley, J., Chiusolo, P., Van Imhoff, G. W., Lenhoff, S., Martinelli, G., Hentrich, M., Pabst, T., Onida, F., Quinn, M., Kroger, N., De Witte, T., & Ruutu, T. (2014). Should the standard dimethyl sulfoxide concentration be reduced? Results of a European Group for Blood and Marrow Transplantation prospective noninterventional study on usage and side effects of dimethyl sulfoxide. Transfusion, 54(10), 2514–2522. https://doi.org/10.1111/TRF.12759

Morrison, S. J., & Scadden, D. T. (2014). The bone marrow niche for haematopoietic stem cells. Nature, 505(7483), 327–334. https://doi.org/10.1038/NATURE12984

Morrison, S. J., & Weissman, I. L. (1994). The long-term repopulating subset of hematopoietic stem cells is deterministic and isolatable by phenotype. Immunity, 1(8), 661–673. https://doi.org/10.1016/1074-7613(94)90037-X

Mosesson, M. W. (2005). Fibrinogen and fibrin structure and functions. Journal of Thrombosis and Haemostasis : JTH, 3(8), 1894–1904. https://doi.org/10.1111/J.1538-7836.2005.01365.X

Müller, S., Nicholson, L., Al Harbi, N., Mancuso, E., Jones, E., Dickinson, A., Wang, X. N., & Dalgarno, K. (2019). Osteogenic potential of heterogeneous and CD271-enriched mesenchymal stromal cells cultured on apatite-wollastonite 3D scaffolds. BMC Biomedical Engineering 2019 1:1, 1(1), 1–10. https://doi.org/10.1186/S42490-019-0015-Y

Murphy, Kaitlin C., Hung, B. P., Browne-Bourne, S., Zhou, D., Yeung, J., Genetos, D. C., & Leach, J. K. (2017). Measurement of oxygen tension within mesenchymal stem cell spheroids. Journal of The Royal Society Interface, 14(127). https://doi.org/10.1098/RSIF.2016.0851

Murphy, Kaitlin C, Whitehead, J., Zhou, D., Ho, S. S., Leach, J. K., & Author, A. B. (2017). Engineering Fibrin Hydrogels to Promote the Wound Healing Potential of Mesenchymal Stem Cell Spheroids HHS Public Access Author manuscript Graphical Abstract. Acta Biomater, 64, 176–186. https://doi.org/10.1016/j.actbio.2017.10.007

Murphy, R. J., Browning, A. P., Gunasingh, G., Haass, N. K., & Simpson, M. J. (2022). Designing and interpreting 4D tumour spheroid experiments. Communications Biology 2022 5:1, 5(1), 1–11. https://doi.org/10.1038/s42003-022-03018-3

Murray, K. A., & Gibson, M. I. (2022). Chemical approaches to cryopreservation. Nature Reviews Chemistry 2022 6:8, 6(8), 579–593. https://doi.org/10.1038/s41570-022-00407-4

Nafar Dastgerdi, J., Koivisto, J. T., Orell, O., Rava, P., Jokinen, J., Kanerva, M., & Kellomäki, M. (2021). Comprehensive characterisation of the compressive behaviour of hydrogels using a new modelling procedure and redefining compression testing. Materials Today Communications, 28, 102518. https://doi.org/10.1016/J.MTCOMM.2021.102518

Najar, M., Raicevic, G., Boufker, H. I., Kazan, H. F., Bruyn, C. De, Meuleman, N., Bron, D., Toungouz, M., & Lagneaux, L. (2010). Mesenchymal stromal cells use PGE2 to modulate activation and proliferation of lymphocyte subsets: Combined comparison of adipose tissue, Wharton's Jelly and bone marrow sources. Cellular Immunology, 264(2), 171–179. https://doi.org/10.1016/J.CELLIMM.2010.06.006

Nakamura-Ishizu, A., Takizawa, H., & Suda, T. (2014). The analysis, roles and regulation of quiescence in hematopoietic stem cells. Development, 141(24), 4656–4666. https://doi.org/10.1242/DEV.106575

National Center for Biotechnology Information (US). (1998). Anemia, sickle cell. National Center for Biotechnology Information (US). https://www.ncbi.nlm.nih.gov/books/NBK22238/

National human genome research institute. (2019). What is genome editing? https://www.genome.gov/about-genomics/policy-issues/what-is-Genome-Editing

National Research Council (US) and Institute of Medicine (US) Committee on the Biological and Biomedical Applications of Stem Cell. (2002). Embryonic Stem Cells. In Stem Cells and the Future of Regenerative Medicine. (3). National Academies Press (US). https://www.ncbi.nlm.nih.gov/books/NBK223690/

Nautiyal, N., Maheshwari, D., Kumar, D., Rao, E. P., Tripathi, D. M., Kumar, S., Diwakar, S., Bhardwaj, M., Mohanty, S., Baligar, P., Kumari, A., Bihari, C., Biswas, S., Sarin, S. K., & Kumar, A. (2024). Rejuvenating bone marrow hematopoietic reserve prevents regeneration failure and hepatic decompensation in animal model of cirrhosis. Frontiers in Immunology, 15, 1439510. https://doi.org/10.3389/FIMMU.2024.1439510/BIBTEX

Navarrete, R. O., Lee, E. M., Smith, K., Hyzy, S. L., Doroudi, M., Williams, J. K., Gall, K., Boyan, B. D., & Schwartz, Z. (2017). Substrate Stiffness Controls Osteoblastic and Chondrocytic Differentiation of Mesenchymal Stem Cells without Exogenous Stimuli. PLoS ONE, 12(1), 170312. https://doi.org/10.1371/JOURNAL.PONE.0170312

Naveiras, O., Nardi, V., Wenzel, P. L., Hauschka, P. V., Fahey, F., & Daley, G. Q. (2009). Bone-marrow adipocytes as negative regulators of the haematopoietic microenvironment. Nature 2009 460:7252, 460(7252), 259–263. https://doi.org/10.1038/nature08099

Nazir, A., Asghar, A., & Aslam Maan, A. (2017). Food Gels: Gelling Process and New Applications. Advances in Food Rheology and Its Applications, 335–353. https://doi.org/10.1016/B978-0-08-100431-9.00013-9

Ndoye, A., Miskin, R. P., & Michael Di Persio, C. (2021). Integrin α3β1 Represses Reelin Expression in Breast Cancer Cells to Promote Invasion. Cancers 2021, Vol. 13, Page 344, 13(2), 344. https://doi.org/10.3390/CANCERS13020344

Neves, M. I., Moroni, L., & Barrias, C. C. (2020). Modulating Alginate Hydrogels for Improved Biological Performance as Cellular 3D Microenvironments. Frontiers in Bioengineering and Biotechnology, 8, 665. https://doi.org/10.3389/FBIOE.2020.00665/BIBTEX

Nie, Y., Han, Y. C., & Zou, Y. R. (2008). CXCR4 is required for the quiescence of primitive hematopoietic cells. Journal of Experimental Medicine, 205(4), 777–783. https://doi.org/10.1084/JEM.20072513

Nielsen, J. S., & McNagny, K. M. (2009). CD34 is a key regulator of hematopoietic stem cell trafficking to bone marrow and mast cell progenitor trafficking in the periphery. Microcirculation, 16(6), 487–496. https://doi.org/10.1080/10739680902941737

Niemeyer, P., Kornacker, M., Mehlhorn, A., Seckinger, A., Vohrer, J., Schmal, H., Kasten, P., Eckstein, V., Südkamp, N. P., & Krause, U. (2007). Comparison of immunological properties of bone marrow stromal cells and adipose tissue-derived stem cells before and after osteogenic differentiation in vitro. Tissue Engineering, 13(1), 111–121. https://doi.org/10.1089/TEN.2006.0114;WEBSITE:WEBSITE:MAL-SITE

Nilsson, S. K., Johnston, H. M., Whitty, G. A., Williams, B., Webb, R. J., Denhardt, D. T., Bertoncello, I., Bendall, L. J., Simmons, P. J., & Haylock, D. N. (2005). Osteopontin, a key component of the hematopoietic stem cell niche and regulator of primitive hematopoietic progenitor cells. Blood, 106(4), 1232–1239. https://doi.org/10.1182/BLOOD-2004-11-4422,

Nishimura, I., Hisanaga, R., Sato, T., Arano, T., Nomoto, S., Ikada, Y., & Yoshinari, M. (2015). Effect of osteogenic differentiation medium on proliferation and differentiation of human mesenchymal stem cells in three-dimensional culture with radial flow bioreactor. Regenerative Therapy, 2, 24. https://doi.org/10.1016/J.RETH.2015.09.001

Nitsche, A., Junghahn, I., Thulke, S., Aumann, J., Radonić, A., Fichtner, I., & Siegert, W. (2003). Interleukin-3 Promotes Proliferation and Differentiation of Human Hematopoietic Stem Cells but Reduces Their Repopulation Potential in NOD/SCID Mice. Stem Cells, 21(2), 236–244. https://doi.org/10.1634/STEMCELLS.21-2-236

Nombela-Arrieta, C., & Manz, M. G. (2017). Quantification and three-dimensional microanatomical organization of the bone marrow. Blood Advances, 1(6), 407. https://doi.org/10.1182/BLOODADVANCES.2016003194

Nombela-Arrieta, C., Pivarnik, G., Winkel, B., Canty, K. J., Harley, B., Mahoney, J. E., Park, S. Y., Lu, J., Protopopov, A., & Silberstein, L. E. (2013a). Quantitative imaging of haematopoietic stem and progenitor cell localization and hypoxic status in the bone marrow microenvironment. Nature Cell Biology 2013 15:5, 15(5), 533–543. https://doi.org/10.1038/ncb2730

Nombela-Arrieta, C., Pivarnik, G., Winkel, B., Canty, K. J., Harley, B., Mahoney, J. E., Park, S. Y., Lu, J., Protopopov, A., & Silberstein, L. E. (2013b). Quantitative imaging of haematopoietic stem and progenitor cell localization and hypoxic status in the bone marrow microenvironment. Nature Cell Biology 2013 15:5, 15(5), 533–543. https://doi.org/10.1038/ncb2730

Nowak-Terpiłowska, A., Śledziński, P., & Zeyland, J. (2021). Impact of cell harvesting methods on detection of cell surface proteins and apoptotic markers. Brazilian Journal of Medical and Biological Research, 54(2), e10197. https://doi.org/10.1590/1414-431X202010197

Nygren, P. (2001). What is cancer chemotherapy? Acta Oncologica, 40(2–3), 166–174. https://doi.org/10.1080/02841860151116204;SUBPAGE:STRING:ABSTRACT;WGROUP:STRING:PUBLICATION

Ode, A., Kopf, J., Kurtz, A., Schmidt-Bleek, K., Schrade, P., Kolar, P., Buttgereit, F., Lehmann, K., Hutmacher, D. W., Duda, G. N., & Kasper, G. (2011). CD73 and CD29 concurrently mediate the mechanically induced decrease of migratory capacity of mesenchymal stromal cells. European Cells & Materials, 22, 26–42. https://doi.org/10.22203/ECM.V022A03

Odorico, J. S., Kaufman, D. S., & Thomson, J. A. (2001). Multilineage Differentiation from Human Embryonic Stem Cell Lines. Stem Cells, 19(3), 193–204. https://doi.org/10.1634/STEMCELLS.19-3-193

Office for Students. (2023). Annual TRAC 2022-23 Sector summary and analysis by TRAC peer group. https://www.trac.ac.uk/tracguidance/.

O'Hagan-Wong, K., Nadeau, S., Carrier-Leclerc, A., Apablaza, F., Hamdy, R., Shum-Tim, D., Rodier, F., Colmegna, I., O'Hagan-Wong, K., Nadeau, S., Carrier-Leclerc, A., Apablaza, F., Hamdy, R., Shum-Tim, D., Rodier, F., & Colmegna, I. (2016). Increased IL-6 secretion by aged human mesenchymal stromal cells disrupts hematopoietic stem and progenitor cells' homeostasis. Oncotarget, 7(12), 13285–13296. https://doi.org/10.18632/ONCOTARGET.7690

Olinga, P., Merema, M., Slooff, M. J. H., Meijer, D. K. F., & Groothuis, G. M. M. (1997). Influence of 48 hours of cold storage in University of Wisconsin organ preservation solution on metabolic capacity of rat hepatocytes. Journal of Hepatology, 27(4), 738–743. https://doi.org/10.1016/S0168-8278(97)80091-8

Omatsu, Y., Sugiyama, T., Kohara, H., Kondoh, G., Fujii, N., Kohno, K., & Nagasawa, T. (2010). The Essential Functions of Adipo-osteogenic Progenitors as the Hematopoietic Stem and Progenitor Cell Niche. Immunity, 33(3), 387–399. https://doi.org/10.1016/J.IMMUNI.2010.08.017/ATTACHMENT/4F6B3B8B-38EC-4546-A647-CEE1B596D6B4/MMC1.PDF

Oriol, A., Vives, S., Hernández-Rivas, J. M., Tormo, M., Heras, I., Rivas, C., Bethencourt, C., Moscardó, F., Bueno, J., Grande, C., del Potro, E., Guardia, R., Brunet, S., Bergua, J., Bernal, T., Moreno, M. J., Calvo, C., Bastida, P., Feliu, E., & Ribera, J. M. (2010). Outcome after relapse of acute lymphoblastic leukemia in adult patients included in four consecutive risk-adapted trials by the PETHEMA Study Group. Haematologica, 95(4), 589. https://doi.org/10.3324/HAEMATOL.2009.014274

O'Shea, J. J., Gadina, M., Sciumè, G., & Meylan, F. (2019). Cytokines and Cytokine Receptors. Clinical Immunology: Principles and Practice, Sixth Edition, 186–214. https://doi.org/10.1016/B978-0-7020-8165-1.00014-9

Ouhtit, A., Thouta, R., Zayed, H., Gaur, R. L., Fernando, A., Rahman, M., & Welsh, D. A. (2020). CD44 mediates stem cell mobilization to damaged lung via its novel transcriptional targets, Cortactin and Survivin. International Journal of Medical Sciences, 17(1), 103. https://doi.org/10.7150/IJMS.33125

Ozturk, S. S., Hu, W.-S., & London, N. Y. (2006). CELL CULTURE TECHNOLOGY FOR PHARMACEUTICAL AND CELL-BASED THERAPIES edited by. http://www.copyright.com/

Paiboon, N., Surassmo, S., Rungsardthong Ruktanonchai, U., Kappl, M., & Soottitantawat, A. (2023). Internal gelation of alginate microparticle prepared by emulsification and microfluidic method: Effect of Ca-EDTA as a calcium source. Food Hydrocolloids, 141, 108712. https://doi.org/10.1016/J.FOODHYD.2023.108712

Palanivelu, S. D., Armir, N. A. Z., Zulkifli, A., Hair, A. H. A., Salleh, K. M., Lindsey, K., Che-Othman, M. H., & Zakaria, S. (2022). Hydrogel Application in Urban Farming: Potentials and Limitations—A Review. Polymers, 14(13). https://doi.org/10.3390/POLYM14132590

Pamphilon, D., Selogie, E., Mckenna, D., Cancelas-Peres, J. A., Szczepiorkowski, Z. M., Sacher, R., McMannis, J., Eichler, H., Garritsen, H., Takanashi, M., Van De Watering, L., Stroncek, D., &

Reems, J. A. (2013). Current practices and prospects for standardization of the hematopoietic colony-forming unit assay: a report by the cellular therapy team of the Biomedical Excellence for Safer Transfusion (BEST) Collaborative. Cytotherapy, 15(3), 255–262. https://doi.org/10.1016/J.JCYT.2012.11.013

Parikh, S., Brochstein, J. A., Wease, S., Martin, P. L., Horwitz, M. E., Schwarzbach, A., & Kurtzberg, J. (2018). A Novel Therapy for Sickle Cell Disease (SCD): Co-Transplantation of Nicord® [Ex Vivo Expanded Umbilical Cord Blood (UCB) Progenitor Cells with Nicotinamide] and an Unmanipulated Unrelated UCB Graft Leads to Successful Engraftment and Cure of Severe SCD. Biology of Blood and Marrow Transplantation, 24(3), S191–S192. https://doi.org/10.1016/j.bbmt.2017.12.302

Park, H., Kang, S. W., Kim, B. S., Mooney, D. J., & Lee, K. Y. (2009). Shear-reversibly crosslinked alginate hydrogels for tissue engineering. Macromolecular Bioscience, 9(9), 895–901. https://doi.org/10.1002/MABI.200800376

Park, S. H., & Bao, G. (2021). CRISPR/Cas9 gene editing for curing sickle cell disease. Transfusion and Apheresis Science : Official Journal of the World Apheresis Association : Official Journal of the European Society for Haemapheresis, 60(1), 103060. https://doi.org/10.1016/J.TRANSCI.2021.103060

Pasovic, L., Utheim, T. P., Maria, R., Lyberg, T., Messelt, E. B., Aabel, P., Chen, D. F., Chen, X., & Eidet, J. R. (2013). Optimization of Storage Temperature for Cultured ARPE-19 Cells. Journal of Ophthalmology, 2013, 216359. https://doi.org/10.1155/2013/216359

Patel, S. A., & Simon, M. C. (2008). Biology of Hypoxia-Inducible Factor-2α in Development and Disease. Cell Death and Differentiation, 15(4), 628. https://doi.org/10.1038/CDD.2008.17

Patient Profile - NHS England Digital. (n.d.). Retrieved January 21, 2026, from https://digital.nhs.uk/data-and-information/publications/statistical/patient-reported-outcome-measures-proms/finalised-hip--knee-replacements-april-2018---march-2019/patient-profile

Pelayo, R., Miyazaki, K., Huang, J., Garrett, K. P., Osmond, D. G., & Kincade, P. W. (2006). Cell Cycle Quiescence of Early Lymphoid Progenitors in Adult Bone Marrow. Stem Cells, 24(12), 2703–2713. https://doi.org/10.1634/STEMCELLS.2006-0217

Peled, T., Shoham, H., Aschengrau, D., Yackoubov, D., Frei, G., Rosenheimer G, N., Lerrer, B., Cohen, H. Y., Nagler, A., Fibach, E., & Peled, A. (2012). Nicotinamide, a SIRT1 inhibitor, inhibits differentiation and facilitates expansion of hematopoietic progenitor cells with enhanced bone marrow homing and engraftment. Experimental Hematology, 40(4), 342-355.e1. https://doi.org/10.1016/J.EXPHEM.2011.12.005

Pham, L. H., Pham, L. H., Vu, N. B., & Pham, P. Van. (2019). The subpopulation of CD105 negative mesenchymal stem cells show strong immunomodulation capacity compared to CD105 positive mesenchymal stem cells. Biomedical Research and Therapy, 6(4), 3131–3140. https://doi.org/10.15419/bmrat.v6i4.538

Pieri, L., Urbani, S., Mazzanti, B., Pozzo, S. D., Santosuosso, M., Saccardi, R., Bosi, A., Faussone-Pellegrini, M. S., & Vannucchi, M. G. (2011). Human mesenchymal stromal cells preserve their stem features better when cultured in the Dulbecco's modified Eagle medium. Cytotherapy, 13(5), 539–548. https://doi.org/10.3109/14653249.2010.542459

Pietras, E. M., Reynaud, D., Kang, Y. A., Carlin, D., Calero-Nieto, F. J., Leavitt, A. D., Stuart, J. A., Göttgens, B., & Passegué, E. (2015). Functionally Distinct Subsets of Lineage-Biased

Multipotent Progenitors Control Blood Production in Normal and Regenerative Conditions. Cell Stem Cell, 17(1), 35–46. https://doi.org/10.1016/j.stem.2015.05.003

Pittenger, M. F., Discher, D. E., Péault, B. M., Phinney, D. G., Hare, J. M., & Caplan, A. I. (2019). Mesenchymal stem cell perspective: cell biology to clinical progress. Npj Regenerative Medicine 2019 4:1, 4(1), 1–15. https://doi.org/10.1038/s41536-019-0083-6

Poisson, J. S., Acker, J. P., Briard, J. G., Meyer, J. E., & Ben, R. N. (2019). Modulating Intracellular Ice Growth with Cell-Permeating Small-Molecule Ice Recrystallization Inhibitors. Langmuir, 35(23), 7452–7458. https://doi.org/10.1021/ACS.LANGMUIR.8B02126/ASSET/IMAGES/LARGE/LA-2018-02126G_0008.JPEG

Ponchio, L., Duma, L., Oliviero, B., Gibelli, N., Pedrazzoli, P., & Della Cuna, G. R. (2000). Mitomycin C as an alternative to irradiation to inhibit the feeder layer growth in long-term culture assays. Cytotherapy, 2(4), 281–286. https://doi.org/10.1080/146532400539215

Ponte, A. L., Marais, E., Gallay, N., Langonné, A., Delorme, B., Hérault, O., Charbord, P., Domenech, J., Lo´, A. L., & Ponte, L. (2007). The In Vitro Migration Capacity of Human Bone Marrow Mesenchymal Stem Cells: Comparison of Chemokine and Growth Factor Chemotactic Activities. Stem Cells, 25(7), 1737–1745. https://doi.org/10.1634/STEMCELLS.2007-0054

Protick, F. K., Amit, S. K., Amar, K., Nath, S. D., Akand, R., Davis, V. A., Nilufar, S., & Chowdhury, F. (2022). Additive Manufacturing of Viscoelastic Polyacrylamide Substrates for Mechanosensing Studies. ACS Omega, 7(28), 24384–24395. https://doi.org/10.1021/ACSOMEGA.2C01817/ASSET/IMAGES/LARGE/AO2C01817_0007.JPEG

Purtill, D., Antonenas, V., Chiappini, P., Tong, D., O'Flaherty, E., Bajel, A., Kabani, K., Larsen, S., Tan, S., Hutchins, C., Curtis, D. J., Kennedy, G. A., Watson, A. M., Bai, L. J., Greenwood, M., Gottlieb, D. J., & Hamad, N. (2020). Variable CD34+ recovery of cryopreserved allogeneic HPC products: transplant implications during the COVID-19 pandemic. Blood Advances, 4(17), 4147–4150. https://doi.org/10.1182/BLOODADVANCES.2020002431

Qian, H., Le Blanc, K., & Sigvardsson, M. (2012). Primary mesenchymal stem and progenitor cells from bone marrow lack expression of CD44 protein. Journal of Biological Chemistry, 287(31), 25795–25807. https://doi.org/10.1074/JBC.M112.339622/ATTACHMENT/47423766-4F20-4D66-9BD0-58B552787CBD/MMC1.ZIP

Qiu, J., Yu, B., Ren, C., Wang, T., Zhang, G., Jian, Z., Ding, J., Xu, F., & Huang, H. (2024). Deep-supercooling preservation of stem cell spheroids for chondral defect repairment. Stem Cell Reports, 19(12), 1665–1676. https://doi.org/10.1016/J.STEMCR.2024.10.008

Qiu, L., Meagher, R., Welhausen, S., Heye, M., Brown, R., & Herzig, R. H. (2004). Ex Vivo Expansion of CD34+ Umbilical Cord Blood Cells in a Defined Serum-Free Medium (QBSF-60) with Early Effect Cytokines. Https://Home.Liebertpub.Com/Scd, 8(6), 609–618. https://doi.org/10.1089/152581699319777

Qiu, Y., & Park, K. (2001). Environment-sensitive hydrogels for drug delivery. Advanced Drug Delivery Reviews, 53(3), 321–339. https://doi.org/10.1016/S0169-409X(01)00203-4

Quentmeier, H., Reinhardt, J., Zaborski, M., & Drexler, H. G. (2003). FLT3 mutations in acute myeloid leukemia cell lines. Leukemia, 17(1), 120–124. https://doi.org/10.1038/sj.leu.2402740

Querceto, S., Santoro, R., Gowran, A., Grandinetti, B., Pompilio, G., Regnier, M., Tesi, C., Poggesi, C., Ferrantini, C., & Pioner, J. M. (2022). The harder the climb the better the view: The impact of substrate stiffness on cardiomyocyte fate. Journal of Molecular and Cellular Cardiology, 166, 36–49. https://doi.org/10.1016/J.YJMCC.2022.02.001

Quereda, V., Hou, S., Madoux, F., Scampavia, L., Spicer, T. P., & Duckett, D. (2018). A Cytotoxic Three-Dimensional-Spheroid, High-Throughput Assay using Patient Derived Glioma Stem Cells. SLAS Discovery : Advancing Life Sciences R & D, 23(8), 842. https://doi.org/10.1177/2472555218775055

Quirici, N., Soligo, D., Bossolasco, P., Servida, F., Lumini, C., & Deliliers, G. L. (2002). Isolation of bone marrow mesenchymal stem cells by anti-nerve growth factor receptor antibodies. Experimental Hematology, 30(7), 783–791. https://doi.org/10.1016/S0301-472X(02)00812-3

Rabbany, S. Y., Pastore, J., Yamamoto, M., Miller, T., Rafii, S., Aras, R., & Penn, M. (2010). Continuous delivery of stromal cell-derived factor-1 from alginate scaffolds accelerates wound healing. Cell Transplantation, 19(4), 399–408. https://doi.org/10.3727/096368909X481782

Ramdhan, T., Ching, S. H., Prakash, S., & Bhandari, B. (2019). Time dependent gelling properties of cuboid alginate gels made by external gelation method: Effects of alginate-CaCl2 solution ratios and pH. Food Hydrocolloids, 90, 232–240. https://doi.org/10.1016/J.FOODHYD.2018.12.022

Rana, D., Tabasum, A., & Ramalingam, M. (2016). Cell-laden alginate/polyacrylamide beads as carriers for stem cell delivery: preparation and characterization. https://doi.org/10.1039/c5ra26447b

Rebar, A. H. (1993). General responses of the bone marrow to injury. Toxicologic Pathology, 21(2), 118–129. https://doi.org/10.1177/019262339302100202

Regmi, S., Raut, P. K., Pathak, S., Shrestha, P., Park, P. H., & Jeong, J. H. (2020). Enhanced viability and function of mesenchymal stromal cell spheroids is mediated via autophagy induction. Autophagy, 17(10), 2991. https://doi.org/10.1080/15548627.2020.1850608

Renders, S., Svendsen, A. F., Panten, J., Rama, N., Maryanovich, M., Sommerkamp, P., Ladel, L., Redavid, A. R., Gibert, B., Lazare, S., Ducarouge, B., Schönberger, K., Narr, A., Tourbez, M., Dethmers-Ausema, B., Zwart, E., Hotz-Wagenblatt, A., Zhang, D., Korn, C., … Trumpp, A. (2021). Niche derived netrin-1 regulates hematopoietic stem cell dormancy via its receptor neogenin-1. Nature Communications 2021 12:1, 12(1), 1–15. https://doi.org/10.1038/s41467-020-20801-0

Revete, A., Aparicio, A., Cisterna, B. A., Revete, J., Luis, L., Ibarra, E., Segura González, E. A., Molino, J., & Reginensi, D. (2022). Advancements in the Use of Hydrogels for Regenerative Medicine: Properties and Biomedical Applications. International Journal of Biomaterials, 2022. https://doi.org/10.1155/2022/3606765

Reyhanoglu, G., & Tadi, P. (2023). Etoposide. XPharm: The Comprehensive Pharmacology Reference, 1–5. https://doi.org/10.1016/B978-008055232-3.61729-5

Rheingold, S. R., Bhojwani, D., Ji, L., Xu, X., Devidas, M., Kairalla, J. A., Shago, M., Heerema, N. A., Carroll, A. J., Breidenbach, H., Borowitz, M., Wood, B. L., Angiolillo, A. L., Asselin, B. L., Bowman, W. P., Brown, P., Dreyer, Z. A. E., Dunsmore, K. P., Hilden, J. M., … Loh, M. L. (2024). Determinants of survival after first relapse of acute lymphoblastic leukemia: a Children's Oncology Group study. Leukemia, 38(11), 2382–2394. https://doi.org/10.1038/S41375-024-

02395-4;SUBJMETA=1541,1990,2125,283,499,692,699;KWRD=ACUTE+LYMPHOCYTIC+LEUKAEMIA,RISK+FACTORS

Ribeiro-filho, A. C., Levy, D., Ruiz, J. L. M., Mantovani, M. da C., & Bydlowski, S. P. (2019). Traditional and advanced cell cultures in hematopoietic stem cell studies. Cells, 8(12). https://doi.org/10.3390/CELLS8121628

Rimac, V., Bojanić, I., Dabelić, S., & Ćepulić, B. G. (2023). Variable recovery of cryopreserved hematopoietic stem cells and leukocyte subpopulations in leukapheresis products. Transfusion and Apheresis Science, 62(5), 103763. https://doi.org/10.1016/J.TRANSCI.2023.103763

Rochefort, G. Y., Delorme, B., Lopez, A., Hérault, O., Bonnet, P., Charbord, P., Eder, V., Domenech, J., Rochefort, L. Y., Hé Rault, O., & Ronique Eder, V. (2006). Multipotential Mesenchymal Stem Cells Are Mobilized into Peripheral Blood by Hypoxia. Stem Cells, 24(10), 2202–2208. https://doi.org/10.1634/STEMCELLS.2006-0164

Rödling, L., Schwedhelm, I., Kraus, S., Bieback, K., Hansmann, J., & Lee-Thedieck, C. (2017). 3D models of the hematopoietic stem cell niche under steady-state and active conditions. Scientific Reports 2017 7:1, 7(1), 1–15. https://doi.org/10.1038/s41598-017-04808-0

Rosnet, O., Bühring, H. J., Marchetto, S., Rappold, I., Lavagna, C., Sainty, D., Arnoulet, C., Chabannon, C., Kanz, L., Hannum, C., & Birnbaum, D. (1996). Human FLT3/FLK2 receptor tyrosine kinase is expressed at the surface of normal and malignant hematopoietic cells. Leukemia, 10(2), 238–248. https://europepmc.org/article/med/8637232

Rovere, M., Reverberi, D., Arnaldi, P., Palamà, M. E. F., & Gentili, C. (2023). Spheroid size influences cellular senescence and angiogenic potential of mesenchymal stromal cell-derived soluble factors and extracellular vesicles. Frontiers in Bioengineering and Biotechnology, 11, 1297644. https://doi.org/10.3389/FBIOE.2023.1297644/FULL

Rowley, S. D. (2009). Hematopoietic Stem Cell Cryopreservation: A Review of Current Techniques. Https://Home.Liebertpub.Com/Scd, 1(3), 233–250. https://doi.org/10.1089/SCD.1.1992.1.233

Ručigaj, A., Golobič, J., & Kopač, T. (2024). The role of multivalent cations in determining the cross-linking affinity of alginate hydrogels: A combined experimental and modeling study. Chemical Engineering Journal Advances, 20, 100678. https://doi.org/10.1016/J.CEJA.2024.100678

Russell, W. M. S. and B. R. L. (1959). The Principles of Humane Experimental Technique. Eweb:789.

Sá da Bandeira, D., Casamitjana, J., & Crisan, M. (2017). Pericytes, integral components of adult hematopoietic stem cell niches. Pharmacology & Therapeutics, 171, 104–113. https://doi.org/10.1016/J.PHARMTHERA.2016.11.006

Sabhachandani, P., Motwani, V., Cohen, N., Sarkar, S., Torchilin, V., & Konry, T. (2016). Generation and functional assessment of 3D multicellular spheroids in droplet based microfluidics platform. Lab on a Chip, 16(3), 497–505. https://doi.org/10.1039/C5LC01139F

Sacchetti, B., Funari, A., Michienzi, S., Di Cesare, S., Piersanti, S., Saggio, I., Tagliafico, E., Ferrari, S., Robey, P. G., Riminucci, M., & Bianco, P. (2007). Self-renewing osteoprogenitors in bone marrow sinusoids can organize a hematopoietic microenvironment. Cell, 131(2), 324–336. https://doi.org/10.1016/J.CELL.2007.08.025

Saleh, M., Shamsasanjan, K., Movassaghpourakbari, A., Akbarzadehlaleh, P., & Molaeipour, Z. (2015). The Impact of Mesenchymal Stem Cells on Differentiation of Hematopoietic Stem Cells. Advanced Pharmaceutical Bulletin, 5(3), 299. https://doi.org/10.15171/APB.2015.042

Atelerix. (2026). Samples Preserved. https://www.atelerix.co.uk/samples-preserved/

Santana, B. P., Nedel, F., Perelló Ferrúa, C., e Silva, R. M., da Silva, A. F., Demarco, F. F., & Lenin Villarreal Carreño, N. (2015). Comparing different methods to fix and to dehydrate cells on alginate hydrogel scaffolds using scanning electron microscopy. Microscopy Research and Technique, 78(7), 553–561. https://doi.org/10.1002/JEMT.22508

Santos, J. M., Camões, S. P., Filipe, E., Cipriano, M., Barcia, R. N., Filipe, M., Teixeira, M., Simões, S., Gaspar, M., Mosqueira, D., Nascimento, D. S., Pinto-Do-Ó, P., Cruz, P., Cruz, H., Castro, M., & Miranda, J. P. (2015). Three-dimensional spheroid cell culture of umbilical cord tissue-derived mesenchymal stromal cells leads to enhanced paracrine induction of wound healing. Stem Cell Research and Therapy, 6(1), 1–19. https://doi.org/10.1186/S13287-015-0082-5/FIGURES/7

Sanz-Horta, R., Matesanz, A., Gallardo, A., Reinecke, H., Jorcano, J. L., Acedo, P., Velasco, D., & Elvira, C. (2023). Technological advances in fibrin for tissue engineering. Journal of Tissue Engineering, 14, 20417314231190290. https://doi.org/10.1177/20417314231190288

Sarker, B., Rompf, J., Silva, R., Lang, N., Detsch, R., Kaschta, J., Fabry, B., & Boccaccini, A. R. (2015). Alginate-based hydrogels with improved adhesive properties for cell encapsulation. International Journal of Biological Macromolecules, 78, 72–78. https://doi.org/10.1016/J.IJBIOMAC.2015.03.061

Sarrigiannidis, S. O., Rey, J. M., Dobre, O., González-García, C., Dalby, M. J., & Salmeron-Sanchez, M. (2021). A tough act to follow: collagen hydrogel modifications to improve mechanical and growth factor loading capabilities. Materials Today Bio, 10, 100098. https://doi.org/10.1016/J.MTBIO.2021.100098

Scaccini, L., Mezzena, R., De Masi, A., Gagliardi, M., Gambarotta, G., Cecchini, M., & Tonazzini, I. (2021). Chitosan micro-grooved membranes with increased asymmetry for the improvement of the schwann cell response in nerve regeneration. International Journal of Molecular Sciences, 22(15), 7901. https://doi.org/10.3390/IJMS22157901/S1

Schajnovitz, A., Itkin, T., D'Uva, G., Kalinkovich, A., Golan, K., Ludin, A., Cohen, D., Shulman, Z., Avigdor, A., Nagler, A., Kollet, O., Seger, R., & Lapidot, T. (2011). CXCL12 secretion by bone marrow stromal cells is dependent on cell contact and mediated by connexin-43 and connexin-45 gap junctions. Nature Immunology 2011 12:5, 12(5), 391–398. https://doi.org/10.1038/ni.2017

Schippel, N., & Sharma, S. (2023). Dynamics of human hematopoietic stem and progenitor cell differentiation to the erythroid lineage. Experimental Hematology, 123, 1–17. https://doi.org/10.1016/J.EXPHEM.2023.05.001

Schmitz, C., Potekhina, E., Belousov, V. V., & Lavrentieva, A. (2021). Hypoxia Onset in Mesenchymal Stem Cell Spheroids: Monitoring With Hypoxia Reporter Cells. Frontiers in Bioengineering and Biotechnology, 9, 611837. https://doi.org/10.3389/FBIOE.2021.611837/BIBTEX

Schubert, T., Xhema, D., Vériter, S., Schubert, M., Behets, C., Delloye, C., Gianello, P., & Dufrane, D. (2011). The enhanced performance of bone allografts using osteogenic-differentiated adipose-derived mesenchymal stem cells. Biomaterials, 32(34), 8880–8891. https://doi.org/10.1016/J.BIOMATERIALS.2011.08.009

Schürch, C. M., Riether, C., & Ochsenbein, A. F. (2014). Cytotoxic CD8+ T cells stimulate hematopoietic progenitors by promoting cytokine release from bone marrow mesenchymal stromal cells. Cell Stem Cell, 14(4), 460–472. https://doi.org/10.1016/J.STEM.2014.01.002/ATTACHMENT/6F1C0CB9-967B-4F55-B755-AA62E7FAA54A/MMC1.PDF

Sei, J., Moses, B., Becker, A. H., Kim, M., Kaur, N., Vemuri, M., & Civin, C. (2019). StemPro™ HSC expansion medium (Prototype) supports superior expansion of human hematopoietic stem-progenitor cells. Cytotherapy, 21(5), S64–S65. https://doi.org/10.1016/J.JCYT.2019.03.448

Seitz, M. P., Song, Y., Lian, X. L., Ma, Z., & Jain, E. (2024). Soft Polyethylene Glycol Hydrogels Support Human PSC Pluripotency and Morphogenesis. ACS Biomaterials Science and Engineering, 10(7), 4525–4540. https://doi.org/10.1021/ACSBIOMATERIALS.4C00923/ASSET/IMAGES/LARGE/AB4C00923_0008.JPEG

Selle, M., Koch, J. D., Ongsiek, A., Ulbrich, L., Ye, W., Jiang, Z., Krettek, C., Neunaber, C., & Noack, S. (2022). Influence of age on stem cells depends on the sex of the bone marrow donor. Journal of Cellular and Molecular Medicine, 26(5), 1594. https://doi.org/10.1111/JCMM.17201

Serp, D., Mueller, M., Von Stockar, U., & Marison, I. W. (2002). Low-temperature electron microscopy for the study of polysaccharide ultrastructures in hydrogels. II. Effect of temperature on the structure of Ca2+-alginate beads. Biotechnology and Bioengineering, 79(3), 253–259. https://doi.org/10.1002/BIT.10287

Severino, P., da Silva, C. F., Andrade, L. N., de Lima Oliveira, D., Campos, J., & Souto, E. B. (2019). Alginate Nanoparticles for Drug Delivery and Targeting. Current Pharmaceutical Design, 25(11), 1312–1334. https://doi.org/10.2174/1381612825666190425163424

Shah, M., LI, H., Harris, M., Paterson, A., & Bhatia, R. (2017). Role of SCF-Expressing Bone Marrow Populations in Hematopoietic and Leukemic Stem Cell Regulation. Blood, 130, 2439. https://doi.org/10.1182/BLOOD.V130.SUPPL_1.2439.2439

Shahrabi, S., Rezaeeyan, H., Ahmadzadeh, A., Shahjahani, M., & Saki, N. (2016). Bone Marrow Blood Vessels: Normal and Neoplastic Niche. Oncology Reviews, 10(2), 72–77. https://doi.org/10.4081/ONCOL.2016.306

Shanbhag, S., Suliman, S., Bolstad, A. I., Stavropoulos, A., & Mustafa, K. (2020). Xeno-Free Spheroids of Human Gingiva-Derived Progenitor Cells for Bone Tissue Engineering. Frontiers in Bioengineering and Biotechnology, 8, 968. https://doi.org/10.3389/FBIOE.2020.00968/PDF

Shao, L., Wang, Y., Chang, J., Luo, Y., Meng, A., & Zhou, D. (2013). Hematopoietic stem cell senescence and cancer therapy-induced long-term bone marrow injury. Translational Cancer Research, 2(5), 397. https://doi.org/10.3978/J.ISSN.2218-676X.2013.07.03

Shenoy, M., Abdul, N. S., Qamar, Z., Bahri, B. M. Al, Ghalayini, K. Z. K. Al, & Kakti, A. (2022). Collagen Structure, Synthesis, and Its Applications: A Systematic Review. Cureus, 14(5), e24856. https://doi.org/10.7759/CUREUS.24856

Shi, G., Chang, Z., Zhang, P., Zou, X., Zheng, X., Liu, X., Yan, J., Xu, H., Tian, Z., Zhang, N., Cui, N., Sun, L., Xu, G., & Yang, H. (2024). Heterogeneous stiffness of the bone marrow microenvironment regulates the fate decision of haematopoietic stem and progenitor cells. Cell Proliferation, 57(12), e13715. https://doi.org/10.1111/CPR.13715

Shin, H. J., Cho, H. U., & Park, J. M. (2023). Alginate as a Soil Conditioner: Properties, Mechanisms, and Agricultural Applications. Biotechnology and Bioprocess Engineering 2023 28:5, 28(5), 734–749. https://doi.org/10.1007/S12257-023-0206-1

Shiroshita, K., Kobayashi, H., Watanuki, S., Karigane, D., Sorimachi, Y., Fujita, S., Tamaki, S., Haraguchi, M., Itokawa, N., Aoyoama, K., Koide, S., Masamoto, Y., Kobayashi, K., Nakamura-Ishizu, A., Kurokawa, M., Iwama, A., Okamoto, S., Kataoka, K., & Takubo, K. (2022). A culture platform to study quiescent hematopoietic stem cells following genome editing. Cell Reports Methods, 2(12), 100354. https://doi.org/10.1016/J.CRMETH.2022.100354

Si, J., Ishikawa, S., Nepal, S., Okada, H., Chung, U. Il, Sakai, T., & Hojo, H. (2024). Osteogenic differentiation capabilities of multiarm PEG hydrogels: involvement of gel–gel-phase separation in cell differentiation. Polymer Journal 2024 57:4, 57(4), 407–417. https://doi.org/10.1038/s41428-024-00955-0

Sim, H. J., Kim, M. H., Bhattarai, G., Hwang, J. W., So, H. S., Poudel, S. B., Cho, E. S., Kook, S. H., & Lee, J. C. (2021). Overexpression of COMP-Angiopoietin-1 in K14-Expressing Cells Impairs Hematopoiesis and Disturbs Erythrocyte Maturation. Molecules and Cells, 44(4), 254–266. https://doi.org/10.14348/MOLCELLS.2021.2155

Simeone, P., Bologna, G., Lanuti, P., Pierdomenico, L., Guagnano, M. T., Pieragostino, D., Del Boccio, P., Vergara, D., Marchisio, M., Miscia, S., & Mariani-Costantini, R. (2020). Extracellular Vesicles as Signaling Mediators and Disease Biomarkers across Biological Barriers. International Journal of Molecular Sciences, 21(7), 2514. https://doi.org/10.3390/IJMS21072514

Simian, M., & Bissell, M. J. (2017). Organoids: A historical perspective of thinking in three dimensions. The Journal of Cell Biology, 216(1), 31. https://doi.org/10.1083/JCB.201610056

Simsek, T., Kocabas, F., Zheng, J., Deberardinis, R. J., Mahmoud, A. I., Olson, E. N., Schneider, J. W., Zhang, C. C., & Sadek, H. A. (2010). The Distinct Metabolic Profile of Hematopoietic Stem Cells Reflects Their Location in a Hypoxic Niche. Cell Stem Cell, 7(3), 380–390. https://doi.org/10.1016/J.STEM.2010.07.011

Sitnicka, E., Bryder, D., Theilgaard-Mönch, K., Buza-Vidas, N., Adolfsson, J., & Jacobsen, S. E. W. (2002). Key role of flt3 ligand in regulation of the common lymphoid progenitor but not in maintenance of the hematopoietic stem cell pool. Immunity, 17(4), 463–472. https://doi.org/10.1016/S1074-7613(02)00419-3/ASSET/19C97BEE-A43B-4360-A984-BD45CBBFD086/MAIN.ASSETS/GR4.JPG

Sjöberg, J., Rydström, A., Larsson, J., Enver, T., Mansell, E., & Sigurdsson, V. (2023). P1333: CHEMOTHERAPY-ACTIVATED HSCS ARE DEFINED BY HIGHLY INCREASED MITOCHONDRIAL MASS AND POTENTIAL INDEPENDENT OF CELL CYCLE STATUS. HemaSphere, 7(Suppl), e4596119. https://doi.org/10.1097/01.HS9.0000972220.45961.19

Smith, A. M., & Miri, T. (2010). Alginates in Foods. Practical Food Rheology: An Interpretive Approach, 113–132. https://doi.org/10.1002/9781444391060.CH6

Smith, N. R., Davies, P. S., Levin, T. G., Gallagher, A. C., Keene, D. R., Sengupta, S. K., Wieghard, N., El Rassi, E., & Wong, M. H. (2017). Cell Adhesion Molecule CD166/ALCAM Functions Within the Crypt to Orchestrate Murine Intestinal Stem Cell Homeostasis. Cellular and Molecular Gastroenterology and Hepatology, 3(3), 389–409. https://doi.org/10.1016/J.JCMGH.2016.12.010

Sneath, R. J. S., & Mangham, D. C. (1998). The normal structure and function of CD44 and its role in neoplasia. J Clin Pathol: Mol Pathol, 51, 191–200.

Sober, S. A., Darmani, H., Alhattab, D., & Awidi, A. (2023). Flow cytometric characterization of cell surface markers to differentiate between fibroblasts and mesenchymal stem cells of different origin. Archives of Medical Science, 19(5), 1487–1496. https://doi.org/10.5114/AOMS/131088

Sohn, H. S., Heo, J. S., Kim, H. S., Choi, Y., & Kim, H. O. (2013). Duration of in vitro storage affects the key stem cell features of human bone marrow-derived mesenchymal stromal cells for clinical transplantation. Cytotherapy, 15(4), 460–466. https://doi.org/10.1016/j.jcyt.2012.10.015

Solanilla, A., Grosset, C., Lemercier, C., Dupouy, M., Mahon, F. X., Schweitzer, K., Reiffers, J., Weksler, B., & Ripoche, J. (2000). Expression of Flt3-ligand by the endothelial cell. Leukemia 2000 14:1, 14(1), 153–162. https://doi.org/10.1038/sj.leu.2401635

Somo, S. I., Brown, J. M., & Brey, E. M. (2020). Dual Crosslinking of Alginate Outer Layer Increases Stability of Encapsulation System. Frontiers in Chemistry, 8, 575278. https://doi.org/10.3389/FCHEM.2020.575278/BIBTEX

Song, L., & Tuan, R. S. (2004). Transdifferentiation potential of human mesenchymal stem cells derived from bone marrow. FASEB Journal : Official Publication of the Federation of American Societies for Experimental Biology, 18(9), 980–982. https://doi.org/10.1096/FJ.03-1100FJE

Sorrentino, A., Ferracin, M., Castelli, G., Biffoni, M., Tomaselli, G., Baiocchi, M., Fatica, A., Negrini, M., Peschle, C., & Valtieri, M. (2008). Isolation and characterization of CD146+ multipotent mesenchymal stromal cells. Experimental Hematology, 36(8), 1035–1046. https://doi.org/10.1016/J.EXPHEM.2008.03.004

Sotiropoulou, P. A., Perez, S. A., Salagianni, M., Baxevanis, C. N., & Papamichail, M. (2006). Characterization of the Optimal Culture Conditions for Clinical Scale Production of Human Mesenchymal Stem Cells. STEM CELLS, 24(2), 462–471. https://doi.org/10.1634/STEMCELLS.2004-0331

Southard, J. H., & Belzer, F. O. (1995). Organ preservation. Annual Review of Medicine, 46, 235–247. https://doi.org/10.1146/ANNUREV.MED.46.1.235,

Spangrude, G. J., Heimfeld, S., & Weissman, I. L. (1988). Purification and Characterization of Mouse Hematopoietic Stem Cells. Science, 241(4861), 58–62. https://doi.org/10.1126/SCIENCE.2898810

Spencer, J. A., Ferraro, F., Roussakis, E., Klein, A., Wu, J., Runnels, J. M., Zaher, W., Mortensen, L. J., Alt, C., Turcotte, R., Yusuf, R., Côté, D., Vinogradov, S. A., Scadden, D. T., & Lin, C. P. (2014). Direct measurement of local oxygen concentration in the bone marrow of live animals. Nature, 508(7495), 269. https://doi.org/10.1038/NATURE13034

Spheroid vs. Organoid: What's the Difference? (n.d.). Retrieved September 4, 2024, from https://www.corning.com/emea/en/products/life-sciences/resources/stories/at-the-bench/organoid-vs-spheroid-what-is-the-difference.html

Steensma, D. P., Bejar, R., Jaiswal, S., Lindsley, R. C., Sekeres, M. A., Hasserjian, R. P., & Ebert, B. L. (2015). Clonal hematopoiesis of indeterminate potential and its distinction from

myelodysplastic syndromes. Blood, 126(1), 9–16. https://doi.org/10.1182/BLOOD-2015-03-631747

Stemcell technologies. (2017). AggreWell^{TM}400 Microwell culture plates for easy and reproducible production of embryoid bodies and spheroids. www.stemcell.com

Stemcell Technologies. (2025). Human Hematopoietic Stem and Progenitor Cell Phenotyping Panels | STEMCELL Technologies. https://www.stemcell.com/human-hematopoietic-stem-and-progenitor-cell-phenotyping-panels.html

Stieglitz, E., & Loh, M. L. (2013). Genetic predispositions to childhood leukemia. Therapeutic Advances in Hematology, 4(4), 270. https://doi.org/10.1177/2040620713498161

Stier, S., Ko, Y., Forkert, R., Lutz, C., Neuhaus, T., Grünewald, E., Cheng, T., Dombkowski, D., Calvi, L. M., Rittling, S. R., & Scadden, D. T. (2005). Osteopontin is a hematopoietic stem cell niche component that negatively regulates stem cell pool size. Journal of Experimental Medicine, 201(11), 1781–1791. https://doi.org/10.1084/JEM.20041992,

Stirewalt, D. L., & Radich, J. P. (2003). The role of FLT3 in haematopoietic malignancies. Nature Reviews Cancer 2003 3:9, 3(9), 650–665. https://doi.org/10.1038/nrc1169

Stowers, R. S., Shcherbina, A., Israeli, J., Gruber, J. J., Chang, J., Nam, S., Rabiee, A., Teruel, M. N., Snyder, M. P., Kundaje, A., & Chaudhuri, O. (2019). Matrix stiffness induces a tumorigenic phenotype in mammary epithelium through changes in chromatin accessibility. Nature Biomedical Engineering, 3(12), 1009. https://doi.org/10.1038/S41551-019-0420-5

Stresser, D. M., Kopec, A. K., Hewitt, P., Hardwick, R. N., Van Vleet, T. R., Mahalingaiah, P. K. S., O'Connell, D., Jenkins, G. J., David, R., Graham, J., Lee, D., Ekert, J., Fullerton, A., Villenave, R., Bajaj, P., Gosset, J. R., Ralston, S. L., Guha, M., Amador-Arjona, A., … Homan, K. A. (2023). Towards in vitro models for reducing or replacing the use of animals in drug testing. Nature Biomedical Engineering 2023 8:8, 8(8), 930–935. https://doi.org/10.1038/s41551-023-01154-7

Subramaniam, A., Žemaitis, K., Talkhoncheh, M. S., Yudovich, D., Bäckström, A., Debnath, S., Chen, J., Jain, M. V., Galeev, R., Gaetani, M., Zubarev, R. A., & Larsson, J. (2020). Lysine-specific demethylase 1A restricts ex vivo propagation of human HSCs and is a target of UM171. Blood, 136(19), 2151–2161. https://doi.org/10.1182/BLOOD.2020005827

Sugiyama, T., Kohara, H., Noda, M., & Nagasawa, T. (2006). Maintenance of the Hematopoietic Stem Cell Pool by CXCL12-CXCR4 Chemokine Signaling in Bone Marrow Stromal Cell Niches. Immunity, 25(6), 977–988. https://doi.org/10.1016/J.IMMUNI.2006.10.016

Sukmana, B. I., Margiana, R., Almajidi, Y. Q., Almalki, S. G., Hjazi, A., Shahab, S., Romero-Parra, R. M., Alazbjee, A. A. A., Alkhayyat, A., & John, V. (2023). Supporting wound healing by mesenchymal stem cells (MSCs) therapy in combination with scaffold, hydrogel, and matrix; State of the art. Pathology - Research and Practice, 248, 154575. https://doi.org/10.1016/J.PRP.2023.154575

Sun, J., & Tan, H. (2013). Alginate-Based Biomaterials for Regenerative Medicine Applications. Materials (Basel, Switzerland), 6(4), 1285–1309. https://doi.org/10.3390/MA6041285

Sun, L., Guo, S., Xie, Y., & Yao, Y. (2023). The characteristics and the multiple functions of integrin β1 in human cancers. Journal of Translational Medicine 2023 21:1, 21(1), 1–13. https://doi.org/10.1186/S12967-023-04696-1

Suto, E. G., Mabuchi, Y., Suzuki, N., Suzuki, K., Ogata, Y., Taguchi, M., Muneta, T., Sekiya, I., & Akazawa, C. (2017). Prospectively isolated mesenchymal stem/stromal cells are enriched in the CD73+ population and exhibit efficacy after transplantation. Scientific Reports, 7(1), 4838. https://doi.org/10.1038/S41598-017-05099-1

SWAN, H., VURTUE, R. W., BLOUNT, S. G., & KURCHER, L. T. (1955). Hypothermia in Surgery. Annals of Surgery, 142(3), 382–400. https://doi.org/10.1097/00000658-195509000-00008

Swioklo, S., & Connon, C. J. (2016). Short-term Storage of Cells for Application in Cell-based Therapies. Bioprocessing for Cell Based Therapies, 187–210. https://doi.org/10.1002/9781118743362.CH7;SUBPAGE:STRING:ABSTRACT;WEBSITE:WEBSITE:PERICLES;CTYPE:STRING:BOOK

Swioklo, S., Constantinescu, A., & Connon, C. J. (2016). Alginate-Encapsulation for the Improved Hypothermic Preservation of Human Adipose-Derived Stem Cells. Stem Cells Translational Medicine, 5(3), 339–349. https://doi.org/10.5966/SCTM.2015-0131/-/DC1

Syed, S., Karadaghy, A., & Zustiak, S. (2015). Simple Polyacrylamide-based Multiwell Stiffness Assay for the Study of Stiffness-dependent Cell Responses. Journal of Visualized Experiments : JoVE, 2015(97), 52643. https://doi.org/10.3791/52643

Takahashi, K., & Yamanaka, S. (2006). Induction of Pluripotent Stem Cells from Mouse Embryonic and Adult Fibroblast Cultures by Defined Factors. Cell, 126(4), 663–676. https://doi.org/10.1016/J.CELL.2006.07.024/ATTACHMENT/A7BA2E0F-99EF-4A86-88AA-418202149347/MMC1.PDF

Takebe, T., Imai, R., & Ono, S. (2018). The Current Status of Drug Discovery and Development as Originated in United States Academia: The Influence of Industrial and Academic Collaboration on Drug Discovery and Development. Clinical and Translational Science, 11(6), 597–606. https://doi.org/10.1111/CTS.12577

Tanaka, Y., Kurosawa, S., Tajima, K., Tanaka, T., Ito, R., Inoue, Y., Okinaka, K., Inamoto, Y., Fuji, S., Kim, S. W., Tanosaki, R., Yamashita, T., & Fukuda, T. (2016). Analysis of non-relapse mortality and causes of death over 15 years following allogeneic hematopoietic stem cell transplantation. Bone Marrow Transplantation, 51(4), 553–559. https://doi.org/10.1038/BMT.2015.330;SUBJMETA=308,499,575,692;KWRD=RISK+FACTORS,TRANSLATIONAL+RESEARCH

Tang, C., Li, M. H., Chen, Y. L., Sun, H. Y., Liu, S. L., Zheng, W. W., Zhang, M. Y., Li, H., Fu, W., Zhang, W. J., Liang, A. Bin, Tang, Z. H., Hong, D. L., Zhou, B. B. S., & Duan, C. W. (2018). Chemotherapy-induced niche perturbs hematopoietic reconstitution in B-cell acute lymphoblastic leukemia. Journal of Experimental and Clinical Cancer Research, 37(1). https://doi.org/10.1186/S13046-018-0859-3,

Testa, U. (2010). Leukemia stem cells. Annals of Hematology 2010 90:3, 90(3), 245–271. https://doi.org/10.1007/S00277-010-1118-7

Thai, V. L., Mierswa, S., Griffin, K. H., Boerckel, J. D., & Leach, J. K. (2024). Mechanoregulation of MSC spheroid immunomodulation. APL Bioengineering, 8(1), 016116. https://doi.org/10.1063/5.0184431

Thermofisher, & eBioscience. (2025). Human Hematopoietic Lineage Antibody, FITC (22-7778-72). https://www.thermofisher.com/antibody/product/Human-Hematopoietic-Lineage-Antibody-clone-RPA-2-10-OKT3-61D3-CB16-HIB19-TULY56-HIR2-Cocktail/22-7778-72

Thompson, E. N., Carlino, M. J., Scanlon, V. M., Grimes, H. L., & Krause, D. S. (2023). Assay optimization for the objective quantification of human multilineage colony-forming units. Experimental Hematology, 124, 36-44.e3. https://doi.org/10.1016/J.EXPHEM.2023.05.007

Tomás-Bort, E., Kieler, M., Sharma, S., Candido, J. B., & Loessner, D. (2020). 3D approaches to model the tumor microenvironment of pancreatic cancer. Theranostics, 10(11), 5074. https://doi.org/10.7150/THNO.42441

Tormin, A., Li, O., Brune, J. C., Walsh, S., Schütz, B., Ehinger, M., Ditzel, N., Kassem, M., & Scheding, S. (2011). CD146 expression on primary nonhematopoietic bone marrow stem cells is correlated with in situ localization. Blood, 117(19), 5067–5077. https://doi.org/10.1182/BLOOD-2010-08-304287

Toyoshima, H., & Hunter, T. (1994). p27, a novel inhibitor of G1 cyclin-Cdk protein kinase activity, is related to p21. Cell, 78(1), 67–74. https://doi.org/10.1016/0092-8674(94)90573-8,

Tratwal, J., Rojas-Sutterlin, S., Bataclan, C., Blum, S., & Naveiras, O. (2021). Bone marrow adiposity and the hematopoietic niche: A historical perspective of reciprocity, heterogeneity, and lineage commitment. Best Practice & Research Clinical Endocrinology & Metabolism, 35(4), 101564. https://doi.org/10.1016/J.BEEM.2021.101564

Trufanova, N., Trufanov, O., Bozhok, G., Revenko, O., Cherkashina, D., Pakhomov, O., & Petrenko, O. (2024). Hypothermic Storage of Mesenchymal Stromal Cell-based Spheroids at a Temperature of 22°C. Problems of Cryobiology and Cryomedicine, 34(3), 186-200–186–200. https://doi.org/10.15407/CRYO34.03.186

Tsuji, W., Rubin, J. P., & Marra, K. G. (2014). Adipose-derived stem cells: Implications in tissue regeneration. World Journal of Stem Cells, 6(3), 312. https://doi.org/10.4252/WJSC.V6.I3.312

Turner, C. H., Rho, J., Takano, Y., Tsui, T. Y., & Pharr, G. M. (1999). The elastic properties of trabecular and cortical bone tissues are similar: results from two microscopic measurement techniques. Journal of Biomechanics, 32(4), 437–441. https://doi.org/10.1016/S0021-9290(98)00177-8

Turney, T. L., Reese-Koç, J., de Lima, M., & Otegbeye, F. (2019). Optimizing cryopreservation of hematopoietic stem cells collected for autologous stem cell transplantation in patients with multiple myeloma. Cytotherapy, 21(5), S39. https://doi.org/10.1016/j.jcyt.2019.03.375

Ullah, M., Liu, D. D., & Thakor, A. S. (2019). Mesenchymal Stromal Cell Homing: Mechanisms and Strategies for Improvement. IScience, 15, 421–438. https://doi.org/10.1016/J.ISCI.2019.05.004

Universities ‘asking how much research they can afford to do’ - Research Professional News. (n.d.). Retrieved May 10, 2025, from https://www.researchprofessionalnews.com/rr-news-uk-universities-2024-12-universities-asking-how-much-research-they-can-afford-to-do/

Valdivia, A., Avalos, A. M., & Leyton, L. (2023). Thy-1 (CD90)-regulated cell adhesion and migration of mesenchymal cells: insights into adhesomes, mechanical forces, and signaling pathways. Frontiers in Cell and Developmental Biology, 11. https://doi.org/10.3389/FCELL.2023.1221306/PDF

Valente, S., Ciavarella, C., Hernández-Aguilera, A., Salvador, F. A., Buzzi, M., Joven, J., & Pasquinelli, G. (2021). Phenotypic, morphological, and metabolic characterization of vascular-spheres from human vascular mesenchymal stem cells. Microscopy Research and Technique, 85(2), 447. https://doi.org/10.1002/JEMT.23918

Valletta, S., Thomas, A., Meng, Y., Ren, X., Drissen, R., Sengül, H., Di Genua, C., & Nerlov, C. (2020). Micro-environmental sensing by bone marrow stroma identifies IL-6 and TGFβ1 as regulators of hematopoietic ageing. Nature Communications, 11(1), 4075. https://doi.org/10.1038/S41467-020-17942-7

van den Boogaard, W. M. C., Komninos, D. S. J., & Vermeij, W. P. (2022). Chemotherapy Side-Effects: Not All DNA Damage Is Equal. Cancers 2022, Vol. 14, Page 627, 14(3), 627. https://doi.org/10.3390/CANCERS14030627

Van Niel, G., D'Angelo, G., & Raposo, G. (2018). Shedding light on the cell biology of extracellular vesicles. Nature Reviews Molecular Cell Biology 2018 19:4, 19(4), 213–228. https://doi.org/10.1038/nrm.2017.125

Van Norman, G. A. (2019). Phase II Trials in Drug Development and Adaptive Trial Design. JACC: Basic to Translational Science, 4(3), 428–437. https://doi.org/10.1016/J.JACBTS.2019.02.005

Vasandan, A. B., Jahnavi, S., Shashank, C., Prasad, P., Kumar, A., & Jyothi Prasanna, S. (2016). Human Mesenchymal stem cells program macrophage plasticity by altering their metabolic status via a PGE2-dependent mechanism. Scientific Reports 2016 6:1, 6(1), 1–17. https://doi.org/10.1038/srep38308

Ventura Ferreira, M. S., Jahnen-Dechent, W., Labude, N., Bovi, M., Hieronymus, T., Zenke, M., Schneider, R. K., & Neurs, S. (2012). Cord blood-hematopoietic stem cell expansion in 3D fibrin scaffolds with stromal support. Biomaterials, 33(29), 6987–6997. https://doi.org/10.1016/J.BIOMATERIALS.2012.06.029

Veronesi, E., Murgia, A., Caselli, A., Grisendi, G., Piccinno, M. S., Rasini, V., Giordano, R., Montemurro, T., Bourin, P., Sensebé, L., Rojewski, M. T., Schrezenmeier, H., Layrolle, P., Ginebra, M. P., Panaitescu, C. B., Gómez-Barrena, E., Catani, F., Paolucci, P., Burns, J. S., & Dominici, M. (2013). Transportation Conditions for Prompt Use of Ex Vivo Expanded and Freshly Harvested Clinical-Grade Bone Marrow Mesenchymal Stromal/Stem Cells for Bone Regeneration. Tissue Engineering. Part C, Methods, 20(3), 239. https://doi.org/10.1089/TEN.TEC.2013.0250

Visnjic, D., Kalajzic, Z., Rowe, D. W., Katavic, V., Lorenzo, J., & Aguila, H. L. (2004). Hematopoiesis is severely altered in mice with an induced osteoblast deficiency. Blood, 103(9), 3258–3264. https://doi.org/10.1182/BLOOD-2003-11-4011

Visvader, J. E., & Lindeman, G. J. (2011). The unmasking of novel unipotent stem cells in the mammary gland. EMBO Journal, 30(24), 4858–4859. https://doi.org/10.1038/EMBOJ.2011.415/FIGURES/1

Vogt, A., Faher, A., Kucharczak, J., Birch, M., McCaskie, A., & Khan, W. (2024). The Effects of Gender on Mesenchymal Stromal Cell (MSC) Proliferation and Differentiation In Vitro: A Systematic Review. International Journal of Molecular Sciences 2024, Vol. 25, Page 13585, 25(24), 13585. https://doi.org/10.3390/IJMS252413585

Vu, N. B., Vu, N. B., & Nguyen, M. T.-N. (2020). A simple and scalable method to generate spheroids from human mesenchymal stem cells for use in tissue engineering. Biomedical Research and Therapy, 7(12), 4139–4151. https://doi.org/10.15419/bmrat.v7i12.652

Wagner, J. E., Brunstein, C. G., Boitano, A. E., Defor, T. E., McKenna, D., Sumstad, D., Blazar, B. R., Tolar, J., Le, C., Jones, J., Cooke, M. P., & Bleul, C. C. (2016). Phase I/II Trial of StemRegenin-1

Expanded Umbilical Cord Blood Hematopoietic Stem Cells Supports Testing as a Stand-Alone Graft. Cell Stem Cell, 18(1), 144–155. https://doi.org/10.1016/J.STEM.2015.10.004

Wang, C.-C., Chen, C.-H., Hwang, S.-M., Lin, W.-W., Huang, C.-H., Lee, W.-Y., Chang, Y., & Sung, H.-W. (2009). Spherically Symmetric Mesenchymal Stromal Cell Bodies Inherent with Endogenous Extracellular Matrices for Cellular Cardiomyoplasty. Stem Cells, 27(3), 724–732. https://doi.org/10.1634/STEMCELLS.2008-0944

Wang, P., Berry, D., Moran, A., He, F., Tam, T., Chen, L., & Chen, S. (2019). Controlled Growth Factor Release in 3D-Printed Hydrogels. Advanced Healthcare Materials, 9(15), e1900977. https://doi.org/10.1002/ADHM.201900977

Wang, T. W., Wu, H. C., Wang, H. Y., Lin, F. H., & Sun, J. S. (2009). Regulation of adult human mesenchymal stem cells into osteogenic and chondrogenic lineages by different bioreactor systems. Journal of Biomedical Materials Research - Part A, 88(4), 935–946. https://doi.org/10.1002/jbm.a.31914

Wang, Y. L., & Pelham, R. J. (1998). [39] Preparation of a flexible, porous polyacrylamide substrate for mechanical studies of cultured cells. Methods in Enzymology, 298, 489–496. https://doi.org/10.1016/S0076-6879(98)98041-7

Wang, Z., Xu, Q., Zhang, N., Du, X., Xu, G., & Yan, X. (2020). CD146, from a melanoma cell adhesion molecule to a signaling receptor. Signal Transduction and Targeted Therapy 2020 5:1, 5(1), 1–15. https://doi.org/10.1038/s41392-020-00259-8

Waskow, C. (2019). Spatiotemporal Resolution of SCF Supply in Early Hematopoiesis. Cell Stem Cell, 24(3), 349–350. https://doi.org/10.1016/j.stem.2019.02.014

Weeks, L. D., & Ebert, B. L. (2023). Causes and consequences of clonal hematopoiesis. Blood, 142(26), 2235–2246. https://doi.org/10.1182/BLOOD.2023022222

Wells, L. A., & Sheardown, H. (2007). Extended release of high pI proteins from alginate microspheres via a novel encapsulation technique. European Journal of Pharmaceutics and Biopharmaceutics : Official Journal of Arbeitsgemeinschaft Fur Pharmazeutische Verfahrenstechnik e.V, 65(3), 329–335. https://doi.org/10.1016/J.EJPB.2006.10.018

Weng, Y., Wang, M., Liu, W., Hu, X., Chai, G., Yan, Q., Zhu, L., Cui, L., & Cao, Y. (2006). Repair of experimental alveolar bone defects by tissue-engineered bone. Tissue Engineering, 12(6), 1503–1513. https://doi.org/10.1089/TEN.2006.12.1503

Wiegand, C., Heinze, T., & Hipler, U. C. (2009). Comparative in vitro study on cytotoxicity, antimicrobial activity, and binding capacity for pathophysiological factors in chronic wounds of alginate and silver-containing alginate. Wound Repair and Regeneration : Official Publication of the Wound Healing Society [and] the European Tissue Repair Society, 17(4), 511–521. https://doi.org/10.1111/J.1524-475X.2009.00503.X

Wielockx, B., Grinenko, T., Mirtschink, P., & Chavakis, T. (2019). Hypoxia Pathway Proteins in Normal and Malignant Hematopoiesis. Cells, 8(2), 155. https://doi.org/10.3390/CELLS8020155

Wilson, A., Fu, H., Schiffrin, M., Winkler, C., Koufany, M., Jouzeau, J. Y., Bonnet, N., Gilardi, F., Renevey, F., Luther, S. A., Moulin, D., & Desvergne, B. (2018). Lack of adipocytes alters hematopoiesis in lipodystrophic mice. Frontiers in Immunology, 9(NOV), 415418. https://doi.org/10.3389/FIMMU.2018.02573/BIBTEX

Wilson, A., Laurenti, E., Oser, G., van der Wath, R. C., Blanco-Bose, W., Jaworski, M., Offner, S., Dunant, C. F., Eshkind, L., Bockamp, E., Lió, P., MacDonald, H. R., & Trumpp, A. (2008). Hematopoietic Stem Cells Reversibly Switch from Dormancy to Self-Renewal during Homeostasis and Repair. Cell, 135(6), 1118–1129. https://doi.org/10.1016/j.cell.2008.10.048

Winter, S., Götze, K. S., Hecker, J. S., Metzeler, K. H., Guezguez, B., Woods, K., Medyouf, H., Schäffer, A., Schmitz, M., Wehner, R., Glauche, I., Roeder, I., Rauner, M., Hofbauer, L. C., & Platzbecker, U. (2024). Clonal hematopoiesis and its impact on the aging osteo-hematopoietic niche. Leukemia 2024 38:5, 38(5), 936–946. https://doi.org/10.1038/s41375-024-02226-6

Wodnar-Filipowicz, A. (2003). Flt3 Ligand: Role in Control of Hematopoietic and Immune Functions of the Bone Marrow. News in Physiological Sciences, 18(6), 247–251. https://doi.org/10.1152/NIPS.01452.2003/ASSET/IMAGES/LARGE/1452-4.C.JPEG

Wong, S. H., Hamel, L., Chevalier, S., & Philip, A. (2000). Endoglin expression on human microvascular endothelial cells association with betaglycan and formation of higher order complexes with TGF-beta signalling receptors. FEBS Journal, 267(17), 5550–5560. https://doi.org/10.1046/j.1432-1327.2000.01621.x

Wood, P. A., & Hrushesky, W. J. M. (1995). Cisplatin-associated anemia: an erythropoietin deficiency syndrome. Journal of Clinical Investigation, 95(4), 1650. https://doi.org/10.1172/JCI117840

Wright, B., Cave, R. A., Cook, J. P., Khutoryanskiy, V. V., Mi, S., Chen, B., Leyland, M., & Connon, C. J. (2012). Enhanced Viability of Corneal Epithelial Cells for Efficient Transport/Storage Using a Structurally Modified Calcium Alginate Hydrogel. Regenerative Medicine, 7(3), 295–307. https://doi.org/10.2217/RME.12.7

Wu, C. C., Liu, F. L., Sytwu, H. K., Tsai, C. Y., & Chang, D. M. (2016). CD146+ mesenchymal stem cells display greater therapeutic potential than CD146- cells for treating collagen-induced arthritis in mice. Stem Cell Research and Therapy, 7(1), 1–13. https://doi.org/10.1186/S13287-016-0285-4/FIGURES/6

Wu, D. T., Diba, M., Yang, S., Freedman, B. R., Elosegui-Artola, A., & Mooney, D. J. (2023). Hydrogel viscoelasticity modulates migration and fusion of mesenchymal stem cell spheroids. Bioengineering & Translational Medicine, 8(3), e10464. https://doi.org/10.1002/BTM2.10464

Xiao Ling, K., Peng, L., Feng, Z. J., Wei, C., Yan, Y. W., Nan, S., Qi, G. C., & Wei, W. Z. (2016). Stromal Derived Factor-1/CXCR4 Axis Involved in Bone Marrow Mesenchymal Stem Cells Recruitment to Injured Liver. Stem Cells International, 2016(1), 8906945. https://doi.org/10.1155/2016/8906945

Xiao, Y., McGuinness, ChanelleA. S., Doherty-Boyd, W. S., Salmeron-Sanchez, M., Donnelly, H., & Dalby, M. J. (2022). Current insights into the bone marrow niche: From biology in vivo to bioengineering ex vivo. Biomaterials, 286, 121568. https://doi.org/10.1016/J.BIOMATERIALS.2022.121568

Xie, A. W., Zacharias, N. A., Binder, B. Y. K., & Murphy, W. L. (2021). Controlled aggregation enhances immunomodulatory potential of mesenchymal stromal cell aggregates. Stem Cells Translational Medicine, 10(8), 1184. https://doi.org/10.1002/SCTM.19-0414

Xu, C., Gao, X., Wei, Q., Nakahara, F., Zimmerman, S. E., Mar, J., & Frenette, P. S. (2018). Stem cell factor is selectively secreted by arterial endothelial cells in bone marrow. Nature Communications, 9(1). https://doi.org/10.1038/S41467-018-04726-3

Xu, Y., Shi, T., Xu, A., & Zhang, L. (2016). 3D spheroid culture enhances survival and therapeutic capacities of MSCs injected into ischemic kidney. Journal of Cellular and Molecular Medicine, 20(7), 1203–1213. https://doi.org/10.1111/JCMM.12651

Xu, Y., Wang, Y. Q., Wang, A. T., Yu, C. Y., Luo, Y., Liu, R. M., Zhao, Y. J., & Xiao, J. H. (2020). Effect of CD44 on differentiation of human amniotic mesenchymal stem cells into chondrocytes via Smad and ERK signaling pathways. Molecular Medicine Reports, 21(6), 2357. https://doi.org/10.3892/MMR.2020.11044

Yagi, H., Chen, A. F., Hirsch, D., Rothenberg, A. C., Tan, J., Alexander, P. G., & Tuan, R. S. (2020). Antimicrobial activity of mesenchymal stem cells against Staphylococcus aureus. Stem Cell Research and Therapy, 11(1), 1–12. https://doi.org/10.1186/S13287-020-01807-3/FIGURES/5

Yahia, E. M. (2010). Cold chain development and challenges in the developing world. Acta Horticulturae, 877, 127–132. https://doi.org/10.17660/ACTAHORTIC.2010.877.9

Yahia, Lh., Chirani, N., Gritsch, L., Motta, F. L., SoumiaChirani, & Fare, S. (2015). History and Applications of Hydrogels. Journal of Biomedical Sciences, 4(2), 0–0. https://doi.org/10.4172/2254-609X.100013

Yamada, T., Park, C. S., & Daniel Lacorazza, H. (2013). Genetic control of quiescence in hematopoietic stem cells. Cell Cycle, 12(15), 2376. https://doi.org/10.4161/CC.25416

Yamaguchi, Y., Ohno, J., Sato, A., Kido, H., & Fukushima, T. (2014). Mesenchymal stem cell spheroids exhibit enhanced in-vitro and in-vivo osteoregenerative potential. BMC Biotechnology, 14(1), 1–10. https://doi.org/10.1186/S12896-014-0105-9/TABLES/1

Yan, X. Q., Briddell, R., Hartley, C., Stoney, G., Samal, B., & McNiece, I. (1994). Mobilization of long-term hematopoietic reconstituting cells in mice by the combination of stem cell factor plus granulocyte colony-stimulating factor. Blood, 84(3), 795–799. https://doi.org/10.1182/BLOOD.V84.3.795.BLOODJOURNAL843795

Yan, X. Q., Hartley, C., McElroy, P., Chang, A., McCrea, C., & McNiece, I. (1995). Peripheral Blood Progenitor Cells Mobilized by Recombinant Human Granulocyte Colony-Stimulating Factor Plus Recombinant Rat Stem Cell Factor Contain Long-Term Engrafting Cells Capable of Cellular Proliferation for More Than Two Years as Shown by Serial Transplantation in Mice. Blood, 85(9), 2303–2307. https://doi.org/10.1182/BLOOD.V85.9.2303.BLOODJOURNAL8592303

Yang, Y., He, X., Zhao, R., Guo, W., Zhu, M., Xing, W., Jiang, D., Liu, C., & Xu, X. (2018). Serum IFN-γ levels predict the therapeutic effect of mesenchymal stem cell transplantation in active rheumatoid arthritis. Journal of Translational Medicine, 16(1), 1–9. https://doi.org/10.1186/S12967-018-1541-4/FIGURES/5

Yang, Yingjun, Wang, X., Wang, Y., Hu, X., Kawazoe, N., Yang, Yingnan, & Chen, G. (2019). Influence of Cell Spreading Area on the Osteogenic Commitment and Phenotype Maintenance of Mesenchymal Stem Cells. Scientific Reports 2019 9:1, 9(1), 1–11. https://doi.org/10.1038/s41598-019-43362-9

Ye, F., Li, J., Xu, P., Xie, Z., Zheng, G., Liu, W., Ye, G., Yu, W., Lin, J., Su, Z., Che, Y., Zhang, Z., Wang, P., Wu, Y., & Shen, H. (2022). Osteogenic differentiation of mesenchymal stem cells promotes c-

Jun-dependent secretion of interleukin 8 and mediates the migration and differentiation of CD4+ T cells. Stem Cell Research and Therapy, 13(1). https://doi.org/10.1186/S13287-022-02735-0,

Ylöstalo, J. H., Bartosh, T. J., Coble, K., & Prockop, D. J. (2012). Human Mesenchymal Stem/Stromal Cells Cultured as Spheroids are Self-activated to Produce Prostaglandin E2 that Directs Stimulated Macrophages into an Anti-inflammatory Phenotype. Stem Cells, 30(10), 2283–2296. https://doi.org/10.1002/STEM.1191

Yoshihara, H., Arai, F., Hosokawa, K., Hagiwara, T., Takubo, K., Nakamura, Y., Gomei, Y., Iwasaki, H., Matsuoka, S., Miyamoto, K., Miyazaki, H., Takahashi, T., & Suda, T. (2007). Thrombopoietin/MPL Signaling Regulates Hematopoietic Stem Cell Quiescence and Interaction with the Osteoblastic Niche. Cell Stem Cell, 1(6), 685–697. https://doi.org/10.1016/J.STEM.2007.10.020

YS, T., T, M., E, J., A, J., A, M., AL, W., A, B., & DE, I. (2016). Modeling Hematopoiesis and Responses to Radiation Countermeasures in a Bone Marrow-on-a-Chip. Tissue Engineering. Part C, Methods, 22(5), 509–515. https://doi.org/10.1089/TEN.TEC.2015.0507

Yu, C., Zhang, M., Song, J., Zheng, X., Xu, G., Bao, Y., Lan, J., Luo, D., Hu, J., Li, J. J., & Shi, H. (2020). Integrin-Src-YAP1 signaling mediates the melanoma acquired resistance to MAPK and PI3K/mTOR dual targeted therapy. Molecular Biomedicine, 1(1), 1–16. https://doi.org/10.1186/S43556-020-00013-0/FIGURES/7

Yuan, M., Hu, X., Yao, L., Jiang, Y., & Li, L. (2022). Mesenchymal stem cell homing to improve therapeutic efficacy in liver disease. Stem Cell Research & Therapy 2022 13:1, 13(1), 1–17. https://doi.org/10.1186/S13287-022-02858-4

Zanetti, A., Grata, M., Etling, E. B., Panday, R., Villanueva, F. S., & Toma, C. (2015). Suspension-Expansion of Bone Marrow Results in Small Mesenchymal Stem Cells Exhibiting Increased Transpulmonary Passage Following Intravenous Administration. Tissue Engineering. Part C, Methods, 21(7), 683. https://doi.org/10.1089/TEN.TEC.2014.0344

Zeddou, M., Briquet, A., Relic, B., Josse, C., Malaise, M. G., Gothot, A., Lechanteur, C., & Beguin, Y. (2010). The umbilical cord matrix is a better source of mesenchymal stem cells (MSC) than the umbilical cord blood. Cell Biology International, 34(7), 693–701. https://doi.org/10.1042/CBI20090414

Zeng, H., Yücel, R., Kosan, C., Klein-Hitpass, L., & Möröy, T. (2004). Transcription factor Gfi1 regulates self-renewal and engraftment of hematopoietic stem cells. The EMBO Journal, 23(20), 4116. https://doi.org/10.1038/SJ.EMBOJ.7600419

Zhang, C., Zhou, Y., Zhang, L., Wu, L., Chen, Y., Xie, D., & Chen, W. (2018). Hydrogel Cryopreservation System: An Effective Method for Cell Storage. International Journal of Molecular Sciences, 19(11), 3330. https://doi.org/10.3390/IJMS19113330

Zhang, H., Zhang, F., & Yuan, R. (2020). Applications of natural polymer-based hydrogels in the food industry. Hydrogels Based on Natural Polymers, 357–410. https://doi.org/10.1016/B978-0-12-816421-1.00015-X

Zhang, N., Wu, J., Wang, Q., Liang, Y., Li, X., Chen, G., Ma, L., Liu, X., & Zhou, F. (2023). Global burden of hematologic malignancies and evolution patterns over the past 30 years. Blood Cancer Journal, 13(1), 82. https://doi.org/10.1038/S41408-023-00853-3

Zhang, P., Iwasaki-Arai, J., Iwasaki, H., Fenyus, M. L., Dayaram, T., Owens, B. M., Shigematsu, H., Levantini, E., Huettner, C. S., Lekstrom-Himes, J. A., Akashi, K., & Tenen, D. G. (2004). Enhancement of hematopoietic stem cell repopulating capacity and self-renewal in the absence of the transcription factor C/EBPα. Immunity, 21(6), 853–863. https://doi.org/10.1016/j.immuni.2004.11.006

Zhang, P., Zhang, C., Li, J., Han, J., Liu, X., & Yang, H. (2019). The physical microenvironment of hematopoietic stem cells and its emerging roles in engineering applications. Stem Cell Research & Therapy 2019 10:1, 10(1), 1–13. https://doi.org/10.1186/S13287-019-1422-7

Zhang, Q., Nguyen, A. L., Shi, S., Hill, C., Wilder-Smith, P., Krasieva, T. B., & Le, A. D. (2012). Three-dimensional spheroid culture of human gingiva-derived mesenchymal stem cells enhances mitigation of chemotherapy-induced oral mucositis. Stem Cells and Development, 21(6), 937–947. https://doi.org/10.1089/SCD.2011.0252;PAGEGROUP:STRING:PUBLICATION

Zhang, Y. H., Hu, Y., Zhang, Y., Hu, L. D., & Kong, X. (2018). Distinguishing three subtypes of hematopoietic cells based on gene expression profiles using a support vector machine. Biochimica et Biophysica Acta (BBA) - Molecular Basis of Disease, 1864(6), 2255–2265. https://doi.org/10.1016/J.BBADIS.2017.12.003

Zhao, L., & Hantash, B. M. (2011). TGF-β1 Regulates Differentiation of Bone Marrow Mesenchymal Stem Cells. Vitamins and Hormones, 87, 127–141. https://doi.org/10.1016/B978-0-12-386015-6.00042-1

Zhou, B. O., Ding, L., & Morrison, S. J. (2015). Hematopoietic stem and progenitor cells regulate the regeneration of their niche by secreting Angiopoietin-1. ELife, 2015(4). https://doi.org/10.7554/ELIFE.05521

Zhou, B. O., Yu, H., Yue, R., Zhao, Z., Rios, J. J., Naveiras, O., & Morrison, S. J. (2017). Bone marrow adipocytes promote the regeneration of stem cells and haematopoiesis by secreting SCF. Nature Cell Biology 2017 19:8, 19(8), 891–903. https://doi.org/10.1038/ncb3570

Zhou, X., Xie, F., Wang, L., Zhang, L., Zhang, S., Fang, M., & Zhou, F. (2020). The function and clinical application of extracellular vesicles in innate immune regulation. Cellular & Molecular Immunology 2020 17:4, 17(4), 323–334. https://doi.org/10.1038/s41423-020-0391-1

Zhu, R. J., Wu, M. Q., Li, Z. J., Zhang, Y., & Liu, K. Y. (2013). Hematopoietic recovery following chemotherapy is improved by BADGE-induced inhibition of adipogenesis. International Journal of Hematology, 97(1), 58–72. https://doi.org/10.1007/S12185-012-1233-4/FIGURES/8

Zimmerberg, J., Cohen, F. S., Finkelstein, A., Baker, P. F., Knight, D. E., Hauser, H., Phillips, M. C., Barratt, M. D., & Biophys, B. (1980). Microencapsulated Islets as Bioartificial Endocrine Pancreas. Science, 210(4472), 908–910. https://doi.org/10.1126/SCIENCE.6776628

Zimmermann, H., Shirley, S. G., & Zimmermann, U. (2007). Alginate-based encapsulation of cells: Past, present, and future. Current Diabetes Reports, 7(4), 314–320. https://doi.org/10.1007/S11892-007-0051-1/METRICS

Zimmermann, J. A., & Mcdevitt, T. C. (2014a). Pre-conditioning mesenchymal stromal cell spheroids for immunomodulatory paracrine factor secretion. Cytotherapy, 16(3), 331–345. https://doi.org/10.1016/J.JCYT.2013.09.004

Zimmermann, J. A., & Mcdevitt, T. C. (2014b). Pre-conditioning mesenchymal stromal cell spheroids for immunomodulatory paracrine factor secretion. Cytotherapy, 16(3), 331–345. https://doi.org/10.1016/J.JCYT.2013.09.004

Zinngrebe, J., Debatin, K. M., & Fischer-Posovszky, P. (2020). Adipocytes in hematopoiesis and acute leukemia: friends, enemies, or innocent bystanders? Leukemia 2020 34:9, 34(9), 2305–2316. https://doi.org/10.1038/s41375-020-0886-x

Zou, Y., Sun, Y., Guo, B., Wei, Y., Xia, Y., Huangfu, Z., Meng, F., Van Hest, J. C. M., Yuan, J., & Zhong, Z. (2020). α3β1 Integrin-Targeting Polymersomal Docetaxel as an Advanced Nanotherapeutic for Nonsmall Cell Lung Cancer Treatment. ACS Applied Materials and Interfaces , 12(13), 14905–14913. https://doi.org/10.1021/ACSAMI.0C01069/SUPPL_FILE/AM0C01069_SI_001.PDF

Zsebo, K. M., Smith, K. A., Hartley, C. A., Greenblatt, M., Cooke, K., Rich, W., & Mcniece, I. K. (1992). Radioprotection of mice by recombinant rat stem cell factor. Proceedings of the National Academy of Sciences of the United States of America, 89(20), 9464–9468. https://doi.org/10.1073/PNAS.89.20.9464